Improving The Visual Stimuli For Brain-Computer Interfaces

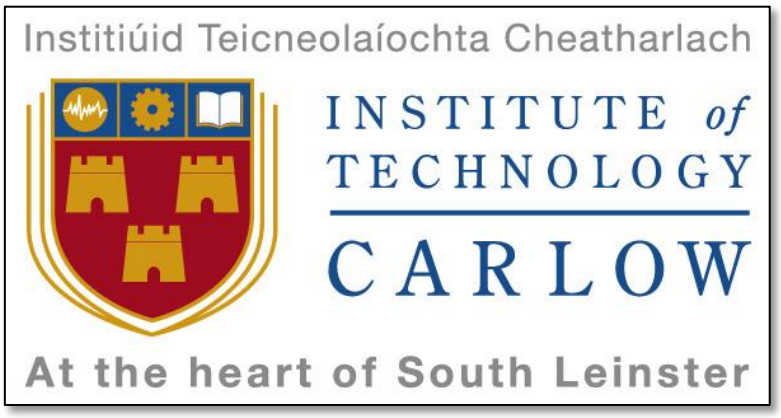

Submitted by: Artur Szalowski

For the award of Doctor of Philosophy

Supervised by: Dr Dorel Picovici

Department of Aerospace, Mechanical & Electronic Engineering

Institute of Technology Carlow

Submitted to the Institute of Technology Carlow, September 2019

Improving The Visual Stimuli For Brain-Computer Interfaces

Artur Szalowski
EngCORE Research Group
Department of Aerospace, Mechanical & Electronic Engineering
Institute of Technology Carlow

Abstract

Visual stimuli are traditionally used to operate Brain-Computer Interface (BCI) systems employing the Steady State Visual Evoked Potentials (SSVEP) technique. In this technique, when a BCI user's visual system is exposed to a flickering stimulus, the brain will generate oscillations with matching frequencies. Such signals will allow the user to control external devices such as computers, games, robots or drones. In non-invasive BCIs, the brain signals available are very weak, usually in the range of microvolts, thus various signal processing methods must be employed in order to facilitate successful system operations. It has been recognised that despite great efforts made by the research community to improve brain signal processing algorithms, improvements can be made at the very source – the brain itself.

A variety of novel testing scenarios have been conceptualised, designed and realised with the sole purpose of formulating and creating flickering graphic that would address this problem by eliciting the strongest, artefacts free, and minimal noise, brain signals. All parameters were individually tested, to evaluate and determine their impact on the brain signals. Among the parameters chosen for evaluation are flicker sizes, patterns, displayed backgrounds, and colours. Specifically, great attention has been put to test the impact of colours. Such determination for the colour flicker testing was directly derived from the fact that the human retina is constructed of photosensitive cells detecting precisely the same primary colours, which are found in digital displays used to present said flickers in the form of pixels. The introduction of colour flickers, not only provided better results, also filled a gap in research: that is, the use of colours in visual stimulation.

In order to achieve the proposed experimental scenarios several hardware and software tools have been used. A bespoke iOS application capable of generating large variety of colour and black-white flickers has been used to elicit brain signals during experiments. Nearly two thousand of raw brain signals have been recorded and analysed. In the final stage of the research, the determined best performing flicker parameters have been used to generate flickers for an off-line BCI application. The resulting flickers delivered strong and clean brain signals, which validated the success of this research.

Declaration

This thesis is presented in fulfillment of the requirements for the degree of Doctorate of Philosophy. It is entirely my own work and has not been submitted to any other University or higher education institution, or for any other academic award in this institution. Where use has been made of the work of other people it has been fully acknowledged and fully referenced.

Signature: _____

Artur Szalowski

September 2019

Acknowledgements

The author would like to express his enormous gratitude towards his supervisor Dr. Dorel Picovici for his unparalleled support, invaluable editorial comments, continued encouragement and guidance throughout the course of this work.

Also, I would like to thank all staff from the Department of Aerospace, Mechanical and Electronic Engineering, Institute of Technology Carlow for creating very positive and friendly environment allowing me to complete this research work.

In addition, I would like to thank all colleagues at Dargan Centre, especially EngCORE and GameCORE research groups for stress relieving conversations, suggestions and overall helpful attitude. Also, I would like to express my appreciation to undergraduate students for participating in experiments so valuable for this research.

Finally, endless appreciation goes to my Family, especially my wife Kamilla, for her patience and understanding, as well as my children; Adam and Amelia, for their smiles and unquestionable love.

Nomenclature

(ɣ)	Gamma waves
(α)	Alpha waves
(β)	Beta waves
(δ)	Delta waves
(θ)	Theta waves
AgCl	Silver Chloride
BIOSIG	Software library for biomedical signal processing
C	Central lobe
dB	Decibel
EEGLAB	Interactive MATLAB toolbox (open source)
ERPLAB	Interactive MATLAB toolbox (open source)
F	Frontal lobe
H.264 or MPEG-4	Block-oriented motion-compensation-based video compression standard
Hz	Hertz
iOS	Apple operating system for mobile devices
K	Kelvin
kHz	Kilohertz
kΩ	Kilo ohm
L	Long wavelengths
M	Medium wavelengths
mm	Millimeter
mV	Millivolt
nm	Nanometer
O	Occipital lobe

P	Parietal lobe
P-300	Positive deflection after 300 milliseconds
S	Short wavelengths
T	Temporal lobe
V1	Visual cortex 1
V2	Visual cortex 2
V3	Visual cortex 3
V4	Visual cortex 4
V5	Visual cortex 5
VLC	Cross-platform media player (open source)
μV	Microvolt

List of Abbreviations

A/D	Analog-to-Digital
ALS	Amyotrophic Lateral Sclerosis
AR	Auto Regressive
BCI	Brain-Computer Interface
BW	Black-White
CCTV	Closed Circuit TV
CLIS	Complete Locked-In State
CMS	Common Mode Sense (active electrode)
CRT	Cathode-Ray Tube
CSP	Common Spatial Patterns
CWT	Continuous Wavelet Transforms
DFT	Discrete Fourier Transforms
DNG	Digital Negative
DRL	Driven Right Leg (passive electrode)
DWT	Discrete Wavelet Transforms
ECG	Electrocardiography
ECoG	Electrocorticography
EDF	European Data Format
EEG	Electroencephalography
EMG	Electromyography
EOG	Electrooculography
ERD	Event-Related Desynchronisation
ERP	Event Related Potentials
ERS	Event-Related Synchronisation
FFT	Fast Fourier Transform

FIR	Finite Impulse Response
fMRI	Functional Magnetic Resonance Imaging
FT	Fourier Transforms
GA	Genetic Algorithm
GNU	GNU General Public License
GPU	Graphics Processing Unit
GUI	Graphic User Interface
HDR	High Dynamic Range
ICA	Independent Component Analysis
IDE	Independent Development Environment
IIR	Infinite Impulse Response
ITR	Information Transfer Rate
LCD	Liquid Crystal Display
LED	Light-Emitting Diode
LIS	Locked-In State
MCF	Multi Colour Flicker
MEA	Multi-Electrode Arrays
MEG	Magneto Encephalography
MF	Matched Filtering
NIRS	Near Infrared Spectroscopy
OLED	Organic Light-Emitting Diode
OSX	Operating System X
PC	Personal Computer
PCA	Principle Component Analysis
PPI	Pixel Per Inch
RGB	Red-Green-Blue

RW	Red-White
SBS	Sequential Backward Selection
SCI	Spinal Cord Injury
SCP	Slow Cortical Potentials
SDK	Software Development Kit
SFS	Sequential Forward Selection
SNR	Signal-to-Noise Ratio
SSVEP	Steady State Visual Evoked Potential
STFT	Short-Term Fourier Transforms
TV	Television
TVEP	Transient Visual Evoked Potentials
UI	User Interface
USB	Universal Serial Bus
VEP	Visual Evoked Potential
WT	Wavelet Transforms

Table of Contents

List of Figures

List of Tables

Chapter 1 Introduction

1.1 Motivation and Rationale

A Brain-Computer Interface (BCI) system is a combination of software and hardware allowing the control of devices such as drones, computers, games etc. using cerebral activity only. In BCIs there are two methods used to obtain brain signals: invasive and non-invasive. The invasive method uses electrodes mounted directly on the surface of the brain thus enabling the obtainment of low amplitude brain oscillations measured in millivolts (mV), which have high resolution, minimal noise and low artefacts. The brain itself can generate the artefacts as well as other body elements through muscle or eye movement. The non-invasive methods do not require any medical intervention; however, they are characterised by much lower spatial and temporal resolution, and provide very weak and noisy signals.

This research focuses on one of the most widespread non-invasive modalities, where electrodes are placed on the scalp. In this method, there are numerous factors both internal (body-based) and external (environmental) that influence the brain signal acquisition process. Because of the distance between electrodes and brain, the signals are of very low amplitude, measured in microvolts (μV), and are prone to artefacts and excessive noise pollution. Therefore, in non-invasive Brain-Computer Interface systems, eliciting and obtaining strong and clean brain signals is a highly challenging task. There are several techniques used to elicit the brain signals. Among them, a very popular one, also adopted in this work utilises visual stimulation and is referred to as Steady State Visual Evoked Potentials (SSVEP). In SSVEP, frequencies between 5 Hz and 15 Hz can be involuntarily elicited in the brain with clearly distinctive amplitude peaks as long as the subject maintains visual contact with the stimulus. It needs to be noted that any brain signals captured can be improved through several post-processing techniques, which will be further discussed in the thesis.

However, the main focus of this work is to establish new and effective methods to improve the signal quality at the source where they originate – the brain itself – during the initial stage of acquisition and before any post-processing is applied. In particular, through designing visual flickers that would be most effective in generating targeted brain waves with maximum amplitude and the least amount of artefacts and noise. Based on previous study and experience in motion graphics design and creation, acquired knowledge about additive colour science and how it relates to the human eye, and newly acquired knowledge during this research about how the brain processes graphic elements and colour, the author decided to investigate how certain parameters of the graphics such as size, pattern, level of contrast and in particular colour will impact the elicited

signals. During the initial stage of the research the author has read over three hundred papers on the subject of BCI development. Only 3% of the studied published work treats about similar problems. Furthermore, the majority of that work is very fragmented, is isolated in terms of methods used, and does not provide comprehensive results as the author intended to do. This presented the author with the opportunity to apprehend and discover new concepts and contribute to the BCI research and development community through publications and conference participations. Since the signal strength generated by the brain is measured on the scalp in the range of microvolts (μV), any qualitative gain, specifically understood as amplitude, will increase the desired portion of the signal by at least a few microvolts, and, in conjunction with noise minimisation and artifact rejection that occurs at the signal source i.e. the brain, it will result in less computing power required to post-process the signals.

The author's belief is that the potential improvement of the signal acquisition process would be very beneficial for the general BCI development. Thus, the main motivation justifying this research is to investigate different parameters of visual stimuli, test them individually to find how they all influence the elicited signal and ultimately propose a set of parameters, which other BCI developers can use to guarantee the best performance of their systems.

1.2 Stimuli Flickers as the Centre of Research

For non-invasive BCIs with sensors contacting the scalp, it is important to note that both spatial and temporal resolutions are significantly lower in comparison to the invasive methods. The non-invasive methods provide ~10 mm spatial resolution and ~0.05 s temporal resolution, while the invasive methods provide ~1 mm spatial resolution and ~0.003 s temporal resolution (Nicolas-Alonso and Gomez-Gil, 2012). Also the signal amplitude provided by the non-invasive techniques is 20 to 100 times weaker compared to the invasively obtained brain signals (Ball et al., 2009). This signal loss is attributed to the distance between the sensors mounted on the scalp and the brain cortex. Between the cerebral cortex, where the majority of electrical activity occurs and sensors/electrodes that capture this activity, there are several layers of anatomic elements protecting the brain. Among them are subarachnoid space, arachnoid matter, subdural space, dura matter, skull bone, periosteum, scalp skin and, usually, hair. They all successfully block the flow of electricity and weaken the signals making them difficult for recording. Due to this complication the chance of signal pollution by artefacts coming from both the body itself and the external environment is increased significantly (Nicolas-Alonso and Gomez-Gil, 2012). Traditionally, BCI researchers and developers who employ visual flicker to elicit certain brain oscillations in order to drive their systems use sources of light that provide maximum contrast ratio. Therefore, quality improvement

of generated signals in the brain through designing the most effective stimuli flickers is of utmost importance for executing a successful visually driven BCI system. For digital screens such as computer monitors, tablets or smartphone screens the use of flickering black and white graphics fulfills this requirement. When using other sources of light such as light bulbs, flashlight or LED panels, electronic circuits are used to make the lights flash and flicker. The common belief always was that such black and white graphics and other sources of white light that are programmed to flicker, will provide the highest possible contrast level between white (light full on) and black (no light) rendering them the most effective choice in exciting the eye's retina. This, in effect, causes brain oscillations, which is the core ingredient in visual-based BCI. This opinion can be derived from the basics of additive colour science, which will be discussed in detail later in Section 1.6. Light is simply an electromagnetic oscillation. A human's visual system can detect wavelengths in the range of approx. 400 nm to 700 nm. The human eye captures and the brain interprets all these frequencies as different colours gradually cross-fading into one another. In additive colour science, mixing together all these electromagnetic wavelengths produces white light. In simple terms, in additive colour science, colour black is to be understood as lack of light, not as a colour per se, while colour white is to be treated as white light.

As accurate as the assumption is about the practicality of black and white stimuli utilisation, the author is convinced that there are other dependencies, especially those existing in the human eye in relation to seeing colours, which potentially are correlated to brain oscillations elicited visually. The eye's retina is equipped with photosensitive cells, which respond to different electromagnetic wavelengths i.e. colours. This presents opportunity for new discoveries when testing colour and multi-colour flickers for eliciting brain signals, which the author intended to test and explore. However, colours and different colour combinations constitute just one parameter of many possible parameters.

Another interesting characteristic of the stimuli elements that is worth experimenting with would be its size. Testing different sizes and comparing their results will be very useful for BCI developers who want to design graphic user interfaces (GUI) for their systems utilising multiple flickering elements within the GUI to achieve a multi-command operation of the system. Finding the ultimate size threshold below which the flickers become unusable will be equally important as finding the perfect stimulus size guaranteeing the best signals. It is quite possible that a flicker occupying too much of the displaying surface induce induce weaker brain signals when compared to smaller counterparts. Testing this dependency seems like a natural choice to include in this work.

When using digital screens for stimuli presentation, flickering graphics usually do not occupy the entire surface of the display and need to be presented on a screen with something serving as a background. Probably, for most researchers a logical choice would be a grey background. In additive colour science grey is a mixture of black and white. In particular, when mixing 50% of black and 50% of white, what is achieved is often referred to as 50% grey. This background has been chosen for multi-colour flicker comparison tests. However, to make the work more complete, a decision has been made to also include white and black backgrounds for stimuli display. The hope is to find another dependency proving to be important in successful stimuli design.

Based on widespread opinion among BCI developers working with visual stimulation, one of the most popular and recommended patterns used to elicit brain signals is a checkerboard (Zhu et al., 2010). As a derivative of this opinion, it was decided to exclusively utilise checkerboard patterns in all experiments using computer generated graphic-based flickers. Many approaches are possible when designing and implementing checkerboard flickers. Among them are the use of graphic design and animation software to create and render individual video files, which can be played back on any operating software using standard media player. A more sophisticated approach would require planning, designing and programming task-specific custom software application executing all the functionality needed for the research.

This work utilises both approaches. In addition, to test other possible pattern variants a different source of light had to be proposed for easy manipulation of the said patterns. For this purpose, a LED panel comprising of 40 LEDs working as an Arduino shield has been chosen for testing. This system is very versatile because it not only fulfills the above-mentioned requirement, but also provides the perfect platform to further test different colours from an RGB colour palette. The above-mentioned proposed methods and techniques to experiment with new and potentially improved stimuli flickers will constitute the backbone of this research. The author's ultimate intention is to experiment with as many parameters of the stimuli elements as possible and from the resulting experiments derive the most optimal set of parameters that can be applied and successfully used by other BCI researchers and developers utilising visual stimulation in their systems. The main research questions this work will address are as follows:

- In what way the size/resolution of the stimuli element will impact the amplitude of elicited portion of the brain signals?

- Is there any dependency between the stimuli presentation background brightness and the generated oscillations?

- How the multi-field flickers (i.e. checkerboard) compare against their counterparts with a single flickering element (i.e. rectangle) for a visually driven BCI system?
- Will the colour flickers offer any improvement in the elicited brain signals in comparison to the greyscale versions?
- How the user training (preliminary exposure to visual stimulation) will impact the performance of the visual stimuli?

For the entirety of this research the 10 Hz frequency has been chosen for flicker presentation. As suggested by Regan (1989) 10 Hz oscillation elicits very high signal peaks in the brain. Additionally, the 10 Hz flickering pattern flawlessly synchronises with most of the digital screens currently used for flicker presentation due to their refresh rate of 60 Hz. For more details please refer to Section 1.7.

1.3 The Eye Retina Function

As described by Falk et al. (1986) in their book titled "Seeing The Light – Optics in Nature, Photography, Color, Vision, and Holography" the best way to describe the retina's function in the eye is to compare it to a film stock in an analogue film camera or to a digital sensor in a modern digital video camera. It is responsible for receiving the real image focused by the eye lens. In the retina there are three layers called the plexiform, choroid, and photoreceptors layers as illustrated in Figure 1-1. The light sensitive layer is built of a very dense array of photosensitive cells referred to as rods and cones (Figure 1-2). Their only function is to absorb light.

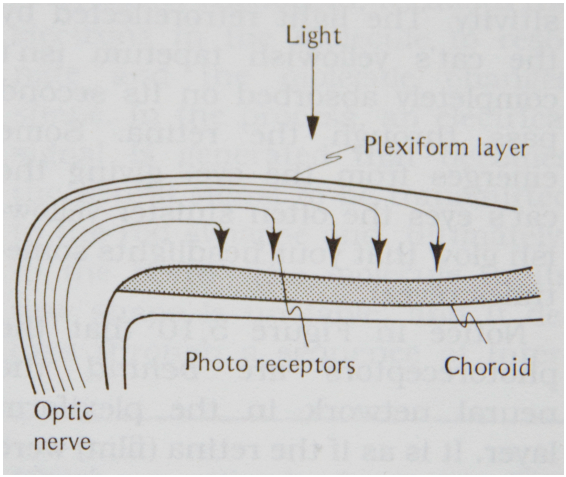

Figure 1-1 Layers of the human retina (Falk et al., 1986)

The plexiform layer is equipped with nerve cells and their main function is processing the signals generated by the said rods and cones and then further relaying them to the optic nerve. The choroid layer finally, has two very distinctive functions in the retina. It carries blood vessels nourishing the retina and works as an anti-halation backing. Essentially, the choroid layer absorbs light after it passes through the rods and cones, preventing it from reflecting back at the photocells. That is why the pupils are so dark since much of the light is almost completely absorbed by the retina layers.

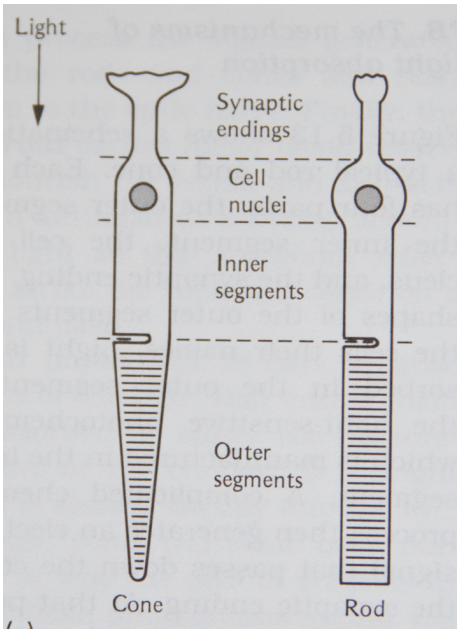

Figure 1-2 Physiology of the photoreceptors; cones and rods (Falk et al., 1986)

In the photoreceptor layer, there are approximately 7 million cones, which are characterised by low sensitivity to light, and about 120 million rods with very high sensitivity to light. Although the cones respond only to high levels of light, they are capable of detecting colour information. There are three types of cones. One type, occupying approximately 64% of the retina responds to colour red. About 32% sees colour green, while the remaining few percent respond to colour blue. The red and green sensitive cones are arranged in the centre of the retina, while the blue ones are mostly located on the edge.

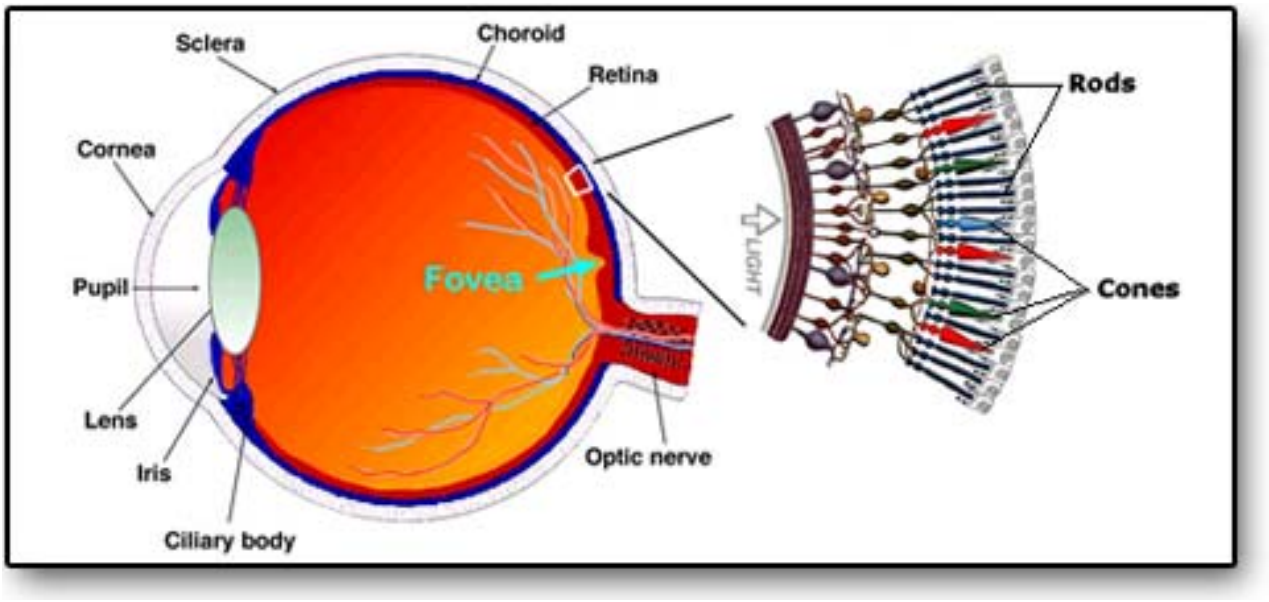

Figure 1-3 Physiology of the human eye (Webvision.med.utah.edu., 2019)

Rods and cones on the human retina.

The rods in contrast, respond to very low levels of light, enabling night vision while not being able to detect colours. Another important characteristic differentiating both types of photocells is their response time in light detection. The scotopic rods detecting greyscale light pallet only are very slow in response, which can be observed when a person enters dark environment and the night vision slowly, usually after a few minutes, adjusts to the lighting conditions and the person starts to see the details. The photopic cones are able to detect changes of light much quicker. This difference in response time is directly related to numbers of rods and cones occupying retina surface. Due to the high number of rods, they are connected to the neural system in bunches, while for cones one-to-one connections are observed. Discovering this information was part of the process encouraging the author to design and conduct this research, which will be substantiated in more detail in the subsequent Sections.

At this stage, however, it can be stated that this research is basing its merit on the premise that in order to process black-white image, multiple colour detections and more complex brain signal processing must be performed to perceive “white light” being represented by the white checker, while single colour detections are possible using more direct neural connections between each colour registering rods and the neural system thus advancing and possibly simplifying signal processing by the brain.

1.4 How the Eye Sees Colours

To fully understand the colour vision one has to include the eyes' processing stage. The colour sensitive cones residing in the retina react to different wavelengths of lights due to their pigmentation. When such cells are exposed to light containing certain wavelengths so called activations take place and signals start to occur in the neural network of the retina. These signals converge onto cells where they are summed in a spectrally opponent manner. As a result, the recipient cell is excited when the eye is stimulated by certain wavelength of light while being inhibited by stimulation of other wavelengths. These interactions that produce spectrally opponent responses originate within the retina's neural network (Dacey, 1999). The idea of spectrally opponent retina response was derived from accurate observations about colour appearance. Hering (Jacobs, 2014) noticed that certain colours such as blueish-greens or reddish-yellows are commonly discerned; others like reddish-greens or blueish-yellows are never seen. This led him to believe that the visual system is based on the operation of three paired, opponent-signed mechanisms, each of them supporting mutually exclusive sensations such as white-black, red-green and yellow-blue (Hering, 1878; Hering, 1964). Among the light sensitive cells there are three types of cones and they can be referred to as S, M and L indicating their maximum light absorption in short, middle and long wavelengths respectively (Figure 1-4). Each cone responds to light stimulation. These receptors generate output signals which are sent to two classes of spectrally-opponent cells where they are merged in a push-pull manner (L-M and S-[M+L]), while in other cells the M and L cone signals are combined additively. These cells are called spectrally non-opponent (Jacobs, 2014).

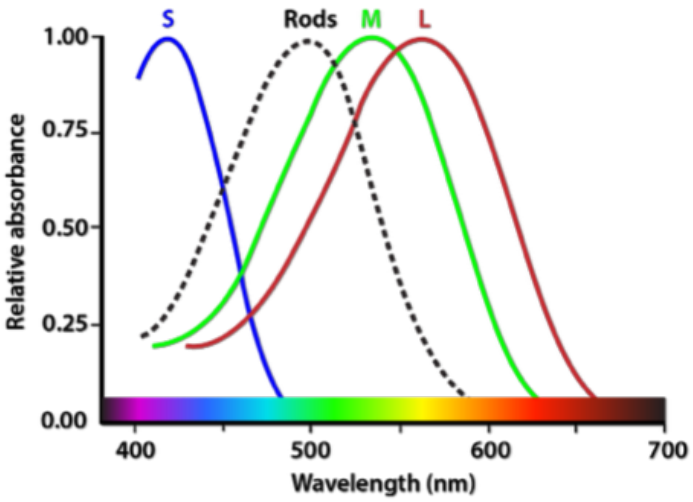

Figure 1-4 Light wavelength vs. retina

Normalised absorption curves for the three classes of cone photo-pigments of the human retina (S, M and L are abbreviations, indicating that the resident pigment has maximum sensitivity to short, middle and long wavelengths, respectively (Jacobs, 2014).

1.5 How the Brain Processes Color Vision

In order to successfully apply visual colour flickers in SSVEP based BCI system it is vital to understand how the brain processes visual colour information. It is well understood that the eye and its retina are just one side of the equation. The brain, with its still not fully uncovered processes, constitutes the other side of the equation, equally important and thus necessary to understand.

Zeki and Marini (1998) in their paper titled "Three cortical stages of colour processing in the human brain" attempted to describe the complexity of processes that occur in the brain while it is exposed to visual elements that contain colour information. They used a technique called functional magnetic resonance imaging (fMRI) that measures brain activity based on detecting changes associated with blood flow (Rinck, 2016). This technique is non-invasive, has high spatial resolution of approximately 1 mm (Nicolas-Alonso and Gomez-Gil, 2012) and enables the viewing of increased brain activity in three-dimensional space through analysing cerebral blood flow which is coupled with neuronal activations (deCharms et al. 2004). As shown in Figure 1-5 the visual cortex in the brain, which is located in the occipital lobe, consists of multiple functional areas called V1, V2, V3, V4 and V5 (Orban, 2008; Astafiev et al., 2004; Schmidt and Thews, 1983). According to Zeki and Marini (1998), there are three stages of colour processing that take place in the brain. The first stage is mainly associated with registering light presence, its intensity and distinguishing different wavelengths of the light that are believed to occur in the V1 and V2 areas. The second stage, based in the V4 area, is related to automatic colour constancy operations, which omits memory, judgment and learning processes. The third stage takes place in the temporal and frontal cortex and is related to object colours.

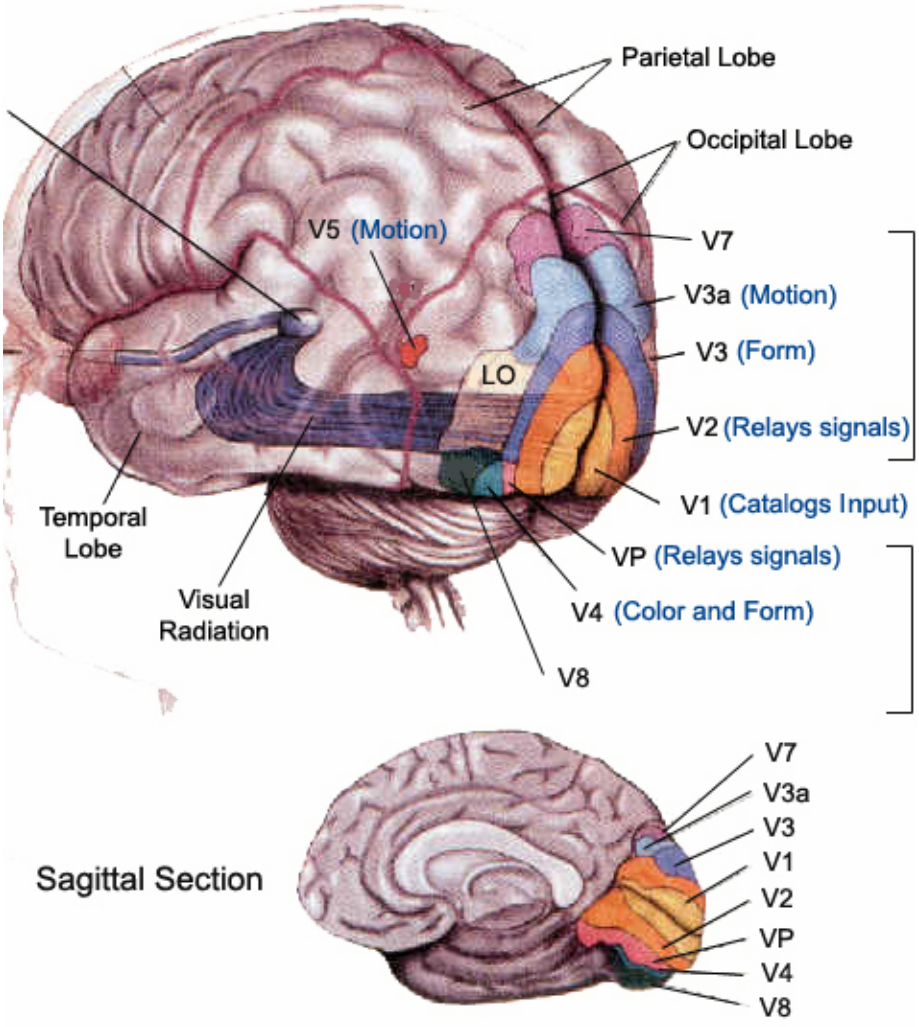

Figure 1-5 Visual cortices with multiple functional areas (Association Visual Cortex, no date)

In a web article titled 'What is color?' (Douma, 2008) colour constancy is explained as the main factor that allows us distinguish known object colours despite ever changing light conditions. Thanks to colour constancy we perceive a banana as being always yellow and thus are always able to recognise it as a known object. According to this article, a colour is a property that our minds create.

A very interesting conclusion regarding colour recognition is drawn in a Harvard University Gazette article titled 'Brain's Color Processor is Located'. A group of medical researchers at Harvard Medical School scanned subjects' brains when they were looking at various colour elements using the same fMRI technique. During the experiments people looked at rotating wheels of different colours and of black and white while their brains were fMRI scanned. Patrick Cavanagh, a psychology professor quoted in this article claims that 'Color information does not flow as a single stream from the eyes to the brain's visual area; rather, it takes parallel paths to other regions that process motion, shape, and texture' (The Harvard University Gazette, 1998).

Inês Bramão et al. (2011) in their paper 'Cortical Brain Regions Associated with Color Processing: An fMRI Study' suggest that colour information improves object recognition and activates a specific neural network associated with visual semantic information that is more extensive than for black and white objects. They, however, differentiate colour's impact in relation to recognition of familiar objects (both natural and artefacts) and non-objects (i.e. random geometric shape) claiming that in the latter colour information does not activate any brain region involved in the recognition process itself.

Muller et al. (2006) used the Steady State Visual Evoked Potential (SSVEP) method to investigate feature-specific attention to colour cues. In their experiments subjects looked at a computer screen displaying spatially intermingled red and blue dots that continually shifted their positions. The red and blue dots flickered at different frequencies thus eliciting distinctive SSVEP signals. Paying attention to one of the dot populations (red or blue) produced enhanced amplitude in SSVEP signals. According to Muller et al. (2006) this selection was based on colour rather than frequency.

Another interesting discussion of the human colour vision is published by Gerald H. Jacobs in his paper 'The Discovery of Spectral Opponency in Visual Systems and its Impact on Understanding the Neurobiology of Color Vision' (Jacobs, 2014). Here Jacobs discusses two opposing colour vision theories that were prominent in the 19th century. The first one promoted by the Young-Helmholtz proposes that the visual system contains three component mechanisms where its individual activations are directly linked to the perception of three principal hues: red, green and blue. The opposing theory proclaimed by Hering (Jacobs, 2014) assumed that there must be three underlying mechanisms in colour processing, each comprising a linked opponency that support contrasting and mutually exclusive colour precepts. Despite skepticism often expressed toward the latter one by many scientists of that time, the most recent discoveries confirmed it to be true supporting the idea that these two theories are applicable to different stages of colour processing. New tools such as single-unit electrophysiology allowed direct examination of links between the eye's spectral stimulation and the visual system's individual cells responses. Due to the research approach it has been revealed that in colour vision there are certain cells that respond in a spectrally opponent way, firing to certain wavelengths of stimulation and inhibiting to others.

1.6 Additive Colour Science

In order to perform informed and valid experiments using colour flickers it is vital to understand the science that determines the way human eyes perceive colours. There are two colour sciences, each being relevant in their own realm. One, called subtractive colour science, deals with physical objects, printed matter, paints, dyes and pigments. The other, called additive colour science, is dealing with light emitting objects such as computer monitors, TV screens, tablets and smartphone screens as well as other light sources such as flashlights, light bulbs and LED lights.

In additive colour science, different colours are produced through adding various wavelengths. A simple experiment carried out by the author using three colour light torches illustrates this phenomenon. Through setting each torch to a different colour i.e. red, green and blue respectively and arranging the light beams as shown in Figure 1-6 (a), it can be observed that three additional colours are generated; yellow, cyan, and magenta.

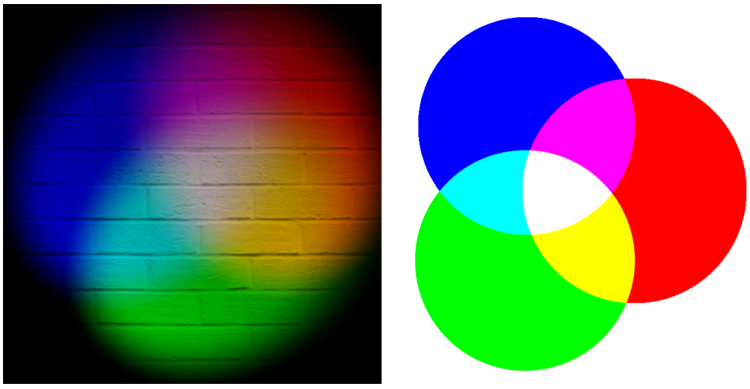

(a) (b)

Figure 1-6 RGB additive colour science

Experiment showing three RGB light torches shining light on a white or neutral grey wall (a) and RGB colours mixed in Adobe Photoshop (b). The following colours can be observed in both (a) and (b) examples: red, green, blue, yellow, cyan, and magenta. Additionally, white light can be seen in the middle (a). In Photoshop the middle of the graphic is occupied by solid white colour.

For this experiment to work a dark room with a neutral colour wall such as white or grey is required for increased effect. By intermixing red with green light beams the resulting colour will be yellow. Mixed red and blue will result in magenta and mixed blue and green produces cyan. In the middle of the arrangement white light can be observed as a result of the summation of all three RGB colours. Scientifically, this demonstrates that adding different colours (wavelengths of visible spectrum) generates new ones and by adding all elements of the visible light spectrum white light is generated, hence the additive colour science. The two experiments, the first (Figure 1-6a) performed using physical objects emitting light in a real life situation and the second (Figure 1-6b) performed in a digital domain confirm the same phenomenon determining how RGB colour science works.

This RGB colour science constitutes the foundation of technology utilised in all digital screens and other colour light emitting objects used today as shown in Figure 1-7.

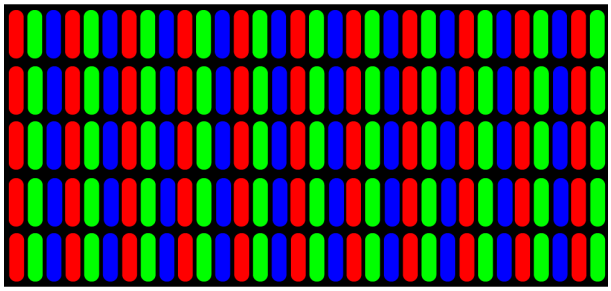

Figure 1-7 Digital screen close-up

All digital screens utilise the RGB colour science to reproduce millions of colours. The higher the bit depth of each RGB colour the higher the number of resulting colours that can be shown through mixing intensity of each colour.

As shown in the Figure 1-7, the extreme close-up of a digital screen unveils three types of pixels, each representing one colour only; red, green, and blue. If only red pixels are lit, the screen will display red colour. The same can be attributed to the remaining green and blue pixels showing green and blue colours respectively. If all RGB pixels are lit with equal light intensity the screen will represent white light. Previously mentioned yellow, cyan, and magenta colours will be displayed by engaging two appropriate colour pixels as explained earlier in this Section. Each RGB pixel can be lit with a certain light intensity. By changing light intensities of the entire screen pixels arrangement millions and even milliards of colours can be shown, depending on the bit depth capability of the screen. A typical 8-bit screen can represent over 16 million of colours and retains the ability to generate the measured level of brightness of approximately 400 nits. Recently introduced 10-bit screen technology generates the brightness level at 1000 nits or more and can display over one milliard of colours. A nit is a measurement of how much light a given source of light sends to the environment within a given area, i.e. a nit is the amount of light output equal to 1 candela per square meter. For more details please see Table 1-1.

Table 1-1 Digital screens bit-depth capabilities

	Light Intensity Levels			
Screen colour bit depth	Red colour pixels	Green colour pixels	Blue colour pixels	All colours which can be displayed
8-bit	256	256	256	16,777,216
10-bit	1,024	1,024	1,024	1,073,741,824

Having previously acquired an academic degree closely related to colour science, digital image manipulation, computer animation, and further gaining the understanding how the human eye is built and eventually how humans perceive colours, the author decided to utilise this knowledge and previous experience to design and execute research described in this thesis. The main inspiration came exactly from the fact that the close relationship between how the digital screens are built and how this technology is correlated to the human eye has been noticed. The author anticipated that utilising the most basic red, green, blue, yellow, cyan, and magenta colours from the RGB colour palette will result in new discoveries in terms of eye/brain reaction to said colours through visual stimulation due to more direct neural connections between the colour detecting photocells and the brain. This anticipation can be further substantiated by the known fact that the retina photocells (cones) responsible for colour detection provide much quicker response compared to the cells (rods) responding only to changes in brightness, i.e. black-white graphics as explained in Section 1.3. Also, it must be mentioned that only a small portion of the SSVEP-related research incorporates stimulation through colour, consequently motivating the author to design and test new flickers using easily reproducible primary and secondary colours. It is expected that these colours incorporated in the stimuli flickers will provide new knowledge, leading to improvements in eliciting brain signals for SSVEP-base BCI systems. In this research, additive colour science is applied and specifically red, green and blue referred to as primary colours as well as yellow, cyan and magenta referred to as secondary colours are used. By using RGB colours and intermixing them in a fully controlled manner (with reported coordinates for all colour channels i.e. red = 255, 0, 0) it is possible to conveniently repeat these experiments (Table 1-2). Also white, grey 50%, and black checkers as well as flicker backgrounds are utilised in the research, where white must be treated as white light, black as no light, and grey 50% as the medium state between the two.

Table 1-2 Colours used in research

Colour	RGB coordinates	Colour example
red (primary)	255, 0, 0	
green (primary)	0, 255, 0	
blue (primary)	0, 0, 255	
yellow (secondary)	255, 255, 0	
cyan (secondary)	0, 255, 255	
magenta (secondary)	255, 0, 255	
white (white light)	255, 255, 255	
grey (50%) (white+black)	127, 127, 127	
black (no light)	0, 0, 0	

The RGB colour coordinates indicated in Table 1-2 can be used to reproduce them in any graphic generating and manipulating software. There are three numbers/coordinates producing any given colour. Each number represents one primary colour channel value; i.e. the first number represents value for color red, the second for colour green, and the third for colour blue. All the primary colours have the maximum value of “255” only for their respective RGB channel. In order to produce secondary colours, two respective primary colour channels must be at their maximum values of “255”. The white colour, representing white light, must have all three RGB channels set at their maximum values of “255”, while the black colour, representing complete lack of light, must have the channels set at the minimum value of “0”. The medium grey also referred to as “grey 50%” is set at the medium value of “127” for all three RGB colour channels. The author intentionally used these colours in the research to provide common platform for other researchers willing to participate, making it possible to repeat experiments and report their results for comparison.

1.7 Limitations of Digital Screens

Despite growing interest in using digital screens for stimuli presentation there are certain limitations inherited from the technology used in these devices. It is obvious that computer/tablet monitors are more convenient since they offer more opportunities for detailed graphics and feedback presentation as well as target alignment (Yijun et al., 2008). Nakamishi et al. (2013) list all the advantages of using a computer screen for the flicker presentation. All the stimulation parameters such as the amount, colour, pattern, size and position can be flexibly configured (Nakamishi et al., 2013). However, the number of targets is limited by the common 60 Hz refresh rate of most screens available today.

In the Alpha range of 8 Hz -12 Hz where the SSVEP is most effective the number of available flickers is very limited (Nakamishi et al., 2014). For instance, for an effective checkerboard flicker an equal amount of black and white frames per period need to be displayed within the 60 Hz refresh rate of the screen. That leaves us with a very limited number of frequencies that can be successfully displayed. For example, 6 Hz (60 Hz/6 Hz gives 10 frames per period, 5 for black and 5 for white fields), 7.5 Hz (8 frames per period), 10 Hz (6 frames per period) and 15 Hz (4 frames per period) (Nakamishi et al., 2013).

Most of the frequencies in Alpha range such as 8 Hz, 9 Hz, 11 Hz, 12 Hz, 13 Hz, 14 Hz when displayed on 60 Hz-based screens will produce a stuttering effect in the graphics presentation disrupting the effectiveness of SSVEP. For more details on brainwaves bands please refer to Table 2-2 in Section 2.4.

There are attempts to overcome this problem by implementing a technique called frequency approximation about which the author learned from the reported work. To illustrate this more clearly a diagram representing standard (constant period) and approximated (variable period) flickering graphic is shown in Figure 1-8 and Figure 1-9.

Figure 1-8 10 Hz flicker displayed by 60 Hz screen

The diagram shows 10 Hz flicker displayed by 60 Hz screen. Two states of the flickering graphics are represented by black and white squares.

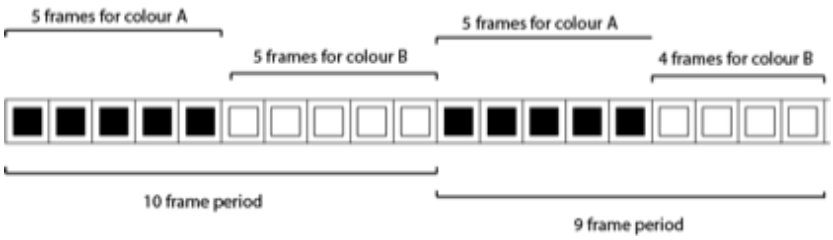

Figure 1-9 6.3 Hz flicker displayed by 60 Hz screen

The diagram shows proposition for 6.3 Hz flicker, which can be achieved by alternating 9 and 10 frame periods. Two states of the flickering graphics are represented by black and white squares.

Wang et al. (2010) proposed a method in which flickering graphics are created by approximation and variable number of frames are utilised to display frequencies that otherwise could not be shown by a 60 Hz screen. In their example they suggested that an 11 Hz flicker can be approximated by mixing 10 Hz and 12 Hz frequencies, where 5 and 6 frames periods can be interleaved as '11100011100111000011100' (Wang et al., 2010). Figure 1-9 above shows a graphic representation of this method used to create 6.3 Hz flicker. The flickers using equal amount of colour A and colour B frames can be referred to as constant period graphics. The approximated period flickers can be referred to as variable period graphics. Using this method, the following frequencies can be approximated and used for stimuli graphics in 60 Hz based screens as explained in Table 1-3.

Table 1-3 Additional Alpha range frequencies through period approximation method

Frequency	Calculation for 60 Hz screen	Remarks
6.3 Hz	60 Hz / 6.3 Hz = 9.52	Approximated period of 9.52, where 1st period has 10 frames (5 colour A and 5 colour B) and 2nd period has 9 frames (5 colour A and 4 colour B).
7.05 Hz	60 Hz / 7.05 Hz = 8.51	Approximated period of 8.51, where 1st period has 8 frames and 2nd period has 9 frames.
8 Hz	60 Hz / 8 Hz = 7.5	Approximated period of 7.5, where 1st period has 8 frames and 2nd period has 7 frames.
9.2 Hz	60 Hz / 9.2 Hz = 6.52	Approximated period of 6.52, where 1st period has 6 frames and 2nd period has 7 frames.
11 Hz	60 Hz / 11 Hz = 5.45	Approximated period of 5.45, where 1st period has 6 frames (3 colour A and 3 colour B) and 2nd period has 5 frames (3 colour A and 2 colour B).
13.3 Hz	60 Hz / 13.3 Hz = 4.51	Approximated period of 4.51, where 1st period has 4 frames and 2nd period has 5 frames.

As suggested by Wang et al. (2010), through combining constant period and variable period flickering graphic, a multi-command BCI system using more frequencies within the Alpha range should be possible. Although the author tried and tested this method, the results were not satisfactory enough to include the method in this research as reported in (Szalowski and Picovici, 2015).

1.8 Colour Response in SSVEP Paradigm

Despite considerable growth of the BCI related publications in recent years, it is important to note that the amount of research focusing on colour response in the SSVEP paradigm as first introduced in Section 1.1 and later detailed in Section 2.6.1.1, is still very limited, lacking in consistency and attempts are very isolated. None of the methods reviewed below offers a comprehensive approach of investigating all possible multicolour combinations of primary and secondary colours.

This Section reviews these investigations and highlights their strengths as well as their limitations. It is worth highlighting that not all of the work discussed herein is within the interest scope of this research, however, certain interpretations and improvements are discussed. Understandably, BCI researchers have begun to recognise that stimulus presentation using colours offers many opportunities. In relation to stimulation methods and the quality of achieved brain signals, colour of the stimulus graphic is increasingly ranked as relevant parameter, which needs to be analysed in detail (Cheng et al. 2001).

One significant detail is the ability to fully exhaust the potential of modern colour displays existent in portable and stationary electronic devices such as smart TVs, laptops, smartphones, tablets, etc. The ever increasing colour depth with its importance illustrated in Figure 1-10 (support for 10-bit colour range in recent iMac desktops) as well as screen resolution being coupled with faster and better performing graphics processing units (GPU) all play a major role for the future development of SSVEP technique and its applications. Today, display driven devices effortlessly stream and process sophisticated animations and video games. The SSVEP-based BCI systems primarily rely on the graphic stimulation quality.

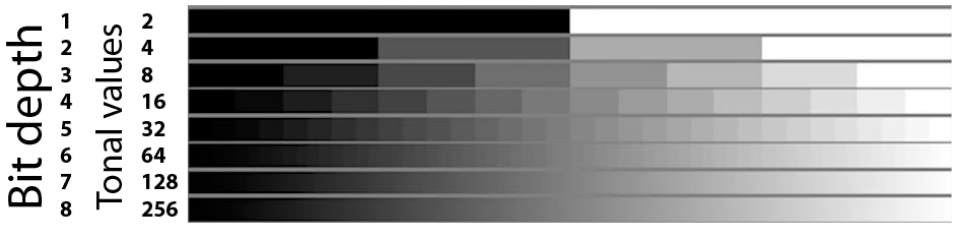

Figure 1-10 Bit depths of digital screens

The figure illustrates tonal ranges associated with bit-depths. Typical computer screens are 8-bit, while the most recent propositions are capable of displaying 10-bit tonal range.

As indicated by Bakardjian et al. (2010), visual graphic employed in BCI systems using SSVEP need the same degree of optimisation as the analysis algorithms in order to maximise the BCI's responsiveness. The author fully agrees with this statement, which in fact was one of the convincing

factors for conducting this research. Further, it is believed that since the graphic's quality influences stability of the SSVEP technique, therefore utilising colourful and visually attractive flickers, instead of traditional black-white stimulators, it will not only improve the user experience but if properly tested and designed should also benefit the performance of the future BCI systems. This advantage of boosting performance is at the core of this research and the results are presented later in Chapter 6, Chapter 4 and Chapter 5. Certain colours are reported to perform better than others. Also, certain colour combinations between the primary Red-Green-Blue (RGB) colours and secondary ones (Yellow, Cyan, Magenta) are giving mixed results, suggesting that certain colour pairs provide different signal characteristics.

Gerloff and Schilling (2012) after testing seven colour combinations and various stimulating frequencies ranging between 6 Hz and 17 Hz state that optimal stimulation combination of colour and frequency varies significantly between the subjects. They suggest that individually optimised adjustment of the stimulus is recommended and denote that for many tested subjects different colours induced better brain signal responses than the black-white combination, questioning its reputation as the best performing stimulus. Gerloff and Schilling confirmed what could be suspected that subjects with red/green blindness reveal lower signal-to-noise ratio for all colour combinations. In their tests, they also suggest the frequency range of 9 Hz to 17 Hz to be the most optimal for colour stimulation (Gerloff and Schilling, 2012).

As reported below, another interesting aspect that should be considered for designing stimuli graphics is the flicker's level of blurriness. Mouli et al. (2013) suggest that most users tested were more comfortable with frosted LED stimuli reporting less fatigue in comparison to clear glass. In their tests, they used visual stimulator in red, green and blue colours based on readily available RGB LEDs with clear and frosted glass in front of them. The lights flickered at 7 Hz, 8 Hz, 9 Hz and 10 Hz. Through measuring EEG signals Mouli et al. investigated performance and qualitative user comfort based on four subjects. In their finding they reported that clear glass with green colour provided the highest SSVEP performance for all four subjects, while the frosted glass was more comfortable for the users. One user did not show notable improvement in glass type.

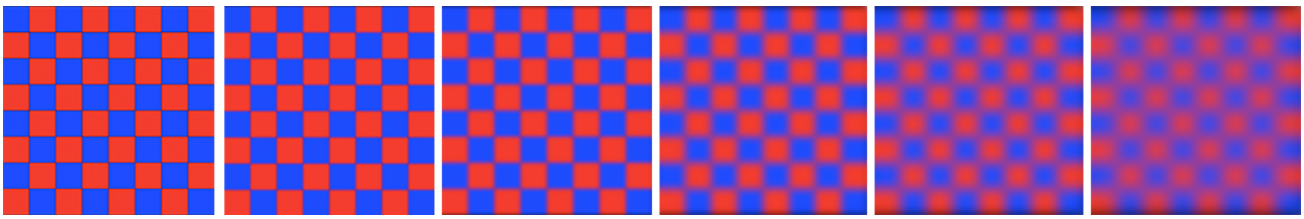

Figure 1-11 Frosted glass effect simulated by Gaussian Blur filter

The diagram shows proposition for RED-BLUE stimuli flicker with applied Gaussian blur filter with increasing intensity to simulate frosted glass effect.

Figure 1-11 shows RED-BLUE stimulus graphic proposition in various states of blurriness starting from a perfectly sharp image. In contrast to above-mentioned hardware testing environment, the author generated this effect using Gaussian Blur filter in Photoshop. This computer-generated graphic imitates the frosted glass effect described earlier. This effect can be applied to motion graphics using a similar procedure. The advantage of this proposed method over the hardware solution provides the ability to test various states of pattern blurriness in order to find the best settings guaranteeing maximum signal peaks with improved user's comfort. It must be stated that this element is beyond the scope of this research.

Cheng et al. (2001) adopted a new stimulation pattern in which the subjects were exposed to two frequencies simultaneously. The resulting SSVEP signals contained both frequencies and their coupling components. In their proposed stimulator they used two colours in one flickering graphic, red and green, each flickering at different frequencies. When both colours red and green were active, the third colour yellow was produced as shown in Figure 1-12.

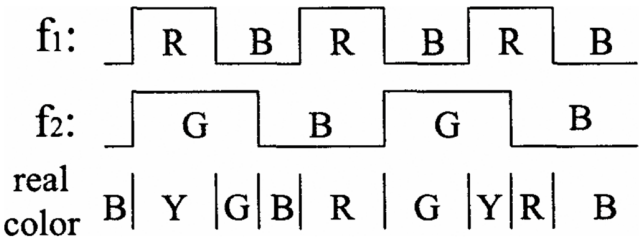

Figure 1-12 Effect of mixing two colours

Three different frequencies produced by R (red) and G (green) flickering graphics. B (black) represents the off state of each colour. Y represents colour yellow produced by mixed green and red. Cheng et al. (2001).

This is in accordance with additive colour science, as discussed in Section 1.6. The report presents an interesting approach where multiple SSVEP signals can be detected using only one multicolour flickering graphic. These authors claim to have found quadratic phase coupling of the stimulus frequencies by using Fast Fourier Transform (FFT) and bispectrum analysis tools (Cheng et al. 2001).

Singla et al. (2014) tested performance of colour induced SSVEP signals in controlling a wheelchair (Figure 1-13). The stimuli graphics were displayed using Liquid Crystal Display (LCD) monitor and LabVIEW System Design Software. Four colours were tested, green, red, blue and violet and the latter was found to produce the strongest response among all colours. Four frequencies 7 Hz, 9 Hz, 11 Hz and 13 Hz were used to control the wheelchair movement in four directions: forward, backward, left and right, and the state of relaxation was used to stop the movement.

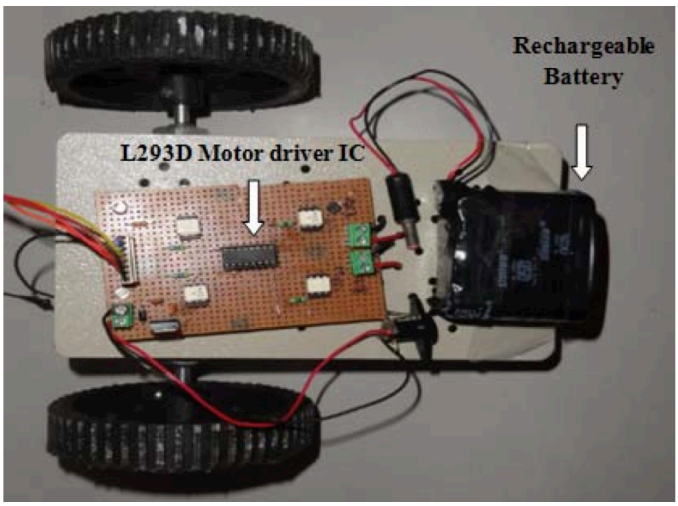

Figure 1-13 The wheelchair prototype for SSVEP controlled BCI (Singla et al., 2014)

This wheelchair prototype was used in Singla et al. experiment utilising colour stimuli to control the device.

Another approach to evaluate colour's influence on the EEG signals using SSVEP paradigm was presented by Teng et al. (2012). They looked at frequency, phase response as well as overall performance of tested white, grey, red, green and blue colour stimuli displayed on a black background. The paper reports that white stimulus has the strongest response in SSVEP signals followed by grey, red, green and blue stimuli. Due to the fact that the authors used 120 Hz screen refresh rate monitor for flicker presentation, they could test more frequencies including 17.14 Hz, 15 Hz, 13.33 Hz, 12 Hz, 10.09 Hz, 10 Hz, 9.23 Hz, 8.57 Hz, 8 Hz and 7.5 Hz. In terms of phase response, white flicker obtained the lowest phase variance followed by grey with both significantly outperforming other tested colours. In green they found that phase variances were more dependent on frequencies compared to other colours. Blue is reported to have the highest phase variance thus negatively affecting SSVEP accuracy.

Tello et al. (2014) in their paper 'Evaluation of different stimuli color for an SSVEP-based BCI' look at SSVEP stimulation induced by colour LEDs in red, green, blue and yellow. Utilising LED panels (Figure 1-14) doesn't restrict the use of any frequencies.

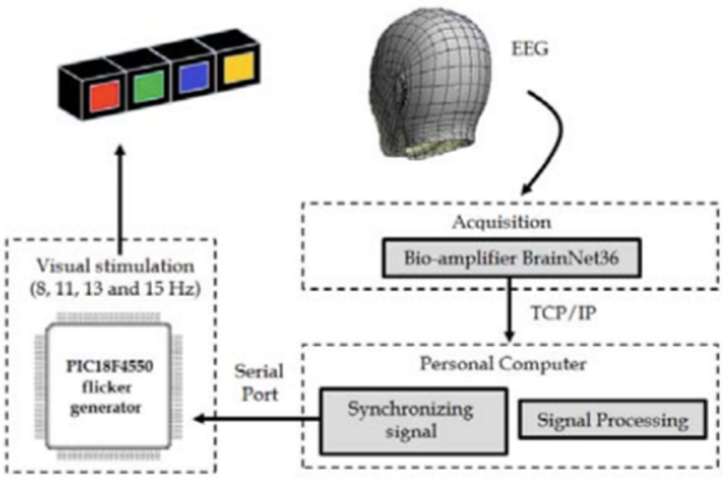

Figure 1-14 Stimulating brain oscillations using LED panel

This block diagram represents the stimulation setup discussed by Tello et al. (2014).

In this experiment 8 Hz, 11 Hz, 13 Hz and 15 Hz were used and specifically Information Transfer Rate (ITR) index and level of user comfort were sought after. They claim that red colour obtained the highest ITR while being reported by the users as uncomfortable. Further, green is claimed to be the most reliable and comfortable at the same time, followed by yellow and blue colour. The paper also denotes that for all colours lower frequencies such as 8 Hz and 11 Hz performed better compared to medium frequencies of 13 Hz and 15 Hz. Additionally, the authors formulate a warning that using red colour, especially in combination with other colours could induce seizures. Figure 1-15 shows the enclosure that was used to house the coloured LED lights to enhance the colour projection during experiment.

Figure 1-15 Stimulating brain oscillations using LED panel

LED housing designed to enhance the intensity of colours (Tello et al., 2014).

Aminaka et al. (2014) investigated SSVEP response by comparing traditional monochromatic LED panel with green-blue panel utilising 7 Hz as well as higher frequencies of 18 Hz, 25 Hz and 39 Hz. Each LED in the panel flickered at different frequency. A microcontroller development board Arduino UNO generated the flickering. The signals were analysed in off-line scenario using OpenVIBE software. The paper concludes that the chromatic (green-blue) stimulators were

successfully implemented in the four command BCI system and are described as performing equally well, and in certain frequencies even better, than the traditional monochromatic (black and white) stimulators. Also, most of the subjects stated they preferred the green-blue stimulator to the monochromatic stimulator due to the increased fatigue experienced with the latter. It is clear that the aspect of colour stimulation is gaining attention in the BCI research community. Employing colour to visual stimulation presents numerous opportunities and possible advantages. Although the majority of the colour related research is focused on panels using physical LED lights and flashlights there are more and more researchers interested in CRT monitors, LCD, LED-backlit and the most recent OLED screens. The most recent technology advances introducing High Dynamic Range technology (HDR) to digital displays and monitor screens are the most promising thanks to significantly increased brightness and contrast ratio.

1.9 Conclusions

The reviewed papers on the colour applications for visually driven BCIs reveal several key findings the author would like to share.

Firstly, the amount of available work in this research area is miniscule in comparison to other elements of the BCI system, such as the signal processing, feature extraction, classification, and even graphic user interface development.

Secondly, the available work lacks in research methods comparability and thus the results are isolated. Many experiments are based on colour descriptions, which are not possible to reproduce (i.e. violet or orange).

Thirdly, the use of colour in most cases demonstrates only practicality of such application just to provide evidence that the colour indeed induces brain signals and can be used in a successful and working BCI. Apparent is the lack of an extended analysis of the brain signals elicited by the colour visual stimuli.

This thesis is attempting to fill the identified gap by providing research methods, tools, and finally experiment results in hope that other researchers, potentially inspired by the novelty of this research, will join and continue the work.

1.10 Organisation of Thesis

Following this general introduction, Chapter 2 introduces a detailed review of all the characteristics describing the structure of a BCI system, its functions, techniques used to operate it, categorisation, feature extraction methods and various artefacts hindering its operation. Chapter 3 describes the research method used including the hardware and software used for the brain signal recording sessions and analysis, as well as the process of flicker design and the testing environment. Chapter 4 concentrates on the aspect of user training for SSVEP-based BCI systems. It presents the test results relating to the very often-neglected importance of the user training element in BCI systems utilising visual stimulation. In Chapter 5 stimuli graphics patterns are analysed and their relationship to elicited brain signals is examined. Chapter 6 investigates multiple parameters of the stimuli graphics such as the graphic's size and resolution as well as the colours' performance in eliciting brain signals. Finally, the conclusions, research contribution, and proposed future work and research directions are presented in the Section 7. The digital version of this thesis is the part of Appendix 1.

Chapter 2 Brain-Computer Interface Overview

2.1 Introduction

A Brain-Computer Interface (BCI) is a system comprised of hardware and software enabling communication between brain and external world using cerebral activity only. In other words, the BCI system permits humans to interact with the environment without the participation of peripheral nerves and muscles using only control signals originated in the brain. The most obvious medical BCI applications are providing communication facilities to severely disabled people with 'locked in' syndrome or spinal cord injury. Among the non-medical applications are gaming, assisted living, environmental control, smart homes, entertainment, education, and neuromarketing studies (Nicolas-Alonso and Gomez-Gil, 2012). In a typical BCI system (Figure 2-1), there are five distinctive stages, which are executed in succession: signal acquisition, pre-processing or otherwise referred to as signal enhancement, feature extraction, classification, and the control interface (Khalid et al., 2009).

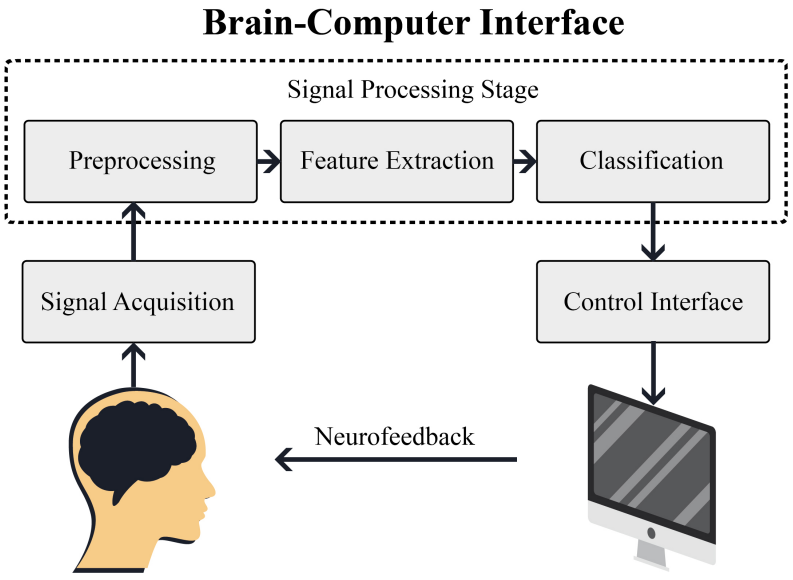

Figure 2-1 Brain-Computer Interface diagram

The diagram shows the five elements found in a typical BCI system.

During signal acquisition stage raw brain signals are captured or recorded by a dedicated hardware. Sometimes at this stage a very basic noise and artifact removal is performed. The preprocessing stage often involves more elaborate signal filtering with high-pass and low-pass filters. It could also include specific channel selection for further processing. The feature extraction stage is a very important and challenging task for a successful operation, as it identifies discriminative information in the captured brain signals and extracts them from different brain activities that overlap both in time and space. Furthermore, such brain signals are polluted with artefacts originating from the

body such as muscle or eye movement, from the environment e.g. electromagnetic field from electrical devices present, or the system itself e.g. electrodes. The classification stage as the name implies, classifies the pre-processed signals looking for feature vectors. In order to obtain effective pattern recognition, choosing the most useable discriminative features is critical. The last stage is the control interface, which in essence assigns the previously classified signals into commands that can be used to control an external device i.e. robot, drone or computer.

Although, initially BCI systems were considered too difficult and expensive to develop, the most recent technological advances have resulted in widespread availability of low-cost brain signal capturing devices and the latest signal processing software development paired with ever increasing computing power increase triggered exponential growth of BCI related research groups, conferences and publications worldwide (Wolpaw, 2007; Konrad and Shanks, 2010). Despite these advances, the majority of the BCI systems still remain in the domain of laboratories within educational and commercial research and development departments. This situation will change and applicability of BCIs will be greater when the ease of use increases by reducing set-up time, calibration and excessive training requirement (Blankertz et al., 2010).

2.2 Neuroimaging Techniques used in BCI systems

The word ‘neuroimaging’ is to be understood as the process of producing images of the brain or other parts of the nervous system structure or activity using various techniques such as magnetic resonance imaging or computerised tomography. Since all BCIs rely on the initial stage of signal acquisition in order to translate the user’s intent into useable commands two types of brain activities can be used: electrophysiological and hemodynamic. Electrophysiological activity can be associated with electro-chemical neuron activity, which serves as an information exchange facility. Ionic currents are generated by neurons, which allow the currents to flow within the neuron cells themselves (primary currents) and through the network (secondary currents). These current streams usually can be observed as a dipole pattern conducting the currents from a source to a sink (Baillet et al., 2001).

Figure 2-2 presents the brain’s response to four stimuli each flickering at different frequency (6 Hz, 7 Hz, 8 Hz, and 9 Hz) showing distinctive amplitude peaks at the elicited frequencies. Figure 2-3 shows spectra and brain maps indicating the dipole patterns occurring for all four frequencies generated in the brain.

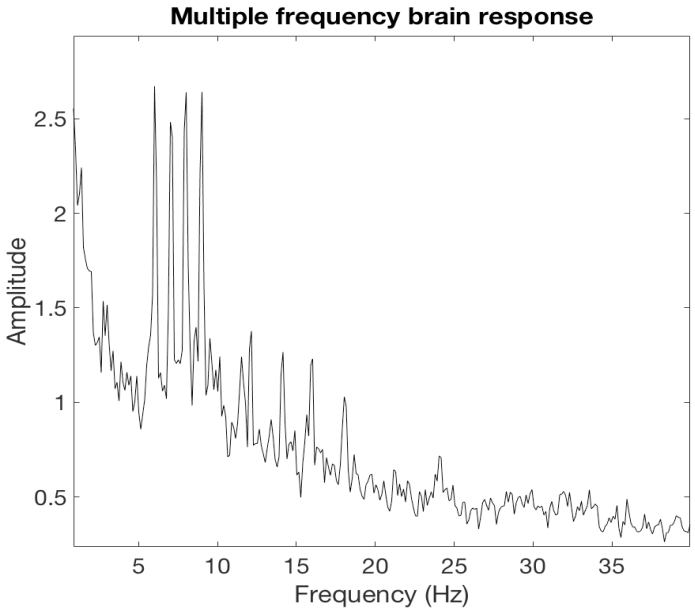

Figure 2-2 Brain's response to four stimuli flickers

The plot shows four frequencies elicited in brain using a setup comprising of four RGB LED panels. Visible in the plot are 6 Hz, 7 Hz, 8 Hz, and 9 Hz peaks accompanied by harmonics.

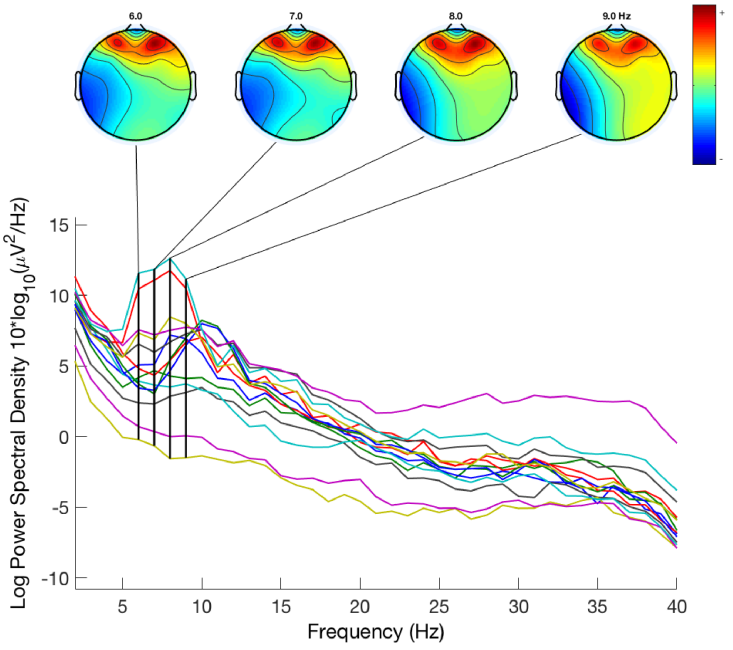

Figure 2-3 Four frequencies reflected in brain maps

The plot exemplifies frequency response of all captured channels as different traces of colours (bottom) and dipole brain activity shown as colour brain maps (top). The colours in the brain maps indicate distribution of brain signal power registered for 6 Hz, 7 Hz, 8 Hz, and 9 Hz. The colour blue reflects low activity of the frequency, while the colour red reflects high activity.

This electrophysiological brain activity can be monitored using electroencephalography, electrocorticography, and magnetoencephalography. Due to advantages presented in Section 2.3 Electroencephalography (EEG) is used in this work.

The hemodynamic brain response relies on the phenomena of blood releasing glucose faster in the active areas of the brain in comparison to the inactive neurons. The glucose and oxygen carried by blood generates a surplus of oxyhemoglobin in the activated brain area, which results in detectable localised ratio change between oxyhemoglobin and deoxyhemoglobin (Laureys et al., 2009). These brain responses can be observed using only selected neuroimaging techniques such as functional magnetic resonance or near infrared spectroscopy. In contrast to electrophysiological activity, the hemodynamic brain response is considered as indirect, because by its nature it is not directly related to neuronal activity. The majority of currently developed BCI systems rely on electrophysiological brain activities using electroencephalography (Nicolas-Alonso and Gomez-Gil, 2012). Table 2-1 presents various neuroimaging techniques used to measure and monitor brain activity.

Table 2-1 Neuroimaging techniques and their characteristics (Nicolas-Alonso and Gomez-Gil, 2012)

Neuroimaging Method	**Activity Measured**	**Direct/Indirect Measurement**	**Temporal Resolution**	**Spatial Resolution**	**Risk**	**Portability**
EEG	Electrical	Direct	~0.05 s	~10 mm	Non-Invasive	Portable
MEG	Magnetic	Direct	~0.05 s	~5 mm	Non-Invasive	Non-Portable
ECoG	Electrical	Direct	~0.003 s	~1 mm	Invasive	Portable
fMRI	Metabolic	Indirect	~1 s	~1 mm	Non-Invasive	Non-Portable
NIRS	Metabolic	Indirect	~1 s	~5 mm	Non-Invasive	Portable

The above table first lists electrophysiological modalities such as electroencephalography (EEG), magnetoencephalography (MEG), electrocorticography (ECoG), which are followed by the hemodynamic modalities including functional magnetic resonance imaging (fMRI) and near infrared spectroscopy (NIRS). Invasive methods such as ECoG involve serious health risks and therefore cannot be used for experimental purposes. They require implanting of microelectrode arrays either on the surface or inside of the cortex (Nicolas-Alonso and Gomez-Gil, 2012).

It is a well known fact that invasive methods are necessary for complex movement restoration in paralysed patients (Lebedev and Nicolelis, 2006) while non-invasive methods are better suited for reacquiring basic communication, simple neuroprosthesis and wheelchair control (Sellers et al., 2010; Muller-Putz and Pfurtscheller, 2008; Cincotti et al., 2008).

2.3 Electroencephalography

Electroencephalography (EEG) is the most popular and widely used neuroimaging technique for BCI research and development. EEG's operation is based on measuring electric brain activity induced by the flow of electric currents during excitations of the neuron dendrites (Baillet et al., 2001). Its main attributes are relatively high temporal resolution, low-cost application compared to other techniques, small size enabling system portability, and risk-free operation for the users due to non-invasive operation process. Through a set of sensors, whose number and spatial arrangement can be easily preconfigured, a typical EEG device acquires electrical signals from different brain areas (Nicolas-Alonso and Gomez-Gil, 2012). Among the main limitations of EEG performance are poor signal to noise ratio (SNR), mainly caused by the scalp, skull, background noise, and high sensitivity to the effects of secondary currents (Baillet et al., 2001). This induces very weak EEG signals in the electrodes, which are difficult to acquire and often of poor quality. Also background noise additionally hinders the EEG performance. The background noise is usually referred to as an artefacts, which can be generated both internally or externally. The artefacts are generated by the brain itself as well as other body elements through muscle or eye movement. External artefacts occur outside of the cortex over the scalp. They can be caused by electromagnetic fields present in the area (Nicolas-Alonso and Gomez-Gil, 2012). More detailed information on the artefacts and methods on how to remove them is provided in Section 2.9.

Figure 2-4 Standard EEG head-cap with passive disc electrodes and conductive agents (Unimed-electrodes.co.uk., 2019)

Traditionally cream, gel or paste must be applied to scalp or electrodes themselves to allow brain signal capture.

Current modern EEG recording system consists of multi-electrode array acquiring the signals from the scalp and feeding them into amplifiers, which process the still analogue signals to enlarge their amplitude. In order to properly carry a useable signal, each electrode is connected to one input of a differential amplifier. The other input of this amplifier is connected to the reference electrode. The operation of these amplifiers is induced by the voltage difference between the active electrode and the system reference electrode and the voltage gain they provide usually ranges between 60-100 dB. The EEG electrical signal by its nature is analogue and with today's availability of digitising devices it is normally more convenient to transcode it to digital form (Teplan, 2002). Therefore, initially the signal is passed through an anti-aliasing filter and then sent to an Analog-to-Digital (A/D) converter. This digitises the signals to make them recognisable by any digital device e.g. computer. Depending on the research objectives various techniques may be used to elicit the EEG signals such as light stimulation, eye closure and opening, and mental commands (Nicolas-Alonso and Gomez-Gil, 2012). After digitisation the EEG signal can be stored as data for further display or manipulation (Teplan, 2002). Figure 2-4 illustrates a typical EEG headset with an array of passive disk electrodes requiring an application of the conductive agents to improve contact with the scalp.

Computers can capture, store, process and display the signals, which are being recorded. The principal technique governing the EEG operation is based on measuring the potential difference that occurs over time between signals that appear at the active electrode and reference electrode. An additional electrode type, referred to as ground electrode is utilised to measure the differential voltage between the active and reference electrodes. Therefore, the most basic EEG device requires at least one active, one reference, and one ground electrode to successfully capture electric brain

activities. In order to properly display the signal a series of filters need to be applied. Those filters include a high-pass filter to remove frequencies between 0.5 Hz to 1 Hz for slow artefacts removal resulting from electro-galvanic signals or movement artefacts, a low-pass filter to remove higher frequencies usually in the range of 35 Hz to 70 Hz. In this band most of the high frequency artefacts such as electromyographic signals reside. Also, it is recommended to incorporate some form of a notch filtration for electrical power line artifact elimination in 50 Hz for Europe or 60 Hz for America (Niedermeyer and Lopes da Silva, 1993).

An EEG system can incorporate several active measuring electrodes and in more advanced devices even up to 256 active electrodes can be found (Teplan, 2002). Usually, the electrodes are made of silver chloride (AgCl) (Sinclair et al., 2007) and to accurately record brain signals, the electrode-scalp contact impedance should measure between 1-10 kΩ. In contact between the electrode and the scalp tissue there are resistance and capacitance occurring both causing low-pass filtration. The resulting impedance will depend on the area that the electrodes cover on the scalp and temperature (Usakli, 2010). To reduce the system impedance, several agents such as EEG gel or paste can be applied to the electrodes thus creating a more conductive path between the skin and electrodes. Some electrodes use felt pads, which for that same purpose can be saturated with saline water. Although very effective, to preserve a good quality signal, this technique often requires reapplication of the agents and continued maintenance.

Figure 2-5 Wireless EEG with active electrodes

An example of one of the latest developments in portable EEG devices for BCI – g.Nautilus (Neurodevice.pl., 2019).

There are also electrodes often referred to as ‘dry’ and they do not need any conductivity improving agents to be applied as shown in Figure 2-5. Usually these agents are made of different materials such as titanium or stainless steel. Among them are ‘dry’ active electrodes equipped with signal boosting circuits, which minimise high impedance between electrode and skin (Fonseca et al, 2007); (Taheri et al., 1994). There are also ‘dry’ passive electrodes, which instead of active circuits are directly linked to ultra-high input impedance EEG capturing devices (Gargiulo et al., 2010). A typical scalp signal amplitude of EEG ranges between 10µV and 100µV (Aurlien et al., 2004). Since the amplitude of the brain signals measured by an EEG device on the surface of the skin is in the range of microvolts, it is very susceptible to different sources of noise. Among the external sources of background noise are power lines and electromagnetic fields generated by other electrical devices present in the room. Other noises in the form of single shot, flicker or burst noise are often called artefacts and are associated process occurring in the body itself (Usakli, 2010).

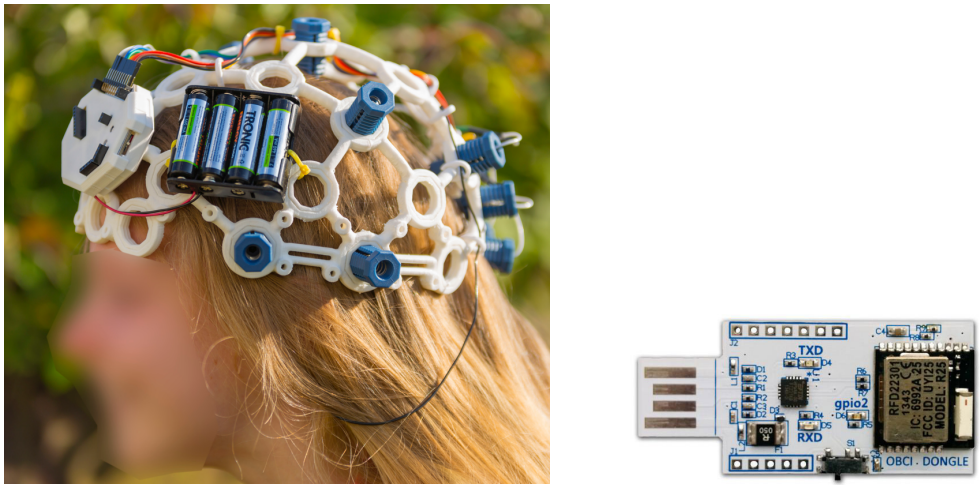

(a) (b)

Figure 2-6 OpenBCI EEG headset with 8 channels/sensors (a) with Bluetooth USB dongle (b)

The headset is equipped with 8 active sensors and connects to PC computers running Windows, Linux, and OSX systems using Bluetooth USB dongle (**Error! Reference source not found.**). The dongle conveniently enables wireless communication between the headset and computer

Figure 2-6 illustrates a low-cost EEG headset utilising eight active electrodes communicating with computers through a USB dongle.

2.4 Frequency Bands of the Brain's Electrical Activities

Brain waves are oscillations that occur naturally in the brain and can be measured by an EEG system. An EEG device with enough sampling resolution and bandwidth can capture signals as low as 0.1 Hz and as high as 100 Hz (Figure 2-7).

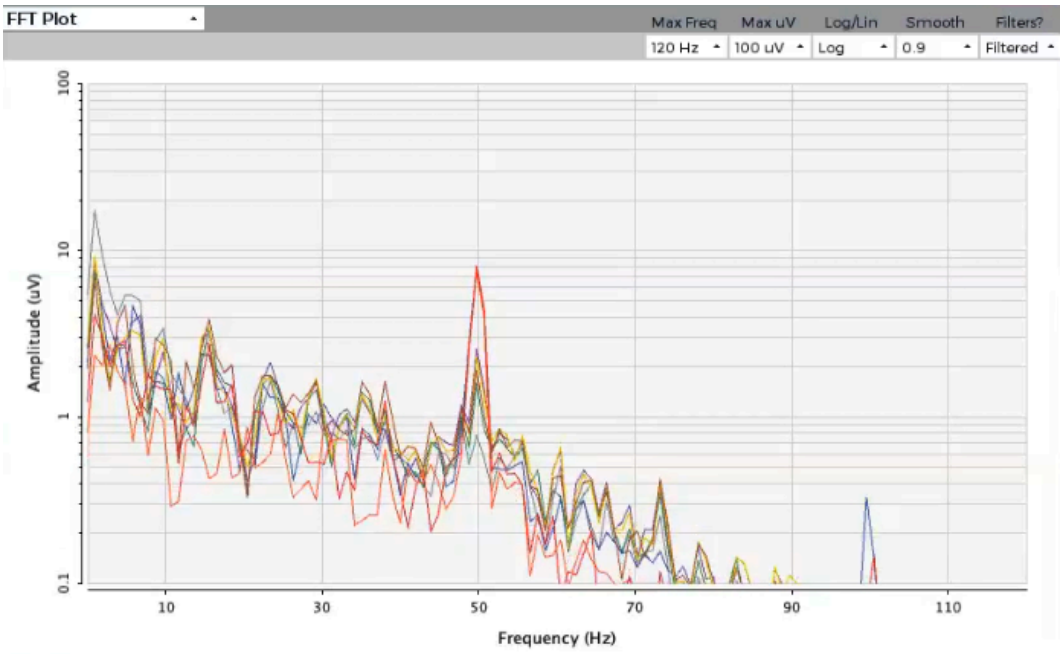

Figure 2-7 Brain signals captured by OpenBCI EEG headset (Figure 2-6)

The headset records brain signals with 250 Hz sampling frequency. By oversampling the frequency range of interest, it is possible to faithfully capture the available range within brain's electrical activity. In the captured frequency domain plot there is visible 50 Hz peak caused by electro-magnetic interference along with its 100 Hz harmonic.

The majority of the cerebral activity represents rhythmic patterns and falls in the range of 1 Hz – 20 Hz. All the lower and higher frequencies should be considered artefactual. There are also transient components that can be observed. These occur as sharp waves and spikes in the waveform and usually are associated with seizure. Vertex waves and sleep spindles seen during sleep are considered normal. There are also so called 'normal variants' which although statistically uncommon are not considered as pathology with Mu waves being one of them. Mu waves also known as Mu rhythms occur between 7 Hz and 13 Hz frequency band and can be mainly observed when body is at rest. The EEG patterns vary with age. Young children have slower oscillation than adults. States of mind and other individual characteristics also have an impact on the EEG patterns (Niedermeyer and Lopes da Silva, 1993). Using several factors such as distribution over the scalp or biological function certain frequency ranges have been defined. Commonly known frequency ranges from low to high are referred to as Delta (δ), Theta (θ), Alpha (α), Beta (β) and Gamma (ɣ).

Detailed below in the Table 2-2 are the main characteristics of these bands.

Table 2-2 EEG rhythmic activity comparison by frequency bands

Bands	Frequency	Characteristics/Location	Activity
Delta [δ]	0.5 - 4	the highest in amplitude the slowest in frequency occur frontally in adults and posteriorly in children, decreases with age and can be confused with artefacts (Nicolas-Alonso and Gomez-Gil, 2012)	most neonatal brain activity in adults represents sleep, occasionally recorded during long attention tasks (Kirmizi-Alsan et al., 2006) large amounts in awake adults is abnormal suggest neurological deceases (Nicolas-Alonso and Gomez-Gil, 2012)
Theta [θ]	4 - 7	locations not related to tasks performed	observed in young and older children, in adults relate to neurological decease (Kübler, et al. 2001) associated with drowsiness or arousal in adults and teenagers (Kübler, et al. 2001) found during relaxation, meditation and creativity (Anand et al., 1961; Aftanas and Golocheikine, 2001; Fernández et al., 1995)
Alpha [α]	8 - 12	mostly found in the occipital lobe of the brain (Pineda, 2005)	found in the state of relaxation and reflection amplitude increases with eyes closed, decreases with open eyes and mental effort (Black, 1997) associated with visual processing (Klimesch, 1997)
Beta [β]	13 - 30	low amplitude waves mostly detected at the frontal and central regions of the head (Nicolas-Alonso and Gomez-Gil, 2012)	associated with motor activities (Nicolas-Alonso and Gomez-Gil, 2012) real movement and motor imagery Beta oscillations are desynchronised symmetrically distributed with no motor activity (Kisley and Cornwell, 2006)
Gamma [ɣ]	30 - 100	somatosensory cortex	during activity requiring combination of two different senses (i.e. smell and taste) (Kisley and Cornwell, 2006; Kanayama et al., 2007) related to certain motor functions or perceptions (Lee et al., 2003) observed in maximal muscle contraction (Brown et al., 1998) and replaced by Beta rhythms during weaker contractions (Mima et al., 1999) less common in BCI applications, prone to eye movement artefacts and muscle contractions (Zhang et al., 2010)
Mu Rhythms	7 - 13	sensorimotor cortex band overlaps with other frequencies	related to motor activities may correlate with Beta rhythms (Pineda, 2005; Pfurtscheller et al., 2006)

2.5 International 10-20 System

The 10-20 system has been developed and standardised by the American Electroencephalographic Society to unify the electrode placement for easy comparison and reproducibility of conducted EEG measurements as detailed in Figure 2-8 Electrode placement according to International 10-20 System. Two reference points in the head are used to define the electrode location. One of these points is called the nasion and it is located at the nose's top at the eyes' level. Inion is the other point and it can be found as the bony lump at the skull's base (Nicolas-Alonso and Gomez-Gil, 2012). The '10-20' refers to the percentage by which the electrodes are spaced away from one another (20%) and from both of the reference points nasion, inion and both ears (10%). The letters F, T, C, P, and O indicate frontal, temporal, central, parietal and occipital lobes. All electrodes marked as 'z' (zero) have been placed in the middle of the skull. Even numbered electrodes such as 2, 4, 6 represent right hemisphere placement while odd numbered electrodes (1, 3, 5) indicate left hemisphere placement (Teplan, 2002) as shown in Figure 2-8 (Jasper, 1958).

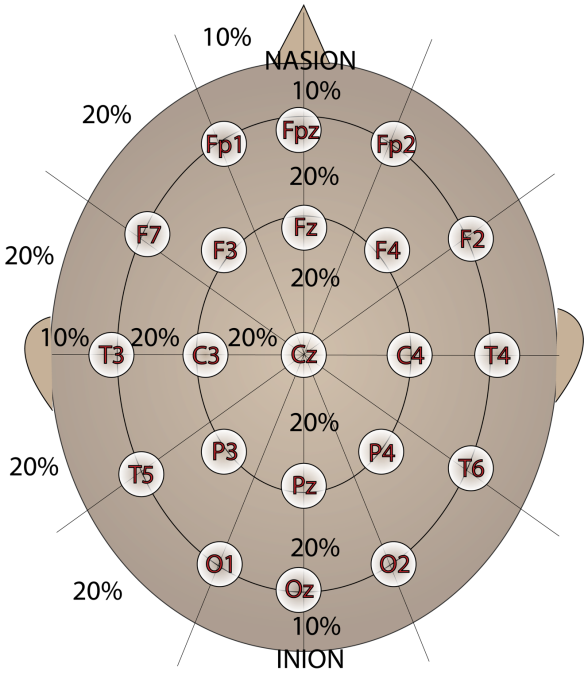

Figure 2-8 Electrode placement according to International 10-20 System (Jasper, 1958)

The initial distance from inion and nasion constitute 10% of the distance, while all the remaining sections occupy 20% hence the name 10-20 system.

2.6 Control Signal Techniques Used in BCI

As a result of many years of research and based on numerous studies carried out in relation to controllable brain signals, several of them have been described and proposed as practically useful to serve as control signals in BCI systems. The main purpose of a BCI is to monitor cerebral activity and read users' intentions in order to utilise them as control commands. It needs to be stated that many of the brain signals remain incomprehensible and their role is still unknown. Nevertheless, various neurological brain activities have been successfully unraveled and people, who undergo certain training sessions designed specifically for this purpose, can learn to modulate them at will. Such controllable brain signals can be recognised by a BCI and used to read their intentions, thus allowing people to control external devices. Among the best-defined control signals implemented in current BCI systems are: Visual Evoked Potentials (VEP), Slow Cortical Potentials (SCP), P300 Evoked Potentials, and Sensorimotor Rhythms (Nicolas-Alonso and Gomez-Gil, 2012). The following table (Table 2-3) summarises these control signals providing basic information about their main characteristics.

Table 2-3 Control signals used in BCIs (Nicolas-Alonso and Gomez-Gil, 2012)

Signal type	Physiological phenomena	Number of choices	Training	Information transfer rate
VEP	Brain signal modulation occurs in the visual cortex as a consequence of visual stimulation	High	No	<60 bits/min
SCP	Slow voltage shifts in the brain signals	Low (2 or 4)	Yes	5-12 bits/min
P300	Positive deflection peaks as a result of infrequent stimuli	High	No	20-25 bits/min
Sensorimotor Rhythms	Brain signal modulation is synchronised with motor activities	Low (2, 3, 4, 5)	Yes	3-35 bits/min

2.6.1 *Visual Evoked Potentials (VEP)*

Visual Evoked Potentials (VEP) are specific electrical modulations occurring in the visual cortex of the brain generated through visual stimulation (Regan, 1989). The brain's visual cortex is located in the occipital lobe as shown in Figure 2-9. The amplitude of VEPs increases when the stimulus is placed at the subject's central visual field making it very easy to monitor through EEG equipment (Yijun et al., 2006). VEPs are categorised by three different criteria: by the optical stimuli form, frequency, and field stimulation (Jinghai et al., 2009). The optical stimuli can be in the form of a flashing source of light including LED panels, light bulbs, flashlights, or graphic patterns such as checkerboards, stripes, and random-dot maps displayed on digital screens in computers, tablets or smartphones. According to frequency, VEPs are categorised as transient VEPs (TVEPs) and steady-state VEPs (SSVEPs). TVEPs occur when the frequency of visual stimulation is ≤ 6 Hz. SSVEPs are generated by stimuli frequencies higher than 6 Hz (Regan, 1989; Xiaorong et al., 2003). Considering field stimulation, VEPs can be distinguished as whole field, half field, and part field VEPs, depending which part of the screen is used.

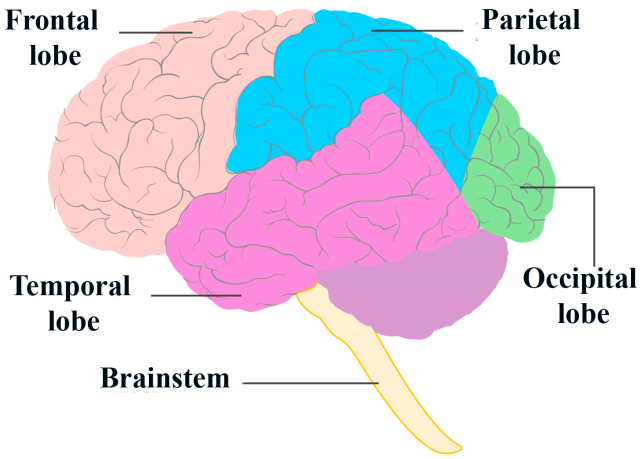

Figure 2-9 Brain Lobes

Visual cortex located in the occipital lobe of the brain.

2.6.1.1 *Steady State Visual Evoked Potentials (SSVEP)*

Steady State Visual Evoked Potentials (SSVEP) is one of the easiest and most effective methods to trigger brain waves. The brain signals can be elicited by exposing the retina to repetitive flickering light or graphic. The frequency of the flicker generates brain waves that carry the same fundamental frequency together with higher order harmonics (Zhu et al., 2010). SSVEPs are a specific case of VEPs and they occur as a consequence of visual stimulation using frequencies ≥ 6 Hz. According to Regan (1989), the strongest signal amplitudes elicited through SSVEP can be observed within 10

Hz range as well as between 16 Hz to 18 Hz bands. The weakest oscillations have been reported in the high frequency range (30 Hz to 60 Hz). In case of a single source of light flashing, the generated SSVEP resembles a sinusoidal-like waveform with the fundamental frequency matching the blinking frequency of the stimulus. However, if the stimulus is presented as a pattern e.g. a checkerboard, the SSVEP occurs at the pattern reversal rate of the checks and harmonics (Zhu et al., 2010). The pattern reversal SSVEP is caused by reversing the phase of the used pattern such as checkerboard lattice, in which the checks change abruptly from black to white and from white to black (Odom et al., 2004).

One of the main and most important characteristics of the SSVEP is the fact that it maintains the amplitude and phase unchanged for longer period of times, usually as long as the subject continues to focus his/her gaze on the stimulator (Galloway, 1990). Compared to other VEPs, SSVEP is less affected by eye blinking and eye movement artefacts (Perlstein et al., 2003). The operation principle of an SSVEP-based BCI allows the user to generate multiple commands in the system and communicate with external devices by changing eye-gaze between stimuli targets flickering at different frequencies (Lee et al., 2008). Each flickering target should elicit brain oscillation within 1-2 seconds and with matching frequency and amplitude high enough to allow the BCI system to effectively detect, extract and classify such features and use them as commands. According to majority of literature published on SSVEP, this type of control signal requires little to no training to be successfully used in BCIs making it one of the main advantages of this technique (Nicolas-Alonso and Gomez-Gil, 2012).

Another advantage of this system is that the user does not have to concentrate on motor action simulation, which is necessary for other BCI systems. The user only needs to switch his/her eye view between different stimuli sources (Muller-Putz and Pfurtscheller, 2008). However, this method requires the user to maintain visual contact with the blinking stimuli as long as the new command needs to be sent making it a major drawback of SSVEP. Therefore, understandable are concerns of the users' safety, health and comfort. Due to nature of the stimuli, prolonged usage could induce the feeling of tiredness, fatigue or even headaches. With some users there is a danger of evoking epileptic seizures and weakening the vision (Fisher et al., 2005; Zhu et al., 2010).

It has been determined that the most annoying flicker frequencies for humans are in the low range of 5 Hz to 25 Hz. Furthermore, the danger of inducing epileptic seizures has been recognised between 15 Hz to 25 Hz frequency bands (Fisher et al., 2005). In cases where the user wants to control a computer cursor or other moving object, the eye contact with the stimulus is lost. One way to mitigate this problem is to program the application in such way

that the stimulus will move together with the controlled object (Martinez et al., 2007; Vasquez et al., 2008).

For SSVEPs, among the most popular light sources are light-emitting diode (LED) panels, different types of computer monitors including cathode-ray tube (CRT), liquid crystal display (LCD) or recent LED backlit displays. It is believed that LED panels perform better than digital screens due to higher light output. However, they require additional hardware and programming to control their behaviour. Digital screens, on the other hand, can be directly connected to computers making it easier to arrange and display multiple graphic stimuli. One caveat of digital screens is the refresh rate, which significantly limits their capabilities to display certain frequencies within the required range. For that reason, LED panels are recommended for multiple targets BCI, where more than 20 commands are required. LED stimulators offer more versatility in terms of programmable frequency and phase. A programmable logic device such as an Arduino board can control each LED independently and any frequency within the most effective range can be generated in the brain without the limitations of digital screens (Yijun et al., 2008). The refresh rate of commonly used digital screens is 60 Hz practically eliminating many frequencies from the preferred range of the Alpha band where most of the visual processing occurs (Klimesch, 1997). The number of available stimuli is directly dependent on the given BCI usability requirement. For BCI systems with low complexity requirement with up to 10 command choices, LCD screens are considered optimal because they introduce less strain on the eyes. For medium complexity BCIs with 10-20 choices LCD and CRT screens can be used. For systems demanding high complexity communication requiring more than 20 choices LED panels are recommended (Nicolas-Alonso and Gomez-Gil, 2012). When more detailed graphics, feedback presentation and better target alignment are required computer and tablet screens are more convenient choices (Yijun et al., 2008).

2.6.2 Slow Cortical Potentials (SCP)

Slow Cortical Potentials (SCP) signals are very slow brain waves that mostly occur below 1 Hz. There are negative and positive potentials within this range and they are correlated with increased or decreased brain activities respectively (Birbaumer et al., 1990). These self-regulated brain waves can be used to control a computer cursor or select different targets on the screen. Thorough user training is necessary to use SCPs effectively. For that purpose, a thought-translation device is used (Hinterberger et al., 2004). During training this device, equipped with a screen cursor constantly provides the user with feedback showing the SCP's amplitude through the cursor's vertical position (Kaiser, 2001). The learning process is heavily dependent on the user's psychological state, mood

or motivation. Therefore, the user's capability to obtain this particular skill has to be determined on an individual basis during initial trials (Hinterberger et al., 2004).

2.6.3 Event Related Potentials (ERPs)

Event Related Potentials (ERP) are very small voltages that can be measured by an EEG system reflecting brain activities which are time locked to and directly induced by specific sensory, cognitive or motor events (Sur and Sinha, 2009). Because an EEG can detect ERPs they produce an opportunity for a non-invasive and safe mode of brain waves research. It is believed that ERPs are generated by thousands to millions of neurons synchronously firing electrical signals when information is being processed by the brain exposed to sensory, cognitive or motor events (Peterson et al., 1995). There are two categories of ERPs that have been detected in humans. The first wave appears during the first 100 ms after the stimulus and is referred to as 'sensory' or 'exogenous' since it is directly related to the physical quality of the stimulus. In the next portion of the brain wave, approximately within 200 ms, another signal peak can be observed which is usually termed as 'cognitive' or 'endogenous', which reflects the subject's attempt to analyse and evaluate the stimulus (Sur and Sinha, 2009). Figure 2-10 illustrates spikes in the brain waves generated by time-synchronised event referred to as P-300, which is detailed later in this Section.

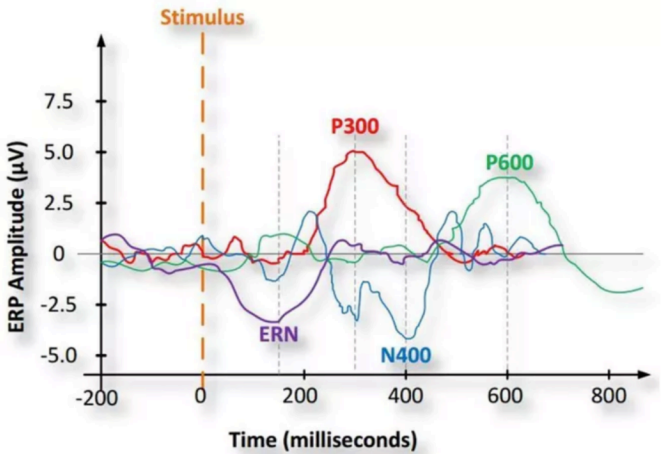

Figure 2-10 Event Related Potentials

Among other examples of ERPs, i.e. electrical signals produced by the brain in response to a stimulus, the P300 is shown. The plot also shows Error-Related Negativity (ERN). The letters P and N represent positive and negative signal deflections and the number, i.e. 300 indicates time at which these deflections occur after the stimulus onset.

2.6.4 P-300 Evoked Potentials and Oddball Paradigm

Oddball Paradigm refers to an experiment mainly used in Event Related Potential (ERP) research. It is based on the idea of presenting sequenced, repetitive, auditory or visual patterns (considered 'standard') occasionally interrupted by a stimulus not expected by the subject (called 'target'). The subject is requested to react to these unexpected elements by either counting them or pressing a button to confirm. The difference between the expected (standard) and unexpected (target) stimuli is that the latter requires a response from the subject (Squires et al., 1975). Although each stimulus triggers an ERP, it has been found that the unexpected target signals that required a reaction from the subject produce brain waves that occur approximately 300 ms after the stimulus presentation and their amplitude is greater compared to a standard (expected) stimuli. The average 300 ms reaction time and positive (P) deflection of the wave contributed to the name of P300 given to this specific potential. Based on published research it is reasonable to state that P300 is a distinct brain signal directly related to decision-making. It means that rather than being a direct product of physical occurrence of either auditory or visual stimuli, the P300 wave is associated with human reaction to it. To be more specific, the P300 is believed to be more dependent on human ability to evaluate and categorise events (Polich, 2007).

The oddball experiment provides a perfect mode for eliciting and evaluating the P300 signal. In electroencephalography (EEG) the P300 shows as a positive peak in voltage with delay ranging between 250 and 500 ms. The two parameters of P300 that are measured are amplitude and latency (delay). Amplitude measured in μV is expressed as the difference between the pre-stimulus baseline voltage level and the greatest registered positive peak of the waveform. The measurement is taken within a pre-defined time window of 250-500 ms, which matches the length of the usual P300 peak, although it may vary depending on various conditions such as a person's age or task intensity. Latency measured in milliseconds is expressed as the time between stimulus onset and the highest registered point in the positive waveform within the same time window (Polich, 2007).

2.6.5 Sensorimotor Rhythms

Beta a rhythms (13 Hz - 30 Hz) that have symmetrical distribution over the central part of the brain possess harmonic relation to the Mu rhythms. Sensorimotor rhythms are a combination of Mu rhythms (7 Hz - 13 Hz) and Beta rhythms (13 Hz - 30 Hz). Mu rhythms also referred to as Mu waves have the form of synchronised patterns of electrical activity that are associated with voluntary movement (Niedermeyer and Lopes da Silva, 1993). Although Mu rhythms occupy a similar frequency band as the Alpha waves, they differ in nature. Unlike Alpha waves, which occur in the occipital lobe and are associated with the state of relaxation and the brain's vision processing

activity, Mu rhythms occur in the motor cortex between the ears and are associated with motor action, although physical movement is not actually required for the oscillations to appear. With training, such brain waves can be triggered by mental rehearsal of a motor act, which results in a paradigm called imaginary movement (Pineda, 2005). Beta rhythms are also closely linked to motor behaviour and have been observed to attenuate during active movements (Pfurtscheller and Lopes da Silva, 1999). Sensorimotor rhythms, as the combination of both Mu and Beta oscillations, can be used to control a BCI as people can be trained to trigger these voluntary modulations. This, however, is time consuming and difficult to do (Pfurtscheller and Neuper, 2001). Imaginary movement can be observed as a decrease in amplitude and signal desynchronisation within the motor cortex along the entire range of Mu and Beta waves (8 Hz - 30 Hz) (Rohani et al., 2013). These amplitude changes and desynchronisation can be utilised to successfully control a BCI. There are two types of amplitude modulations found in sensorimotor rhythms. These are Event-Related Desynchronisation (ERD) involved in amplitude suppression and Event-Related Synchronisation (ERS) linked to amplitude enhancement (Pfurtscheller and Neuper, 2001).

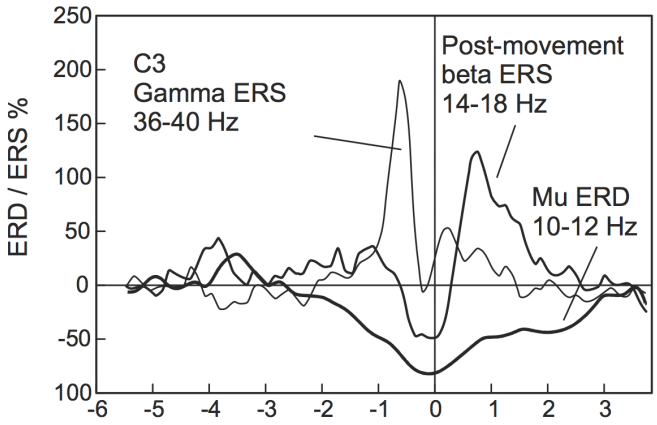

Figure 2-11 Example of ERD and ERS desynchronisation (Pfurtscheller and Neuper, 2001)

Negative time represents time before the movement onset.

Figure 2-11 illustrates the process of desynchronisation during a voluntary index finger lifting experiment. In this example ERD (suppression) of Mu wave starts approximately two seconds before the onset of the movement, reaches its maximum at the movement, and returns to its original level after three seconds. At the same time, we can observe different behaviours of the Beta wave where a short ERD (suppression) occurs at the movement start and then it shows ERS (enhancement) peaking immediately after the movement execution. This is the moment of the maximum desynchronisation where Beta ERS appears while the Mu wave is still being suppressed. In the above illustration we can also notice a short ERS peaking of the Gamma wave right before the movement execution. Gamma waves (36 Hz - 40 Hz) that are the fastest brain oscillations registered by the EEG are also known to be linked to human motor activity (Pfurtscheller and

Neuper, 2001). In the BCI design sensorimotor rhythms are very useful since the brain generates them voluntarily without the actual movement (Pfurtscheller et al., 1997).

2.7 Categorisation of BCI Systems

Based on the various BCI control signal types discussed earlier in this thesis, it is possible to categorise BCI systems into the following categories: exogenous, endogenous, synchronous (cue-paced) and asynchronous (self-paced) (Nicolas-Alonso and Gomez-Gil, 2012). The first two categories refer to the nature of the signals that the BCI system receives, while the last two depend on the input data processing modality. BCI systems can also be invasive and non-invasive depending on the method of electrode placement with and without surgical intervention.

2.7.1 Exogenous vs. Endogenous BCI

In exogenous BCI an external stimulus is required for the specific brain activity to be elicited (Nicolas-Alonso and Gomez-Gil, 2012). Previously discussed SSVEP and P300 are good examples of such BCI systems. There are numerous advantages of the exogenous BCI systems. Among them are minimal to no training required and easy management of control signals (Kleber and Birbaumer, 2005). Another very crucial parameter for any control system is Information Transfer Rate (ITR) (Yijun et al., 2008). This determines how many individual commands can be sent through the system within a certain timeframe. Exogenous BCI systems excel in this area and they can provide up to 60 bits per minute (Nicolas-Alonso and Gomez-Gil, 2012). This means that using this method, an average person, after minimal training, can send 60 different commands per minute. In most situations this is more than enough to control any type of domestic device or computer application (Kleber and Birbaumer, 2005). Stimulus based control signals require only one EEG channel, which significantly simplifies the system and lowers the overall cost (Nicolas-Alonso and Gomez-Gil, 2012). The list of disadvantages is not very long but they may cause problems in various situations.

Firstly, this type of BCI requires the user to be constantly focused on the stimulus. This means that if the eye contact is lost the elicited signal also disappears. One way to overcome this problem would be to programme the application in such a way that when the controlled object moves the stimulus moves along with it, or, the controlled objects are presented as flickers themselves (Chumerin et al., 2012). Secondly, the quality of the flickering graphics and their accuracy in terms of frequency plays an important role in the overall robustness of the system. As indicated by Bakardjian et al. (2010), visual graphics employed in BCI systems using SSVEP need the same degree of optimisation as the analysis algorithms in order to maximise the brain's response.

Thirdly, as Wang et al. (2008) reported, the number of commands (targets) has a considerable impact on the tiredness of the person using the system. The more flickering graphics that are presented to the user the more discomfort the system will cause. They also suggested that systems with more targets provide higher transfer rates, giving an example of 13-target system versus 2-target system, where the first one operated at 43 bits per minute and the second one at just 10 bits per minute of transfer rate. They also pointed out that the number of targets implemented in the BCI needs to be considered as a tradeoff between the performance and user comfort. In summary, the exogenous BCI systems won't allow the user to freely move a computer cursor or a mechanical arm in any desired direction. Instead it constrains the device's control by the choices the stimuli graphics present (Nicolas-Alonso and Gomez-Gil, 2012).

In contrast, endogenous BCI systems are operated on the principle of self-regulation and self-control of the brain waves without the use of any kind of external stimulation (Kleber and Birbaumer, 2005). Endogenous BCI systems are based on sensorimotor rhythms (Mu band) and the user needs to be trained how to change brain oscillations based on motor imagery (Nicolas-Alonso and Gomez-Gil, 2012) or on Slow Cortical Potentials (SCPs) where a thought-translation device is used (Hinterberger et al., 2004). In this training the user performs certain motor imagery tasks while the EEG records the signal, which then further needs to be extracted and classified by comparing to the reference data. Based on the results a visual feedback is presented to the user enhancing the learning experience (Nicolas-Alonso and Gomez-Gil, 2012). It is a time-consuming task and the results are never guaranteed and depend on the individual's abilities (Hwang et al., 2009). Another disadvantage of this method is the need to use multichannel EEG systems in order to increase the performance and stability of the system. It also delivers a significantly lower bit rate of approximately 20-30 bits/minute compared to exogenous systems. However, the fact that it operates at free will and is stimulation independent makes it a good choice for systems where cursor control is required (Nicolas-Alonso and Gomez-Gil, 2012).

2.7.2 Synchronous vs. Asynchronous BCI

Endogenous systems can further be classified according to the input data processing modality i.e. synchronous and asynchronous. In synchronous systems there are predetermined time slots during which the brain signal is analysed and recorded. Any brain activities that occur outside this time are ignored. During this predefined time frame the user is presented with auditory or visual cues (Tsui and Gan, 2007). The most obvious advantage of this method is the ability to simplify the system's design and brain signal evaluation methods. Eye blinks, eye movement and most of other biological artefacts can be eliminated since the signal recording is only limited to the allocated time windows

and it is easier for the user to focus during this time. Asynchronous BCI presents a more natural mode of interaction where brain signals are recorded at all times. In consequence, this approach requires an elaborate system where signal evaluation is much more difficult and the demand for computation is much higher (Nicolas-Alonso and Gomez-Gil, 2012).

2.7.3 Invasive vs. Non-Invasive BCI

The main difference between invasive and non-invasive BCIs is attributed to the mode of interaction between the device used to obtain brain signals and the brain itself. In non-invasive systems, such as EEG, where electrical signals are captured from the subject's scalp, or Magnetoencephalography (MEG), where the brain's magnetic activity is registered by means of magnetic induction (Pfurtscheller and Lopes da Silva, 1999), no surgical intervention is necessary. As has been already noted, brain signals originating from non-invasive devices such as EEG require thorough noise and artifact removal before they are useable for BCI applications. There are numerous factors inherent in this technique that hinder recording clean signals.

Firstly, electrical fields produced by neurons decay exponentially with distance. In EEG in particular, the activity of small neuronal clusters is undetectable or, when recorded such signals are heavily polluted with noise. Furthermore, brain signals can reach the scalp and be detected by EEG mainly due to morphology of pyramidal neuron fields with long and parallel dendrites and their profuse presence in the cortex. This causes a variety of smaller electrophysiological processes underlying EEG signals to be difficult to read.

Secondly, skin tissue acts as a low-pass filter attenuating high frequency signals and practically burying them inside the background noise. In consequence, non-invasive systems are mostly suitable for low-frequency neural activity analysis in the range between 0.1 Hz – 90 Hz.

Thirdly, spatial distortion of the signal is affected by different electrophysiological properties of the media composing brain cortex, which cause electrical fields to spread and distort. This is further enhanced by cerebrospinal fluid, skull and scalp, leading to additional spatial distortion of the fields before the EEG electrodes can detect them. All these constraints render non-invasive systems inappropriate and inefficient for natural motor recovery and control in disabled patients due to under sampling of the neural network (Waldert, S. (2016).

Invasive systems, on the other hand, require medical intervention where the electrodes are placed inside of the brain cortex. There are many forms of invasive electrodes. They can be installed as single electrodes, multi-contact electrodes, multi-electrode arrays (MEA), or as any combination of

the aforementioned. When comparing purely the quality of signals and depth of information the invasive systems can provide, it is commonly agreeable they yield much higher performance than non-invasive systems. Signals captured by invasive methods convey information up to several kHz. With invasive systems, high implementation accuracy is not of utmost importance as long as the electrodes' contact remains in grey matter of the brain. For higher and more accurate performance though, placing the electrodes in deeper layers is preferable, especially for accurate motor control. In general, unlike in non-invasive systems, invasive signals reflect input to local processing and output of cortical areas making them undeniably capable of producing much higher information transfer rates. Internally installed electrodes can be used for stimulation and recording, performing both tasks at the same time (Henze et al., 2000). This stimulation could be used to provide feedback to the brain cells, effectively closing the loop of BCI. It is believed that the lack of such direct feedback impoverishes current BCI systems relying mainly on visual or acoustic responses (Waldert, 2016).

All the advantages aside, it must be stated that the user acceptance for invasive systems is much lower compared to non-invasive techniques due to medical concerns related to neurosurgery and the implant itself (Blabe et al., 2015). Among the main challenges is biocompatibility, degradation of recording quality progressing over time, and eventual implant failure. It is suggested that once all the challenges related to technical, socio-ethical, and neuro-scientific issues cease to exist, user concerns would diminish, and invasive methods will eventually prevail in future applications, including non-medical. At present, all the commercially available BCI systems are non-invasive (Waldert, 2016).

2.8 Feature Extraction Methods

The main function of a successful BCI system is to recognise different patterns of brain signals and classify them into classes based on their features. Feature extraction in BCIs operates on the principle of recognising similarities to a certain class as well as differences from the rest of the classes. Feature recognition in properties of the brain signals is founded on the discriminative information required to distinguish their different types. Properly designed feature extraction constitutes one of the most challenging and important elements of any BCI system. Since brain signals reflect multiple activities taking place simultaneously, the useful information is usually concealed in a very noisy environment. Different brain tasks can effectively overlap both in time and space portions of the signal, which are of interest for a BCI developer. Therefore, simple filtration is not usually sufficient to extract the features that are to be used in the system. In the EEG technique, multiple channel recording is executed and that provides large portions of unnecessary

information, which often is referred to as signal noise. In order to preserve the system's computational resources for other tasks, various dimension reduction techniques such as independent component analysis (ICA) or principal component analysis (PCA) need to be employed. Their role is to reduce the dimension of the acquired signals by removing redundant information. Using time domain view of recorded brain signals the information about when certain features occurred can be obtained. One approach is to slice the incoming data stream into short sections thus allowing the detection of any signal peaks, patterns or other relevant parameters that may be present. This windowing technique can be very effective but settings such as window length and overlap need to be carefully adjusted (Nicolas-Alonso and Gomez-Gil, 2012). If the data segmentation is exaggerated, peak-detecting transformation such as Fast Fourier Transform (FFT) can be compromised (Ghafar et al., 2008). This Section examines deferent methods to acquire relevant brain signal features and applied selection techniques. Discussed are dimension reduction, time and frequency analysis, common spatial pattern algorithm application, and various feature selection methods.

2.8.1 Independent Component Analysis (ICA)

Independent Component Analysis uses a statistical approach by splitting mixed signals into their sources based on the assumption that these sources are statistically mutually independent. The assumption made by the ICA algorithm is based on incoming EEG signal, which is being treated as a mixture of independent source signals originating from various cognitive activities. The following equation shows how the ICA interprets EEG signal ***x(t)*** referring to its sources ***s(t)***.

$$\mathbf{x}(t) = \mathbf{f}(\mathbf{s}(t)) + \mathbf{n}(t) \quad (1)$$

In this basic equation function ***f*** works as an unknown mixer function and ***n(t)*** functions as a random noise vector that is added to the input signal. The number of sources determines the dimension of the input vector ***s(t)***. The resulting dimension of output vector ***x(t)*** equals the number of channels captured. The ICA algorithm assumes the number of sources to be less than or equal to the number of channels (Te-Won et al., 1999).

Another method of using ICA allows reconfiguring the equation as a matrix multiplication with ***A*** functioning as the mixing matrix.

$$\mathbf{x}(t) = \mathbf{A}\mathbf{s}(t) + \mathbf{n}(t) \quad (2)$$

Although equation (2) appears to be too simplified, it is proven to work well with brain signals. If an assumption is made that the signal has minimum noise, the n(t) component can be removed altogether from the equation to simplify the calculations (Castellanos and Makarov, 2006; Kun et al, 2009). ICA is often used to remove eye movement and blinking artefacts as a method of pre-processing and before the actual feature extraction and is considered as a powerful and robust tool for this task (Gao et al., 2010). Yet, some studies claim that such artifact removal may negatively impact the power spectrum of valuable neural activities in certain scenarios (Wallstrom et al., 2004).

2.8.2 Principal Component Analysis (PCA)

Principal Component Analysis (PCA) is a feature extraction technique based on statistics. PCA uses linear transformation in order to convert possibly correlated observations into uncorrelated variables, referred to as principal components. A set of components originated from the input data is generated by a linear transformation. They are sorted based on their variance such that the first principal component is of the highest possible variance. This function allows the PCA to extract different components in the brain signals. PCA projects the input data on a *k*-dimension eigenspace of *k* eigenvectors, which are calculated from the covariance matrix $\sum$ of the training data $p = [p_1 p_2 \dots p_n]$ (Lin and Hsieh, 2009). In the equation (3) below p_i is *i*-th *d*-dimension training sample, and *n* is the number of samples.

$$\sum = \sum_{i=1}^{n} (p_i - m)(p_i - m)^t \quad (3)$$

In the equation (3) $m = \frac{1}{n} \sum_{i=1}^{n} p_i$ is the mean vector of the training samples p_i.

The covariance matrix $\sum$ is a real and symmetric *d x d* matrix, thus $\sum$ has *d* different eigenvectors and eigenvalues. Through the eigenvalues, it is possible to find which eigenvectors represent the most meaningful brain signals in the captured dataset. Therefore, the principal component of the training dataset *p* is represented by the eigenvectors with the highest eigenvalue. One of the main reasons PCA is used for brain signal processing is its ability to reduce dimensions of the features. In

other words, since the number of columns is less than the number of eigenvectors, the dimension of the output data is smaller than the dimension of the input data. This allows simplifying the next important stage of signal processing called classification, which will be explained in the subsequent Section (Nicolas-Alonso and Gomez-Gil, 2012). Sometimes, the best discriminating components cannot be found within the largest principal components (McFarland et al., 2006). PCA reduces data dimensions by always searching for new optimal representation of data using mean-square-error between the original data and newly found representation. It is not guaranteed that the discriminative features are best for classification. Even still, PCA is considered to be a very effective noise reduction technique. Additionally, PCA is a robust artefacts reduction method when applied in BCI systems.

It can identify components of an artifactual nature such as eye blinks or eye movement, and reconstruct the signals without them present in the output signal (Lins et al., 1993; Boye et al, 2008).

2.8.3 Matched Filtering (MF)

Matched Filtering (MF) uses predetermined known signal patterns or templates and attempts to extract features seeking for matches of such patterns present in the signals analysed. The user's intention is recognised by correlating between the unknown input brain signals and the existing signal templates. Each intention of the user is correlated to a separate template and better matching is achieved by a higher correlation between them. By finding harmonically similar sinusoidal signal components each matched filter can be modeled as their summation (Krusienski et al, 2007):

$$\mathrm{MF}\ (n) = \sum_{k=1}^{N} a_k \cos\left(\frac{2\pi k f_F}{f_s} n + \Phi_k\right) \tag{4}$$

In equation (4) n represents the template sample number, and f_s is the sampling frequency while f_F is the fundamental frequency of the rhythm template. *N-1* represents the number of harmonics, a_k is the amplitude while Φ_k represents the phase of the individual harmonics. The Fast Fourier Transform (FFT) spectrum provides all the necessary information to determine a_k and Φ_k parameters (Krusienski et al, 2007). According to Brunner et al. (2010) MF method can be used for SSVEP feature extraction.

2.8.4 Auto Regressive Components (AR)

Auto Regressive Components (AR) is a signal modeling method using spectral estimation. It models the EEG signal as the output random signal derived from a linear invariant filter. For the signal input AR uses white noise with a mean of zero. AR's main task is to find filter coefficients since it assumes that different brain activities will be reflected in them, thus they can be used as the signal features. Another assumption that the AR is based on declares that the transfer function of the filter will only contain poles in the denominator. The number of poles expressed in the denominator coincides with the autoregressive model's order. To make the filter coefficients computation easier an all-pole filter assumption is needed, which means only linear equations need to be solved.

To express AR mathematically, the following model of order p describes the EEG signal $y(t)$ as:

$$y(t) = a_1 y(t-1) + a_2 y(t-2) + a_3 y(t-3) + \ldots + a_p y(t-p) + n(t) \quad (5)$$

where, a_i is i-th filter coefficient, and $n(t)$ represents the noise. In the AR model, determining the appropriate p order for a given input signal needs to be properly balanced. If the input signal is modeled using order set too low, the spectrum may be too smooth and therefore not accurately represent the signal. Conversely, if the order is set too high, the resulting spectrum may present invalid peaks (Nicolas-Alonso and Gomez-Gil, 2012). AR spectral calculation is considered to perform better in a short time segments than Fourier Transform because it provides better resolution (Krusienski et al., 2006). For non-stationary signals AR is not recommended due to poor performance in such scenario (Florian and Pfurtscheller, 1995).

2.8.5 Common Spatial Patterns (CSP)

Common Spatial Patterns (CSP) extracts features from a multichannel EEG data by converting it to subspace, minimising similarities and maximising differences between classes detected in the signals. CSP creates a specific spatial filter, which effectively transforms input data into a set of new output data with an optimal variance to make the subsequent classification easier (Ramoser et al., 2000). Although CSP is most effective in solving 2-class problems in multichannel EEG recordings, other versions for multiclass applications have also been proposed (Grosse-Wentrup and Buss, 2008). CSP is most effective in synchronous systems where signals are detected in predefined time periods. Its decreased functionality in asynchronous BCIs is associated with non-stationary properties of EEG signals (Mousavi et al., 2011). Another parameter determining CSP's effectiveness is spatial resolution. Furthermore, certain electrode arrangements seem to work better than others for specific brain tasks.

2.8.6 Wavelet Transform (WT)

Wavelet Transform (WT) is a very effective mathematical algorithm used to analyse and extract information from complicated sets of data such as audio or video. WT works best with non-stationary signals since the time and frequency of signals can be flexibly represented by the algorithm (Ghanbari et al., 2009). Wavelets are functions of varying frequency and limited duration, allowing simultaneous signal analysis in both the time and the frequency domain. Fourier Transform (FT), provides only information about the frequency content of the signal. To mitigate this problem a newer version called Short-Term Fourier Transform (STFT) was developed. The main difference between FT and STFT is that the latter divides the signal into successive epochs and applies FT within them. In this method the window length remains constant and usually presents various problems. Smaller window designs produce higher temporal resolution and lower frequency resolution at the same time. To overcome this difficulty WT is applied, which is able to decompose the analysed signal in both the time and the frequency domain at various resolutions. This is achieved by using a modulated window, which can be moved within the signal at multiple scales. Thus, a resulting algorithm referred to as Continuous Wavelet Transform (CWT) was developed, which defines the convolution of the signal $x(t)$ with the wavelet function $\psi_{s,\tau}(t)$ (Samar et al., 1999):

$$w(s,\tau) = \int_{-\infty}^{\infty} = x(t)\,\psi^{*}_{s,\tau}(\mathrm{t})dt \tag{6}$$

Where $w(s,\tau)$ is the wavelet coefficient corresponding to the frequency associated with the scale s and the time τ of the wavelet function $\psi_{s,\tau}(t)$. The symbol '*' expresses the complex conjugation. The wavelet function $\psi_{s,\tau}(t)$ is an expanded and transposed version of a *mother wavelet* $\psi(t)$:

$$\psi_{s,\tau}(t) = \frac{1}{\sqrt{s}}\psi\left(\frac{t-\tau}{s}\right) \tag{7}$$

Although the mother wavelet can be expressed in many ways it always complies with the following condition:

$$\int_{-\infty}^{\infty} \psi(t)dt = 0 \tag{8}$$

The equation (6) defining CWT can be treated as a template matching, as described in the matched filter paragraph, where the cross variance between the signal and a predefined waveform is calculated (Krusienski et al, 2007). It needs to be mentioned however that the CWT's advantage over classic template matching methods are due to the fact that wavelets are more efficient in transient signal analysis, where the signal spectral properties change over time. Wavelet Transform, due to its inherent relationship to frequency and temporal position of the analysed signals, allows distinguishing signals of identical frequency ranges using temporal position, and vice versa separating temporally overlapping processes comparing different frequency content (Demiralp et al., 1999). To combat excessive data redundancy and complexities introduced by CWT, the Discrete Wavelet Transform (DWT) was proposed. The DWT translates and expands the mother wavelet only in certain discrete values (Hubbard, 1998). Selecting a mother wavelet is necessary when using WT. In various BCI applications many different wavelets have been successfully used depending on the type of features that are to be extracted from the signal. The wavelet called Mexican Hat is suitable for time domain based feature extraction and works well with Event Related Potentials (ERP) occurring in time (Bostanov, 2004). For frequency domain the Morlet wavelet is commonly used and found to be very effective in gamma band activity detection (Senkowski and Herrmann, 2002). For successful imaginary movement detection in 1 Hz - 4 Hz frequency range the bi-scale wavelet was used (Mason and Birch, 2000).

2.8.7 Genetic Algorithm (GA)

Genetic Algorithm (GA) is a procedure aiming to establish the most efficient set of features in EEG signals. In BCI research it is usually applied as an automatic method extracting an optimal set of features (Fatourechi et al., 2007; Dal Seno et al., 2008). The following diagram shown in Figure 2-12 explains the steps that GA undertakes to extract useful data from EEG signals.

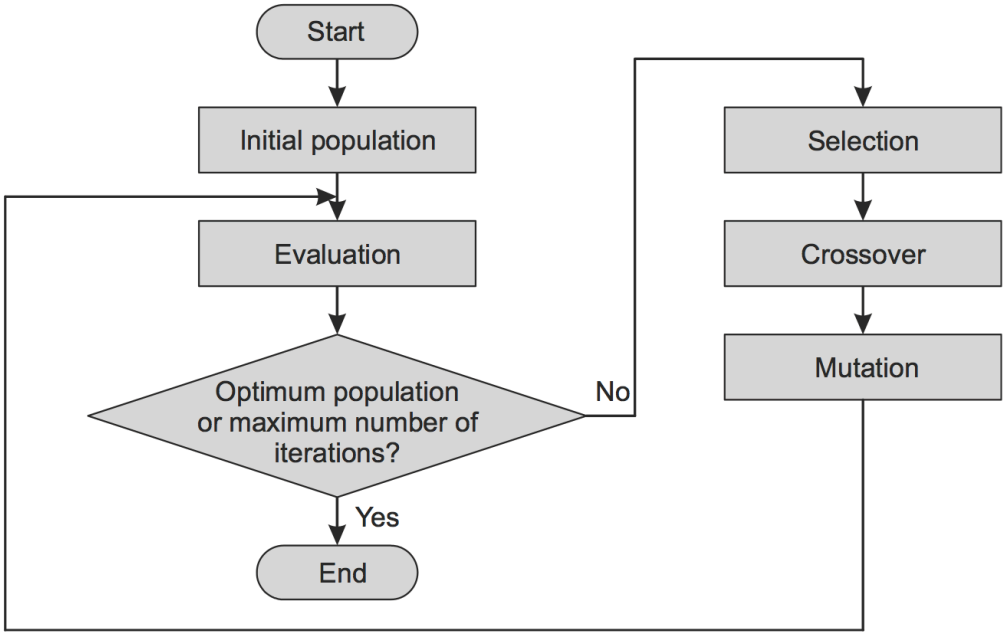

Figure 2-12 Genetic Algorithm signal processing steps

The basic operation of GA algorithm is to populate candidate solutions, which are called individuals. They are encoded by strings named chromosomes, which can either be encoded by binary or no binary information. The operation is started with a randomly generated initial population. If some initial information is possessed by the algorithm, the first population can be sent to areas where optimal solutions are likely to minimise possible iterations. Next, an evaluation of individual population fitness is performed by the algorithm. As a result, certain population representatives are discarded in order to make space for newly generated individuals. Other individuals may be used as future parents, which in turn will generate new individuals.

To prevent premature convergence, certain individuals may be stochastically selected allowing diversity of the population. Past the selection procedure, the individuals are cross referenced with each other. In this step, using the selected parents a process called mating generates one or more offspring. Since keeping the population size constant is essential, the number of generated offspring should match the number of discarded individuals. Next, the parents' genes are split and then combined again forming new offspring. After the crossover step, new population is altered by mutations. This helps to avoid the state of convergence towards something that is called a local suboptimum solution before the entire search space is exhausted. Due to resulting mutations, the areas that cannot be explored by the crossover process can be discovered. In the last step, the new population is evaluated for its fitness. The GA algorithm is terminated when an acceptable solution is found or the maximum number of generations has been produced (Nicolas-Alonso and Gomez-Gil, 2012).

2.8.8 Sequential Selection

Sequential Selection adds and removes features sequentially in order to find the optimal subset of features. This optimisation approach utilises a pair of algorithms performing sequential selection, one forward and one backward. Sequential Forward Selection (SFS) is an algorithm that proceeds upwards. Once the best feature is found it is treated as the first feature in the subset. Next, from the remaining set of features, for all subsequent steps the algorithm choses another feature, which yields the best subset of features in combination with the already found features. The algorithm stops working when the required number of features is achieved. The SFS however, cannot remove redundant features after it adds new ones. In contrast to SFS, Sequential Backward Selection (SBS) uses a top down process starting from the entire set of features and proceeds towards more specific ones by removing them sequentially, thus introducing minimum error (Ciaccio et al, 1993). In consequence, it may discard very useful features in the process. Successful SFS applications in BCI development have been documented (Lakany and Conway, 2007; Dias et al., 2010).

2.9 Artefacts in BCI

Artefacts are unwanted parts of the brain signals, which can significantly contaminate them and they are usually of non-cerebral origin. They can affect the brain activity signals and completely change the shape of the neurological response thus reducing any BCI's performance (Nicolas-Alonso and Gomez-Gil, 2012). Fisch (2002) revealed in his publication "Fisch and Spehlmann's EEG Primer: Basic Principles of Digital and Analog EEG" that artefacts shown in the EEG signals are of non-cerebral origin and they are one of the main factors confusing and sometimes distorting EEG readout. They can be divided into two main categories, which Fisch called physiological artefacts and non-physiological artefacts. Physiological artefacts are generated by various body activities that are caused by head movement, body or scalp (e.g. pulsations of the scalp arteries), which directly affect the electrode scalp interface. They can also occur as bioelectrical potentials produced by other moving signal sources within the body itself such as eyes, tongue, jaw or stationary sources like the scalp muscles, heart or even sweat glands.

For the non-physiological artefacts two main sources are distinguished: external electrical interference originating from other power sources such as power lines or electrical equipment located in the same room as the EEG system; and internal electrical defects and malfunctioning of the EEG recording system developing from recording electrodes (electrodes integrity, positioning and application), leads, amplifiers and filters (Fisch, 2002).

2.9.1 Physiological (body-based)

This Section reviews the scenarios when physiological artefacts usually occur. Physiological artefacts mostly originate from different activities such as muscular, called electromyography (EMG), ocular known as electrooculography (EOG), and heart referred to as electrocardiography (ECG) (Fatourechi et al., 2007). EMG artefacts are caused by different types of muscular contractions including talking, chewing, teeth clenching, swallowing or head turning and are responsible for substantial brain signal pollution. Muscle artefacts are known to cause very short potential changes, which usually recur. Muscle artefacts produced by scalp and face muscles mainly show in the frontal and temporal lobes. Head and body movement artefacts appear even if all the electrodes make good mechanical and electrical contact.

During the recording, simply avoiding body movement can eliminate many of the artefacts associated with movement. Tongue movements produce intermittent or repetitive slow oscillations in a wide distribution showing their maximum amplitudes in the mid-temporal region. Tongue artefacts can be caused by speaking, swallowing, chewing and coughing (Fisch, 2002). EOG are associated with all sorts of eye movements and blinking. The former is usually responsible for low-frequency patterns while the latter generates rather high-amplitude momentary peaks, both contaminating brain signals. Blinking and eye movements cause potential changes which are mainly picked up by the nearest frontal electrodes; Fp1 and Fp2 for blinking, F7 and F8 for horizontal (lateral) eye movement (see Figure 2-8 on p. 37 for electrode placement). Artefacts linked to eye activities are usually identifiable by their frontal distribution, bilateral symmetry and characteristic shape (Fisch, 2002).

ECG, due to its rhythmic nature introduces a continuous pattern into brain signals that reflect heart activity (Fatourechi et al., 2007). The EEG with wider electrode arrangements effectively picks up heart activity potential changes. Unlike most other artefacts the ECG usually cannot be avoided by simply improving the electrode contact or replacing it (Fisch, 2002). This statement however is contradicted by other opinion submitted in Section 2.9.3.

2.9.2 Non-physiological (environment-based)

Non-physiological artefacts are electrical interference artefacts caused externally. They emanate from electrical equipment and power lines. In Europe it causes 50 Hz, while in the US and other overseas countries 60 Hz interference. Wherever electrical equipment powered by alternating current is used, the artefacts will occur regardless, even if the electrodes are faulty or working properly. These artefacts can be introduced as either electrostatic interference produced by moving

charged objects or electromagnetic interference by strong currents flowing through cables and equipment i.e. transformers or electric motors. Both types can be minimised by shielding the offending power cables and by the proper wiring of the power cables (Fisch, 2002).

2.9.3 Artefacts Removal Techniques

The BCI developers and researchers mainly focus on physiological artefacts removal since the process is much more challenging compared to non-physiological artefacts reduction (Nicolas-Alonso and Gomez-Gil, 2012). Artefacts can be avoided or automatically rejected during the brain signal acquisition. They can also be manually removed after the recording. Avoiding artefacts is very helpful during the acquisition and it does not consume any computing resources. The subject just needs to be instructed to avoid any unnecessary activities including body movements or eye blinking during the experiments (Vigário, 1997). Manual artifact removal requires visual inspection of the recorded signal and can be very labour intensive. It can also be applied in off-line systems only. Huster et al. (2004) also concluded that the most problematic are the artefacts caused by physiological functions and processes of the body. These artefacts can be either corrected or rejected. They suggest that pronounced cardiac artefacts can be avoided by proper electrode placement while most of the signal power linked to muscle movement occupy higher frequency bands which are usually neglected by the current BCI designs. Huster et al. (2004) confirmed that simply instructing the subject not to clench teeth or move the head can significantly eliminate all myographic artefacts while stating that no such easy solution is available for the eye movement artefacts. Blinks or eye movement cannot be avoided during longer EEG recording sessions. They also contaminate the frequency bands frequently used for neurofeedback training. Simply monitoring and rejecting suspiciously high (75 μV) signal amplitudes is the most effective method since eye blinks and horizontal movement generate signals shifts larger than the normal EEG (Huster et al., 2014).

There are various Independent Component Analysis (ICA) techniques available today that can be used to analyse, correct and remove unwanted signals from the EEG system (Jung et al., 2000; Keren et al., 2010). Their main function is to extract separate components from the EEG signals. Whatever the method used, after determining which part of the signal is useable, the noise is nullified and the remaining components are mixed back together. Some of the methods used in ICA are so advanced that the process of ‘unmixing’ signal, purifying it and mixing it back together is fully automated (Nolan et al., 2010).

As researched in the last few years by comparing EEG data between paralysed and healthy subjects, it has been observed that muscle movement plays a significant role in the EEG signal contamination. This occurs particularly in the range of higher Gamma frequencies above 20 Hz. Surface Laplace is used to remove muscle artefacts and it works best with EEG systems comprising of at least 64 electrodes (Fitzgibbon et al., 2013).

2.10 Classification Techniques of Extracted Features in BCIs

Classification is the second most important step after feature extraction in BCI development. In this step all of the user's mental intentions, based on the feature vector matching brain activity, are decoded and used to drive external devices or applications. This can be achieved either through the use of regression or classification algorithms. In regression algorithms EEG extracted features are used as independent variables to decode the user's intent. Classification algorithms however, use the same features as independent variables but their role is to define boundaries between the targets. To best describe the difference between the two approaches two scenarios can be discussed, one with two-target and one with four-target cases. In a two-target case scenario both regression and classification methods can work with single function parameters as shown in Figure 2-13.

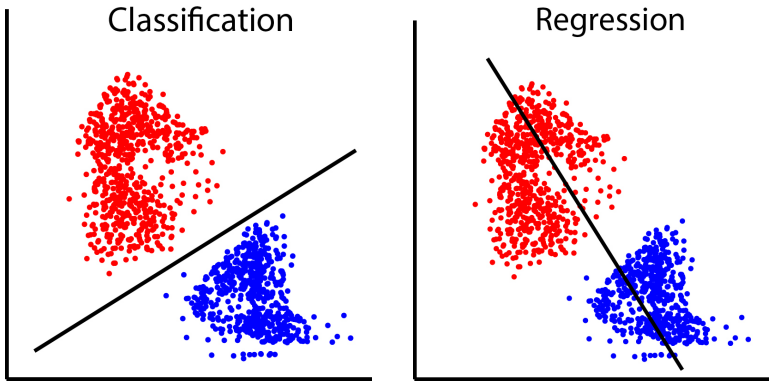

Figure 2-13 Two-target classification and regression methods example

Each set of colour dots illustrate two separate targets being classified by both methods.

In a four-target situation, with linearly distributed targets, the regression method can work with a single function, while the classification methods have to use three separate functions to determine each of the three boundaries between the four targets (Figure 2-14). For that reason, the regression method is usually recommended for applications with multiple targets and the classification works best with two-target scenarios. Also, BCIs with continuous feedback requirement such as computer cursor control are reported to work better with the regression algorithms (McFarland and Wolpaw, 2005). Online BCIs work with real time data streams and provide an important opportunity to evaluate the system's applicability in real-world environments, where decoding spontaneous user

intentions are an essential mode of operation. Offline systems are based on prerecorded trials and are very useful to test, evaluate and fine-tune new classification algorithms in a more controlled scenario.

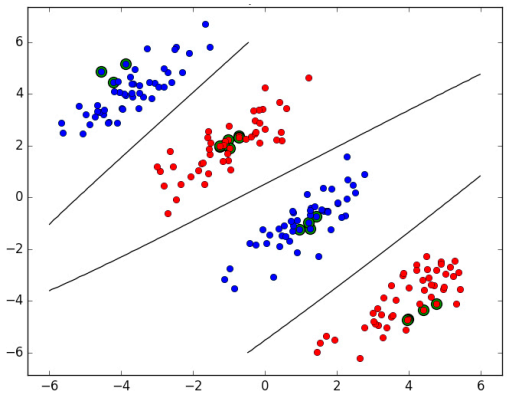

Figure 2-14 Four-target classification example

Each set of colour dots illustrate four separate targets being classified in this example.

Online systems are more complex and demanding since the users' changing motivation and fatigue may impact on the system's effectiveness. Classification algorithms can be successfully used in online, offline and a combination of both setups. It is crucial to always test any new BCI system using both offline simulation and cross-validation. Only online operation however can accurately verify the system's usability (McFarland et al., 2006; Daly and Wolpaw, 2008; Townsend et al., 2010).

In order to understand classification, a technique referred to as supervised learning needs to be explained. Supervised learning should be understood as one of the methods used in machine learning. It is a specific task of learning a new function, which maps an input to an output based on example input-output pairs (Russell and Norvig, 2010). The function is generated using existing, categorised training data usually including a predefined set of training examples (Mohri et al., 2012). Each example is a pair, which contains a vector input signal and a required output, which is also called supervisory signal. The algorithm analyses the prerecorded training data and generates a resulting function. This new inferred function can be used to map new examples. Ideally, the learning algorithm should generalise useable output data from the new examples using the training data.

Traditionally, BCI researchers use supervised learning to calibrate classification algorithms. In online sessions it is believed that constant feedback is beneficial for the classifier to properly detect brain signals. However, due to non-stationarity of the brain signals the effectiveness of the BCI

system can be compromised. According to Shenoy et al. (2006) there are two main reasons for the non-stationary nature of the brain signals.

Firstly, often the prerecorded training data used for calibration often differs drastically from the signals streamed during the online sessions.

Secondly, brain signals are prone to change over time depending on concentration, motivation, attentiveness or fatigue of the user. To improve BCI rigidness, it is suggested to develop and use algorithms, which are able to adapt to changing conditions. This is especially important in asynchronous and non-invasive systems (Millan and Mourino, 2003; Galán et al., 2008). It is a recognised fact that supervised learning does not provide optimal performance for classification of non-stationary signals. Therefore, long and extensive training sessions and calibration are necessary to achieve good results. The solution could be semi-supervised learning to minimise the initial training period and at the same time allow the continuous updating of the online session classification algorithm (Li et al., 2008). In such case, a small dataset can be used to initially train the classifier, which during the process, can be updated using the online data.

Realistically, in any online BCI setting, the subject's intentions are not known until the training data is provided in which case using unsupervised learning or reinforcement learning is suggested. In order to use such unlabeled data for classification, unsupervised learning attempts to find hidden patterns in them. Reinforcement learning techniques utilise the phenomenon in which discriminating EEG signals occur when the subject recognises an incorrect decision. These elicited signals are used as learning data to eliminate similar errors in subsequent sessions (Ferrez and Millan, 2008). Although adaptation algorithms usually increase BCI performance, a situation may occur when a given BCI adapts too fast, thus confusing the user, as the training will continually be performed in ever changing conditions (Millan, 2004). Furthermore, the process of adaptation can hide important signal features, which otherwise could be useful. Therefore, a tradeoff can be observed, where proper classification can be hindered or even compromised by adaptation process being too sensitive to signal changes.

There are also two other problems impacting classification algorithms, commonly known as the curse of dimensionality and the bias-variance tradeoff. The curse of dimensionality refers to a situation when the amount of training data required for proper operation of the system increases exponentially with the feature vector dimensionality (Jain et al., 2000). Since the training process is very time consuming and can be very tedious and tiring for the users, there is very little training data available. The bias-variance is the natural tendency of the classification process towards high variance with low bias and vice versa. High bias with low variance results in a reasonably stable

classification, while the opposite situation, high variance with low bias, results in a rather unstable classifier. The least amount of errors is achieved when bias and variance are at their lowest value simultaneously. Either a single classification algorithm or a combination of multiples can be used to design the required classification step. Among the commonly used algorithms are linear classifiers, *k*-nearest neighbour classifiers, support vector machines and various neural networks as summarised in Table 2-4. The tendency is always to start with the simplest one to avoid the unnecessary complexity of the system. The simpler algorithms, also due to their inherent nature, are more effective in the adaptation process. However, whenever they lack in performance, simple algorithms should be replaced with more advanced variants (Daly and Wolpaw, 2008).

Table 2-4 Classification techniques summary

Technique	Properties	Applications
Bayesian analysis	Not popular in BCI applications, non-linear decision boundaries	(Pires et al., 2008; Ruiting et al., 2009)
Linear Discriminant Analysis	Usually two-class with low computational requirements and acceptable results, fails with strong noise	(Garrett et al., 2003; Bostanov, 2004; Scherer et al., 2004; Hoffmann et al., 2008; Vidaurre et al., 2009; Blankertz et al., 2011)
Support Vector machines	Fast working classifier allowing for binary or multi-class operation with linear and non-linear modalities, fails with strong noise	(Garrett et al., 2003; Schlögl et al., 2005; Xiang et al., 2007; Rakotomamonjy and Guigue, 2008)
k-Nearest Neighbour Classifiers	Multi-class, efficient classifier with low dimensional feature vectors	(Borisoff et al., 2004; Kayikcioglu and Aydemir, 2010)
Artificial Neural Network	Multi-class, very flexible classifier using multiple architectures	(del R Millan et al., 2002; Millan and Mourino, 2003; Felzer and Freisieben, 2003; Palaniappan, 2005),

Despite unquestionable importance and usability of classifiers in BCI development it needs to be pointed out that inappropriate use could introduce problems. Namely, the phenomenon of bias and variance over-fitting of the algorithms' estimated error are among the main sources of difficulties. When over-fitted, the classification algorithm will only classify data very similar to the existing training data. This phenomenon can be avoided when restrictions to the classification complexity are applied. Cross validation procedure is used to estimate any classification errors. After completing the classification algorithm training, the validation is executed based on validation data set, which needs to be independent of the training data. This process can be run through multiple

times, each time applying different partitions of the sample data, in which case the resulting validation errors can be averaged across multiple trials (Lemm et al., 2011).

2.11 Applications for BCI Systems

In recent years new BCI applications have emerged due to rapid growth of new technologies, especially in the field of mobile computing using smartphones and tablets. BCI offers the users completely new communication and control channels when interacting with computers and other digital devices utilising recognition of mental state. This technique can replace or augment already existing control interfaces traditionally employing peripheral nerves, muscles and limbs when using computer mouse, control panel or touch screens. The BCI is a very promising new technology, encouraging developers and researchers around the world to focus on continuous improvement and advancement of the systems. Extensive BCI development and research facilitates EEG-based brain signal acquisition due to significant advances, offering acceptable signal quality, ease of use, portability, accessibility and low-cost operation of this method (Nicolas-Alonso and Gomez-Gil, 2012). One of the main applications and original motivations for the BCI development was to improve the quality of life of severely disabled people who cannot use their limbs or communicate in traditional ways. Potentially, BCI may help in revealing hidden processes occurring in the subject's brain during many activities that otherwise could not be monitored. BCI will become increasingly important and potentially attractive for a wider base of end-users of non-medical applications, allowing healthy people to use this technology for environmental control, future smart homes, game control, entertainment and even neuromarketing.

Due to many difficulties inherent in the BCI usage it becomes more apparent that future hybrid systems, utilising brain signal acquisition combined with eye trackers or other muscle-based devices, should be beneficial and improve overall user experience. Also, the combination of multiple BCI paradigms such as SSVEP and imaginary movement with other existing assistive technologies, appears to be the natural consequence of ever growing computing power paired with miniaturisation of digital devices (Treder and Blankertz, 2010; Pfurtscheller et al., 2010). The number of paper publications reporting successfully working BCI applications such as word processors, web browsers, simple games, brain controlled wheelchairs, robots and neuro-prostheses is growing exponentially every year. However, the majority of these systems have been solely developed for training or demonstration purposes working as proof of concept. Shortcomings inherent in the BCI technology still prevent widespread commercialisation. Many parameters describing BCI performance present significant challenges limiting control for real-world tasks (Moore, 2003). One of them is the information transfer rate, which is still considered to be too low

for natural interactive communication and the high error rate complicates interaction even further. Disabled people cannot set up and use the system autonomously since the capturing electrodes need to be properly applied and the recording session initiation requires assistance.

A technical pitfall, often described as 'Midas touch', refers to a situation where the system can be switched off by the user using mental command as input, but without the ability to switch it back on again. Moreover, BCI systems usually require the users to be highly attentive for prolonged periods of time, demanding a high cognitive load. This is easily achievable in fully controlled laboratory conditions with trained, well-prepared, and accustomed subjects, but very difficult to perform by an average user. Nonetheless, the independent home use of a BCI system is virtually inevitable, considering the amount of research taking place globally (Sellers et al., 2010). In order to properly judge the BCI practicality it is important to make a clear distinction between the specific functions it can perform and the application these functions should serve. In other words, a BCI system may capture, process, analyse and translate the input signals into commands effectively, but to fully evaluate its usability for any application, it must be checked as to how well it performs its designated purpose (Wolpaw et al., 2000). This designated purpose can be understood as the application that denotes the environment in which the estimated BCI output commands are employed. The subsequent Sections explain various BCI applications grouped as medical and non-medical applications.

2.11.1 Medical Applications

When considering medical applications for BCI several categories of disabilities need to be considered. The first category includes patients with Complete Locked-In State (CLIS), who have entirely lost their motor control either due to severe cerebral palsy or they are at a terminal stage of Amyotrophic Lateral Sclerosis (ALS). The second category comprises Locked-In State (LIS) patients who suffer almost complete paralysis with remaining some minor voluntary movement, such as lip twitches, eye blinks and eye movement. The last category consists of abled-bodied users with existing neuromuscular control, including speech or hand control, but who suffer from neurological disorders such as schizophrenia or depression. The performance of a BCI system is directly related to the level of impairment. According to Kübler and Birbaumer (2008) a CLIS patient could not control BCI. Communication with voluntary brain control was reported only for LIS patients. Therefore, it is worth mentioning that the BCI systems as assistive technology can be attractive for severely disabled people only if other methods are not available. Even though BCI provides a relatively low information transfer rate, the severe disabilities of LIS patients encourage

them to use BCI rather than other more reliable and conventional systems such as muscle or eye-movement based (Liu et al., 2011; Treder et al., 2011).

2.11.1.1 Communication and Environmental Control

With neurologically impaired patients, the main BCI's function is to restore the communication as the most essential human activity. Usually these kinds of applications display a virtual keyboard, where the BCI enables them to select letters to build words and sentences and there can be multiple methods to achieve this goal. After long training, paralysed patients can generate positive and negative deflections in their Slow Cortical Potentials (SCP) and drive cursor movement to select letters (Hinterberger et al., 2004). ALS patients were able to select 2 characters per minute when writing a text (Birbaumer et al., 1999).

EEG artefacts such as eye blinks can also be used to execute similar tasks (Chambayil et al., 2010). Another popular protocol that is commonly used to drive a spelling program is P-300, which occurs spontaneously and does not require extensive training. P-300 responses have been reported as adequate for ALS patients (Silvoni et al., 2009). Some of the best P-300 spelling applications have been developed by Farwell and Donchin, which are commercially available to the general public (Farwell and Donchin, 1988). Figure 2-15 shows the 6 x 6 matrix of symbols displayed as P-300 interface where rows and columns are flashing, allowing the user to concentrate on selected characters. The BCI registers these responses and generates commands to write desired words.

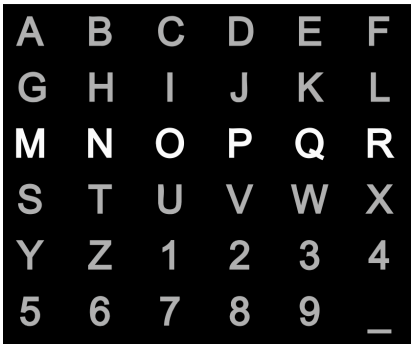

Figure 2-15 P-300 spelling program interface

Due to perceptual errors, which occurred with this traditional interface layout, a new design has been introduced, where letters were grouped in regions instead of rows and columns. This design uses two separate screens for character distribution.

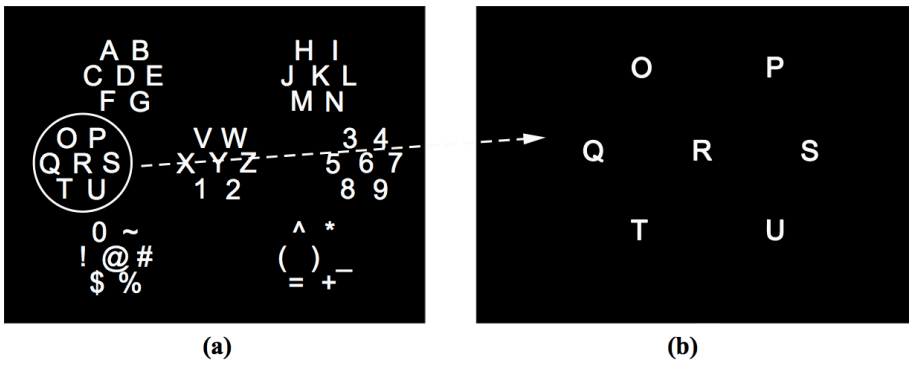

Figure 2-16 Alternative P-300 design

Perceptual error correcting interface with 2 screens approach: (a) the first screen of flashing character groups, (b) the selected group is expanded as individual letter ready for further selection (Fazel-Rezai and Abhari, 2009).

After initial selection of one group, the program redistributes its letters on the second screen as separate targets. The procedure is repeated until the desired word is written as shown in Figure 2-16 (Fazel-Rezai and Abhari, 2009). For patients with severe vision impairment an auditory stimulation can be used in P-300 paradigm (Furdea et al., 2009). Besides spelling programs, web browsing became an equally important mode of communication due to the increasing importance of the Internet in our daily routines. One of the first web browsers using SCP is called 'Descartes' (Karim et al., 2006). The links are alphabetically arranged as a tree, which the user can select or reject by positive or negative SCP shifts. A better approach presents a browsing program called 'Nessi', which overcomes some of the problems existing in 'Descartes' (Bensch et al., 2007). This approach creates coloured frames around the links or other selectable object such as graphics discarding tree design altogether.

Apart from communication, environmental control is becoming equally important for people with disabilities. Being able to control home appliances such as TV, light, and ambient temperature is crucial to improve the quality of life for people with severe motor disabilities. Achieving certain level of independence is beneficial for the patient's rehabilitation and lessens the caregiver's work intensity, thus reducing the costs. There are examples of both non-invasive and invasive modalities applied for testing. A pilot research has been reported by Cincotti et al. (2008) proposing BCI technology integration in a home environment. Multiple patients with motor disabilities were tested, using various control interfaces including computer keyboard, mouse, joystick, head trackers, microphones with voice recognition, and finally a BCI system utilising voluntary modulations of sensorimotor rhythms. For signal output, several domestic devices such as Lights control, TV, Stereo set, Mobile bed, Sound alarm, Door opener, Telephone, and Wireless CCTV cameras were targeted.

An invasive system was tested and documented by Hochberg et al. (2006) an EEG reading sensor was planted in patient's primary motor cortex. The patient could successfully use computer cursor, send email messages, and operate TV, by imaginary limb movement, which could be executed even during conversation.

2.11.1.2 Motor Restoration and Locomotion

Another neurological disability called spinal cord injury (SCI), which is still treated as a life-long disease, presents an opportunity to test BCI's potential to offer patients certain degree of motor independence and alleviate their social hardship, and psychological distress. As demonstrated by Pfurtscheller et al. (2000), a patient with an upper spinal cord injury, after undergoing extensive training, controlled a hand orthosis, opening and closing the hand without any errors, using imaginary movement. After a few years of development, the same research group successfully used an implanted neuroprosthesis, proving the concept of controlling such device with brain signals, was possible. This implanted neuroprosthesis demonstrated that BCI was able to detect EEG patterns with decreased power in certain frequency bands, generated by the user's imaginary movement (Müller-Putz et al., 2005). A different concept was introduced to move a dual-axis neuroprosthetic hand using an SSVEP-based BCI. Four blinking LEDs were placed, each on a different finger, flickering at different frequencies 6 Hz, 7 Hz, 8 Hz and 13 Hz which allowed the turning, opening and closing of the hand (Muller-Putz and Pfurtscheller, 2008).

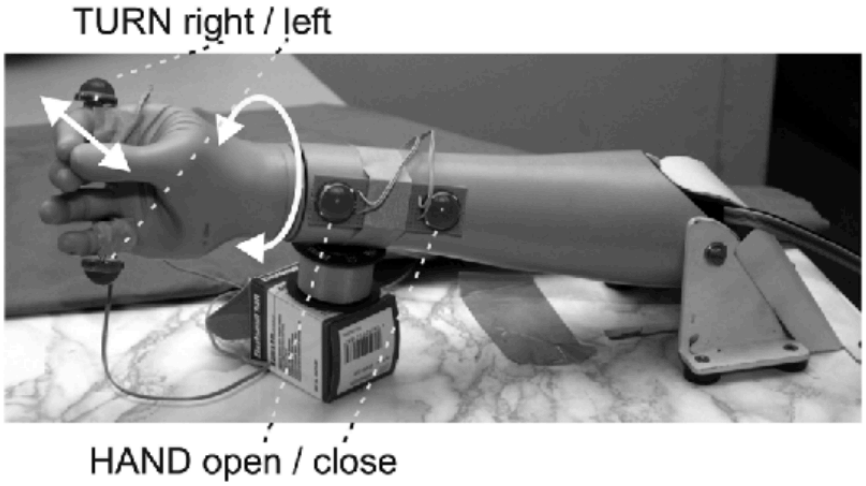

Figure 2-17 SSVEP-operated prosthetic hand (Muller-Putz and Pfurtscheller, 2008)

Four blinking LEDs allow controlling two-axis robotic arm by changing the user's gaze between the stimuli elements.

Portable and relatively lightweight BCIs, usually EEG-based, can also be used to enable people with disabilities to control and autonomously drive different means of transportation, e.g. wheelchairs. Due to noisy signals and low ITR the main challenge is to ensure that the commands

are sufficiently accurate to evoke a correct response. As already mentioned in this work, invasive methods work best with devices requiring continuous control (Serruya et al., 2002). Due to the high health risk with humans, non-invasive systems are preferred and suggested as most appropriate. Pilot experiments illustrate the feasibility of BCI application for mobile robot continuous control, especially indoors with rooms, corridors and doorways (Millan and Mourino, 2003). Tanaka et al. (2005) reported the first wheelchair fully driven using only EEG signals. Using left and right hand imaginary movement protocol, the 6 users were able to drive a wheelchair over square-segmented floor. To combat low ITR and accuracy, a synchronous P-300-based BCI was proposed. A simplified wheelchair control was designed to limit the number of needed user commands. The system was fed with data about environment guide-paths. Using P-300 the patient controlled the wheelchair by selecting predefined destination points and the wheelchair automatically followed the path. An odometer and a bar code scanner were used to enable the guided movement. The real shortcoming of such approach is limited flexibility of movement in unknown and populated environments (Rebsamen et al., 2007).

2.11.2 Non-Medical Applications

The use of Non-medical BCI systems present the widest group of applications due to a much less restrictive nature where no harm is presented to human health and wellbeing. Naturally in this group of applications non-invasive, portable and low-cost systems are preferred to guarantee potential attractiveness to a future wide end-user base. The majority of non-medical usage can be expected in the gaming and entertainment industries with potentially high economic incentives for early developers and adapters. Gaming and entertainment are already established industries, always looking for new and emerging technologies to accommodate their expansion. Consequently, the development of BCI applications is increasingly imminent and just a matter of time. A very promising concept is the idea of assisted learning with prospects of introducing new and revolutionary BCI assistive systems making learning more flexible, effective and attractive for learners. Such systems could help to fine-tune tutorials and improve learning tasks based on the individual capabilities of the learners. Neuromarketing is a new and innovative way of discovering a customer's buying preferences, based on their natural and usually involuntary response to products and services. Neuromarketing therefore, has the potential to replace problematic surveys and questionnaires. However, certain ethical issues associated with this method need to be critically addressed and solutions proposed.

2.11.2.1 *Gaming and Entertainment*

For gaming and entertainment applications the BCI should be based on relatively small, portable and low-cost devices. EEG is the one technique most suitable for such applications for the following particular reasons. There are already available commercial devices working as entertainment and gaming BCI interfaces. Among them is the Emotiv EPOC 14-channel EEG headset, which is also used for this research by the author (Figure 2-18). The headset can be purchased with an accompanying software development kit (SDK) and demo games such as Cortex Arcade and Spirit Mountain Demo game. The SDK helps game developers to adapt the headset to their games and other applications (Epoc, 2015). A company called NeuroSky has also developed a gaming system called MindWave accompanied with software application responding to the user's changing brainwaves and mental states (Figure 2-19). Similar to EPOC it also provides a set of programing tools allowing developers to create games and other software applications utilising the headset's control abilities.

Figure 2-18 Emotiv EPOC EEG headset with 14 sensors (Epoc, 2015)

The company also provides a set of biometric algorithms matching certain mental states such as attention, meditation, mental effort, familiarity or appreciation. This headset also allows the detection of eye blinks giving the programmers a very comprehensive set of features ready for application (EEG Headsets | NeuroSky Store, 2014).

Figure 2-19 NeuroSky MindWave EEG headset with 1 channel (EEG Headsets | NeuroSky Store, 2014)

Some of the largest software companies such as Microsoft have already expressed their interest in BCI technology integration in their future products (Microsoft Research—Computational, no date). Besides obvious control functionality, integration of BCI technology can augment the gaming possibilities and raise it to a higher level of user experience. For first-person games with avatars the BCI can help to convey the user's authentic attitude and even display facial expressions. This level of technology assimilation will create technological platforms to develop games and entertainment applications, which will be closer to real-life experience (Fun of gaming: Measuring the human experience of media enjoyment, no date). Successful implementation of SSVEP was reported by Middendorf et al. (2000) in a simple flight simulator game. The gaming object position could only be moved in one axis, in the direction of left and right. For this experiment two methods were tested. The first test detects signal strength and the second test detects signal frequency. According to test participants, the frequency method was preferred because it required no training and participants experienced no adverse effect.

2.11.2.2 Neuromarketing

New and innovative attempts have been made to commercially exploit brain signal in neuromarketing for marketing research proving reasonable usability in some areas, (Ambler et al., 2000; Ambler et al., 2004; Vecchiato et al., 2010; Cook et al., 2011). The neuromarketing method could significantly improve product testing at the very early stages of development saving unnecessary prototyping costs (Ariely and Berns, 2010). It is also believed that neuroimaging, as opposed to standard studies, would provide more precise and errorless data, revealing hidden customer preferences, where expressing them explicitly is usually problematic. Also, the

measurement methods of advertisement campaigns effectiveness could be improved by additionally quantifying them using natural brain response. There are already several companies exploiting such possibilities commercially. Among them are Neurofocus (Neuromarketing, Neuroscientific Consumer Testing. NeuroFocus, no date), Neuroconsultant (Neuroconsult, no date), Neuro Insight (Neuro Insight, no date), and EmSense (EmSense: Quantitative Biosensory Metrics, no date). However, despite attracting attention among commercial marketing providers and research communities, these methods have proven to be controversial regarding the ethical issues involved. Furthermore, the policy of employing technology to acquire information that is primarily involuntary raises more questions as to the possible compromise of human rights and the moral principles involved (Fisher et al., 2010).

2.12 Summary

This Section investigated all the crucial elements of most BCI systems concentrating on features used in this research. Firstly, the BCI block diagram has been presented pointing to all the stages involved in proper operation of a typical BCI system. Next, all the neuroimaging techniques have been briefly introduced and their main characteristics presented in Table 2-1. As the main technique used for this research, EEG has been discussed in detail along with the frequency bands and their characteristics, which can be observed in a healthy human brain using EEG as shown in Table 2-2.

Being a necessary element of worldwide neural research unification, the International 10-20 System has been briefly reviewed.

Next, in Table 2-3 the most popular in BCI development control signal techniques have been listed and their functionality and mode of operation have been comprehensively discussed, focusing on SSVEP as the paradigm intrinsic to this research. Due to the great variety of BCI topology used in research and working applications nowadays, different categories of BCI had to be established to differentiate between them.

The following categories have been distinguished and compared: exogenous vs. endogenous, detailing BCI dependency or lack of thereof on external stimulation; synchronous vs. asynchronous presenting distinction between BCI systems recording brain signals continuously or only during predetermined time slots; and finally invasive vs. non-invasive systems, where the former require surgery to place electrode array on the surface of the brain, while non-invasive is the completely safe and risk free option preferred by most of the research groups worldwide.

Various feature extraction methods have been described in great detail presenting their strengths and weaknesses along with most suitable applications. Artefacts in BCI systems constitute one of the most problematic features that confront researchers and developers. This forces them to search assiduously for new and effective methods to avoid, to minimise or completely remove unwanted transient or rhythmic parts of the brain signals. One of the last stages of the BCI signal processing described in this Section is referred to as Classification.

In Classification, after feature extraction, the system's algorithms are able to distinguish between similar portions of the signal based on periodic patterns, different frequency bands, phase, and amplitude strength. The classification stage assigns them to separate classes, which then can be used as separate commands driving and controlling a given application, which constitutes the last stage of BCI. Finally, different BCI applications are discussed regarding the main distinction between medical and non-medical applications.

The medical applications are associated with life improving communication and environmental control abilities, particularly in patients with locked-in-syndrome. They are also involved with motor restoration and locomotion in patients with spinal cord injury and other disabilities. The non-medical application has been presented as having the most potential for commercial applications that are suitable and more appropriate for a wider customer base, including activities such as gaming, entertainment and neuromarketing.

Chapter 3 Research Methods Used

3.1 Introduction

This Section demonstrates in detail the research methods employed as well as the software and hardware setup that was used for experiments. The overall research methodology, although in concept always consistent, evolved over time with the main objective being the improvement of the recorded brain signals quality by implementing different approaches based on gained experience. The methodology evolved also to improve the workflow, making the experiments easier to carry out. Vast changes have been introduced, especially in software, implementing a bespoke iOS tablet application. As it became clear during the work, certain new aspects potentially interesting for testing would always emerge, thus encouraging the author to adapt new equipment such as an RGB capable LED matrix for stimuli presentation**.** In addition to the software and hardware used, this Section also introduces a brain signal analysis approach, stimuli flicker design methods and their evolution, as well as the testing environment.

3.2 Hardware and Software Setup

3.2.1 Brain Signal Recording

For this research brain signals were always recorded using an off-line method for convenience and practical reasons. This means that the signals were recorded first as separate trials based on the experiment requirement. The number of trials and recording times varied, generally based on specifics of a given experiment, and usually resulted in tens and sometimes hundreds of recorded trials with duration between 10 to 60 seconds per trial. This factor determined the length of each experiment, which usually oscillated around 2-3 hours including hardware setup.

Firstly, the visual system of the subject was unaltered and remained the same over the entire period. Secondly, certain element of training resulting from repeated preliminary tests was noticeable and was especially manifested when testing similar scenarios with voluntary subjects including undergraduate students or the author's family members. This unfortunately, usually gave unsatisfactory results despite employing identical conditions. At the early stage of the flickering stimuli design, the tests were executed with only one subject, the author himself. It was a very long and tedious process requiring dedication and patience. During this time various parameters were adjusted and experimented with, including square wave vs. sine wave performance for transition between the flicker's animated frames. To overcome the common problem of achieving unrepresentative results by chance, all of the tests included multiple trials, especially important in

single scenario situations. This provided enough material to select best trials for analysis. Nevertheless, to satisfy the multiple subject-testing requirement, the final test with primary and secondary colour stimuli flickers was carried out with the results submitted for publishing.

3.2.1.1 Electroencephalograph Headset Emotiv EPOC

Raw EEG brain signals were captured as European Data Format files (EDF) by an Emotiv EPOC headset (Figure 2-18) wirelessly communicating with a Windows 7 based PC computer running Emotiv Xavier Test Bench software.

Figure 3-1 Emotiv EPOC - portable EEG headset (Epoc, 2015)

The headset conveniently allows for wireless brain signal streams to a PC computer via supplied Bluetooth dongle.

The signals were then analysed in MATLAB using EEGLAB and ERPLAB plugins for basic filtration and plots. To achieve better coverage of the occipital lobe, which is crucial for accurate SSVEP response analysis, the EPOC headset was rotated (Figure 3-2) as suggested by Manyakov et al. (2011).

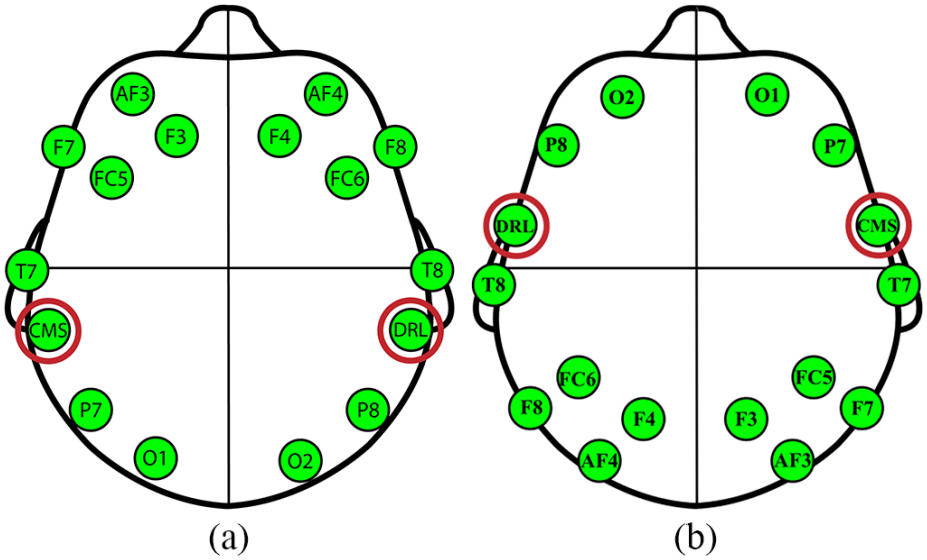

Figure 3-2 Emotiv EPOC sensor arrangement

(a) Shows default arrangement of the sensors, (b) shows rotated arrangement for better occipital lobe coverage. Sensors circled in red are reference electrodes (Research Use of Emotiv EPOC, 2015).

The EPOC device is equipped with 14 EEG electrodes accompanied by 2 reference ones (circled electrodes CMS and DRL as shown in Figure 3-2). It uses the following EEG locations for channels 1 to 14 in accordance with the 10-20 international system (Teplan, 2002) for signal acquisition: AF3, F7, F3, FC5, T7, P7, O1, O2, P8, T8, FC6, F4, F8, AF4. Although all channels were recorded, only channel 1 (AF3) was analysed. It needs to be clarified that the AF3 electrode in normal default position of the EPOC headset does not belong to the occipital lobe and it is located at the front of the headset. However, after the headset rotation this naming convention was maintained throughout this work. Whenever the AF3 electrode is discussed in this thesis, it indicates the actual AF3 electrode on the headset after rotation. The 10-20 System as detailed in Section 2.5, has been developed to unify the electrode placement for easy comparison and reproducibility of conducted EEG measurements.

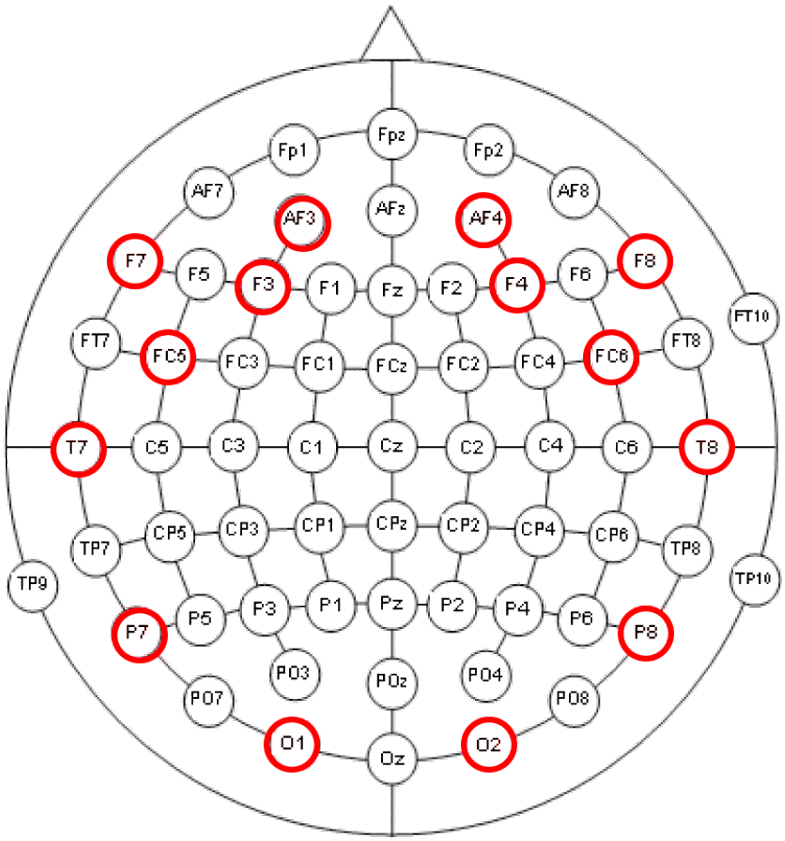

Figure 3-3 Emotiv EPOC electrode placement according to 10-20 System (Darah Juang and Dr. Dro!, 2017)

Circled in red are Emotiv EPOC electrodes.

The ’10-20’ refers to the percentage by which the electrodes are spaced away from one another (20%) and from nasion, inion and both ears (10%). The letters F, T, C, P, and O indicate frontal, temporal, central, parietal and occipital lobes. All electrodes marked as ‘z’ (zero) have been placed in the middle of the skull. Even numbered electrodes such as 2, 4, 6 represent right hemisphere placement while odd numbered electrodes (1, 3, 5) indicate left hemisphere placement (Teplan, 2002). EPOC headset is capable of capturing signal frequencies between 0.16 Hz and 43 Hz with internal sampling rate of 2048 Hz and 18 bits resolution (Emotive.Store.Compare, 2014). The signals are internally filtered and down-sampled to 128 Hz.

The sensors are saline soaked felt pads, which need to be kept wet while in operation as illustrated in Figure 3-4. The EPOC EEG device connects to computers with any operating system via the supplied USB wireless dongle (Figure 3-1). The accompanying software records raw EEG data, which then can be further processed and analysed (Epoc, 2015).

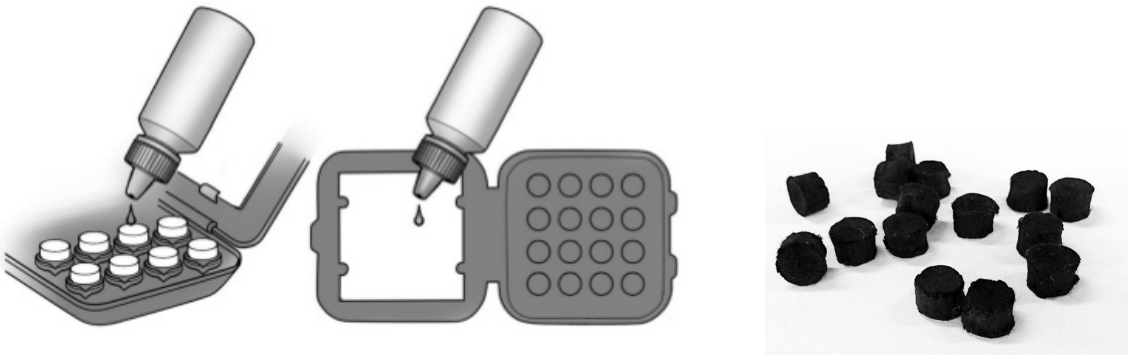

Figure 3-4 Saline soaked felt pads for EPOC headset (Epoc, 2015)

The saline solution can be applied to the sensor pads through the supplied storage box or directly on the headset.

3.2.1.2 Recording Software and Hardware Implementation

Signals for all tests were recorded using a USB dongle, which enabled wireless communication between the EEG headset and a standard PC computer running Windows 7 operating system. All the recorded EDF files were stored locally.

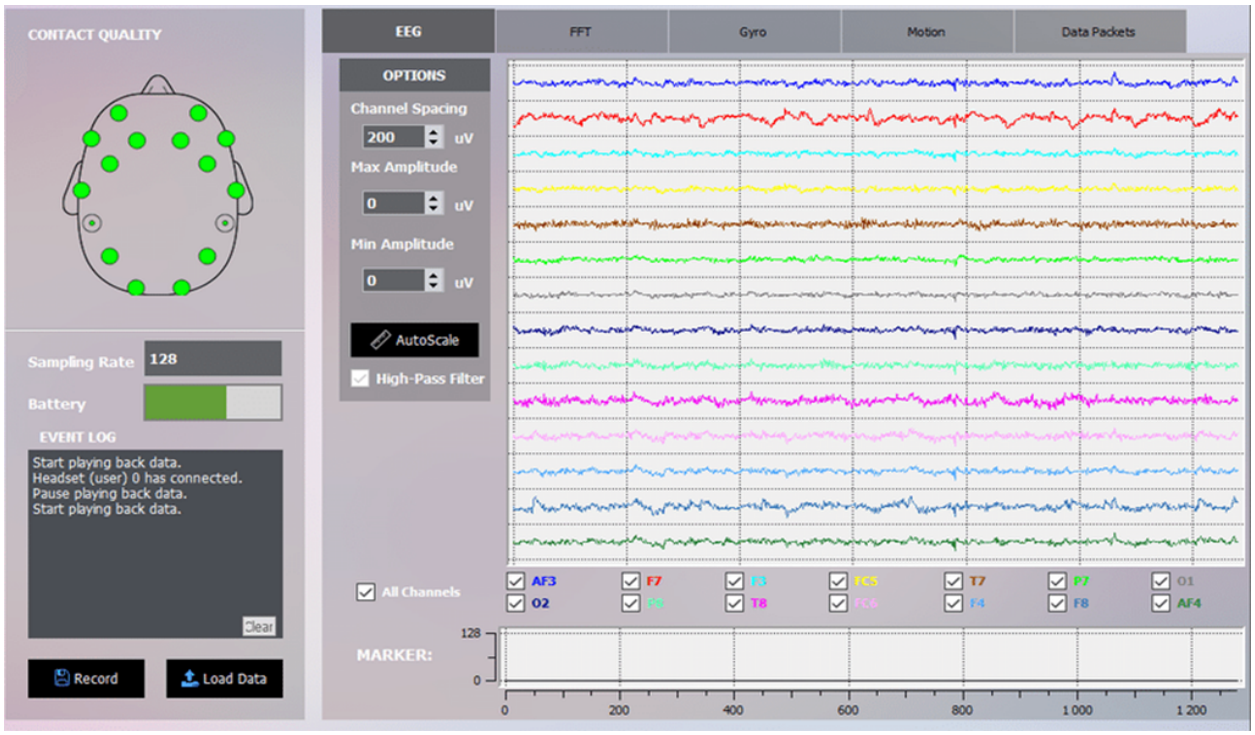

Figure 3-5 Emotiv Xavier Test Bench 3.1.19 application (Epoc, 2015)

Recording raw EEG signals from the headset's 14 channels.

For raw EEG signal capturing Emotiv EPOC's accompanying software called Emotiv Xavier Test Bench application was used. A screenshot of its GUI is shown in Figure 3-5. The application can

only record and playback the signals as an EDF file. The visible signal preview window can be used to monitor the brain activity and if necessary adjust sensor placement to avoid excessive noise and artefacts from the recorded signals. Also a contact quality widget is used to ensure that all the sensors are making proper contact with the scalp. This widget is using color-coded visual feedback. When all the sensors are green, the recording session may begin. All tests were recorded using maximum signal quality with the sensor icons green lit. The window also provides information about the state of the sampling rate, in this case indicating the default 128 Hz and state of internal battery charge of the headset.

3.2.1.3 Stimuli Presentation Setup

For the digital graphic stimuli presentation, a tablet with 12.9" screen running iOS system has been selected, as detailed in Figure 3-6. The most obvious caveat of such screen lays in its technical specification. Current panels lack the ability to display higher contrast ratios, which inherently impacts the quality of elicited EEG signals in the brain. However, the most recent developments in display technology promises improvements in this department. The latest development of Apple's iPad line up (iPad Air2, iPad Pro) employs screen performance enhancements called Photo Aligned Liquid Crystal Display (LCD) providing higher contrast ratios compared to the more common mechanical alignment of the iPad Mini 4. The display's maximum contrast is the ratio between the brightest white peak and the black darkest luminance and is considered to be one of the most important measurement factors in LCD quality tests (Soneira, 2015). All of the iPad devices score very highly in this department from 967 for the iPad Mini 4, 1,064 for the iPad Air 2 up to 1,631 for the iPad Pro, which is the highest score ever measured in any LCD tablet as reported by the testers from www.displaymate.com webpage (Displaymate.com, 2019). Additionally, the iPad Pro is equipped with metal oxide TFT back plate, which essentially increases the light throughput, thus improving its power efficiency (Soneira, 2015).

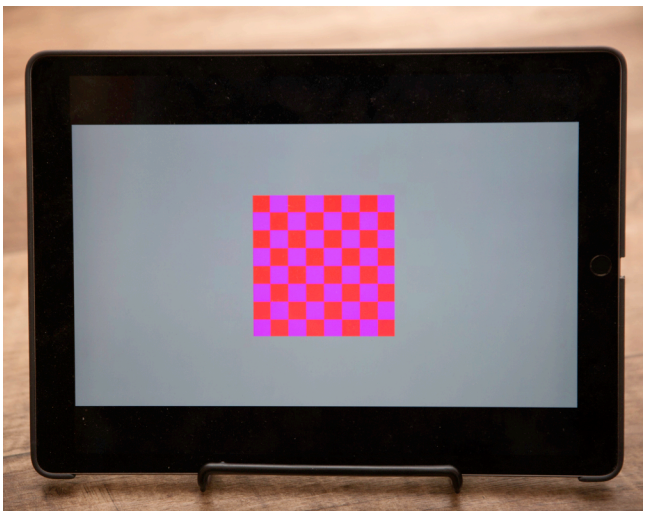

Figure 3-6 Tablet with 12.9" screen for stimuli presentation (iPad Pro 12.9" second generation)

Colour spectrum and absolute colour accuracy of the used display are of utmost importance when judging how certain colours impact the EEG signals in the brain. Most of the manufacturers calibrate the display to a very high accuracy with only minor shifts towards cooler (blueish white point) or warmer (yellowish white point) of the displayed colours. These technological advancements in the quality of LCD displays require more structured and organised research where human vision response to different colours, their mixtures with white, black and different shades of greys, can be more accurately tested and possibly implemented to future BCI systems. Such complete systems could be entirely operated by modern tablet devices with their ever increasing computing power and the quality of graphics.

3.2.1.4 Alternative Solution Using Arduino Uno

In one of the experiments described in Chapter 4, an RGB Arduino shield with an array of 40 RGB full-colour LEDs was used as shown in Figure 3-7 for testing the brain's response to visual stimulation, using different patterns. The shield is very versatile for this kind of research as well as final BCI application. It can display any colour from the RGB palette at any desired light intensity. After programming, it can generate any flickering pattern at any frequency. This shield, even mounted on Arduino board, is very small and lightweight making it a perfect solution for portable, multi-command BCI systems.

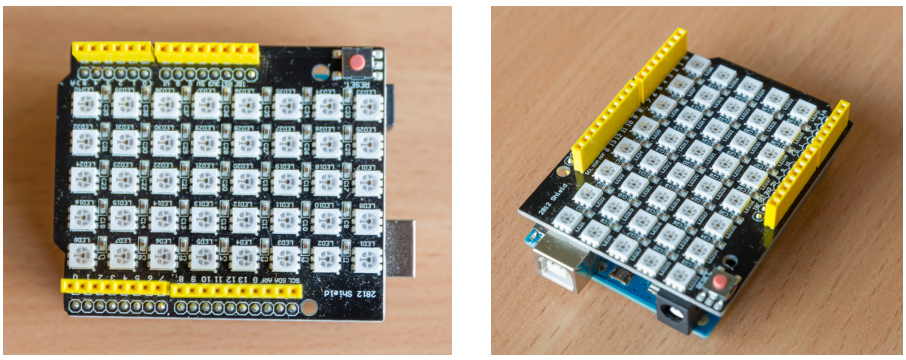

Figure 3-7 Keystudio WS2812 RGB LED shield for Arduino board

The matrix has 40 LEDs, which can be individually addressed, capable of displaying full range of RGB colours.

For this research ten different patterns have been programmed. For each pattern all possible single RGB primary and secondary colours with both white colour (light) and black colour (no light) combinations have been prepared along with a variety of two-colour and multicolour varieties bringing the total number of flicker designs to 749. For each programmed pattern facilities have been provided to quickly adjust light intensity level as well as flickering frequency.

3.2.2 Brain Signal Analysis

Although a few aspects evolved over the course of research such as the tablet replacing a laptop screen for stimuli presentation, or a custom tablet application replaced individually generated stimuli graphic flickers, one aspect remained the same. From the very beginning, all the recorded raw brain signals were processed using a very minimalistic technique in order to maintain a high degree of result comparability. The main purpose of this approach was to minimise any possible impact of excessive signal filtering or any other destructive processing on the results. From the very start of the research, the main focus was to achieve the highest possible raw brain signals prior to any filtration, which is associated with the initial signal processing stage in BCI. Therefore, after signal capture in EDF file format, the signals were imported to MATLAB using EEGLAB plugin (Sccn.ucsd.edu., 2019). In a majority of the tests conducted for this research, before the final signal plots were generated, only data detrending (in EEGLAB called ‘remove baseline’) was applied. Very basic filtration, usually in the form of low-pass and high-pass filters was applied to individual signals bearing traces of signal pollution in the lowest band between 0.1 Hz – 1 Hz. The filter parameters were always set in such a way that their filtering boundaries would never overlap the frequency band of interest. The EPOC headset automatically removes the common 50 Hz electromagnetic pollution during the signal capture.

3.2.2.1 *Brain Signal Analysis Hardware Setup*

For the signal processing tasks, a MacBook Pro 17” laptop running MATLAB, EEGLAB plugin, and ERPLAB toolbox was used as shown in Figure 3-8 (ERP Info, 2019). At the very early stage of the research, before employing the aforementioned 12.9” tablet, this computer was also used for stimuli presentation.

Figure 3-8 MacBook Pro laptop with 17" screen

The computer was used to perform signal processing and plots. Initially also used for stimuli presentation.

3.2.2.2 *Brain Signal Analysis Software Setup*

MATLAB was used to import raw brain signals, process and generate plots. Early on, two signal-processing open-source add-ons EEGLAB and ERPLAB were installed to speed up the workflow. EEGLAB is considered by many BCI researchers a popular and useful plugin for MATLAB enabling quick signal review, manual or automatic artifact removal, signal detrending, filtering and generating plots. Although ERPLAB has been mainly developed to assist researchers utilising Event Related Potentials (ERP) approach, it also has useful alternative filtering and plot generating functions often used in this research. EEGLAB GUI (Figure 3-9) is initiated by typing ‘eeglab’ in MATLAB’s command window. ERPLAB plugin however shows as part of the EEGLAB’s main menu giving access to multiple useful functions such as filter design or quick single channel frequency response plotting.

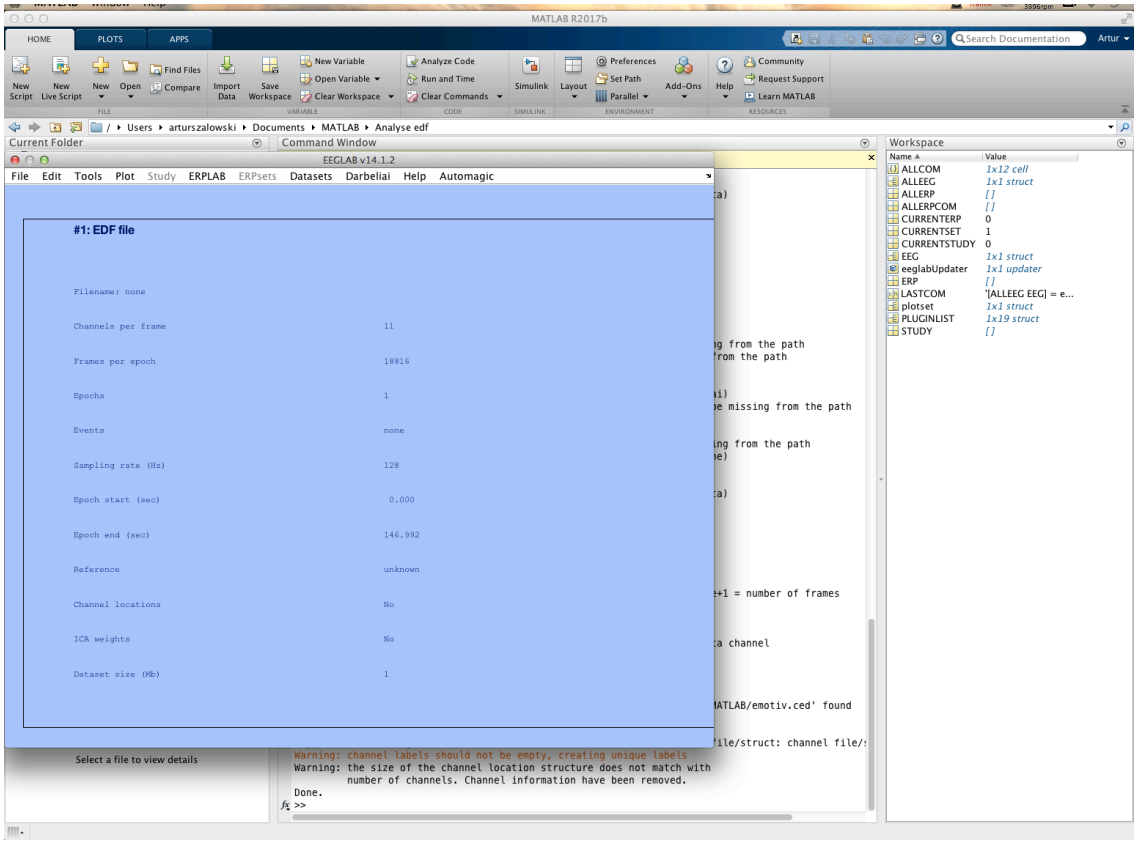

Figure 3-9 EEGLAB plugin with GUI initiated in MATLAB

To import an EDF file format through the plugin one must download the 'BIOSIG data import' add-on. 'Load data using BIOSIG' window pops up (Figure 3-10) enabling to specify which EEG channels are to be investigated. The raw brain signal data recorded by EPOC headset is assigned to channels 3 to 16 in the software since channels 1 and 2 carry other types of data not related to brain signals.

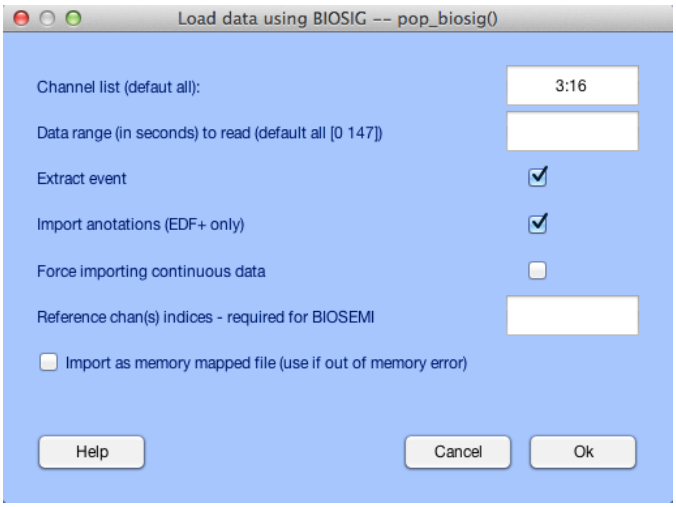

Figure 3-10 EDF loading window in EEGLAB

Channel list parameter shows channels 3 to 16 chosen for processing.

A very important stage of signal processing involved signal detrending, referred to as 'baseline removal' in EEGLAB. Function Tools-Remove baseline was used opening the window 'pop_mbase' as shown in Figure 3-11. Baseline signal shift can be caused by poor contact of the electrodes, perspiration under the electrodes, variations in temperature as well as by instrumentation or amplifiers bias. This may change the electrode's impedance, which in turn affects low frequency artefacts. This type of signal disturbance is undesired in EEG data and must be removed before any further signal processing is undertaken, mainly for proper analysis, displaying and plotting EEG signals.

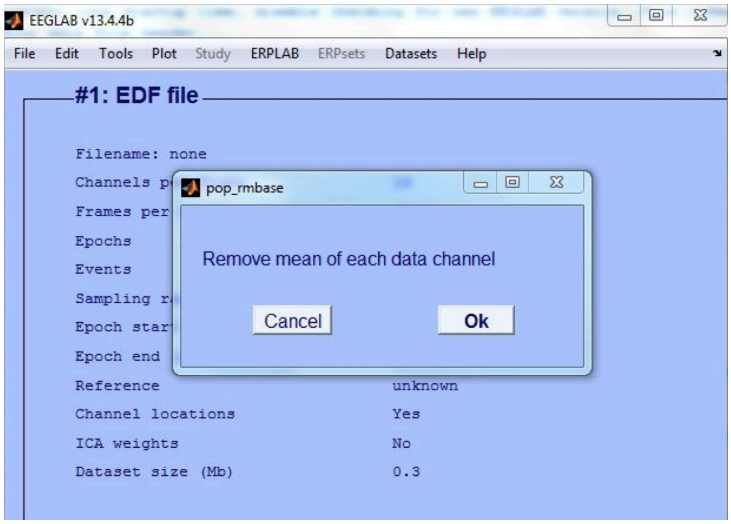

Figure 3-11 'Remove baseline' function in EEGLAB

The remove baseline function is the EEGLAB's equivalent to MATLAB's detrending.

To quickly review all 14 channels of captured brain signals as waveform the function 'Plot-Channel data (scroll)' can be initiated (Figure 3-12). It allows visual inspection of the recorded data in order to detect any sudden transient spikes artefacts in the signal.

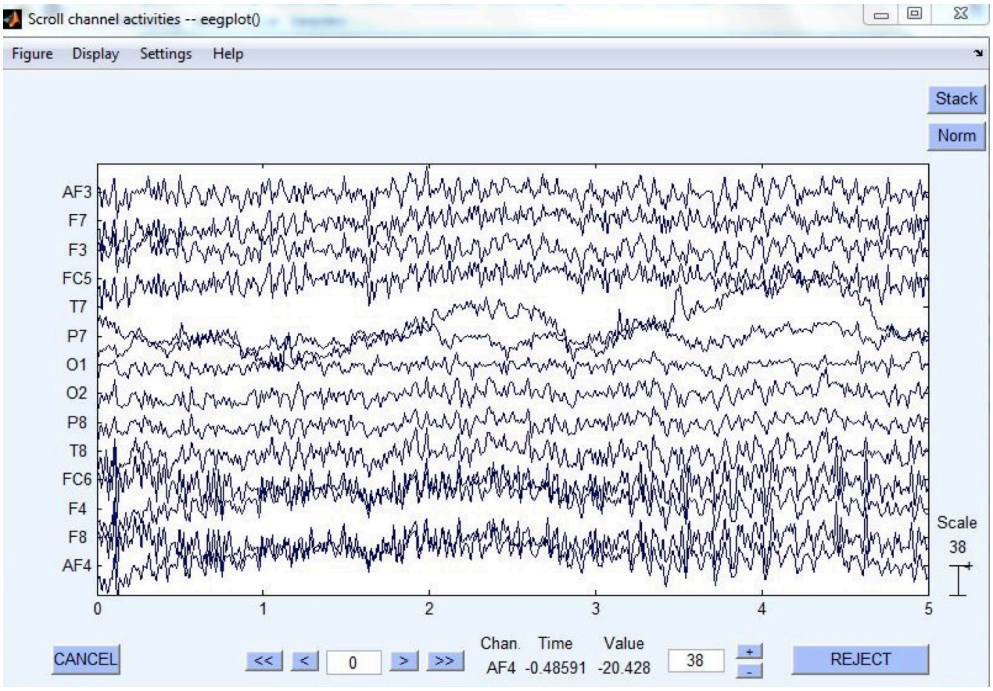

Figure 3-12 'Scroll channel activities' window shows signals as waveform in EEGLAB

This window conveniently allows manually selecting and removing the unwanted portions of the data. After highlighting the problematic section 'Reject" button removes the section and saves the dataset as a new file (Figure 3-13). Due to this functionality the original dataset can be retrieved at any stage of the signal processing.

EEGLAB is also equipped with basic feature extraction algorithms and among the most popular for SSVEP is Independent Component Analysis (ICA) as detailed in Section 2.8.1. The function (Figure 3-14) can be found under Tools-Run ICA. Decomposing data by ICA involves a linear change of basis from data collected at single scalp channels to a spatially transformed "virtual channel" basis. This means that a collection of simultaneously recorded single-channel datasets is transformed into the signals that represent a collection of simultaneously recorded outputs of spatial filters applied to the whole multi-channel EEG recording.

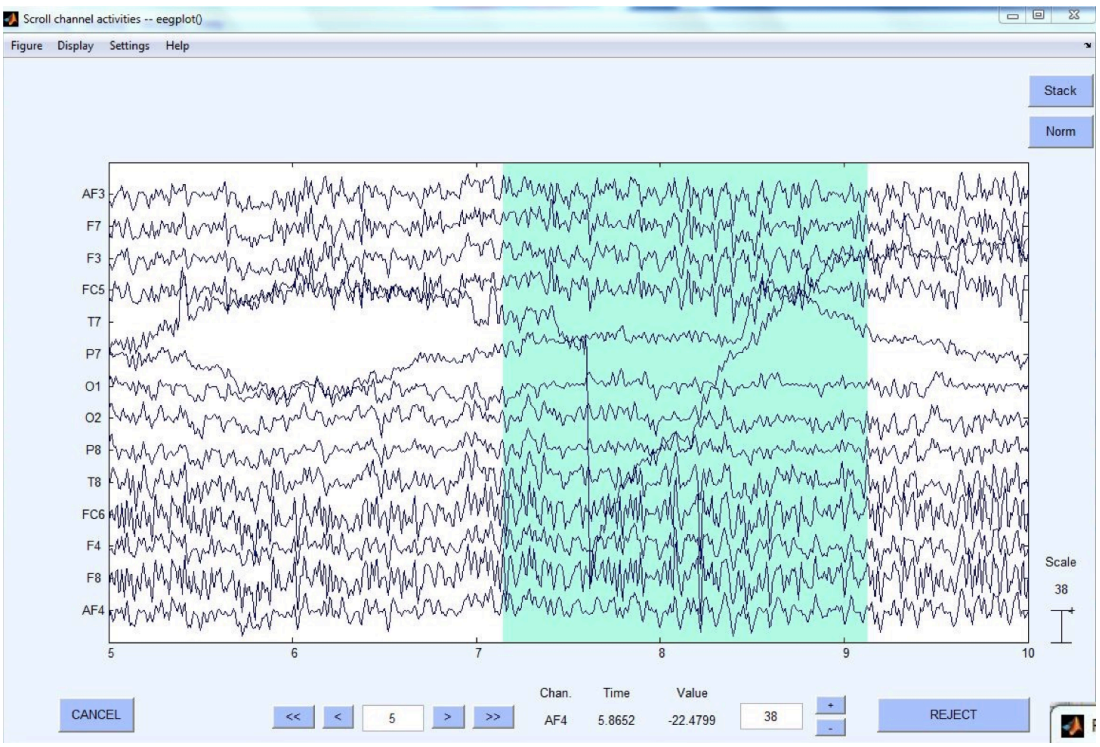

Figure 3-13 Manual artifact selection and rejection

An example of such signal transformation can be observed in Figure 3-15. The upper plot shows signal waveforms across all channels as they appear during raw EEG recording. The lower plot shows patterns found by the ICA algorithm and assigned to corresponding channels.

Figure 3-14 ICA algorithm in EEGLAB

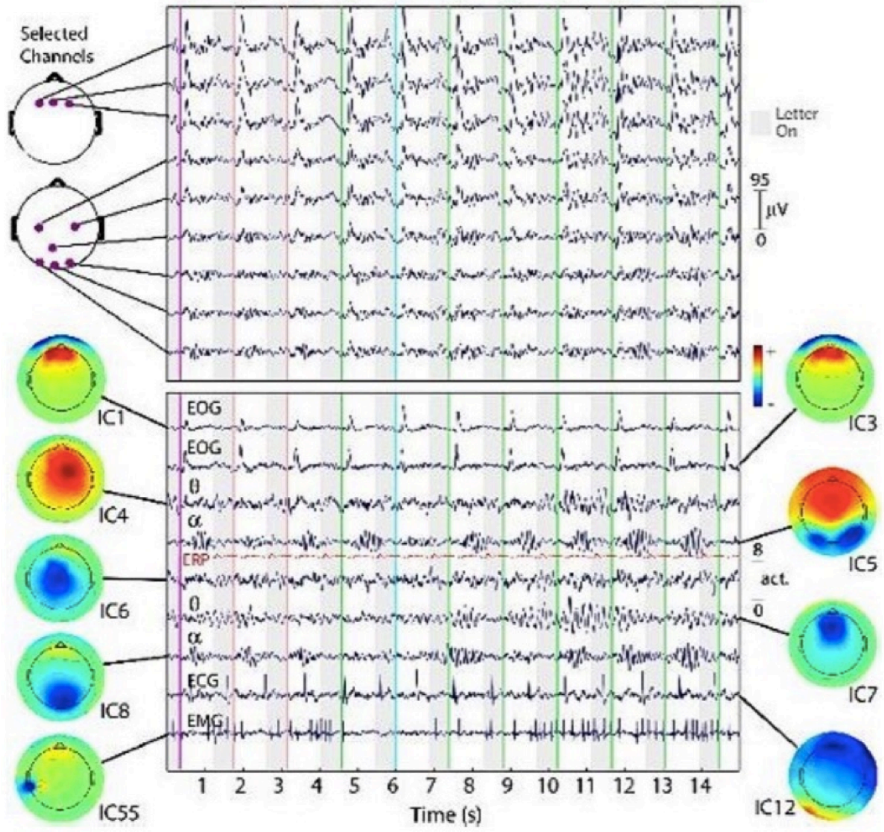

Figure 3-15 EEG channels before and after ICA transformation (Sccn.ucsd.edu, 2019)

Different colours shown in the brain maps indicate distribution of power for specific frequency or pattern. Colours red and blue represent positive and negative polarities of dipoles.

Another EEGLAB's very useful plotting option allows viewing peaks in captured brain signals using all available channels. This is called 'Channel spectra and maps' and is available under 'Plot' menu. In this function it is possible to specify exactly which frequencies are of interest and the range at which the search is to be performed as seen in Figure 3-16.

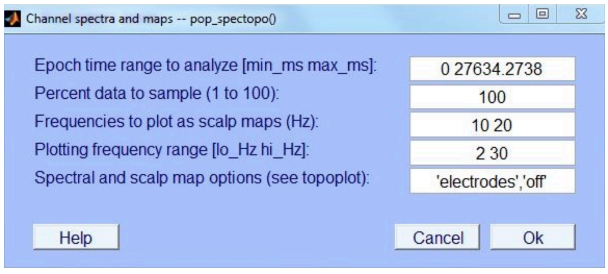

Figure 3-16 'Channel spectra and maps' function parameter window in EEGLAB

The resulting plot displays EEG signals using colour brain maps where red represents the highest (positive) and blue represents the lowest (negative) potential of a dipole. This allows determining at which parts of the brain certain activities take place. At the same time frequency peaks, which are correlated to these activities are shown (Figure 3-17). Plot exhibited in Figure 3-17 shows brain

maps and signals peaks after the EPOC headset rotation. The increased brain activity indicated by the red colour showed in the frontal lobe actually occurred in the occipital lobe. Henceforth, all the brain maps presented in the figures reflect signals present at the occipital lobe after the headset rotation.

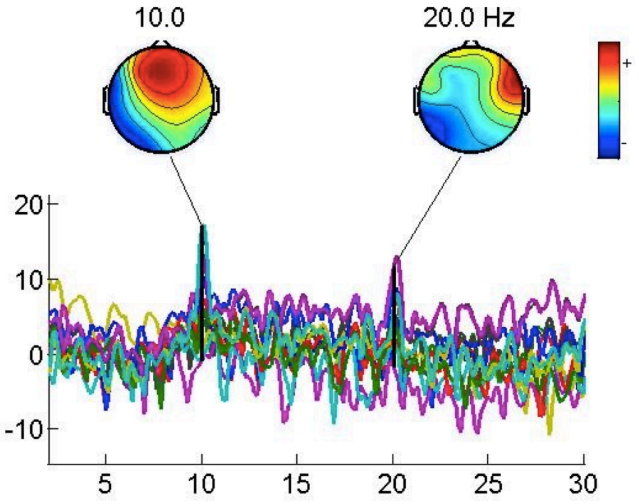

Figure 3-17 'Channel spectra and map' plot in EEGLAB

Plot showing increased brain activity at 10 Hz and 20 Hz.

ERPLAB plugin was used for signal filtration and an alternative view of elicited signal peaks. This plugin is particularly convenient since it provides the facility to select individual EEG channels and display their spectral response. Only a very simple high-pass filter was used in extreme situations where excessive low frequency pollution appeared in individual recordings. Usually a IIR Butterworth filter was applied in such a scenario with cutoff boundary set between 1 Hz and 2.5 Hz (Figure 3-18) to avoid any signal distortion within the frequencies of interest i.e. 6 Hz to 12 Hz for the Alpha range and beyond up to 40 Hz in some cases, where harmonics could be expected.

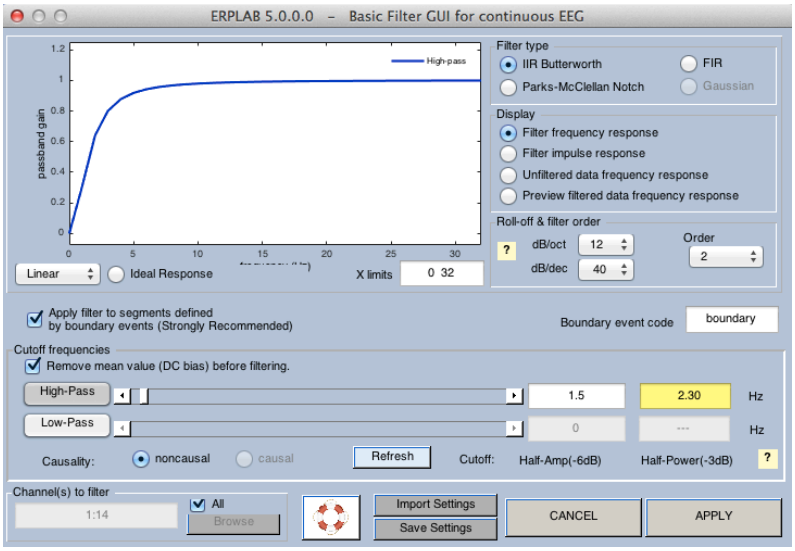

Figure 3-18 Filter GUI in ERPLAB plugin

These exemplify various processing and plotting functions used when analysing brain signals recorded during research experiments.

3.2.2.3 Fast Fourier Transform in Brain Signal Peaks Extraction

Brain signals can be compared to sound. A sound that exists in nature is constructed of many sinusoidal oscillations added together. These sinusoidal sound waves are referred to as pure tones, which do not exist in nature and usually can be generated by sound synthesisers or audio manipulating software. Each pure tone has its own frequency. The more frequencies are added together, the more complex and richer in harmonics the resulting sound is. By reversing this process, one can apply mathematical calculations to a complex sound in order to reveal its sinusoidal frequency components. The same process can be applied to the brain signals, which can be viewed as multiple frequencies in the range between 0.1 Hz and 90 Hz with amplitudes fluctuating over time. In order to deconstruct these frequencies into sinusoids from a data source, a mathematical operation known as Discrete Fourier Transform (DFT) is required. The DFT is one of the most powerful and often used tools applied in signal processing enabling the viewing of spectral content in a finite duration signal. For the DFT processing, digitisation of the signal is needed, by acquiring data samples for the duration of T seconds (Tan, 2007). Thus, the periodic signal $x(n)$ is captured by copying the obtained N data samples with the duration of T to itself repetitively. Fourier series coefficients can be determined by using one-period N data samples and Equation (9).

$$c_k = \frac{1}{N}\sum_{n=0}^{N-1} x(n)e^{-j\frac{2\pi kn}{N}},\ k = 0,1,\ldots,\ N-1 \tag{9}$$

Next, Fourier series coefficients are multiplied by a factor of N to obtain the Equation (10)

$$X(k) = Nc_k = \sum_{n=0}^{N-1} x(n)e^{-j\frac{2\pi kn}{N}},\quad k = 0,\ 1,\ldots,\ N-1 \tag{10}$$

where $X(k)$ constitutes the DFT coefficients. It should be noted that the factor of N is a constant and does not affect the relative magnitudes of the DFT coefficients $X(k)$. Applying DFT with N data samples of $x(n)$ sampled at a rate of f_s (sampling period is $T = 1 / f_s$) produces N complex DFT coefficients $X(k)$ (Tan, 2007).

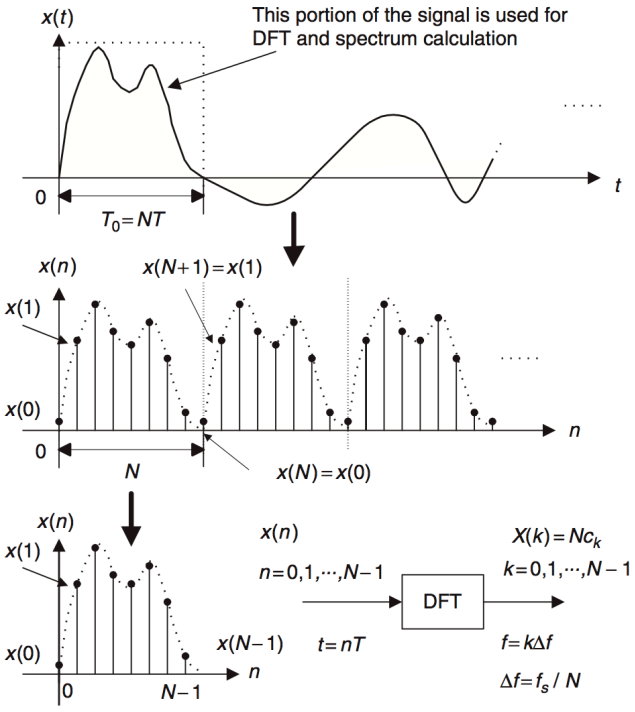

Figure 3-19 Development of DFT formula (Tan, 2007)

The index n is the time index representing the sample number of the digital sequence, whereas k is the frequency index indicating each calculated DFT coefficient, and can be further mapped to the corresponding signal frequency expressed in Hz. To conclude the DFT definition, with a given sequence $x(n)$, $0 \le n \le N-1$, its DFT is defined as

$$X(k) = \sum_{n=0}^{N-1} x(n) e^{-j2\pi kn/N} = \sum_{n=0}^{N-1} x(n) W_N^{kn}, \text{ for } k = 0, 1, \ldots, N-1 \tag{11}$$

and the Equation (11) can be expanded as

$$X(k) = x(0)\, W_N^{k0} + x(1)\, W_N^{k1} + x(2) W_N^{k2} + \ldots + x(N-1) W_N^{k(N-1)}, \quad \text{for } k = 0, 1, \ldots, N-1, \tag{12}$$

where the factor W_N is defined as

$$W_N = e^{-j2\pi/N} = \cos\left(\frac{2\pi}{N}\right) - j \sin\left(\frac{2\pi}{N}\right). \tag{13}$$

As illustrated in Figure 3-19, the sample number or time index *n* for indexing the digital sample sequence *x(n)* is used. In frequency domain, index *k* is used for indexing *N* calculated DFT coefficients *X(k)*. In Equations (11) and (12) *k* is referred to as the frequency bin number (Tan, 2007).

In MATLAB, the function **fft**() can be used to compute the DFT coefficients and the function **ifft**() for computing the inverse DFT with the following syntax:

Table 3-1 MATLAB FFT functions

X = fft(x)	**% Calculate DFT coefficients**
x = ifft(X)	% Inverse DFT
x = input vector	
X = DFT coefficient vector	

Fast Fourier Transform (FFT) was used throughout the entire research to identify the brain signal peaks from the recorded EEG signals. The DFT is a mathematical operation that transforms a discrete signal from its original time domain characterisation into its discrete frequency domain

representation. Computing the DFT of *n* points, which represent the data size, in any signal using the DFT's definition although very useful in many applications, is time consuming and often impractical task. The process is expressed by the following:

$$\text{Complex multiplications of} \quad \text{DFT} = N^2 \tag{14}$$

The same result can be computed by using the FFT algorithm, in which the amount of steps required to finish the calculation is expressed by the following:

$$\text{Complex multiplications of} \quad \text{FFT} = \frac{N}{2} \quad \log_2(N) \tag{15}$$

The reduction of DFT's calculation complexity arises from the FFT's ability to rapidly compute such transformations. To evaluate the effectiveness of FFT, a sequence with 1,024 data points can be considered. Applying DFT will require 1,024 x 1,024 = 1,048,576 complex multiplications. By comparison, applying FFT will need only (1,024/2) $\log_2$ (1,024) = 5,120 complex multiplications.

For large data sequences such as long epochs of brain signal recordings, this algorithm offers substantial gain in terms of time required to compute the transformation.

3.2.3 Stimuli Flicker Design

The author holds the Bachelor of Science (Honours) degree in TV and Media Production. The education and personal interest in professional graphics designing software were essential in developing stimuli graphics for the research. It has been envisaged by the author, from the very beginning that designing and executing stimuli flickers employing colour would be at the centre point of this work. However, after preliminary tests it was recognised that not just the colours need to be taken into consideration, but also other parameters must be tested such as graphics size/resolution and various flicker patterns. To achieve these goals the research methodology had to evolve incorporating different processes and techniques including hardware and software applications to finally arrive at the most efficient approach. Several changes were also introduced to stimuli presentation. Initially a 17" screen laptop running OSX operating system was used to display designed and generated flickers. As the work progressed, new challenges were apparent, such as the need to obtain a portable digital screen with best possible performance. The purchased iOS tablet with 12.9" screen presented new opportunities such as longer working hours on a single battery charge, a brighter screen with a more accurate colour reproduction. A bespoke iOS application was developed for this research to streamline the workflow. Also, the methods used to

design and generate stimuli flickers evolved with the main scope to arrive at timesaving processes. Furthermore, additional testing methods were proposed during the research to satisfy certain testing scenarios such as testing the brain's response to various stimuli patterns. This can be exemplified by the use of LED panel controlled by Arduino UNO (details in Section 4.2).

3.2.3.1 Flicker Design Using Vector Graphic Software

Adobe Illustrator CS6 is a professional vector graphic design application. It was used during the early stage of the multi-colour checkerboard flicker creation process. The main advantage of vector graphics is their unlimited scalability without the loss of resolution. In vector graphic software the design elements are not built out of pixels but rather using mathematical formulas, which work in the background of the software. When drawing a rectangular shape, the software does not "paint" pixels on an empty canvas, but instead it uses mathematical formulas and algorithms representing shapes, their colours, transparency and many other useful transformations. The shape being created can be transformed, its colours can be changed without the need to "erase and repaint" new pixels. Any drawn shape using available tools can be resized without losing resolution. In Adobe Illustrator CS6, there are over 100 tools for shape creation and manipulation as shown in Figure 3-20.

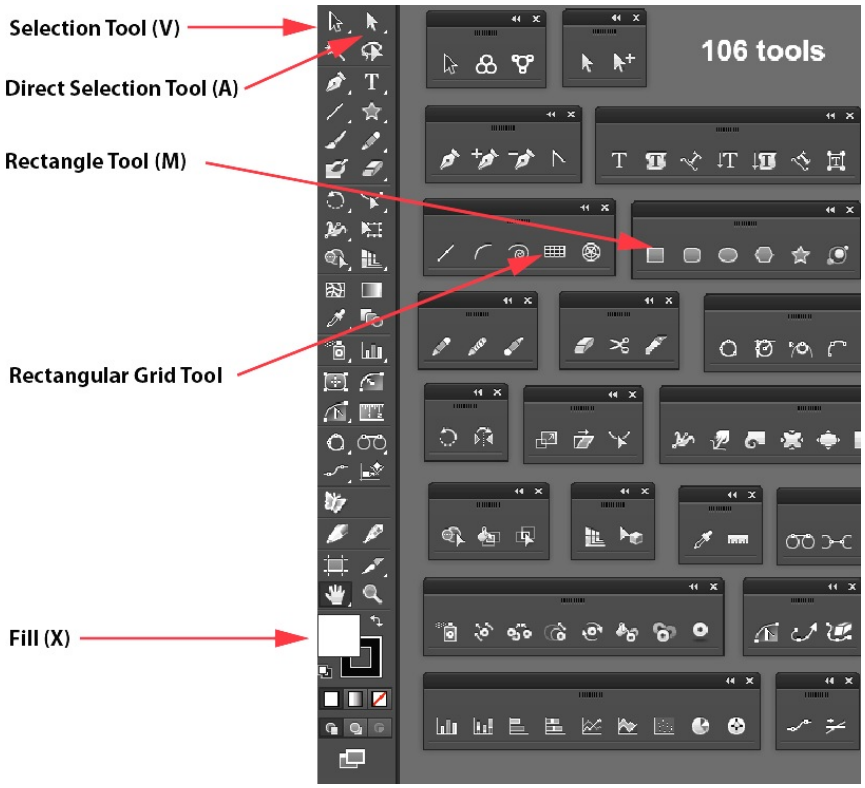

Figure 3-20 Adobe Illustrator available tools

There are over 100 graphic shape manipulation tools available in Adobe Illustrator.

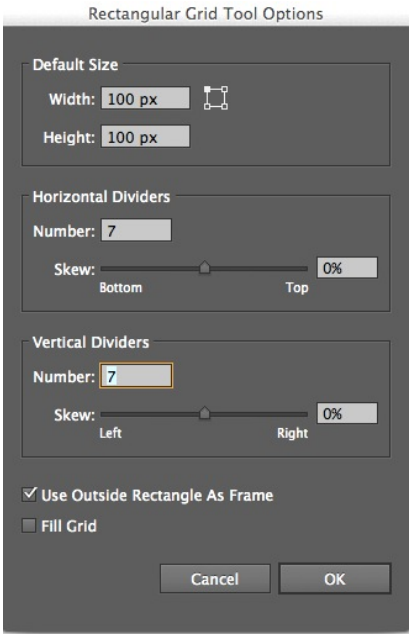

Figure 3-21 Rectangle Grid Tool Options window in Illustrator

The tool can generate rectangular grids by specifying horizontal and vertical dividers.

Some of the tools can be selected through keyboard shortcuts such as 'V' for Selection Tool, which is crucial when designing a graphic. Other tools used for the task described above were Direct Selection Tool (A), Rectangle Tools (M), Rectangle Grid Tools, and Fill (X). The Selection tool is used for general shape selection, moving or resizing, while the Direct Selection Tool allows selecting individual anchor points and segments within the shape in order to delete or move them, significantly changing appearance of the shape. After creating a square shaped Artboard (the design canvas) it can be filled with desired shapes. To create a checkerboard, pattern the Rectangular Grid Tool was used (Figure 3-20). After double-clicking the tool, a Rectangle Grid Tool Option window is presented giving many useful options including choosing required number of horizontal and vertical dividers to automatically generate any desired grid (Figure 3-21). The rectangle Tool was used to fill in all the fields with square shapes (Figure 3-22). To change colour of the rectangles the Fill (X) tool was used.

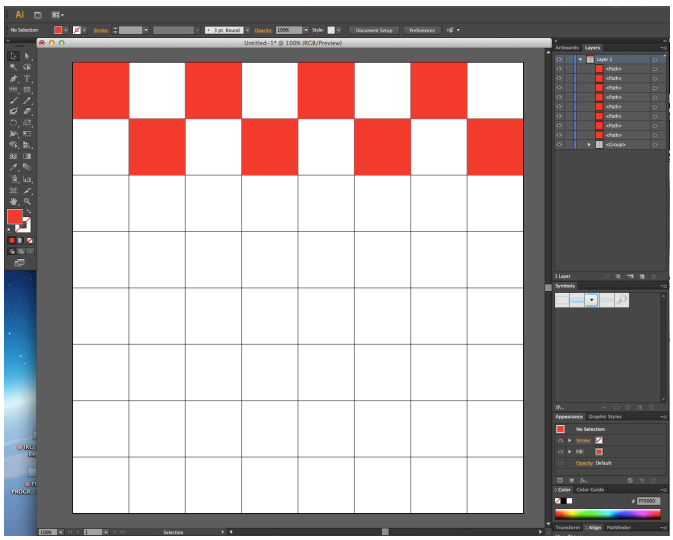

Figure 3-22 Rectangular grid with red and white checkerboard fields in Illustrator

By copying and pasting coloured squares the grid can be populated with the shapes.

When the basic checkerboard was created, all the remaining colour variants could be generated by selecting appropriate rectangle shapes and changing their colours using the Fill (X) tool. For each multi-colour checkerboard two states of the graphic had to be prepared: one starting with colour sequence ABAB etc. and one with reversed pattern BABA etc. (see Figure 3-23), so when animated they would generate the flickering animation.

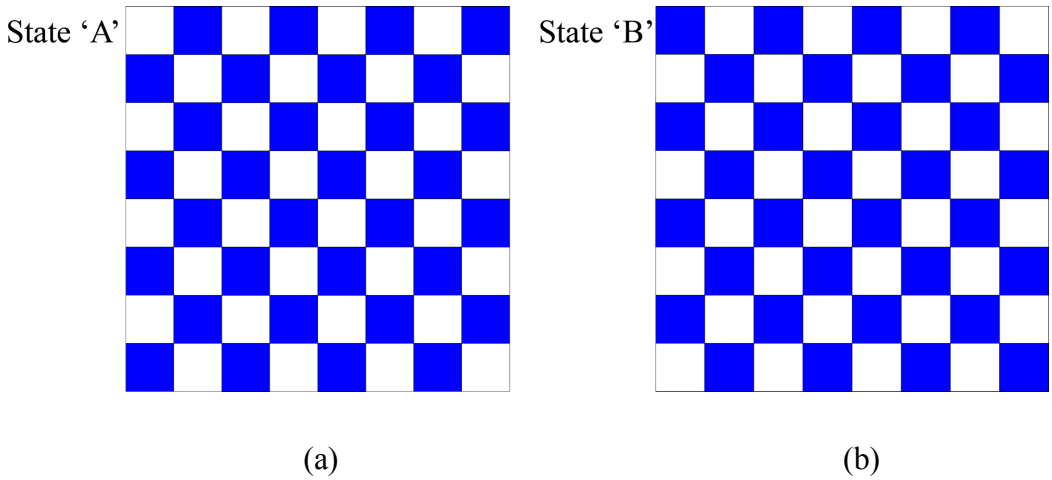

Figure 3-23 Two states of the checkerboard graphic using blue and white fields

Graphic (a) represents given sequence of colours ABAB forming state ‘A’ of the animation and graphic (b) represents pattern reversal BABA forming state ‘B’.

Despite automation facilities and design tool convenience available in the software, the process proved to be quite tedious and required dedicated attention to detail during the creation and rendering process. The multi-colour checkerboard combinations had to be composed of primary and

secondary RGB colours, as well as white, grey, and black, giving 34 variants for checkerboard flickers to be generated.

After the patterns were generated and rendered as Digital Negative (DNG) lossless raw image format files, they were imported into Adobe flagship animation, compositing and motion graphics software called After Effects CS6. In After Effects CS6 the two separate states 'A' and 'B' of the checkerboard pattern were animated as detailed in Section 3.2.3.2.

3.2.3.2 Flicker Design Using Animation Software

Adobe After Effects CS6 is professional animation software used for special visual effects compositing, motion graphics, titles and other animation tasks. Again, gradual evolution of the production technique can be observed with this software. In the preliminary flicker versions, the more manual and time-consuming method was used. The pre-designed multi-colour checkerboard patterns were imported into the software workspace. Each graphic constituted a single frame of the animation, therefore the animation's length had to be adjusted in order to generate any desired flickering frequency. The normal and reversed patterns were placed on separate layers to enable necessary manipulations as shown in Figure 3-25. First and third layers contain state 'A' and second and fourth layers contain state 'B' of the checkerboard pattern. When playing back the project, a short animation showing checkerboard pattern flicker could be observed. This phase of flicker design was crucial to achieve the desired frequency of the oscillation by calculating the relative number of animation frames per displayed sequence. The refresh rate of the display screen is 60 Hz. When dividing this value by the desired flicker frequency, e.g. 6 Hz, the resulting number of frames per cycle can be determined (Figure 3-24 and). Next this number needs to be divided by 2 to achieve the number of frames per each state of the graphic.

60 Hz / 6 Hz = 10 frames per cycle;

10 frames / 2 = 5 frames per each graphic state

i.e. 5 frames per state 'A' and 5 frames per state 'B'

Figure 3-24 Calculation determining number of animation frames per frequency cycle

Example for the 6 Hz frequency.

In order to generate an alternating flicker animation between the two states 'A' and 'B', 5 frames per cycle for each state of the graphic need to be adjusted as shown in Figure 3-25. In this figure (a) state 'A' is produced by sequences 1 and 3, while in (b) state 'B' is produced by sequences 2 and 4.

To achieve the final animation length, i.e. 60 seconds, further sequence pre-composing was necessary.

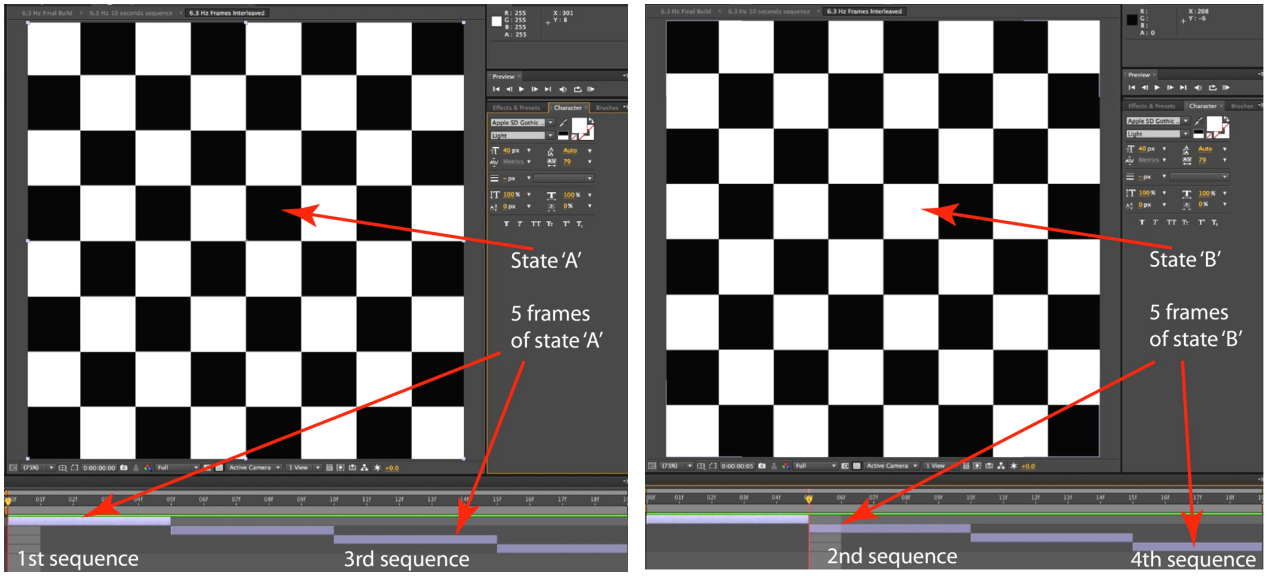

(a) (b)

Figure 3-25 Normal (a) and reversed (b) checkerboards animated in After Effects

By adjusting number of frames of each graphic different frequency could be achieved. This is an example of a very short sequence of alternating black and white patterns. The graphic (a) represents aforementioned state 'A' of the animation and the graphic (b) represents the reversed state 'B'. The lower part of the window indicated by 2 arrows shows short sequences composed of 5 animation frames each.

In subsequent steps, after determining the required flicker frequency, the short sequences were pre-composed, first into the 10-second pre-comp (Figure 3-26a) and then into the final 60-second animation as illustrated in Figure 3-26b. This animation project pre-composing approach enabled convenient frequency selection by only changing the relative number of frames in the initial short sequence presented in Figure 3-25. Each flickering animation had to be individually rendered as a separate video file, which then could be played back on any digital device.

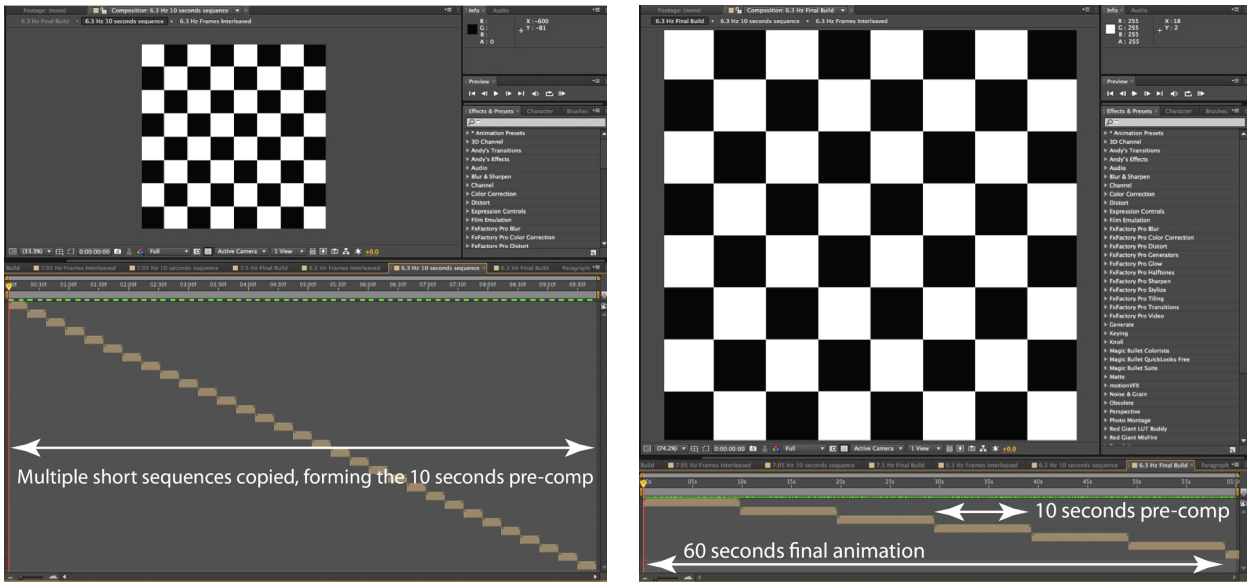

(a) (b)

Figure 3-26 Checkerboard flicker animation in main composition window of After Effects

The animation time length was adjusted by pre-compositing and multiplying the short sequence shown in Figure 3-25. In (a) the pre-composed segments of above mentioned short sequences generate a 10 second composition and in (b) the animation is achieved with the pre-composed 10 second sections multiplied and arranged into a 60 second final animation. In both (a) and (b) the relevant pre-composed sections are illustrated in the lower parts of the screenshots indicated by the arrows.

A more advanced method of checkerboard flicker animation using After Effects was developed in order to streamline the workflow. Through researching available animation options in After Effects, the expressions functionality and available pattern generators were used. Employing these features allows avoiding the unnecessary step of using the Adobe Illustrator graphics. Using the application's Effects & Presets one can select the Generate function allowing the use of the Checkerboard generator as shown in Figure 3-27. In this figure, there is visible the width parameter controlled by the slider determining how many squares in the checkerboard are generated. Also the available, the colour picker enables colour selection for desired set of checker squares. In order to create a two-colour flickering checkerboard, four graphic layers were used in the composition, two layers per one checkerboard colour as shown in Figure 3-29. The two layers work together, where one of them acts as a static pattern background and the other uses a sine expression to animate the checker's squares as detailed in Figure 3-28. Additionally, Toggle Transparency Grid had to be switched on in global composition settings to freely control the flicker checker's colours.

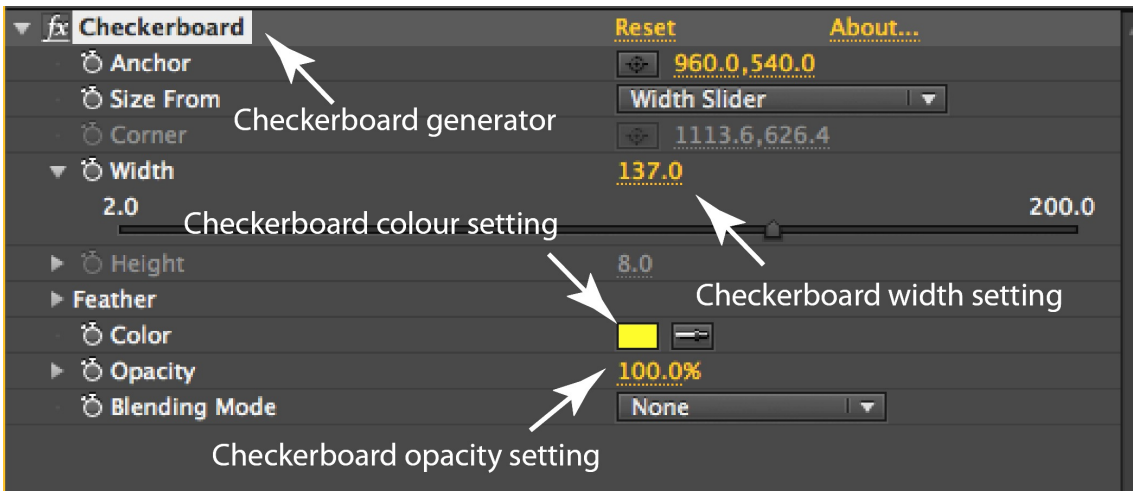

Figure 3-27 Checkerboard generator function in After Effects

The function allows creating a checkerboard of any size and field color, in this example yellow. The opacity parameter was used to generate the flickering behaviour.

The expression functionality was used to create graphic's animation. The expression used is shown in Figure 3-28 and it employs the trigonometric sine function enabling oscillation of the flicker. There are two parameters governing the flicker's behaviour; 'freq' adjusts the oscillation frequency and 'amp' regulates the amplitude.

```
freq = 10;
amp = 200;
value + amp*Math.sin(freq*time*Math.PI*2)
```

Figure 3-28 Expression formula in After Effects

By assigning the formula to layers' opacity parameter the flicker effect was achieved. The 'freq' parameter adjusts the flicker oscillation at 10 Hz and the 'amp' representing amplitude is set to 200.

By reversing the generated checkerboard pattern in the second pair of layers the flickering animation was achieved. In order to produce different frequencies in the flicker, the frequency parameter in the formula must be adjusted for both animation layers with the expression active. The expressions were linked to the active layer's opacity parameter, effectively controlling the overall flicker effect as illustrated in Figure 3-29. With the opacity parameter constantly changing between the values of 0 % and 100 % the flicker can be generated in the animation.

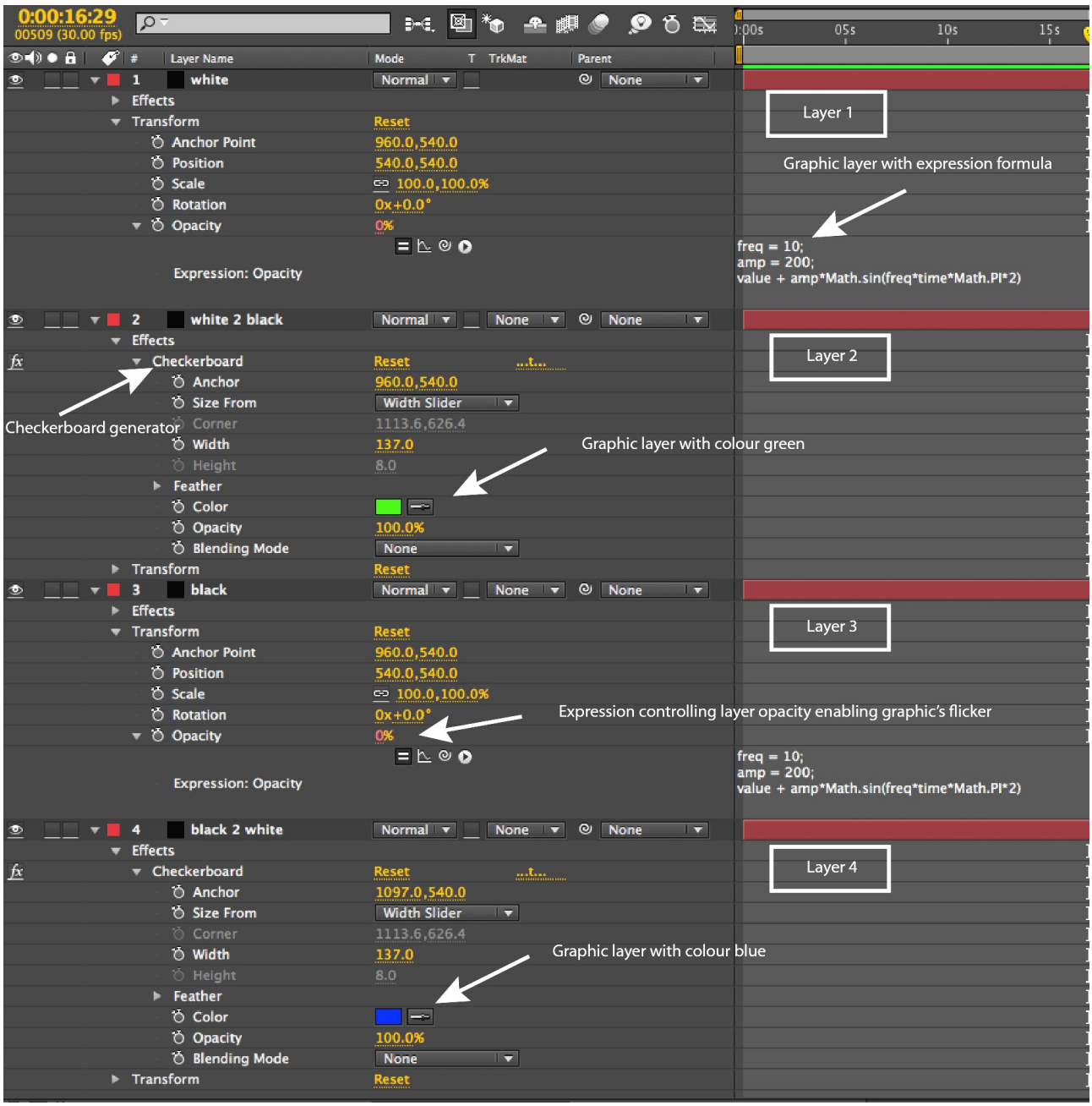

Figure 3-29 Expression formula in After Effects controlling layer's opacity parameter

In order to generate a 2-colour flickering checkerboard, in this example green-blue, four layers of graphic elements were used. Two layers contain static graphics and two other employ expression formula generating flickering behaviour.

As an added bonus, in the main composition window (Figure 3-30), the option of selecting black, white, and grey backgrounds for the flickering animations were added to expand on available testing scenarios.

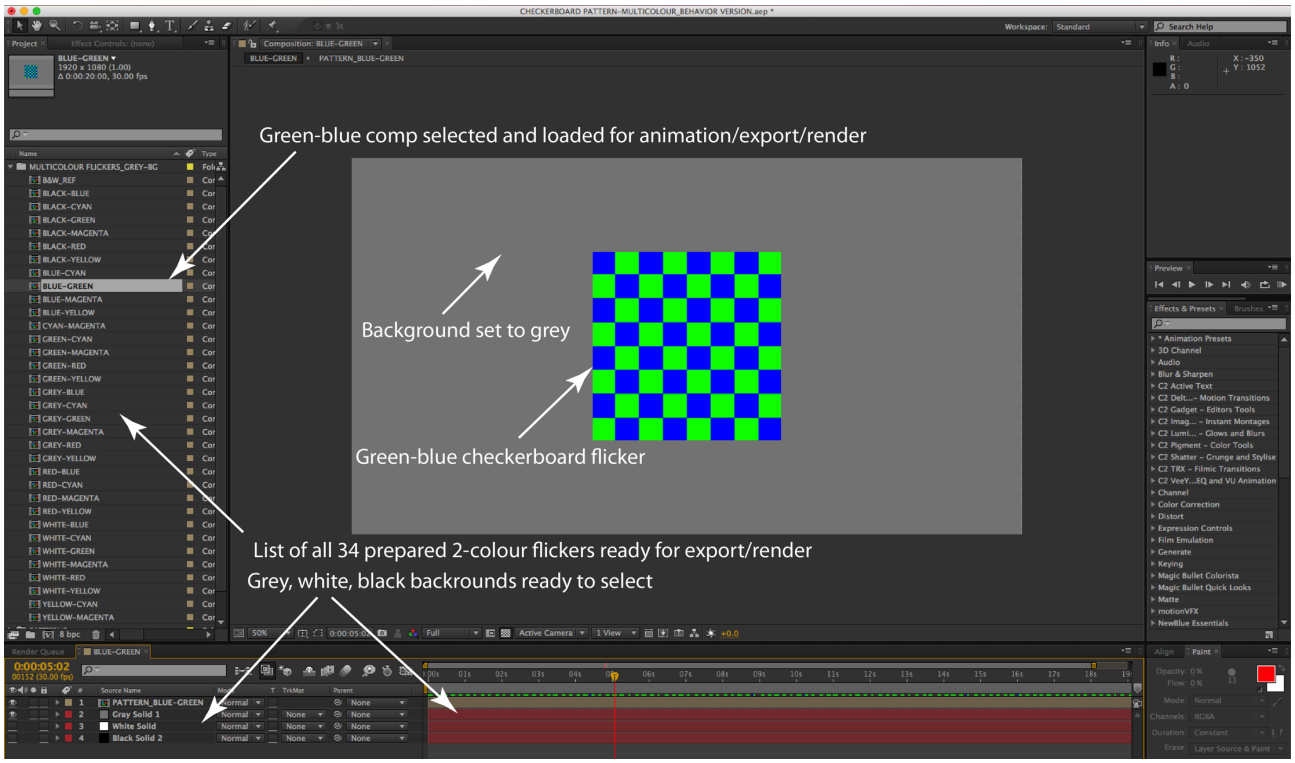

Figure 3-30 Main composition window in After Effects with added background choice option

In this window black, white, and grey background can be selected for the flicker before final render.

Despite this significant workflow improvement, the flickers still had to be individually rendered as before and played back during experiments. The rendered files occupied approximately 1.5 GB of storage space for the entire set of colours including primary, secondary, and black, grey, and white. The rendering time was approximately 20 minutes per flicker. The computer used for this task was an iMac 27" (late 2013) desktop with 3.5 GHz Intel Core i7 processor, 8 GB RAM and NVIDIA GeForce GTX 760M 4 GB graphic card.

3.2.3.3 Multi-Colour Flicker (MCF) Application

Specifically, for this research a bespoke iOS application called Multi Colour Flicker (MCF) has been developed to streamline the workflow and provide a unified colour-testing tool for BCI developers.

The MCF application was created in Apple IDE Xcode version 7.3.1 environment using Swift 2.0 programming language. According to the author's knowledge, this type of application has not been developed for any platform at the time of writing this thesis. The choice for iOS platform and iPad tablet device was made for the following reasons.

Firstly, because of the tablet's high accuracy in colour rendition and high contrast display capabilities, and secondly because of streamlined, easy to use and very popular way of application

distribution possibilities through Apple's app store. Also Swift was used instead of Objective-C as it is continually expanding its user base and gaining the potential of a programming language of the future. Development of this application required the use of UIkit and CoreImage libraries (Processing Images, 2017). The UIkit library provides all the necessary facilities such as window view, Multi-touch input, and animation support, enabling the implementation of a graphic user interface. The CoreImage library uses near-real-time image processing technology consisting of many useful filters and graphic generators. The one that was used to create the main components of the application was CICheckerboardGenerator (Figure 3-31).

```
func checkergenJ(_a:UIColor, _b:UIColor) ->UIImage{
    print ("Generating User checkerboard...")

    // Create a couple of colors on RGB depending on the parameter's values.
    let color0 = CIColor.init(color: _b)
    let color1 = CIColor.init(color: _a)

    // Create a CPU-driven rendering context.
    let glContext = EAGLContext(API: EAGLRenderingAPI.OpenGLES2)
    let ciContext = CIContext(EAGLContext: glContext)

    // Create the basic checkerboard CIImage, guarding against failure.
    guard let checkers = CIFilter(name: "CICheckerboardGenerator", withInputParameters: [
        "inputColor0" : color0,
        "inputColor1" : color1,
        kCIInputWidthKey : (width10/8)] // Manage the square size and by deviding the width by 8
        )?.outputImage else {
            // This code executes when the filter creation fails.
            print("ERROR: Unable to create checkerboard image.")
            return UIImage()
    }

    // Set up our drawing rectangle. The output size of the checkerboard is infinite, so we need
    let drawRect = CGRectMake(0.0, 0.0, width10, width10)

    // Create the output image. SWIFT BONUS: No need to manually release the returned CGImage!
    let outputImage = ciContext.createCGImage(checkers, fromRect: drawRect)

    // Wrap the CGImage in a UIImage and return it.
    return UIImage(CGImage: outputImage)
}
```

Figure 3-31 CheckerboardGenerator function creating inverted pattern

To accommodate the preselected colours of white, black, grey, green, red, blue, yellow, cyan and magenta, in the code, there are 10 checkerboard generator functions created called checkergenA to J (Figure 3-32). Each of these functions uses two standardised colours, Acolor and Bcolor, from the UIkit library, as parameters and returns a different checkerboard. The 10 checkerboards are working in pairs, for example A and B are the full-size checkerboards, A being black and white and B being white and black (reversed pattern) to create the flickering effect between the two states of the checkerboard. Furthermore, the width variable allows the control of the size of the checkerboard and by dividing the width value by an *n* number, *n-by-n* checkerboards are generated. All the variable declarations are added. First in line are Acolor and Bcolor, the two UIColor elements that will constitute the colour of the A and B square groups as shown in the application GUI (Figure 3-33). Next, the 5 different checkerboard sizes i.e. the default 100% and resized 66%, 50%, 25%

and 10% are declared and the 10 checkerboards are preloaded with black and white default patterns (Figure 3-34).

```
@IBAction func ClickOnWhite0(sender : UIButton){
    Acolor = UIColor.whiteColor()
    checkerA = checkergenA(Acolor, _b: Bcolor)
    checkerB = checkergenB(Acolor, _b: Bcolor)
    checkerC = checkergenC(Acolor, _b: Bcolor)
    checkerD = checkergenD(Acolor, _b: Bcolor)
    checkerE = checkergenE(Acolor, _b: Bcolor)
    checkerF = checkergenF(Acolor, _b: Bcolor)
    checkerG = checkergenG(Acolor, _b: Bcolor)
    checkerH = checkergenH(Acolor, _b: Bcolor)
    checkerI = checkergenI(Acolor, _b: Bcolor)
    checkerJ = checkergenJ(Acolor, _b: Bcolor)
}
    // Function triggered when the user click on the white button on the left
    // Change the color of the first half of the the squares to white
    // Reload the ten checkerboards with the new colours
```

Figure 3-32 ClickOnColor function allowing to select colours for checkerboards

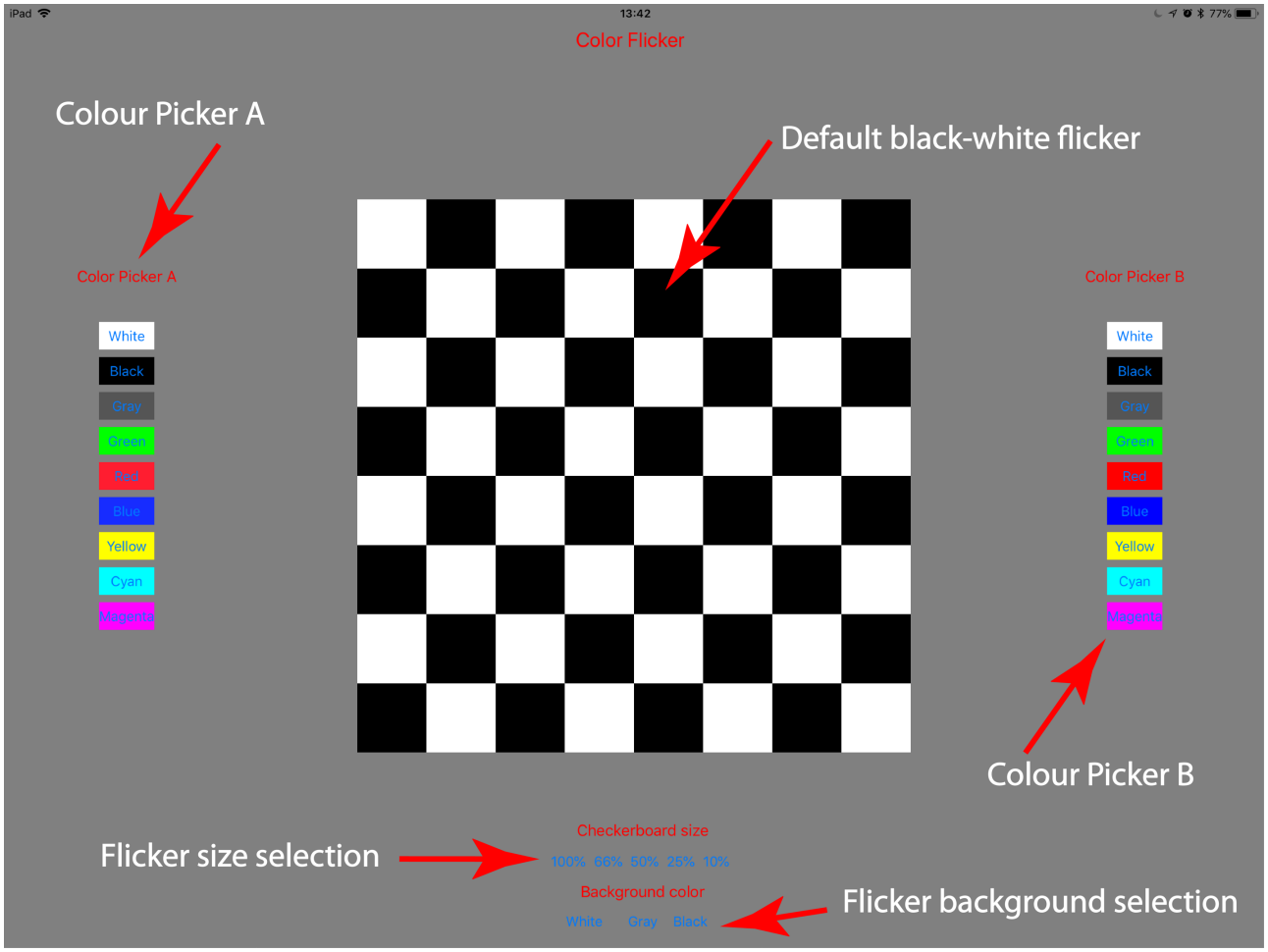

Figure 3-33 MCF application GUI

Default screen of the MCF application after starting the program.

Finally, the ViewController component of the application is entered. This part of the program contains all the code lines related to the User Interface. In this segment of the code, there are a few more variables, the most important being the use of two timers and a *sizecontrol* variable. The

timers are used to produce the 10 Hz and 20 Hz flickering effect in respective versions of the MCF application. The *sizecontrol* manages the size of the checkerboards. There are 10 outlets used to link the buttons from the User Interface (UI) to the application's engine. In the ViewController, there is a standard function called Viewdidload (Figure 3-35), which acts as an infinite loop commencing when the UI is loaded and running until the application is closed.

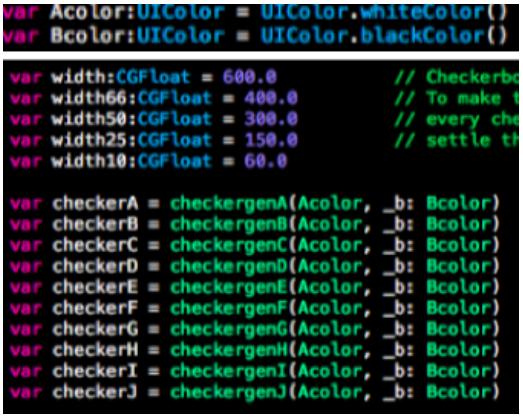

Figure 3-34 Variables describing flicker size and default colours

This part of the code represents the most important elements of the application.

The two previously mentioned timers are used in this loop. The timers are continuously operating in such a way that timer 1 runs from 0 to 0.05 of the second and timer 2 from 0.05 to 0.1 of the second, which results in a total animation period of 0.1s and thus the 10 Hz oscillation is achieved. At the end of their period, the timers launch the function managing the size selection made by the user when touch-selecting one the size buttons, which modifies the *sizecontrol* value. Three background colour functions are called when one of the backgrounds colour buttons (white, black or grey) is pressed by the user. These buttons change the background colour attribute of the UI. Next, a function determining the checkerboard element colour is applied in the form of *ClickOnColor0* and *ClickOnColor1* (Figure 3-36).

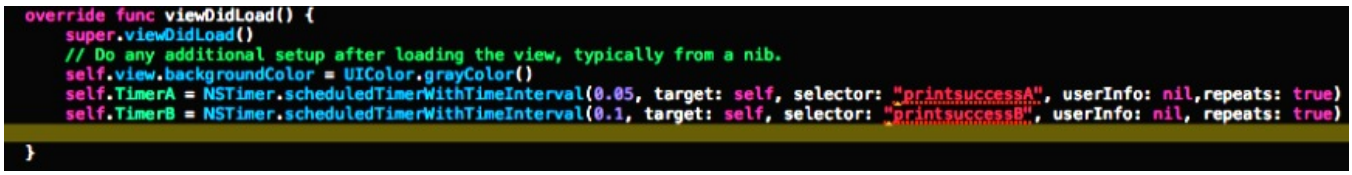

Figure 3-35 Viewdidload function code

This is the infinite loop, which is initiated once the application is initiated.

Every colour picker button on the left side the GUI is linked to a ClickOnColor0 function and their counterparts on the right side of the GUI to *ClickOnColor1*. The *ClickOnColor0* functions change the Acolor value to the one assigned to one of the GUI colour picker square buttons. When the

button is selected, all the checkerboards are reloaded to apply this change. The *ClickonColor1* work the same way with Bcolor code elements. Both colour pickers are shown in GUI (Figure 3-33).

Finally, the two functions launched by the timers are declared. Using a switch case instruction looking at the *sizecontrol* variable, these functions will load the right pair of checkerboards on the screen to match the size selected by the user (A and B for a 100% checkerboard size display, C and D for 66% etc.). The first one will return the first checkerboard (A, C, E etc.) and the second one works with the other checkerboard (B, D, F, etc.).

```
@IBAction func ClickOnWhite0(sender : UIButton){
    Acolor = UIColor.whiteColor()
    checkerA = checkergenA(Acolor, _b: Bcolor)
    checkerB = checkergenB(Acolor, _b: Bcolor)
    checkerC = checkergenC(Acolor, _b: Bcolor)
    checkerD = checkergenD(Acolor, _b: Bcolor)
    checkerE = checkergenE(Acolor, _b: Bcolor)
    checkerF = checkergenF(Acolor, _b: Bcolor)
    checkerG = checkergenG(Acolor, _b: Bcolor)
    checkerH = checkergenH(Acolor, _b: Bcolor)
    checkerI = checkergenI(Acolor, _b: Bcolor)
    checkerJ = checkergenJ(Acolor, _b: Bcolor)
}
    // Function triggered when the user click on the white button on the left
    // Change the color of the first half of the the squares to white
    // Reload the ten checkerboards with the new colours
```

Figure 3-36 ClickOnColor function selecting checkerboard colours

The following flowchart diagram represents all the functions and parameter settings available in the MCF application and their relationship (Figure 3-37).

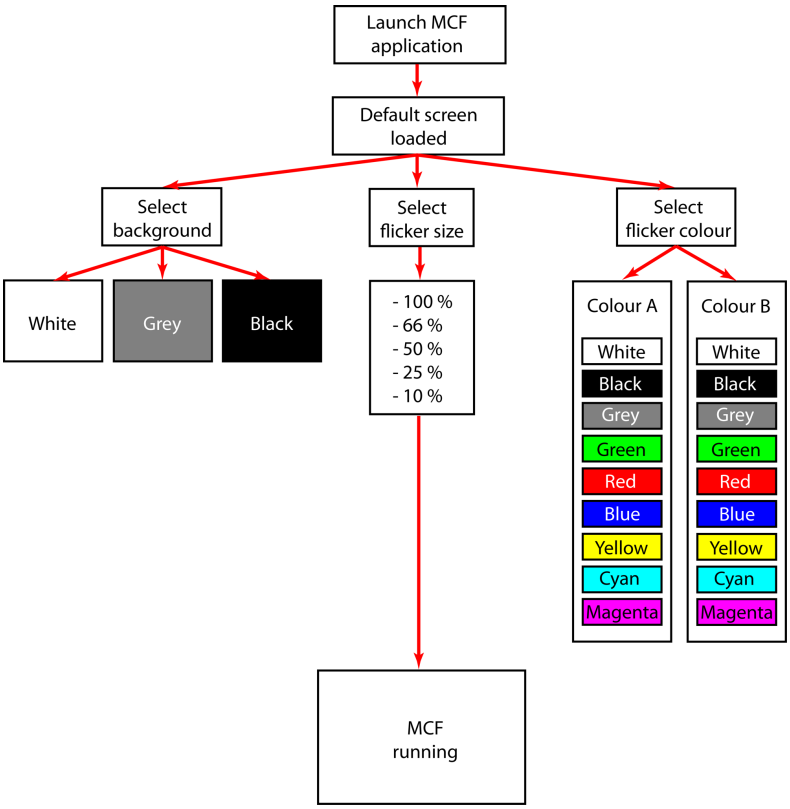

Figure 3-37 MCF application operation flowchart

The flowchart represents the application's operation. It is possible though to change background and flicker colour while the application is running.

After initiating the MCF application, the default screen shows 50% grey background, two colour pickers on both sides of the screen and flicker size selection buttons as well as background selection buttons at the bottom of the screen as illustrated in Figure 3-38. To start the flicker, one of the flicker size selection buttons must be touch-clicked.

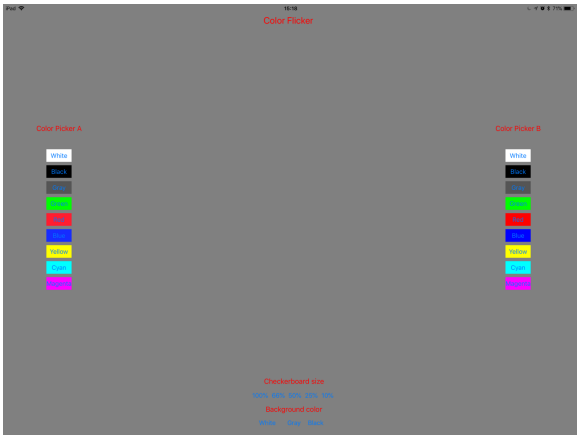

Figure 3-38 MCF default screen is loaded after initiating the application.

The flicker starts after selecting one of the flicker size buttons at the bottom of the screen.

Figure 3-39 presents the MCF application after engaging one of the flicker size selection buttons. The flicker's both colours can be determined through colour picker selection buttons prior the initiation or after the flicker is started.

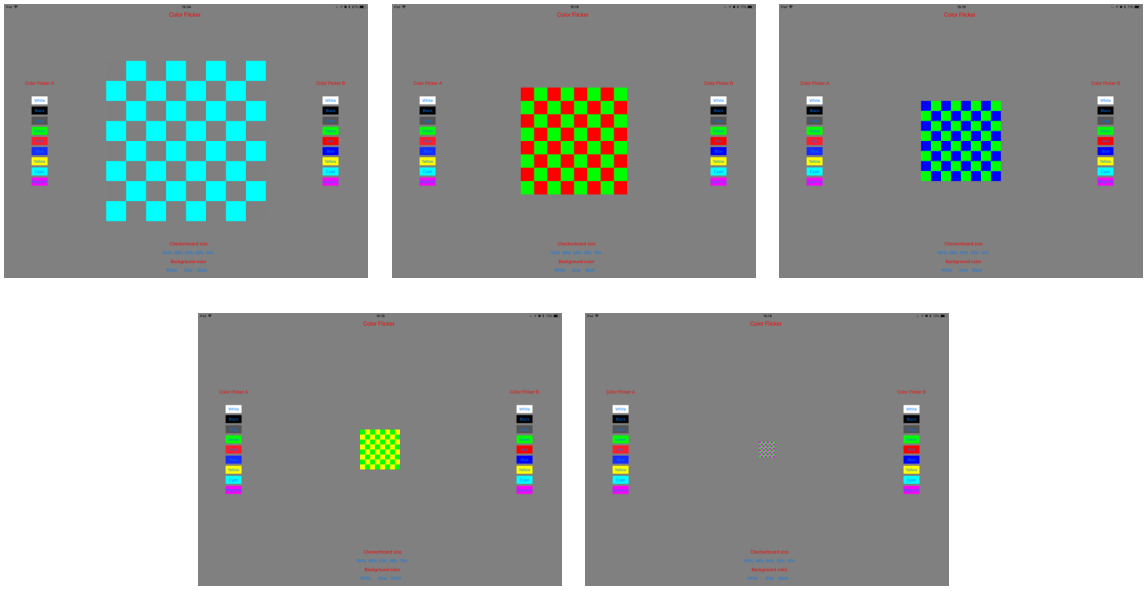

Figure 3-39 MCF application flickers at various sizes

The following sizes can be selected in MCF application: 100 %, 66 %, 50 %, 25 %, and 10 %.

All the parameters of the application can be changed when it is active. Figure 3-40 demonstrates different states of the application being changed while in operation with different backgrounds and flicker colours.

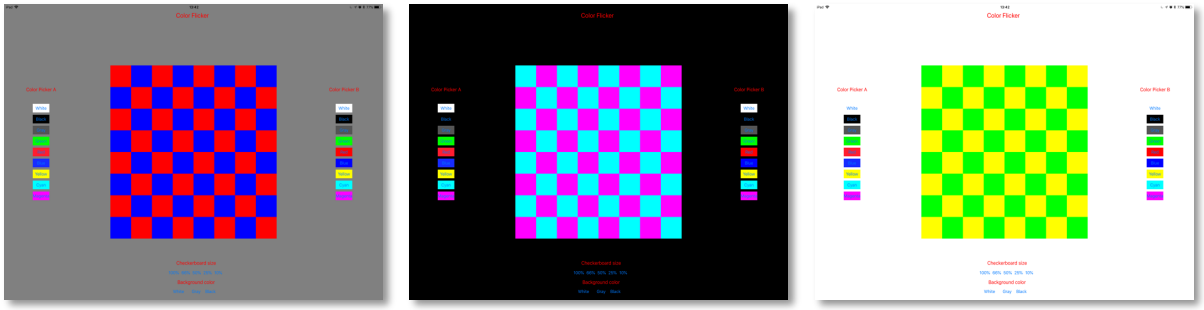

Figure 3-40 MCF application running various states of the flickering scenarios

Three application settings while running the programme with different backgrounds and flicker colors.

3.2.3.4 Flicker Design Using Arduino Development Board

Arduino (ver. 1.8.6) Integrated Development Environment (IDE) is written in Java programming language as a cross-platform application working in Windows, OSX, and Linux operating systems (Figure 3-41a). Its main purpose is to write and upload programs called 'sketches' to Arduino boards (Figure 3-41b). It is an open source program and the IDE's source code is released under the

GNU General Public License (Store.arduino.cc, 2019). Arduino IDE is a very popular programming environment and usually it requires additional libraries installed in order to address and work with specific hardware devices.

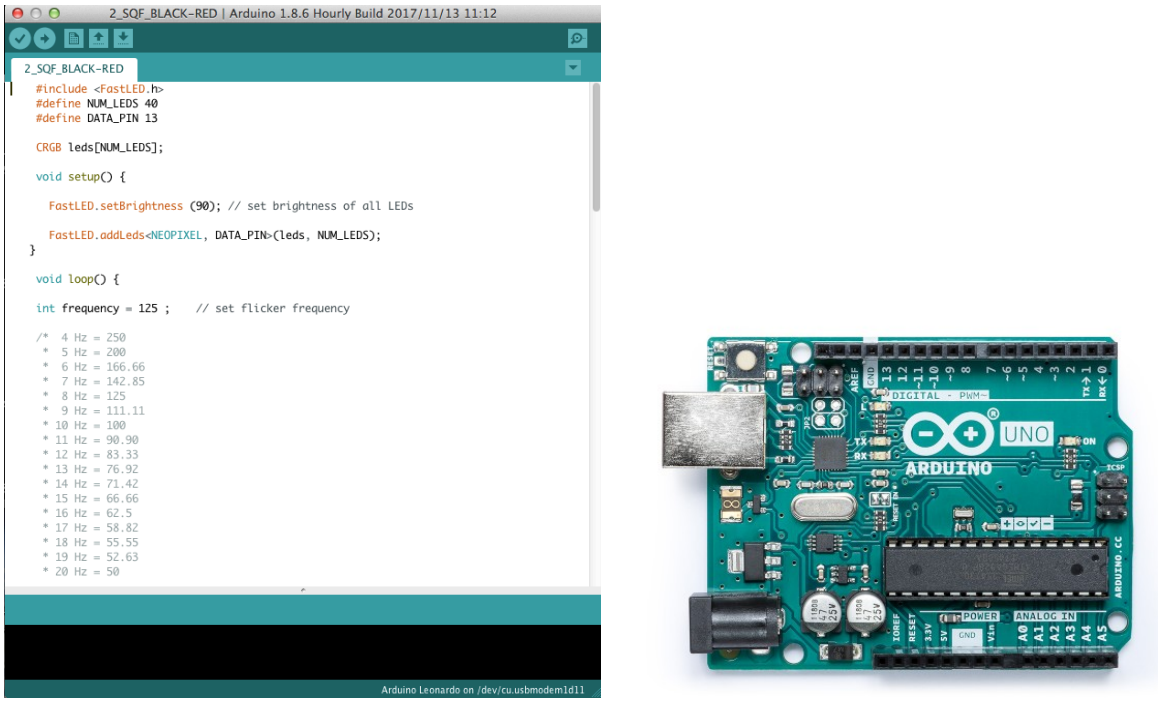

(a) (b)

Figure 3-41 IDE interface (a) and Arduino UNO microcontroller board (b)

One of the important features of Arduino board is the fact that it is equipped with the analogue and digital connection ports, which can be used to communicate with other external devices. Such third party devices utilising this facility are referred to as 'shields'. There are many types of shields offering additional features such as port expansions, sensors, memory card readers, wireless networking etc. For this research, it was decided to use an RGB LED matrix (Figure 3-42) serving as a light source generating stimuli flickers of various programmed patterns as detailed on page 79.

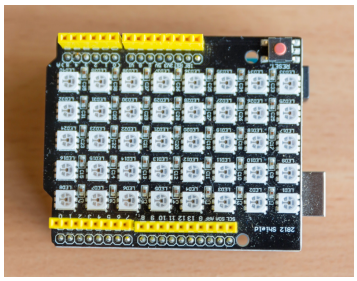

Figure 3-42 RGB LED matrix shield for Arduino UNO board

The shield is equipped with 40 full colour LEDs referred to as 'pixels'.

For one of the experiments carried out during this research a custom library called FastLED was installed. This library enables addressing and programming RGB LEDs that are used in a wide variety of third-party Arduino controllable products often taking a form of LED stripes or matrices. As exemplified in Figure 3-43, the FastLED library was included in the sketch using '#include' command. Additionally, '#define' component enables Arduino to recognise the number of LEDs and communication pin number in the device thus allowing the data transmission between Arduino and the LED shield. This is a convenient way of giving a name to constant values in the syntax before compiling the program (Store.arduino.cc, 2019).

Next, the 'setup()' function is called where the LEDs brightness parameter can be adjusted using integer numbers between 0 and 255, where 0 means LED is off and 255 represents the maximum brightness. The second line of code establishes a connection between the FastLED library and the LEDs called 'NEOPIXEL', which are installed in the shield (Figure 3-44).

```
#include <FastLED.h>
#define NUM_LEDS 40
#define DATA_PIN 13

CRGB leds[NUM_LEDS];
```

Figure 3-43 FastLED library loaded in Arduino IDE

FastLED library enabling communication between the LED shield and Arduino UNO board.

```
void setup() {

  FastLED.setBrightness (100); // set brightness of all LEDs

  FastLED.addLeds<NEOPIXEL, DATA_PIN>(leds, NUM_LEDS);
}
```

Figure 3-44 Arduino IDE 'setup()' syntax

LED brightness set to 100, which represents medium brightness.

The setup function is part of the code, which initialises and sets the initial program values. In this example it sets the LED panel brightness to the value of 100 and establishes connection between the LEDs and the program. After initiating the 'setup()', the 'loop()' function is added. As the name implies, this section of the code runs a consecutive loop, which controls how the board responds to various sections of the code.

In this example the ‘loop()’ function was used to generate a flickering behaviour of the LEDs. Again integer ‘int’ primary data-type was used to set the required flickering frequency. Syntax ‘/**/’ defining block comment was used as a description exemplifying integers corresponding to useful frequencies, which can be set in the sketch. Figure 3-45 illustrates frequency parameter set to 111 generating 9 Hz flicker oscillation.

```
void loop() {

int frequency = 111        // set flicker frequency
/*  4 Hz = 250
 *  5 Hz = 200
 *  6 Hz = 166
 *  7 Hz = 142
 *  8 Hz = 125
 *  9 Hz = 111
 * 10 Hz = 100
 * 11 Hz = 90
 * 12 Hz = 83
 * 13 Hz = 76
 * 14 Hz = 71
 * 15 Hz = 66
 * 16 Hz = 62
 * 17 Hz = 58
 * 18 Hz = 55
 * 19 Hz = 52
 * 20 Hz = 50
   */
```

Figure 3-45 Arduino IDE 'loop()' syntax

The grey-coloured descriptive portion of the code informs values to be used to generate frequencies, e.g. variable value of 111.11 for 9 Hz flicker.

The LED’s flickering behaviour was created in such a way that the sketch contained two separate, opposite states of the pattern lit with the LEDs. This could be achieved due to direct LED addressability guaranteed by the FastLED library coding. The left-hand side of the code represents the LED’s address starting with first LED at position ‘0’. The right-hand side determines the LED’s colour. The colour ‘Black’ means the LED is turned off. The basic RGB colours can be conveniently generated in the LED matrix by selecting ‘Red’, ‘Green’, ‘Blue’, ‘Yellow’, ‘Cyan’, and ‘Magenta’ as defined in FastLED library. To generate white light in the LED one need to select ‘White’ in the code.

```
// state A of the flicker

  leds[0] = CRGB::Black;
  leds[1] = CRGB::Black;
  leds[2] = CRGB::Black;
  leds[3] = CRGB::Black;
  leds[4] = CRGB::Green;
  leds[5] = CRGB::Green;
  leds[6] = CRGB::Green;
  leds[7] = CRGB::Green;
  leds[8] = CRGB::Black;
  leds[9] = CRGB::Black;
```

Figure 3-46 State 'A' of the LEDs programmed in Arduino IDE

Figure 3-46 and Figure 3-47 represent a portion of the code showing two opposing states of the LEDs. The programmed infinite loop causes frequent changes between the two states according to frequency set in the loop, thus generating the flicker.

```
// state B of the flicker

leds[0] = CRGB::Green;
leds[1] = CRGB::Green;
leds[2] = CRGB::Green;
leds[3] = CRGB::Green;
leds[4] = CRGB::Black;
leds[5] = CRGB::Black;
leds[6] = CRGB::Black;
leds[7] = CRGB::Black;
leds[8] = CRGB::Green;
leds[9] = CRGB::Green;
```

Figure 3-47 State 'B' of the LEDs programmed in Arduino IDE

For the flicker to work, each LED state ‘A’ and ‘B’ must be accompanied by the portion of code as shown in Figure 3-48, activating the LEDs’ given state. It is possible to generate more complicated flickers with different colours displayed by the same LEDs at different times of the running program by creating more LED states in the code.

```
FastLED.show();

delay(frequency);
```

Figure 3-48 'FastLED.show()' command in Arduino IDE

Over 750 different flickers have been created with varying patterns and colour combinations. Many of them include three or four different colours.

3.3 Testing Environment

Although the main purpose of this research is to establish stimuli graphics parameters resulting in the highest signal to noise ratio and minimal artifact pollution, it has been determined that the testing conditions should be as close to normal human living conditions as possible. It would not be very useful to design a very clean, noise free environment, as this would be unrealistic. It is important that the knowledge acquired through this research should be applicable for commercial systems, where laboratory environment cannot be recreated. Thus, in the testing room, the lighting conditions and common environmental sounds, which included people engaging in their normal daily activities as well as electrical devices such as computers, monitors, and ceiling lighting fixtures, were always factored in as part of the testing setup. The room shown in Figure 3-49 and Figure 3-50 is of the following dimensions: length 12.3 m, width 9.5 m, height 3.4 m.

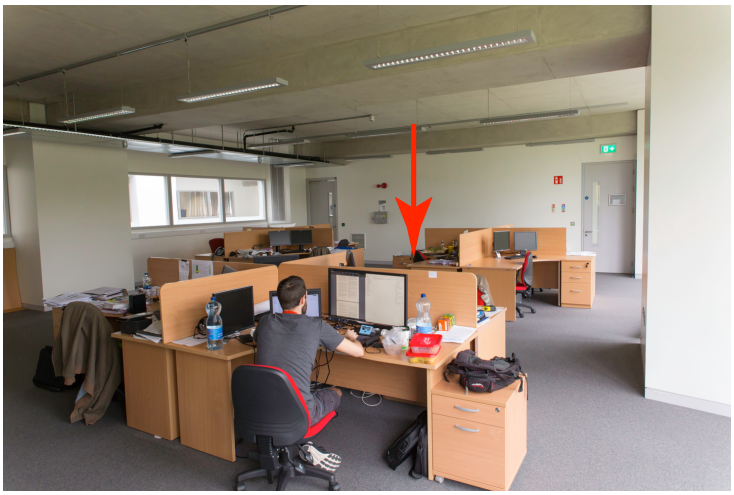

Figure 3-49 Testing environment – front perspective

The red arrow indicates the desk where the experiments were conducted.

Figure 3-50 Testing environment – back perspective

There is a large window beside the desk where the experiments were conducted.

3.3.1 Lighting Conditions and Light Reflection Minimisation

The experiments were usually carried out in the room (Figure 3-51) between 11 am and 3 pm at different times of the year, therefore the environmental light was never consistent and sometimes even fluctuated during the test. Most of the times, the available light was a mixture of natural daylight and artificial light emanating from fluorescent lighting fixtures normally found in offices (Figure 3-52).

Figure 3-51 Testing environment – back perspective

Close-up perspective of the room and desk showing the usual lighting conditions accompanying the experiments.

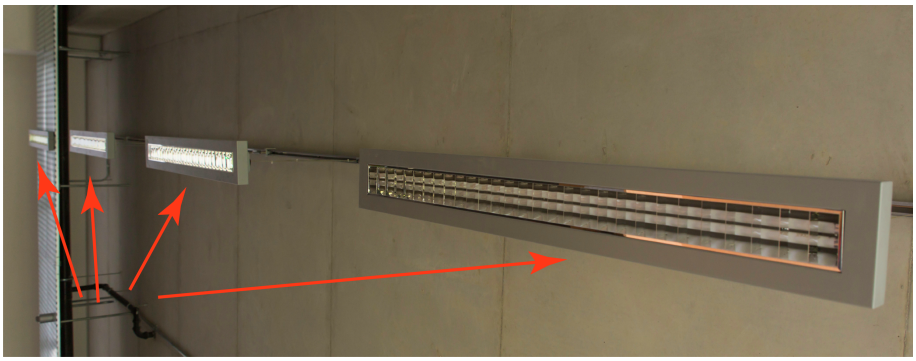

Figure 3-52 Room light fixtures

There are 15 light fixtures in the room mounted as 3x4 plus 1x3 grid filling it with light of 4000 K colour temperature (Table 3-2).

It should be noted how colour temperature impacts the way people see colours. Figure 3-53 illustrates the same graphic presented by digital screen set to three different colour temperature values to compensate the lighting conditions the screen is surrounded with.

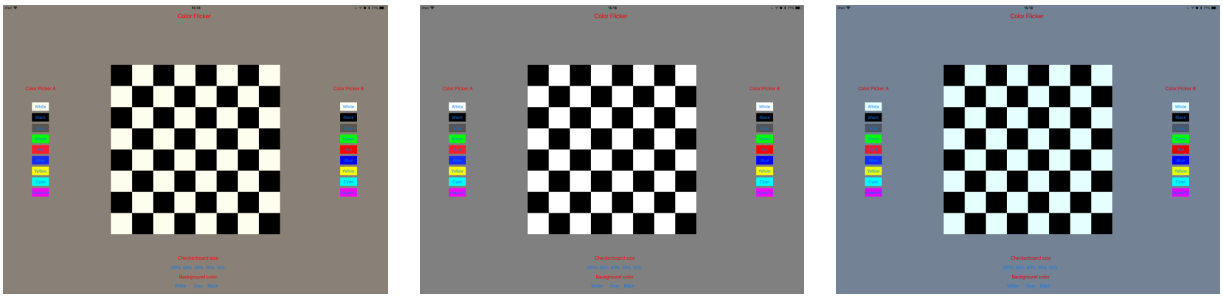

(a) (b) (c)

Figure 3-53 The impact of colour temperature on digital screen

The figure represents three states of digital screen with varying colour temperature settings to match: yellowish warm tungsten light (a), normal daylight (b), and blueish cool lighting conditions (c).

Observing the three states of presented graphics one can notice that the overall colour cast is changing and it is most evident when observing areas lacking in colour saturation, e.g. grey or white. The changing tonality from warmer 'yellowish' to cooler 'bluish' in colour science is referred to as 'white point shifting'. This phenomenon is explained in detail in Figure 3-54. The colour temperature is referenced to a black body radiator with colour changing from red through orange, yellow to white and bluish white, thus it is expressed and measured in temperature Kelvin (K).

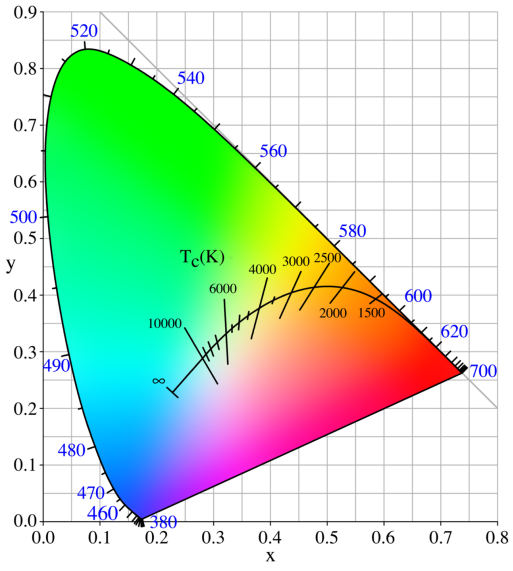

Figure 3-54 Chromaticity colour space with black body chromaticity line

The black line in the middle of the colour space graph indicates the black body's different states of chromaticity (CIE, 1932). The image is a modern version of the colour space map.

The human eye has a natural ability to adjust to even the most extreme lighting conditions so that the colour of the light source appears to be white. However, the source of light will appear coloured when it is strongly shifted towards one of the primary colours. When daylight and tungsten light are seen together, daylight appears bluer. When an observer is standing outside on an overcast day and looks into a room lit by a typical light fixture, incandescent or tungsten, the interior light will appear significantly more yellow than it really is. This is due to the observer's visual system adjusting to the exterior, bluer light conditions. When the same observer enters the previously observed room, his/her vision will adjust to the new conditions. Now the interior light will appear white and the outdoor light will seem very blue. Colour temperature of various light sources is measured in Kelvin (K) as shown in Table 3-2. This phenomenon influences the way people perceive colours in various lighting conditions. The situation is even more complex in environments, where different sources of light mingle together (Ascher and Pincus, 2012).

For this reason, maintaining constant colour temperature of the flicker presentation was not possible throughout the entire research. Thus, the author undertook precautionary measures and tried to minimise the impact of the environmental lighting conditions by placing the stimuli presenting devices (tablet and LED matrix) in a light and reflection-blocking box (Figure 3-55).

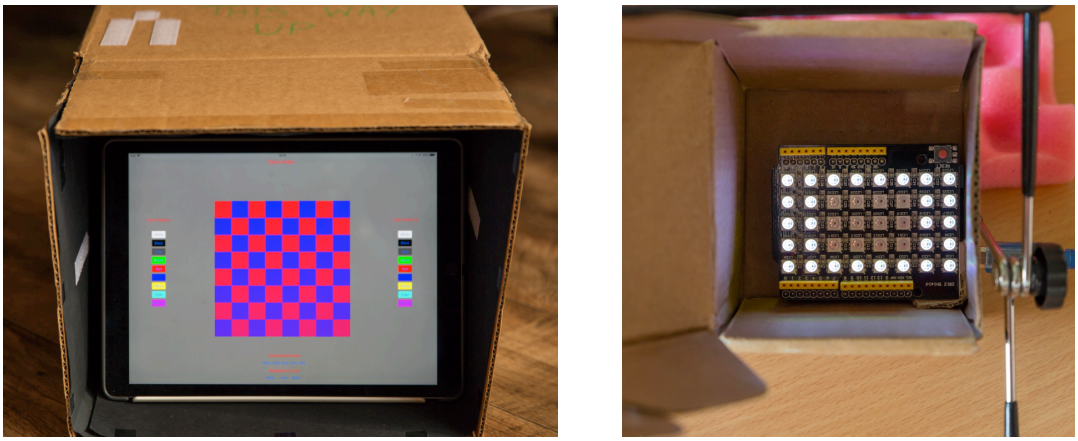

(a) (b)

Figure 3-55 Flicker presenting devices: (a) tablet and (b) LED matrix in light blocking boxes

Table 3-2 Approximated colour temperatures of common light sources (Ascher and Pincus, 2012)

Light source	Degrees Kelvin (K)
Candle flame	1850 - 2000
Household bulb	2900
Fluorescent warm white tube	3500
Fluorescent daylight tube	4300
Summer sunlight at noon	5400
Overcast sky	6000 - 7500
Summer shade	8000

3.3.2 Subject Positioning

Regarding subjects' positioning, the tests have all been maintained at a constant distance of 50 cm from the stimulus, as illustrated in Figure 3-56. This distance had certain advantages and seemed to be the most comfortable for the vision system. It was not tiring and provided enough room for small individual adjustments requested by testing subjects in order to maintain precise sharpness of the stimuli graphics.

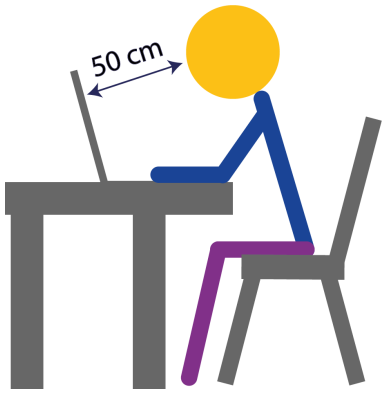

Figure 3-56 Subject positioning during experiment

3.3.3 Plots and Statistical Data

The subsequent Sections: Chapter 4, Chapter 5, and Chapter 6 present all the experiments conducted during this research. In these Sections various plots and statistical data calculations are presented. All the amplitude peak plots have been obtained from MATLAB. The provided statistical data has been calculated using spreadsheet software called 'Numbers' produced by Apple. All the bar-graph plots representing the statistics also have been generated in 'Numbers'.

3.4 Summary

In this Section, the author presented detailed information about the research methods applied during the work including software, hardware and overall workflow approach to experiments. Since the tools and methods changed and expanded during the course of research, the process of progression and evolution constitutes a significant portion of this Section.

First, the process of brain signal acquisition was described, giving details of how the signals were captured. Next, as part of the hardware used, the Emotiv EPOC EEG headset was introduced providing technical specifications of the device, specifically referencing them to the International 10-20 System. Continuing the data acquisition method description, the raw brain signal recording software Emotiv Xavier Test Bench software was discussed. Further, the devices used to present visual stimuli during experiments such as 12.9" iOS tablet and Arduino driven LED matrix were described including their most fundamental characteristics. Following, the brain signal analysis process was explained including hardware and software applications. In particular, MATLAB and its plugin add-ons such as EEGLA and ERPLAB were characterised, focusing specifically on the functions and signal processing methods used. Next, various methods of stimuli design developed for the research work were described, introducing the original iOS tablet application developed to streamline the research workflow. Arduino IDE software was also detailed outlining its usability in designing various flickering patterns giving examples of utilised programming functions and parameters. Finally, different environmental issues such as lighting conditions and subject positioning during experiments were described.

Chapter 4 Analysis of Stimuli Graphics Patterns

4.1 Introduction

In order to fully analyse the impact of stimuli graphics on the quality of brain signals one must consider all the possible parameters that relate to graphics designs. One of the parameters is the frequency at which the graphic oscillates. The chosen 10 Hz oscillation for the stimuli graphics testing has been determined and discussed based on Regan's suggestions (Regan, 1989). This frequency was also tested against other suggested frequencies in the Alpha range by the author and confirmed to provide the most robust and consistent results. Another reason for choosing 10 Hz frequency was determined by the technical specifications of most digital screens used today. That is their refresh rate of 60 Hz, which considerably limits presentation of frequencies that do not conform to this standard. This phenomenon was described in detail in Section 1.7.

During the research, the author came across various publications mentioning the possible impact of various stimuli shapes on the elicited brain signals (Embrandiri et al., 2015). Based on results achieved from resolution/size experiments, which will be presented in Chapter 5, it was decided to design a testing setup to additionally evaluate the brain's response to different patterns. This would enable the author to arrive at more complete and comprehensive set of parameters, which he would like to propose, as the result of this research. Since programming a variety of patterns using graphic design software or Xcode environment would require substantial amount of time, the author decided to implement a more streamlined approach. For that purpose, an Arduino board was used with a 40 LED matrix shield. Using the Arduino programming environment, a variety of flickering patterns were designed and tested.

Moreover, introducing this novel research method presents new perspectives for future work, where a brain signals' dependency on different pattern presentations could be combined with other parameters such as multi-colour combinations of said patterns. These could be further tested with the whole range of frequencies frequently used in SSVEP technique.

The following Sections present and discuss visually elicited brain signal dependencies related to various flickering patterns.

4.2 Experiment Setup

This Section focuses its attention on finding flickering patterns that provide the most robust brain signals containing desired peaks with minimum noise and artefacts. In contrast to many tests performed for early publications, constituting the foundation and inspiration for this research, where either a 17" computer screen or a 12.9" tablet displaying checkerboard flickers were used, for this test the author decided to use a multi-LED panel controlled by the Arduino board. This hardware device in combination with the Arduino programming environment allowed the free design and testing of a variety of flickering patterns. The LED panel is capable of displaying true RGB colours through the provided 40 LEDs arranged in 5 x 8 matrix as shown in Figure 3-7. This device potentially could be used to drive colour-stimuli driven multi-command BCI system with the ability to display unlimited colour combinations and overcome some of the common digital screen limitations such as refresh rate. Using the Arduino IDE, a total of 10 patterns as detailed in Figure 4-2 were designed.

For details on the hardware/software used for brain signals recording and testing environment please refer to Chapter 3. Raw EEG brain signals were captured as European Data Format files (EDF) by Emotiv EPOC headset wirelessly communicating with Windows 7 based PC computer running Emotiv Xavier Test Bench software. The signals were then analysed in MATLAB using EEGLAB (Sccn.ucsd.edu., 2019) and ERPLAB plugins for basic filtration and plots. A Keystudio WS2812 RGB LED shield with Arduino UNO and accompanying IDE software were used to design, program and display stimuli flickers. Since it was decided to use 10 Hz oscillation during the research, to satisfy the results comparability and compatibility requirement, all 10 flickers were presented at 10 Hz frequency. Subject (User 1), wearing correcting glasses was exposed to visual stimulation in a normal office environment in daylight. The LED panel was placed inside of a small cardboard box to minimise the influence of the ambient light on the panel as the dominant light source stimulating the subject's visual system as detailed in Figure 3-55b. The subject was placed approximately 50 cm from the LED panel wearing an EEG headset, which streamed digitised signal to the PC. Each flicker was presented in 9 to12 trials for the duration of 10 seconds for each trial. From the recorded trials, after performing peak extraction using FFT, the best performing 6 trials were selected for further analysis and comparison resulting in 60 signals being analysed for the final results presentation as detailed in Figure 4-1.

10 Patterns x 6 trials = 60 signals analysed

Figure 4-1 The total number of tested flickers

Each trial was captured as a separate EDF file. To achieve better coverage of the occipital lobe, which is crucial for accurate SSVEP response, the EPOC headset was rotated as illustrated in Figure 3-2 and suggested by Manyakov et al. (2011). The technical details on the headset used can be found in Section 3.2.1.1. Again all 14 channels were recorded and only signals captured by the AF3 channel were analysed as explained in Section 1.2. The remaining three channels covering the occipital lobe carried similar brain responses.

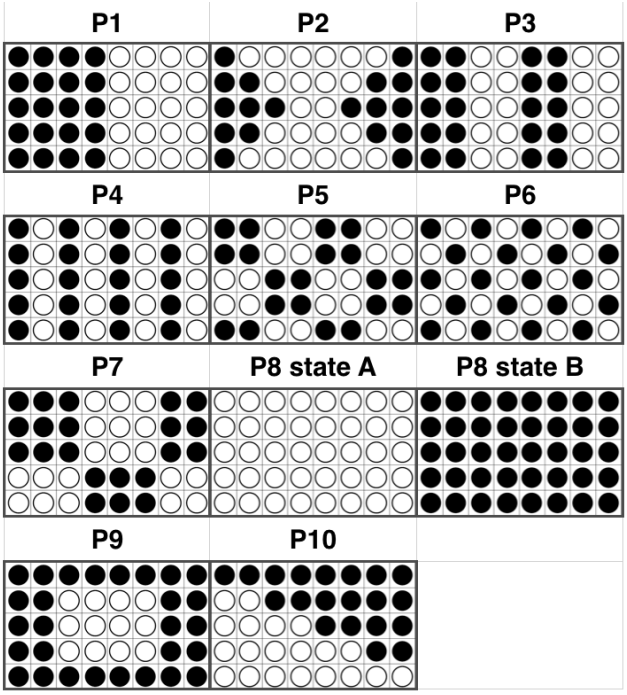

Figure 4-2 Graphic representations of the 10 patterns used for the experiment

Figure 4-2 shows all the 10 patterns used in the tests. The black dots indicate switched off LEDs and the white dots indicate switched on LEDs. The way each flicker works is that there are two states for each flicker, from now on referred to as 'State A' and 'State B'. The first state, 'State A' for all tested flickers is shown in Figure 4-2 and the second state, 'State B' is a complete reverse of the pattern. This concept is explained with more detail in Figure 4-3 showing pattern P8 in two states of the flicker. The patterns were designed in order to test different checkerboard versions, wide and narrow stripes, triangles, two-field and single field rectangles, and dots. Also introducing a certain degree of variance to the scatter factor of the patterns was important. The main intention was to observe whether any dependencies could be detected between the elicited brain signals and the proposed flicker patterns.

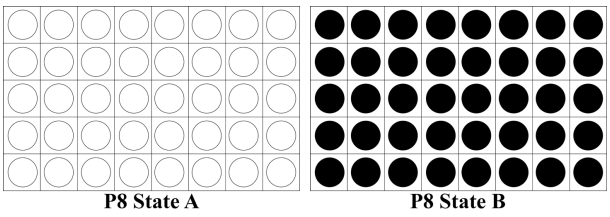

Figure 4-3 Flicker pattern P8

Two states of the flicker; state A and state B. By rapid repetition of the two states, the flickering pattern is generated.

These two states are alternating at 10 Hz frequency. Although the LED panel is capable of displaying colours, for this test only the black and white flickers were used. Henceforth, the patterns from 1 to 10 will be referred to as P1 to P10.

4.3 Test Results

The obtained test results are presented in this Section. Each set of individual pattern results consists of pattern graphic, frequency domain plot with best result chosen from all analysed trials, bar graph illustrating fundamental 10 Hz frequency peak with harmonics if present and finally bar graph presenting statistical data derived from all 6 analysed trials i.e. maximum, minimum, and average values. The best plots for each pattern selected from all trials were chosen based on the power of the elicited peak expressed by 'Amplitude (μV)' axis. The level of noise and other artefacts such as harmonics were also considered. According to Isa et al. (2012) typical signal amplitudes evoked by visual stimulation in the Alpha band (7 Hz – 15 Hz) and measured by the EEG range between 8-10 μV. Interestingly, a typical level of random (considered as noise) brain oscillations, measured at rest without any visual stimulation, also can reach similar value of 10 μV. With the elicited fundamental frequency, the noise level seems to decrease in amplitude reaching values below 2 μV in the most successful trials. In this experiment, signals with the highest main component peak (10 Hz), the lowest noise and minimal harmonic content are considered as the most useful for BCI systems.

Pattern 1 (P1) results

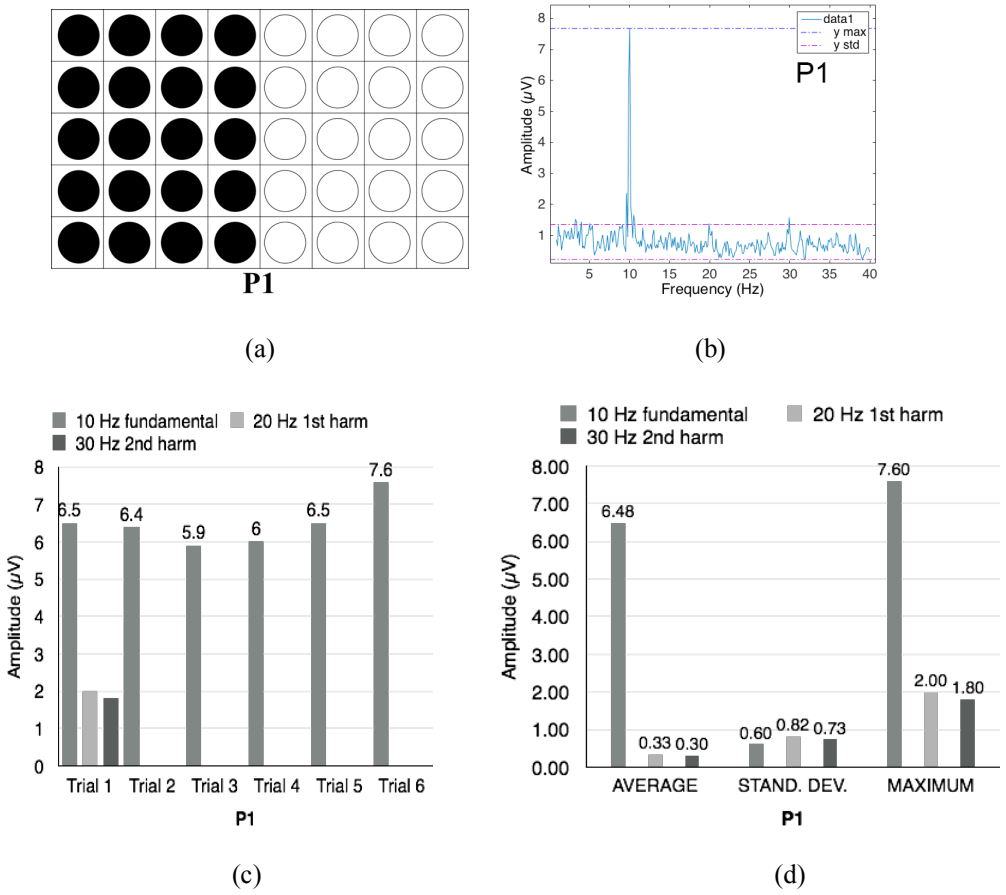

Figure 4-4 Results for P1 (a): best 10 Hz peak (b), peak amplitudes (c) and statistics (d) for 6 best trials

The first pattern, P1 has the form of 2 vertical rectangles, each occupying one side of the LED panel revealed in Figure 4-4a. The 10 Hz flickering bevaviour is realised in such a way that both sides blink, reversing the pattern and causing apparent image horizontal movement. In essence the flicker contains 2 shapes. As illustrated in Figure 4-4b, showing the best 10 Hz peak generated by this flicker, the peak with value of 7.6 μV is strong and clean without any visible artefacts. The noise level is low with the average value below the 1.4 μV. Harmonics are almost non-existent. Figure 4-4c shows the bar graph indicating the best 6 results for 10 Hz peaks and harmonics. Trial 1 shows the fundamental peak with harmonic content of 20 Hz and 30 Hz with levels below 2 μV. The remaining trials are free of any harmonics. In Figure 4-4d statistical data on average, standard deviation, and maximum values are presented showing very consistent fundamental 10 Hz peak response with standard deviation below the value of 1. The average values of harmonic contamination are very low when compared to the average fundamental 10 Hz peak. The P1 flicker generated very useable signals in all 6 trials.

The target 10 Hz signal peaks would be very easy to extract with very minimal signal preprocessing, thus valid for BCI applications.

Pattern 2 (P2) results

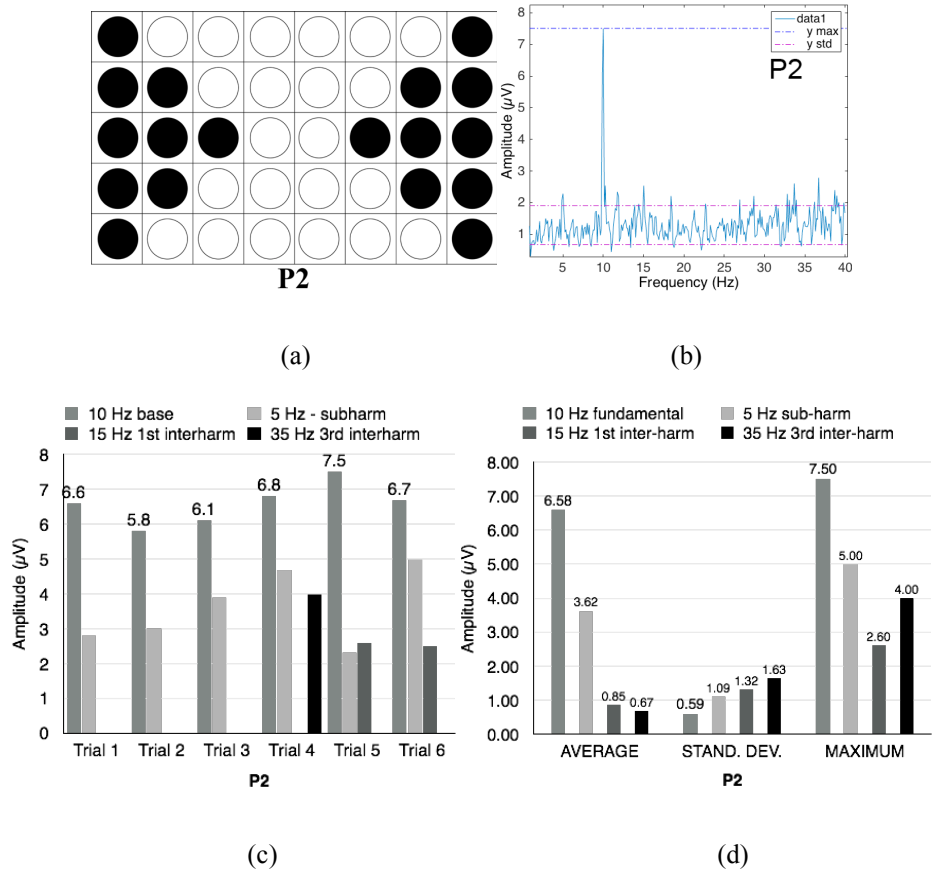

Figure 4-5 Results for P2 (a): best 10 Hz peak (b), peak amplitudes (c) and statistics (d) for 6 best trials

The second pattern, P2 has the form of 2 triangles residing on both sides of the LED panel. The LEDs in the middle resemble an hourglass shape (Figure 4-5a). The 10 Hz flickering bevaviour is realised in such a way that the 2 triangles and the hourglass-like shape blink, reversing the patterns. In this flicker one can distinguish 3 separate shapes. As illustrated in Figure 4-5b, the P2 generated 10 Hz peak with maximum best value of 7.5 μV. The peak is well defined with no visible artefacts in low frequency range. The noise level is higher with the average value slightly below the 2 μV. Minor inter-harmonic contamination of 5 Hz and 15 Hz are present. Figure 4-5c shows the bar graph indicating the best 6 results for 10 Hz peaks and harmonics. All trials show the unusual presence of 5 Hz sub-harmonics. In three trials out of five other harmonics can be observed with slightly lower levels. In Figure 4-5d statistical data on average, standard deviation, and maximum values, confirm strong presence of 5 Hz sub-harmonics with the average value of 3.62 μV, which is relatively high in comparison to the main 10 Hz component average value of 6.58 μV. For BCI operations, clever signal pre-processing would need to be factored in when extracting the targeted features. Positive is the fact that standard deviation parameter for the 10 Hz oscillation is low at 0.59 μV.

Pattern 3 (P3) results

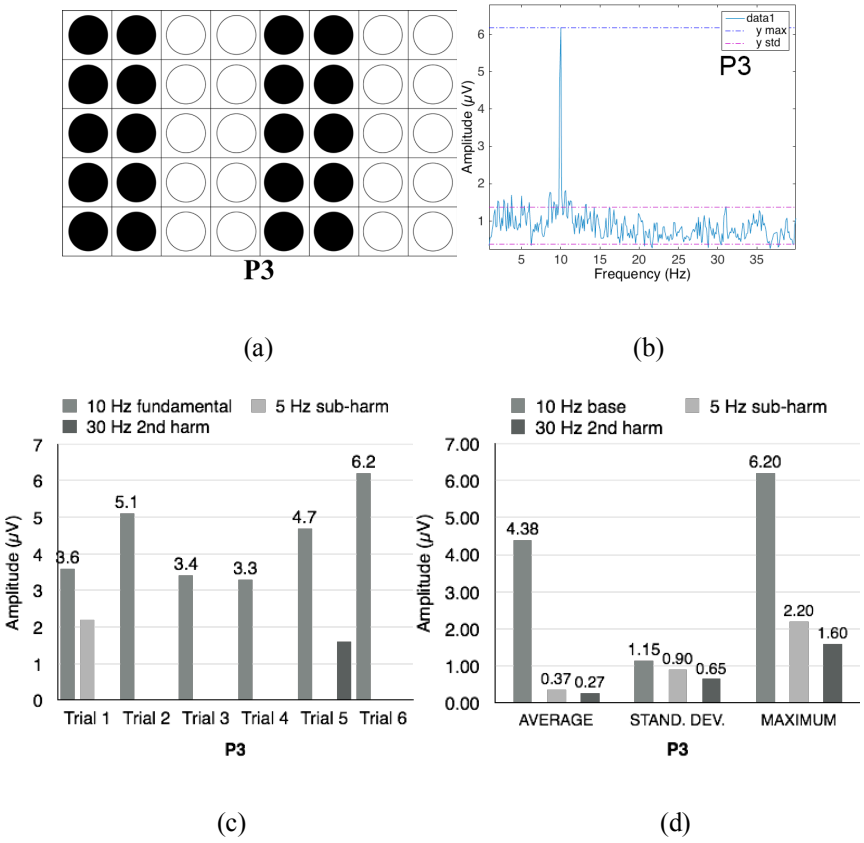

Figure 4-6 Results for P3 (a): best 10 Hz peak (b), peak amplitudes (c) and statistics (d) for 6 best trials

The third pattern, P3 has the form of 4 vertical rectangles, each occupying 2 rows of LEDs (Figure 4-6a). The 10 Hz flickering bevaviour is realised in such a way that each 2-row rectangle is replaced by the reversed pattern inducing horizontal movement of the apparent image. There are 4 shapes constituting the flickering pattern. The Figure 4-6b illustrates the best 10 Hz peak generated by this flicker. The peak value reads 6.2 μV. The frequency domain plot reveals very low noise level with average value below 1.5 μV and clean target 10 Hz peak. No harmonic content has been noted. Figure 4-6c with all registered peaks within the 6 trials suggests very inconsistent 10 Hz peak responses with rather minimal harmonic content at the same time. This can be further acknowledged in Figure 4-6d, where the average target 10 Hz peak is of rather low 4.38 μV value and standard deviation at 1.15 μV suggests problem with consistency. The same figure indicates equally low average levels for detected harmonics, which are well below 0.4 μV.

Altogether, despite low fundamental 10 Hz peak results, the flicker should be useful in BCI operations due to relatively low noise base and minimal harmonic content.

Pattern 4 (P4) results

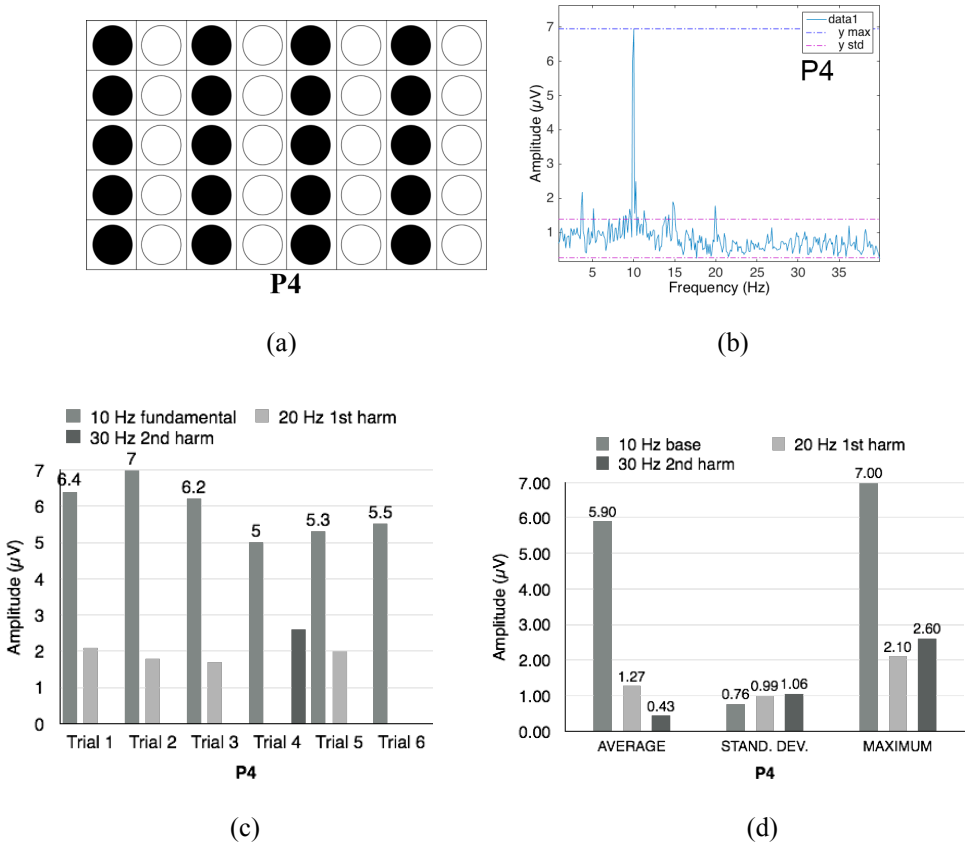

Figure 4-7 Results for P4 (a): best 10 Hz peak (b), peak amplitudes (c) and statistics (d) for 6 best trials

The fourth pattern, P4 has the form of vertical stripes each occupying 1 row of LEDs in the panel (Figure 4-7a). The 10 Hz flickering bevaviour is realised in such a way that each row of LED is replaced by the reversed pattern causing horizontal movement of the apparent image. There are 8 separate shapes flickering in this pattern. The Figure 4-7b exemplifies the best result achieved with this pattern. The maximum amplitude peak registered at 10 Hz shows 7 µV, which represents a very good value. The average noise is below 1.5 µV, however, there is visible slight trace of 20 Hz harmonic, accompanied by low frequency artefacts. Figure 4-7c indicates consistent 10 Hz peak responses in all 6 trials, however only 1 trial is free of harmonics. Equally consistent seems to be the occurrence of 20 Hz component in 4 trials, which is rather problematic. Generated 30 Hz harmonic in trial 4, although as a very isolated result, seems to be coupled with the lowest fundamental 10 Hz peak at just 5 µV value. Figure 4-7d confirms a solid 10 Hz response generated by the pattern with the average value of 5.9 µV and low standard deviation of 0.76 µV, while common existence of the 20 Hz component influenced its high 1.27 µV average level, especially considering the fact that it was found in 4 trials only.

Consistent high fundamental peak response should guarantee usefulness of this pattern for BCI systems, especially after 20 Hz harmonic removal through filtration.

Pattern 5 (P5) results

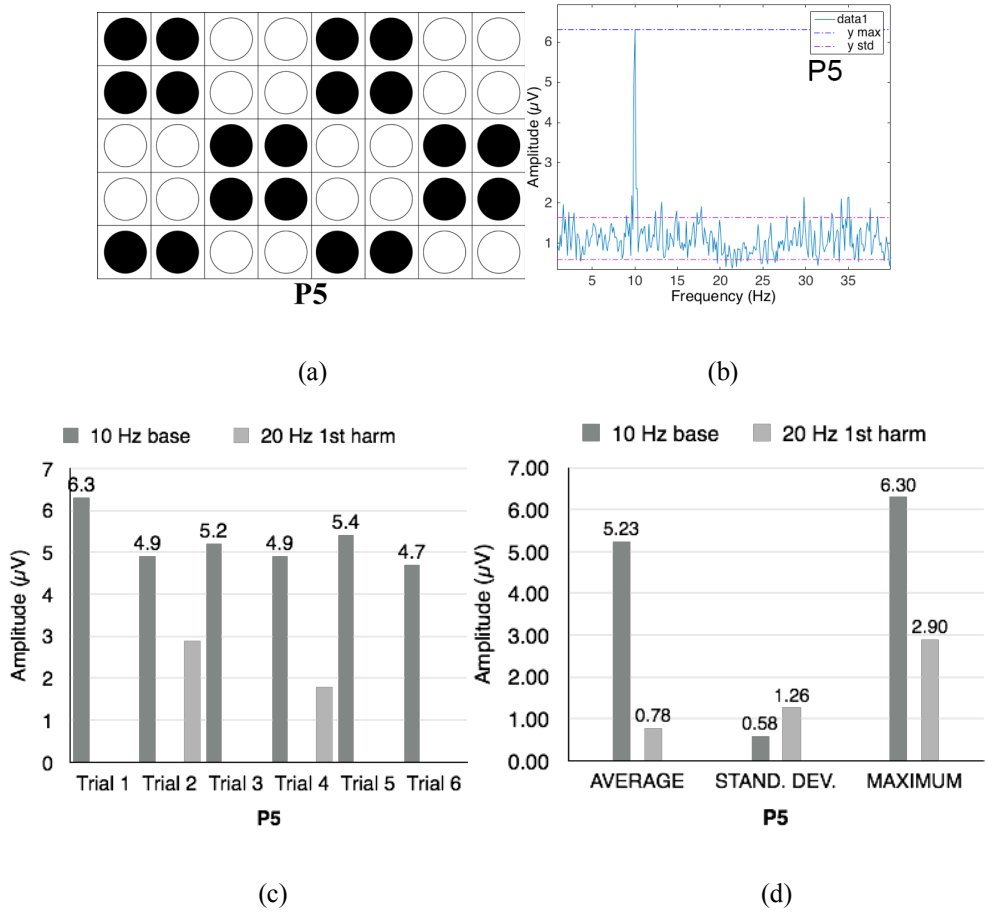

Figure 4-8 Results for P5 (a): best 10 Hz peak (b), peak amplitudes (c) and statistics (d) for 6 best trials

The fifth pattern, P5 has the form of a medium size checkerboard with incomplete pattern (Figure 4-8a). The upper part of the LED board contains 2 rows of checkers, each constructed of 4 LEDs. At the bottom of the panel one can notice the incomplete checkers with only 2 LEDs each. In total, there are 12 flickering elements in this pattern. The 10 Hz flickering behaviour is realised in such a way that all the patterns are reversed causing apparent horizontal image movement. In Figure 4-8b the best plot of 10 Hz shows the value of 6.3 μV with no visible harmonics and slightly higher noise level measured close to 1.7 μV. The bar graph plot shown as Figure 4-8c indicates even response of the fundamental 10 Hz with 2 instances of 20 Hz harmonic in trials 2 and 4. Except for the trial 6, it seems that the harmonics start to accumulate whenever the fundamental 10 Hz peak reaches levels below 5 μV. The average peak and harmonic results shown in Figure 4-8d illustrate safe gap between the two. Low standard deviation value at 0.58 μV registered for the 10 Hz component is characteristic for stable signal response induced by this pattern's visual stimulation.

The pattern produced very useable 10 Hz peaks for BCI with very minor harmonic content.

Pattern 6 (P6) results

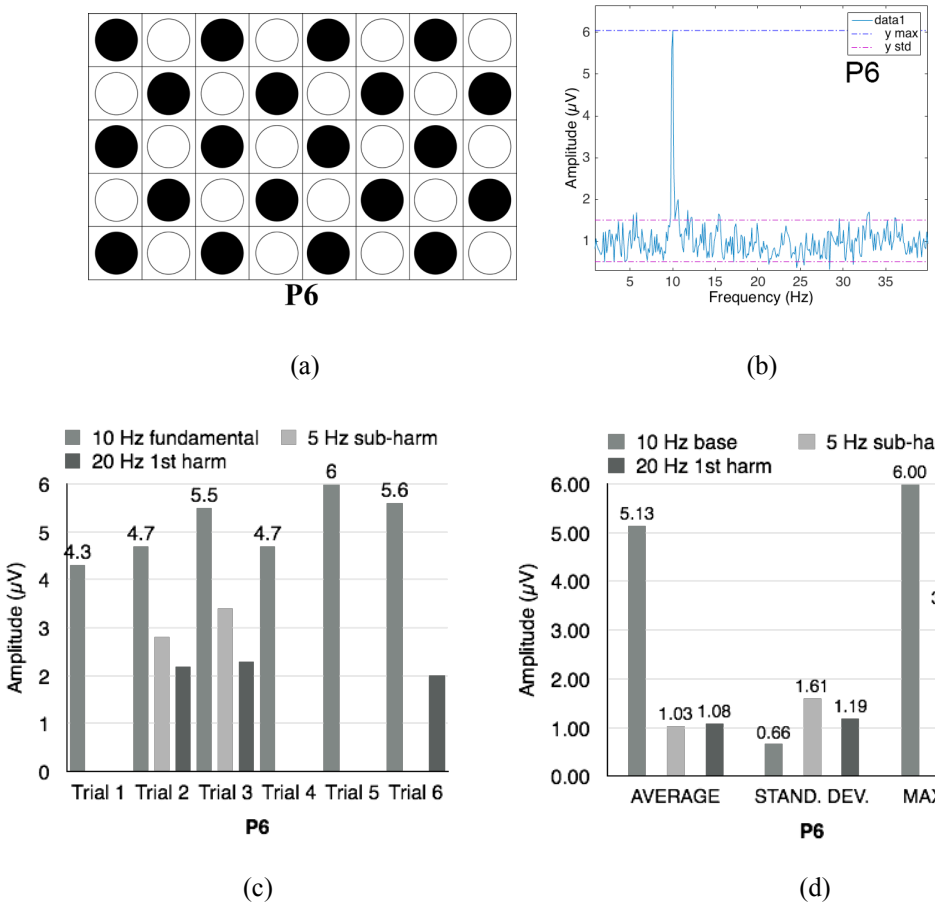

Figure 4-9 Results for P6 (a): best 10 Hz peak (b), peak amplitudes (c) and statistics (d) for 6 best trials

The sixth pattern, P6 represents the most scattered arrangement of LEDs forming flickering patterns resembling a checkerboard with the smallest checkers (Figure 4-9a). This pattern is composed of 40 separated flickering elements, the largest number tested in this experiment. The complete pattern reversal generates the 10 Hz flicker inducing apparent image movement both horizontally and vertically. Figure 4-9b reveals a clean 10 Hz peak registered at 6 μV with low noise level averaging at 1.5 μV and no harmonic content. Figure 4-9c reveals rich harmonic contamination in trials 2 and 3 of both 5 Hz and 20 Hz. The average levels shown in Figure 4-9d are in favour of the fundamental 10 Hz oscillation but the maximum values exhibit high levels of 5 Hz and 20 Hz peaks.

Although standard deviation for 10 Hz peak displays low value of 0.66 μV, the presence of many harmonics would be problematic for a successful feature extraction and thus usefulness in a BCI system could be limited.

Pattern 7 (P7) results

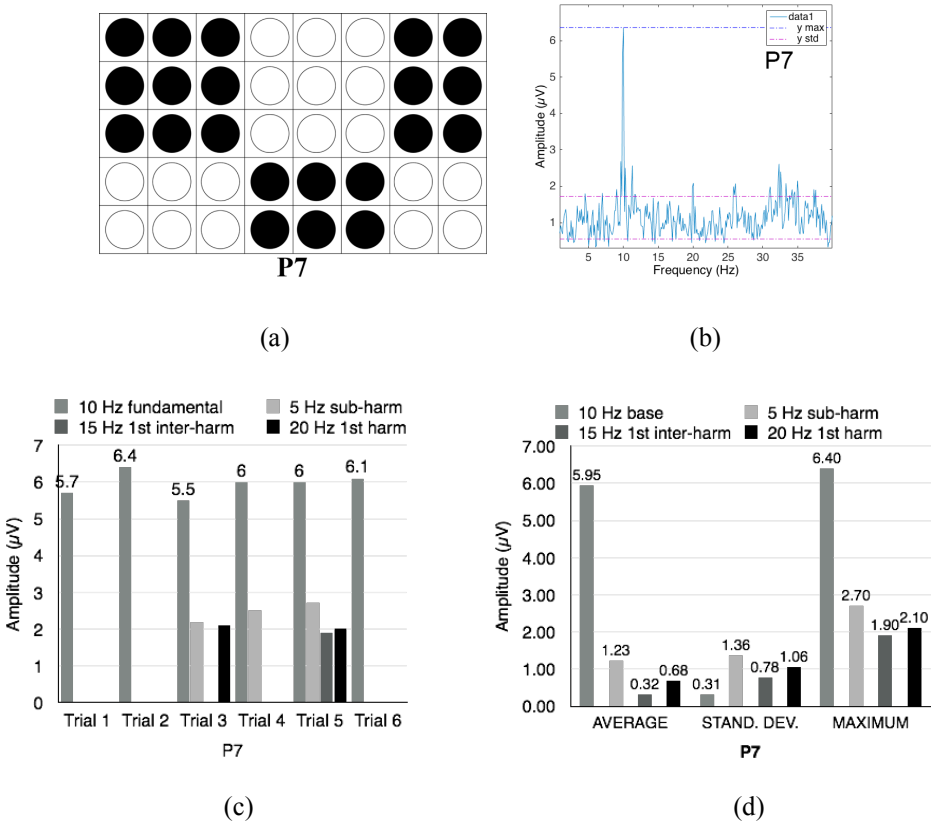

Figure 4-10 Results for P7 (a): best 10 Hz peak (b), peak amplitudes (c) and statistics (d) for 6 best trials

The seventh pattern, P7 has the form of a large size checkerboard again with the pattern incomplete, this time both at the bottom and at the right-hand side of the panel (Figure 4-10a). The upper part of the LED board contains 1 row of 2 complete checkers, each constructed of 9 LEDs and 1 incomplete checker using 6 LEDs. At the bottom, there are 2 incomplete checkers present, again with only 6 LEDs, forming 2/3 of the checker. In the right lower corner, there is a small checker field consisting of only 4 LEDs. In total, there are 6 flickering elements in the pattern. The 10 Hz flickering behaviour is realised by reversing the pattern inducing the apparent image movement along both horizontal and vertical lines. The frequency domain plot (Figure 4-10b) exposes 10 Hz peak at 6.4 μV amplitude with an average noise level readout of 1.8 μV. There is also visible slightly raised noise in the upper frequency range past 20 Hz mark. Bar graph with all 6 trials' peaks show very even 10 Hz response (Figure 4-10c), which can be further confirmed by the very low level of standard deviation at 0.31 μV (Figure 4-10d). In 3 trials however, harmonic contamination can be observed, especially in trial 5 with exceedingly rich harmonics of 5 Hz, 15 Hz, and 20 Hz. Although low average results for harmonics are positive, their maximum amplitudes, which occurred in one of the trials are substantial, which will introduce errors during feature extraction process for BCI operations (Figure 4-10d).

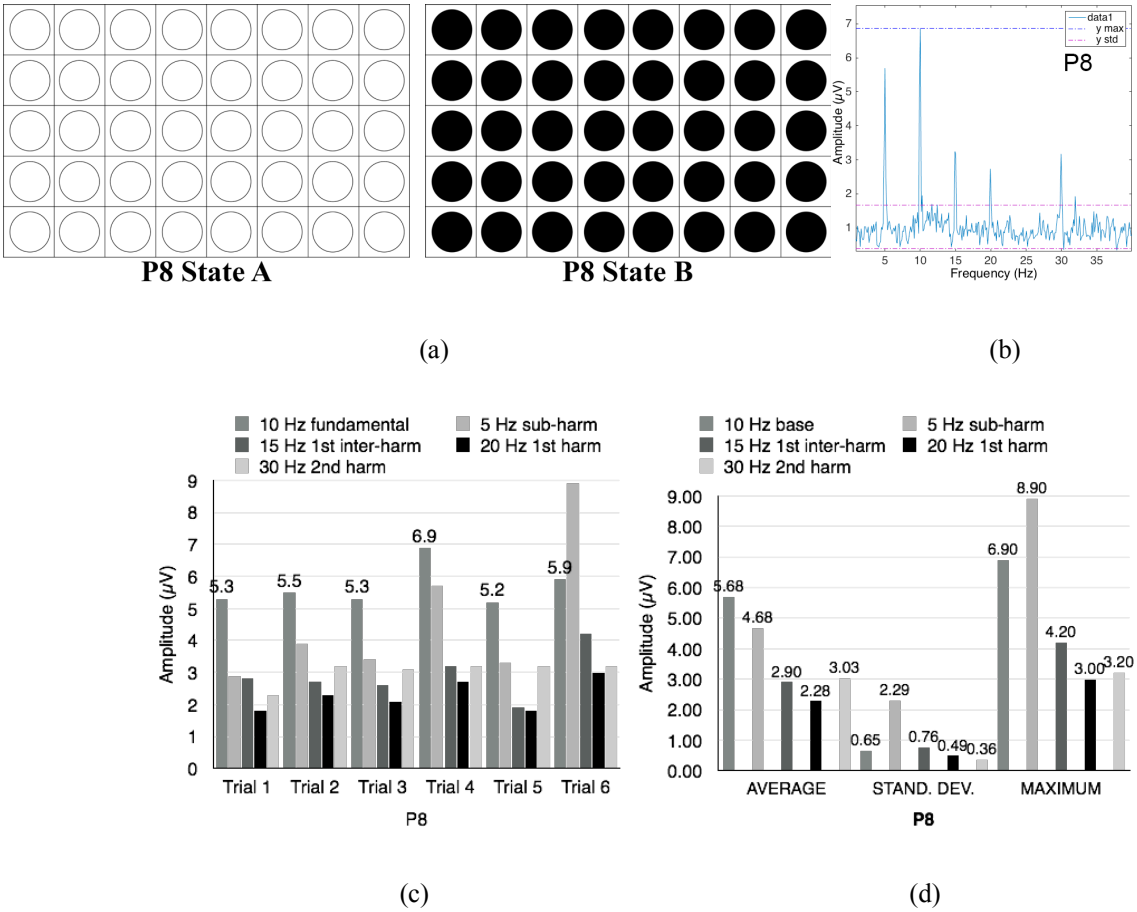

Figure 4-11 Results for P8 (a): best 10 Hz peak (b), peak amplitudes (c) and statistics (d) for 6 best trials

The eighth pattern, P8 has the form of a complete rectangle. The shape fills in the entire panel (Figure 4-11a). The 10 Hz flickering behaviour is realised in such a way that all LEDs light on or off. There is only 1 element flickering. Shown in Figure 4-11b, the best 10 Hz peak from trial 4 reveals 6.9 μV, with substantial amounts of harmonics present. Abnormally high level of 5 Hz contamination is accompanied by further harmonics such as 15 Hz, 20 Hz, and 30 Hz. The averaged noise level shows 1.8μV. Comparable signal contamination with harmonics can be reconfirmed by confronting this result with the remaining 5 results as in Figure 4-11c. Practically, in all of the recorded trials, high levels of multiple harmonics can be observed with moderate amplitudes registered for the main 10 Hz component. Figure 4-11d shows the relationship between the achieved average results, where the 10 Hz frequency at 5.68 μV only slightly exceeds the 5 Hz sub-harmonic. The remaining harmonics' results of 15 Hz, 20 Hz, and 30 Hz indicate abnormally high levels, never registered with any of the other patterns. Surprisingly, the highest amplitude level of 8.9 μV belongs to 5 Hz sub-harmonic as illustrated in Figure 4-11cd.

Due to high harmonic contamination, the pattern P8 is not recommended for BCI systems.

Pattern 9 (P9) results

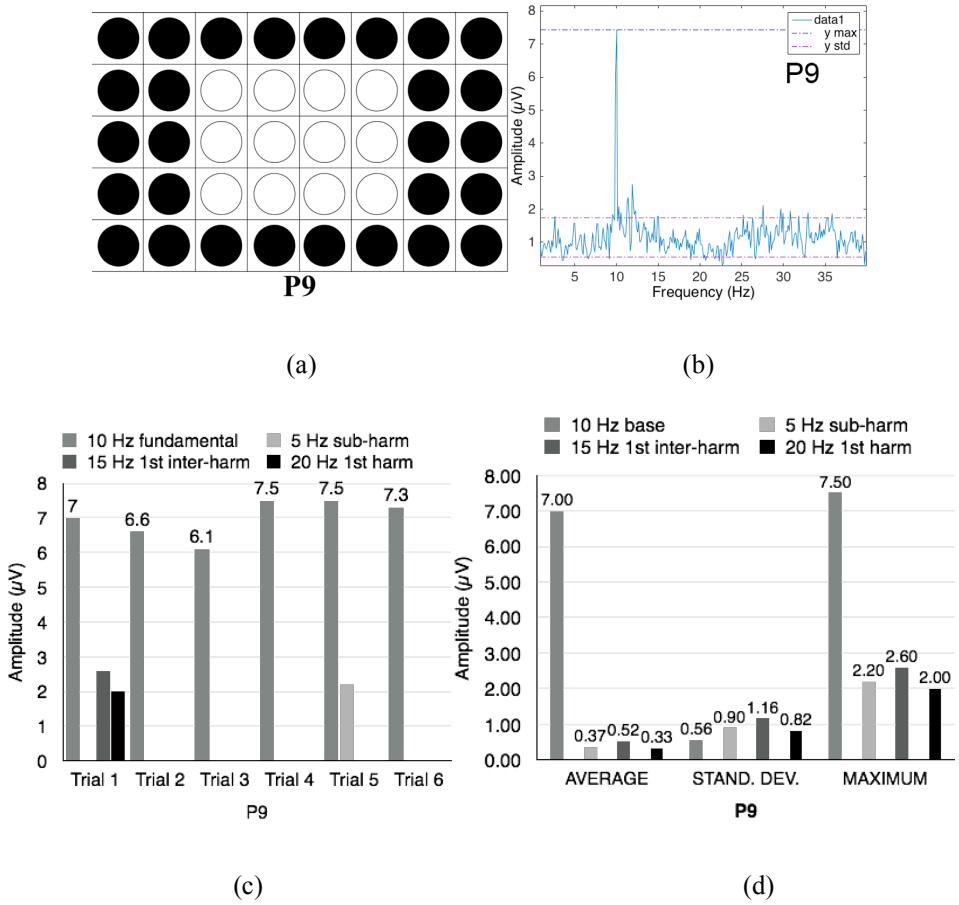

Figure 4-12 Results for P9 (a): best 10 Hz peak (b), peak amplitudes (c) and statistics (d) for 6 best trials

The ninth pattern, P9 has the form of a small rectangle placed in the middle of the LED board surrounded by a rectangular frame (Figure 4-12a). The 10 Hz flickering behaviour is realised through reversing the pattern. The apparent image movement is from center to the edges and vice versa. There are 2 shapes constituting the flickering pattern. The Figure 4-12b illustrates the best 10 Hz peak generated by this flicker in trial 4. The peak amplitude value is at 7.5 µV and is free of harmonics and artefacts. The average noise level present in this plot reads 1.8 µV, which is not as low as other successful patterns generated. A visible noise amplitude can be noticed around the fundamental 10 Hz peak as well as past 25 Hz mark. Figure 4-12c, showing all peaks registered in 6 trials, reveals 3 instances with very high 10 Hz peaks above 7 µV. Very little harmonic contamination is evident. These good results can be further instantiated by the statistical data bar graph represented in Figure 4-12d. One can notice huge amplitude difference between the average targeted 10 Hz peaks and evoked accompanied harmonics. In generated by the pattern 10 Hz peak, the standard deviation parameter is very low at 0.59 µV.

This pattern guarantees high reliability of a BCI operation due to consistent high 10 Hz peaks and minimal harmonic contamination observed in the elicited brain signals.

Pattern 10 (P10) results

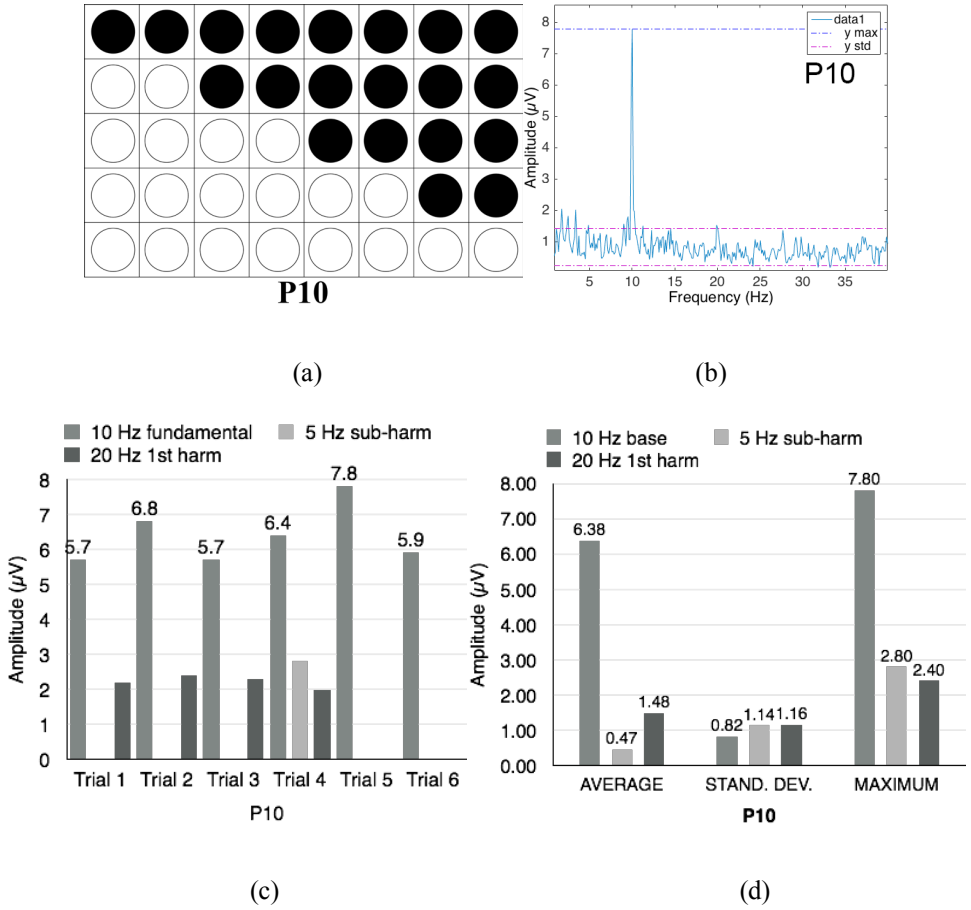

Figure 4-13 Results for P10 (a): best 10 Hz peak (b), peak amplitudes (c) and statistics (d) for 6 best trials

The tenth pattern, P10 has the form of 2 identical, reversed triangles sharing their longest side across the diagonal line of the LED panel (Figure 4-13a). In total there are 2 elements flickering in this pattern. The 10 Hz flickering behaviour is realised through reversing the pattern inducing the apparent image movement along the diagonal line. The frequency domain plot (Figure 4-13b) exposes very clean 10 Hz peak with 7.8 μV amplitude and average noise level readout below 1.5 μV. There is however, slight noise increase visible in the plot below 5 Hz. Bar graph with all 6 trials' peaks shows 10 Hz response with some variance in amplitude levels and harmonic content across all trials (Figure 4-13c). Only trial 6 is free of any harmonics. Statistics in Figure 4-13d indicate reasonably low standard deviation of 0.82 μV, high average at 6.38 μV and maximum at 7.80 μV amplitudes registered for the main 10 Hz component. At the same time, the 20 Hz harmonic occurred in 4 trials with statistical average value of 1.48 μV.

This suggests that a certain degree of filtration needs to be incorporated in the signal pre-processing in order to properly extract 10 Hz features and use them in a BCI.

4.4 Experiment Discussion and Conclusions

Recording brain signals in a normal office environment where computer screens, lighting fixtures and people moving around are present, a potential distraction and source of unwanted artefacts. In these circumstances it is to be expected that not all of the recordings will be clean and useable. Therefore, for this particular test a decision was made that multiple recordings would be carried out numbering 9 to 12 trials per pattern. It is also worth explaining the decision not to use a perfectly isolated laboratory room. At its origin, the author's core focus was to determine all the possible techniques and methods, which could lead to developing low-cost stimuli driven BCI system. This system could eventually be commercialised and applied to a variety of applications with potential appeal to a wide base of end-users. Therefore, testing in normal condition is crucial for this research. When looking at the signal plots assembled in Figure 4-14 it is quite clear that all of the prepared patterns are capable of eliciting 10 Hz peak that is distinguishable from the noise floor.

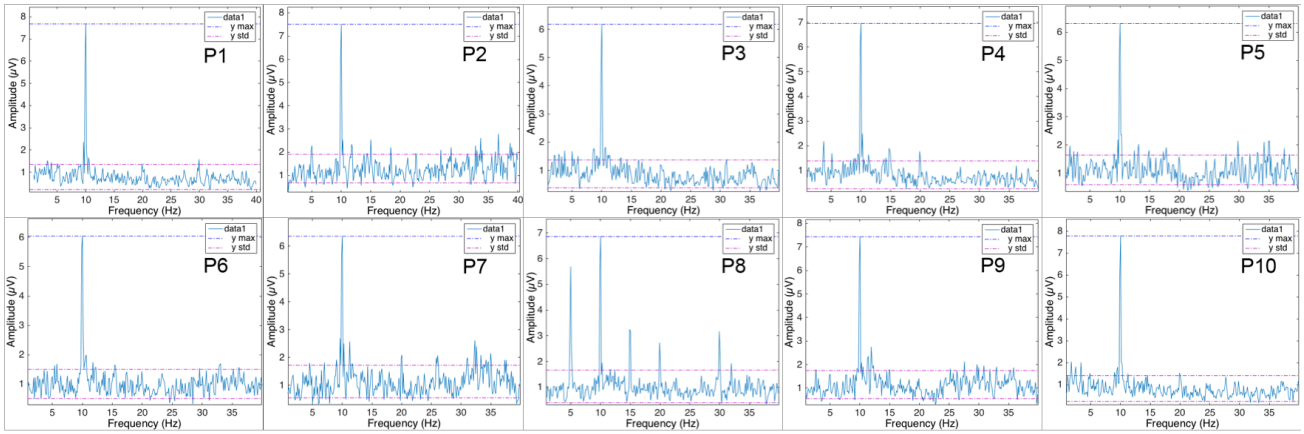

Figure 4-14 All the best signal plots for patterns P1 to P10

All the patterns except for the pattern P8 generated very clean and free of harmonics 10 Hz peaks.

However, in a system where every microvolt is important, it is significant that the evoked brain signals contain not only a strong peak that can be classified into a system command, but also are free of noise and harmonic artefacts to conserve the computing power, thus making the system more portable and low-cost.

Figure 4-14 reveals that P8 produced plenty of harmonic content, which certainly would distract the classification process. It is then recommended that this type of flickering pattern (P8) should be avoided. The next characteristic that can be noticed in Figure 4-14 plots are differences in the noise floor.

Patterns P2, P5, P7 and P9 produced slightly elevated noise floor compared to the remaining patterns P1, P3, P4, P6 and P10 which produced the cleanest signals within the best trials.

However, it should be stated that the average difference in noise floor is approximately within 0.5 μV and probably would be negligible in most classification scenarios.

From Figure 4-15 presented in Section 4.5 it can be noted that the strongest fundamental 10 Hz peak was produced by P10, followed by P1, P2 and P9. Patterns P4 and not recommended P8 registered the fundamental peaks close to the average score of 6.82 μV with the remaining patterns P3, P5, P6 and P7 registering slightly below the average.

The weakest peak was produced by P6 with value of 6.04 μV. Further analysis of the summarised data derived from the 6 best trials reveals new information about harmonic content which in most BCI system is rather considered as an artifact and an unwanted portion of the signal.

As mentioned before, the author does not recommend P8 pattern and its harmonic pollution can be observed in Figure 4-11. Clearly in all 6 trials the signals are rich in harmonics of multiple frequencies and in trial 6 the sub-harmonic of 5 Hz even overpowers the fundamental 10 Hz oscillation.

The smallest amount of harmonics can be observed in patterns P1 (Figure 4-4) with 2 harmonics in 1 trial, P3 (Figure 4-6), P5 (Figure 4-8) with 1 harmonic in 2 trials each and P9 (Figure 4-12) with 2 harmonics in 1st trial and 1 harmonic in 5th trial. However, out of these patterns only P1 (Figure 4-4) and P9 (Figure 4-12) registered exceptionally high peak levels, which ideally should be accompanied by low noise and minimum harmonics for best BCI performance. Pattern P3, despite good harmonic rejection and low noise, presented the lowest average peak level of 4.38 μV accompanied by the highest standard deviation of 1.15 μV (Figure 4-6). Pattern P5 shows good overall performance with little harmonic content, slightly elevated noise floor and average peak level of moderate 5.23 μV as shown in Figure 4-8.

Pattern P2 with slightly elevated noise floor shows good peak level with repeating strong appearance of 5 Hz sub-harmonic pollution, therefore it could prove to be problematic for BCI classification, unless a strong high-pass filtration set at 5 Hz was applied during signal processing prior to the classification (Figure 4-5). At the same time, it demonstrated low standard deviation for the fundamental 10 Hz peak with value of 0.59 μV.

Pattern P4 demonstrated low noise and useable peaks with average score of 5.9 μV (Figure 4-7). At the same time, it exposed low but noticeable harmonic content of 20 Hz and in one instance of 30 Hz. Setting a moderate low-pass filtration at 20 Hz would be advisable to improve the signal usability for BCI.

Pattern P6 although low in noise response did not deliver consistent peak response with standard deviation at 0.66 μV and average fundamental 10 Hz peak at 5.13 μV (Figure 4-9). It also exhibited a considerable amount of 5 Hz and 20 Hz harmonics in two trials, which should be successfully filtered during signal pre-processing.

Pattern P7 was one of the noisiest signals, and a noise elevation can be observed in the higher range of 30 Hz to 35 Hz (Figure 4-10). The peak response was very consistent and reached the average level of 5.96 μV with the lowest calculated at 0.31 μV standard deviation. In 2 trials however, a noticeable harmonic content can be observed with trial 5 exhibiting 3 different harmonics of 5 Hz, 15 Hz and 20 Hz. Properly tuned signal filtration would be necessary for P7. P8 as previously rejected, they will not be considered or further analysed (Figure 4-11). Pattern P10 demonstrated low noise and a very good peak response of average 6.38 μV (Figure 4-13). Although it needs to be noticed that in 4 trials 20 Hz harmonic pollution was detected. Again, a moderate low-pass filter at 20 Hz should remove the pollution. Concluding this discussion, the following observations can be made.

- Observation #1

Pattern P8 should be avoided since its results although, showing good peak level at the fundamental 10 Hz, they all contained plenty of harmonics, which renders the signals practically not useable for BCI.

- Observation #2

Pattern P3, with low noise and very good harmonic rejection demonstrated very inconsistent peak response with average level of 4.38 μV, very high standard deviation of 1.15 μV and maximum level of 6.2 μV.

- Observation #3

Patterns P1 and P9 produced the best results by eliciting high, consistent signal peaks in the fundamental 10 Hz frequency and at the same time displayed very few harmonics within the 6 trials analysed. In addition, P1 demonstrated exceptionally low noise. P9 produced the highest average peak level for fundamental 10 Hz scoring 7 μV. These 2 patterns are the most recommended for stimuli-driven BCI development using flickers.

- Observation #4

Pattern P10 achieved the highest registered peak level at 7.8 µV for the fundamental 10 Hz frequency with very low noise response. With careful rejection of the first harmonic it should prove to be very useful for BCI.

- Observation #5

Many examples of the presented flicker patterns such as P2, P4, P5 and P7, should still be useful, but they require signal processing and careful filtration to eliminate noise and harmonic artefacts.

4.5 Summary

By visual analysis of the bar graph presented in Figure 4-15a, exhibiting the summary of all the best 10 Hz peaks elicited by the tested patterns, 3 distinctive groups can be isolated by referencing to the averaged value of 6.82 µV, illustrated by the graph's last blue bar. The first group, marked by green colour bars, includes patterns P1, P2, P9, and P10 as per Figure 4-15b. These flickers generated maximum 10 Hz peak amplitude levels ranging between 7.43 µV and 7.77 µV, greatly exceeding the average (blue bar) value. The second group, marked as grey bars, includes P4 with 6.94 µV and P8 with 6.86 µV amplitude values, whose levels approximately match the computed average level. And finally, the third group coloured in red constitutes the flickers with peak values registered below the average. These flickers are: P3, P5, P6, and P7 and their values range between 6.36 µV and 6.04 µV.

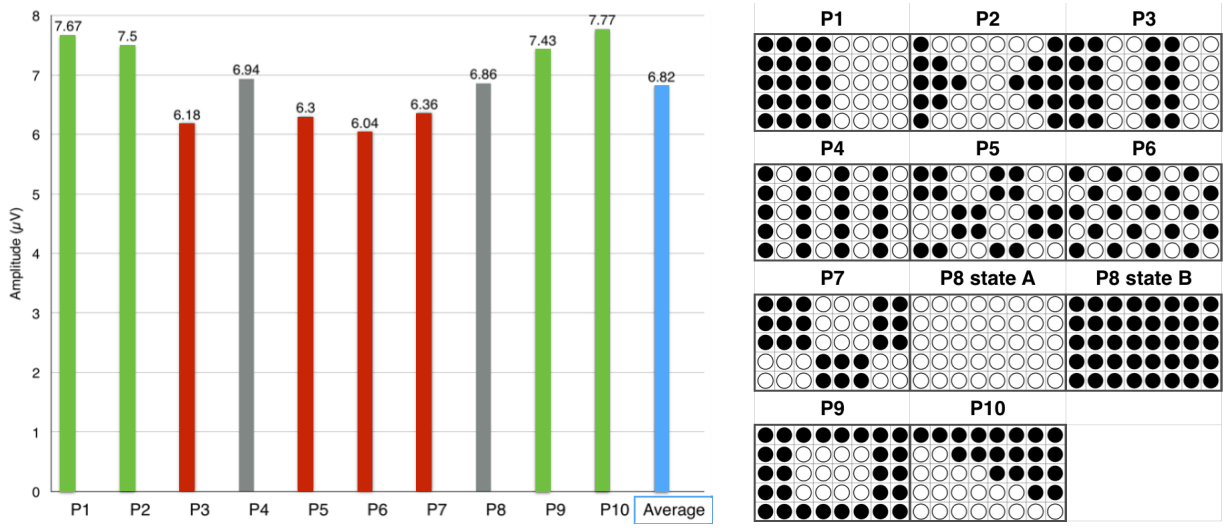

(a) (b)

Figure 4-15 Summary of best signal peaks for patterns P1 to P10 (a), all patterns tested (b)

Interestingly, almost identical results in terms of pattern grouping in relation to their performance are evident when analysing averaged 10 Hz peak levels computed from each pattern's six trials. Although as shown in Figure 4-16, the average (cyan bar) calculated from all averaged results is lower by ~1 µV when compared to the average (blue bar in Figure 4-15) derived from all maximum results, one can agree that the brain's overall response to the presented flickers is very positive. Also, the pattern grouping based on their performance is comparable. Again, three very distinctive groups can be designated. Patterns P1, P2, P9, and P10, presented as magenta bars, constitute the first group with the best performing flickers with the amplitudes raging between 7 µV and 6.38 µV. Patterns P4, P7, and P8 (yellow bars) are grouped as flickers with results between 5.95 µV and 5.68 µV, which are close to the average (cyan bar).

Patterns P3, P5, and P6 are categorised as the worst performing flickers (orange bars) and the achieved results range between 5.23 µV and 4.38 µV. It can be noted that only P7 was catalogued differently and moved from the worst performing group to the average group as displayed in Figure 4-16. The two different colour schemes used in Figure 4-15 and Figure 4-16 were introduced intentionally to discriminate between maximum and averaged values.

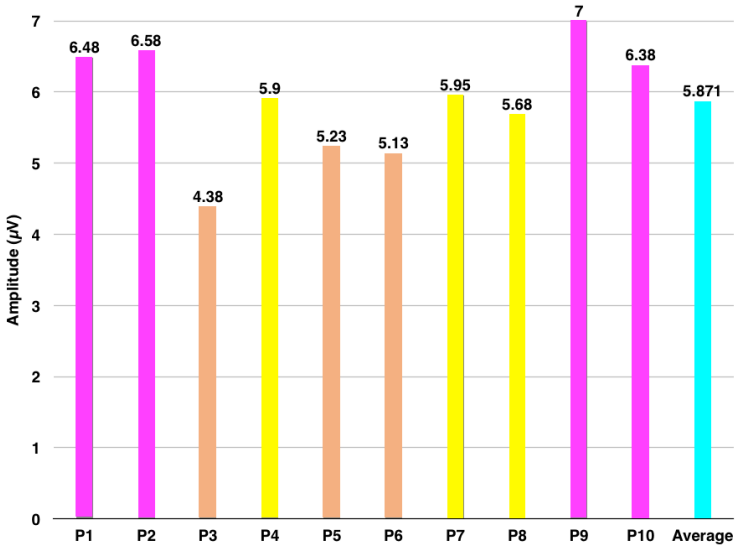

Figure 4-16 Summary of averaged signal peaks for patterns P1 to P10

This allows the author to assume that the maximum amplitudes selected from all trials as shown in Figure 4-14 are very representative and can be used as such to evaluate the patterns' performance in this experiment. The patterns, which generated the best signals with the highest amplitude peaks, the least amount of artefacts and lowest noise, are the ones with at least 2 and no more than 3 flickering elements. These are the patterns most recommended for visually controlled BCI system as shown in Figure 4-17.

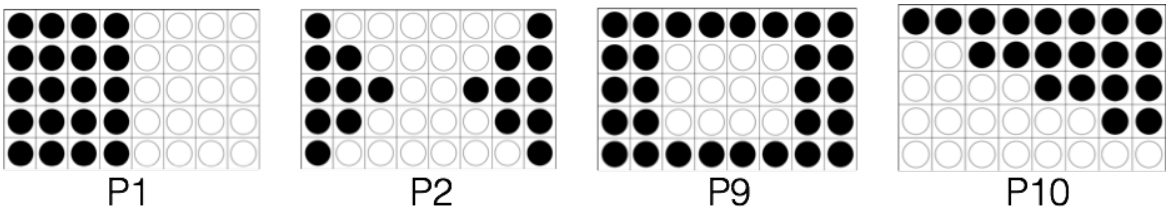

Figure 4-17 The best performing patterns with peak amplitudes above average

The patterns, which generated the worst signals with the lowest amplitude peaks, the highest amount of artefacts and the highest noise, are the ones with more than 3 flickering elements in them as illustrated in Figure 4-18.

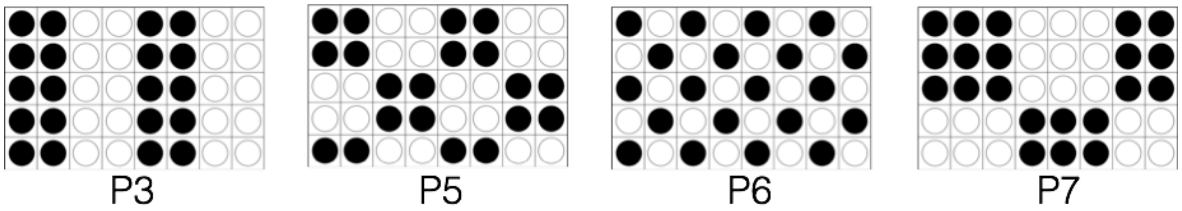

Figure 4-18 The worst performing patterns with peak amplitudes below average

Although these signals, after signal pre-processing, eliminating harmonics, noise and other artefacts, can be useful, they are not the most recommended for BCI use, especially when compared against the cleanest signals generated by the best performing patterns (Figure 4-17).

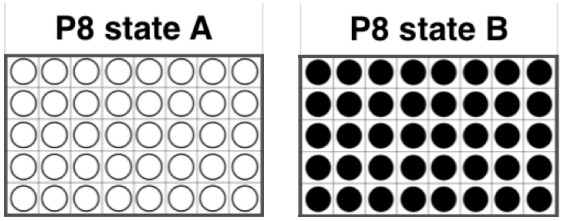

Figure 4-19 Example of the pattern producing the highest number of harmonics in the brain signals

The pattern represented in Figure 4-19 is an example of a flicker, which despite producing reasonable amplitudes of the main 10 Hz component, should rather be considered as unjustifiable for a visually driven BCI system, due to excessive harmonic content manifested in all recordings. It is a typical example of a light source with a 'full on – full off' flickering behaviour. Its very poor performance against the rest of the patterns with at least 2 or more flickering shapes suggests that indeed this type simple light is not very effective in eliciting SSVEP signals.

The patterns P1 and P10 generated the highest maximum peak amplitudes, while the pattern P9 produced the highest average score. This can be attributed to the fact that they all represent flicker patterns with only two flickering fields. The final conclusion is that for this type of small light source (3.5 cm x 6.5 cm), patterns with highly scattered LED elements should be avoided.

Chapter 5 Analysis of Stimuli Graphics Resolution and Colour

5.1 Introduction

Another potentially crucial parameter found in computer graphics is resolution, which for simplicity reasons can be referred to as graphic size or dimension. Usually, these terms are used in relation to digital screen parameters. In digital screens these terms are often confusing. The screen resolution describes the number of distinct pixels that can be displayed vertically and horizontally. The screen size however, is measured in inches and it represents its physical size. Today, the pixel size can vary between the screens, therefore the parameter known as Pixel-Per-Inch (PPI) determines the real screen resolution, i.e. the pixel density of the screen. In digital graphics it is possible to increase the graphic's dimensions by digital transformation known as 'resizing', which physically changes the graphic's size but does not change its resolution. In this research the terms size and resolution can be interchanged since no artificial resizing ever occurred. Meaning, each dimension of the graphics always contained the right amount of pixels for that size thus matching the resolution. The stimuli graphics size/resolution was tested using rendered checkerboard flickers displayed on a 12.9" tablet screen.

Multiple colour checkerboard flickers were also tested with 3 subjects to find any possible correlation between the fundamental 10 Hz and harmonic 20 Hz response and brain lobe activations. Specifically, the occipital and parietal lobes were considered.

Furthermore, the performance of colour checkerboard flickers was tested against their greyscale versions. For this test the total of 33 colour flickers were tested and compared against the greyscale versions. The motivation for this test was to establish, whether the impact of saturated colour on the elicited brain signals could be proved.

Finally, selected colour flickers and the black and white reference version were tested with multiple users to investigate the effectiveness of colours in eliciting target 10 Hz brain signals. The expanded user base is crucial to obtain credible results constituting the finalisation of this research.

All the achieved results for the graphic resolution/size, pattern and colour dependencies found in brain signals are presented in the subsequent Sections.

5.2 Testing Resolution with Black-White and Red-White Flickers

This Section investigates brain signal peaks and their relationship to flicker size and resolution using colour red-white (RW) and monochrome black-white (BW) graphics. Experiments using more colours will be discussed later in this thesis. The raw electroencephalograph (EEG) signals were recorded using a rotated Emotiv EPOC headset into Windows based PC running Emotiv Xavier Test Bench software. The flickers oscillating at 10 Hz of different resolutions were displayed over black and white backgrounds using a 12.9" screen tablet. The signals were analysed and their amplitude and noise levels were measured using MATLAB with EEGLAB and ERPLAB plugins. In this experiment the BW flickers served as a reference and the main purpose was to examine, whether introducing a colour flicker, in this case RW, would introduce any detectable difference in the signals quality. Choosing two types of background for flickers presentation where black served as a dark background, and white served as a bright background had its own purpose. The idea is to establish, whether the element of background brightness could be considered as another factor influencing the elicited brain signals. In essence, during this extensive experiment there were numerous factors taken into consideration for brain signal quality improvement: flicker size/resolution using 6 dimensions, background brightness using black and white, and the brain's response to colour using red-white checkerboards versus the reference black-white checkerboards.

5.2.1 *Experiment Setup*

Most of the SSVEP-based systems utilise only black and white graphics due to the increased contrast ratio. Therefore, incorporating colour into stimuli graphics tests is vital in order to discover new dependencies between the elicited brain signals and colour flickers. Equally important is investigating the graphics resolution/size in relation to quality of the EEG signals they induce.

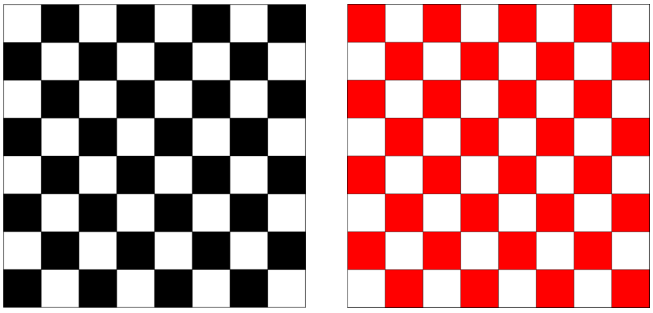

Figure 5-1 BW and RW flickers used in the experiment

This Section investigates brain signal peaks and their relationship to flicker size/resolution using colour red-white (RW) and monochrome black-white (BW) checkerboard flickers as shown in Figure 5-1.

For the standard red colour, RGB coordinates of 255, 0, 0 were chosen (Hex Colour Code FF0000). The 10 Hz flickers were displayed over black and white backgrounds for testing scenario variety as shown in Figure 5-2.

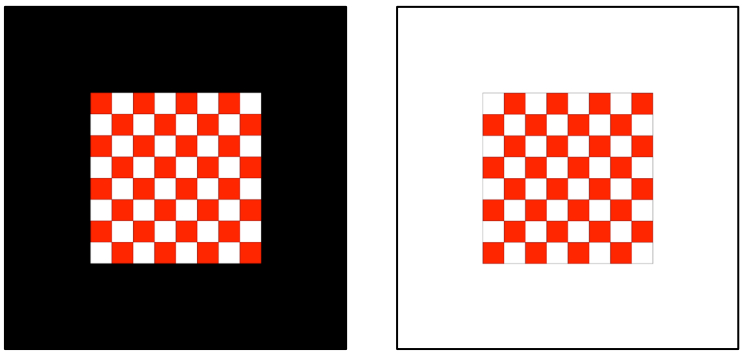

Figure 5-2 RW flicker with 50% resolution on black and white backgrounds

This figure exemplifies RW flicker in 50% resolution displayed over the two types of backgrounds; black and white used during this experiment. The resolution relationship is detailed later in this Section.

The flickers were designed in Adobe Illustrator CS6 and rendered in multiple resolutions as H.264 MPEG-4 video files using Adobe After Effects CS6 motion graphics software. For testing they were displayed on a 12.9" tablet screen using open source VLC media player. For more details on graphics design method please refer to Section 3.2.3.

The hardware and software setup was as follows. Raw EEG signals were captured as European Data Format files (EDF) by a rotated Emotiv EPOC headset wirelessly communicating with Windows 7 based PC computer running Emotiv Xavier Test Bench software. The signals were then analysed in MATLAB using EEGLAB and ERPLAB plugins. For more details on the hardware and software used during this experiment please refer to Section 3.2.

The brain signals were recorded from one male 'subject 1' wearing glasses in 4 repeated trials for each flicker type in sessions of approximate 30-40 seconds per trial. The flickers were presented from a distance of 50 cm. The tablet screen was set to full brightness in a brightly lit office room environment with normal level of ambient noise.

The 10 Hz checkerboard black-white (BW) and red-white (RW) flickers in square shape were presented both on white and black backgrounds in multiple resolutions where 1080 x 1080 pixels served as 100% reference. The other resolution used are listed in Table 5-1.

Table 5-1 Flicker resolutions/sizes

Flicker size in %	100%	75%	50%	25%	15%	10%
Flicker resolution in pixels	1080 x 1080	756 x 756	540 x 540	270 x 270	162 x 162	108 x 108

In total, for this experiment 88 brain signal recordings were performed. During visual inspection of the flickers, it was determined that all flickers presented in 100% resolution, filled in the entire screen estate and there was no difference between black or white background. Therefore, the results achieved for 100% with black background were copied and used for white background scenario as detailed in Table 5-2 and Table 5-3

Table 5-2 Black-white (BW) flicker trials

Flicker resolution (%)	100%	75%	50%	25%	15%	10%	**Total no of trials**
No of trials on black background	4	4	4	4	4	4	**24**
No of trials on white background	Results copied from black background	4	4	4	4	4	**20**

Table 5-3 Red-white (RW) flicker trials

Flicker resolution (%)	100%	75%	50%	25%	15%	10%	**Total no of trials**
No of trials on black background	4	4	4	4	4	4	**24**
No of trials on white background	Results copied from black background	4	4	4	4	4	**20**

Figure 5-3 shows examples of BW checkerboard flickers displayed by the tablet on black background in 100%, 50%, 25% and 10% resolutions. Each recording was stored as a separate EDF file for analysis.

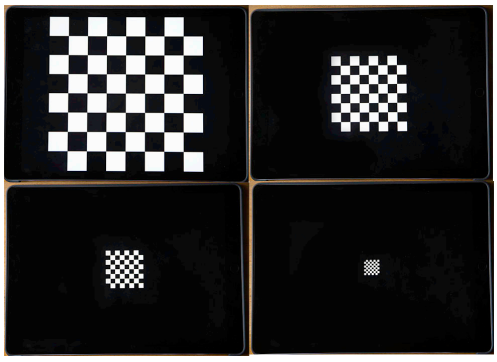

Figure 5-3 Comparison of 100%, 50%, 25%, and 10% flicker resolutions

The black-white checkerboards of four different resolutions displayed on the 12.9" tablet on the black background.

The signals were then opened in MATLAB using EEGLAB plugin's BIOSIG toolbox. Before generating frequency domain plots for each captured signal, only very basic pre-processing operations were performed. First sensor locations were assigned, next signal detrending, also referred to as baseline removal, was performed. Finally, automatic artifact rejection set equally for all signals was done as illustrated in Figure 5-4, followed by low pass and high pass FIR filtration (Figure 5-5) with boundaries set at 1 Hz and 20 Hz.

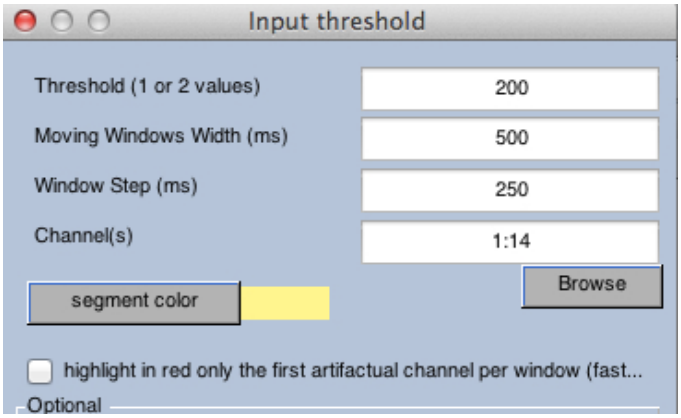

Figure 5-4 Automatic artifact rejection settings for captured EEG signals

Frequency domain signal peaks were derived from ERPLAB plugin. Channel 1 (AF3 location) was selected as the most representative for all recordings. In most of the cases channels 1 (AF3), 3 (F3), 12 (F4) and 14 (AF4) carried signal peaks of equal amplitudes.

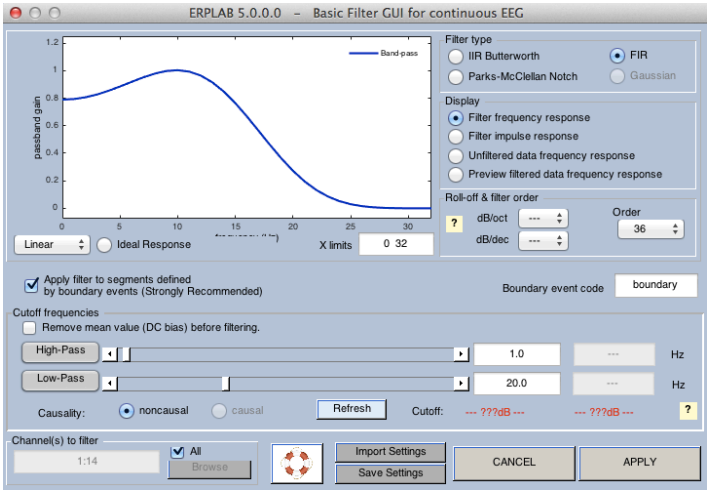

Figure 5-5 Filter settings for EEG signals

5.2.2 Test Results

The following set of figures represents amplitude levels vs noise floor achieved during this experiment for all flicker resolutions per individual trial. First, presented are individual trial results for BW and RW checkerboard flickers displayed over black and white backgrounds. Next, comparison plots are arranged to find whether any possible common trends can be observed. Finally, averaged results for all peaks and noise levels registered are submitted for even more conclusive signal tendency analysis. The values for the plots were obtained from the individual FFT plots from MATLAB as exemplified in Figure 5-6.

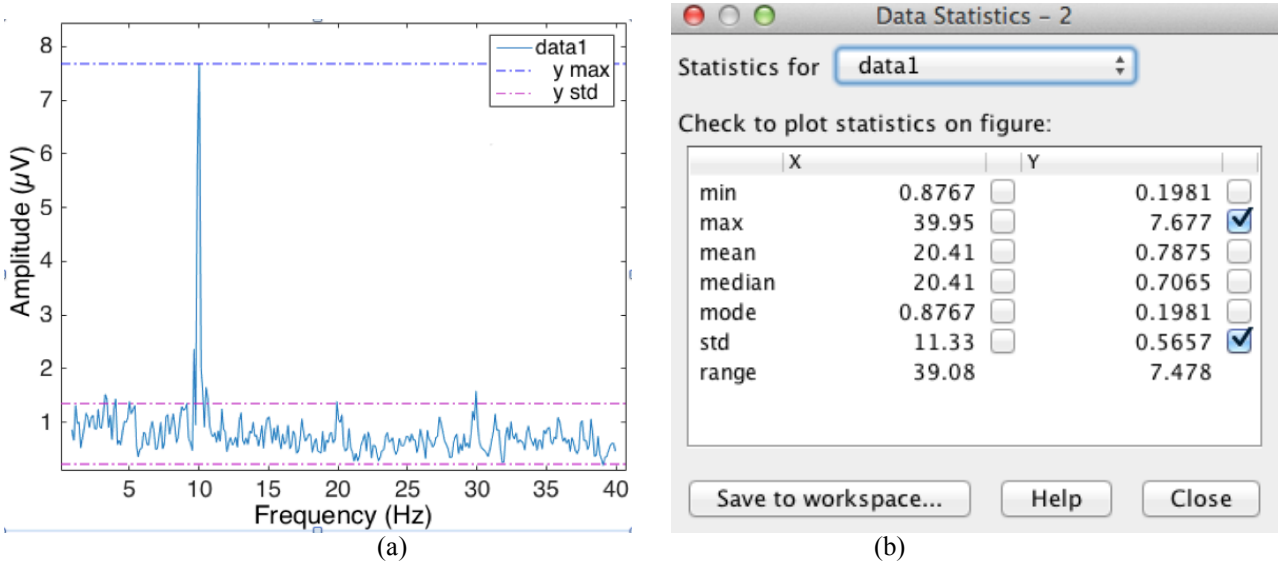

(a) (b)

Figure 5-6 Example of elicited peak and noise readout generated by FFT in MATLAB.

Single channel peak plot (a), and data Statistics function with 'max' and 'std' values selected for the Y axis. Individual plots were generated for each recorded signal and the values entered into the spreadsheet software (Numbers by Apple) to generate plots used in this Section.

A. BW flickers – individual trials

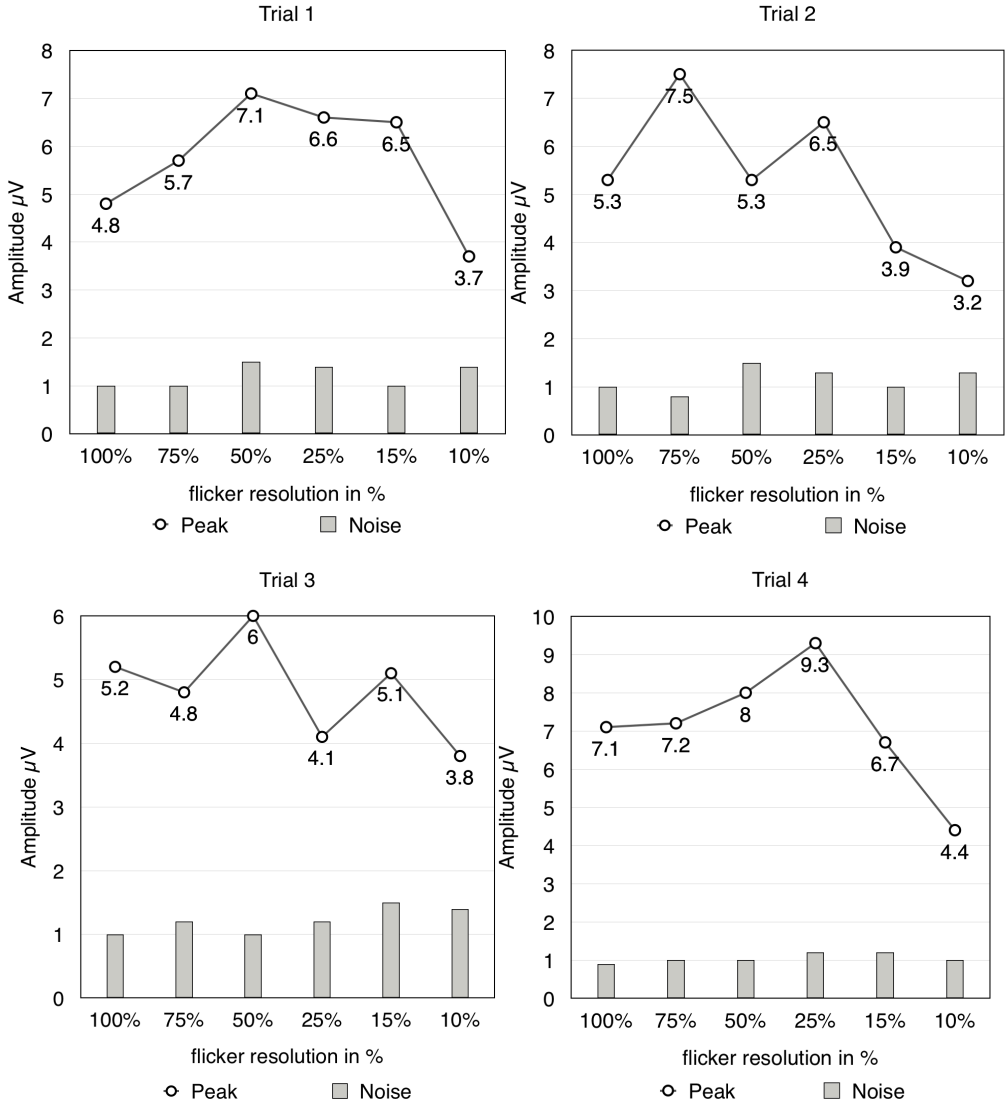

Figure 5-7 BW flickers over black background

Figure 5-7 represents four trials of SSVEP elicited brain signals using BW flickers over black background in six sizes from 100% to 10% resolution. In all of the graphs the X-axis represents flicker resolution expressed as a percentage, while the Y-axis shows amplitude values expressed in μV. At the bottom of the plots, there are grey bars indicating noise levels.

The circled line joins peak levels achieved by each flicker. In this example Trial 1 and Trial 4 produced balanceds response with the tendency of improved signal level for the medium sized flickers. The 10% resolution flickers generated the lowest amplitude levels in all 4 trials. In three trials the 100% flicker versions elicited noticeably weaker signals than the medium sizes. The noise is low in all 4 trials.

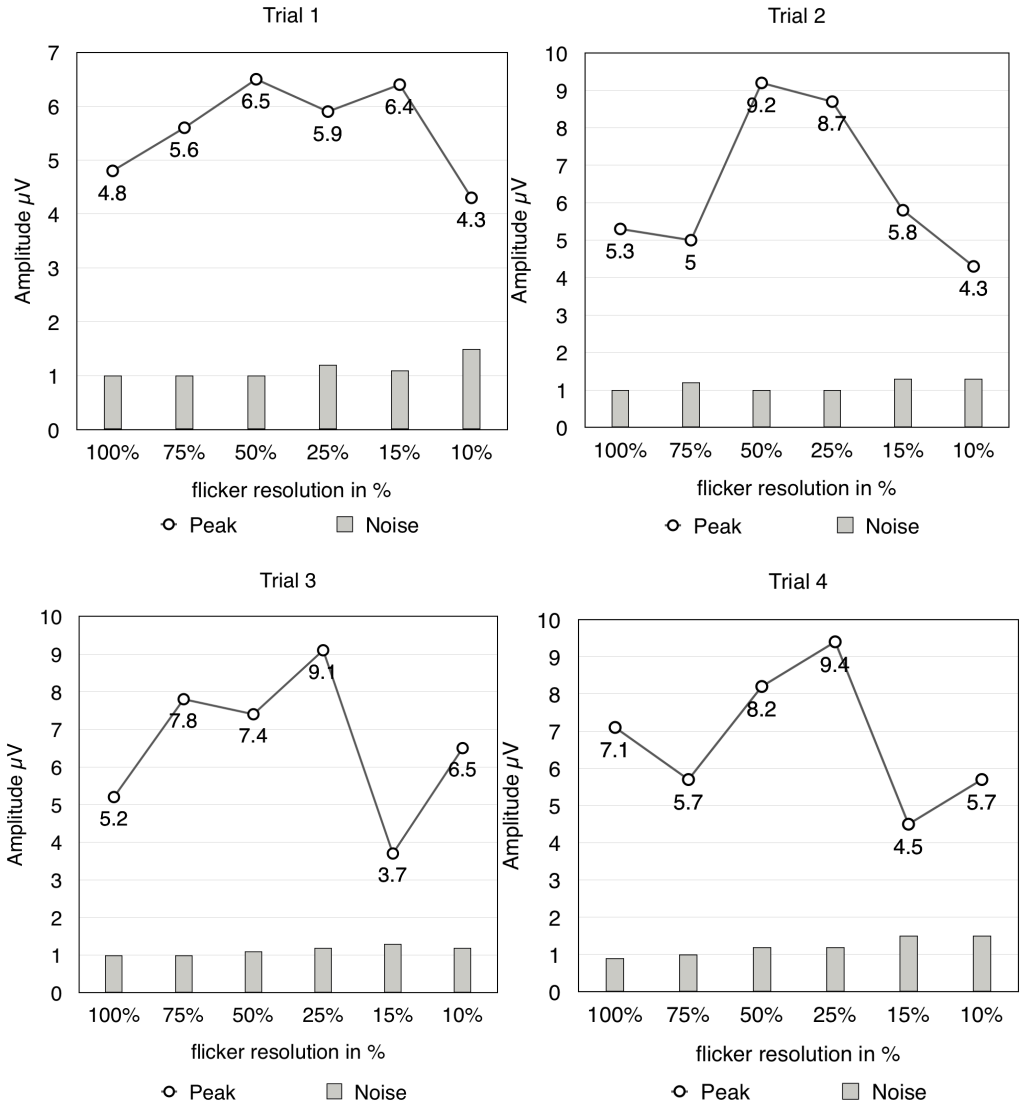

Figure 5-8 BW flickers over white background

Figure 5-8 illustrates a similar scenario with BW flickers, this time displayed over a white background. Very similar behavior can be observed with peaks gaining in value with decreasing flicker size compared to 100% variant. Trial 1 illustrates the most balanced response. The remaining trials, although more erratic in response, also present the tendency of increased peak levels within the medium flicker sizes. In comparison to black background results, in some of the instances; higher peak levels can be confirmed especially in Trial 2, Trials 3, and Trial 4. Similarly, a considerable drop in signal strength can be noticed with resolution decreasing below 25% mark.

Surprisingly, in two instances, it was the 15% flicker that generated the lowest signal amplitude. Noise level is low across all trials with values between 1 µV and 1.5 µV.

B. RW flickers – individual trials

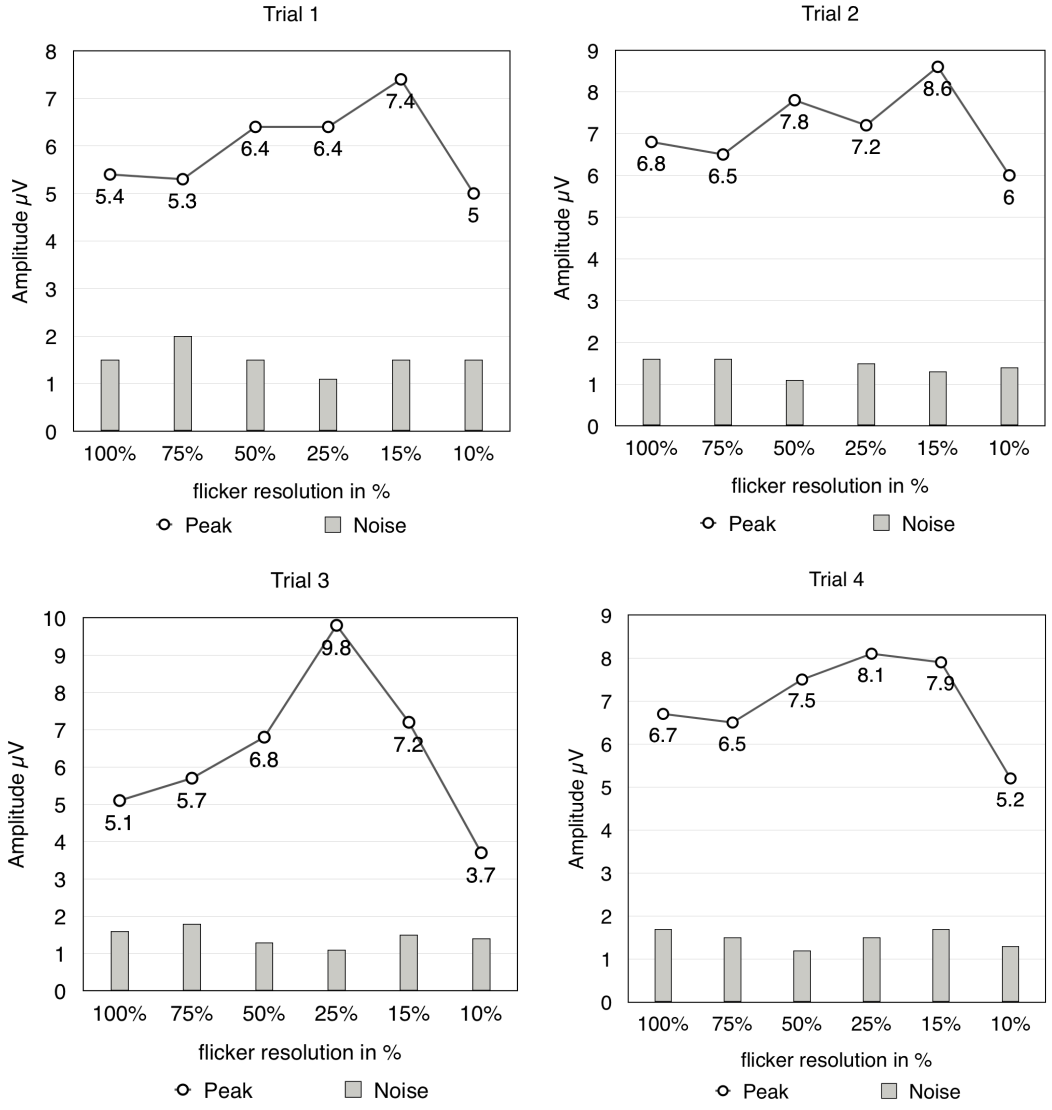

Figure 5-9 RW flickers over black background

Figure 5-9 shows RW flickers displayed over black background. These flickers introduce colour, red paired with white, as the alternative to traditional black and white graphics. The recorded 4 trials exhibit very similar brain response to visual stimuli. Medium sized flickers, when compared to extremities; e.g. 100% and 10% sizes, appear to perform better, eliciting higher signal amplitudes. When analysing the curvature of the plots, they seem to possess fewer erratic characteristics when compared to BW flicker responses, which suggests a more dependable response. In three trials, the lowest 10% size performed surprisingly well with amplitudes equal or higher than 5 µV. In Trial 3, the 25% resolution flicker generated very high 10 Hz peak at 9.8 µV, a level never achieved by any of the BW flickers.

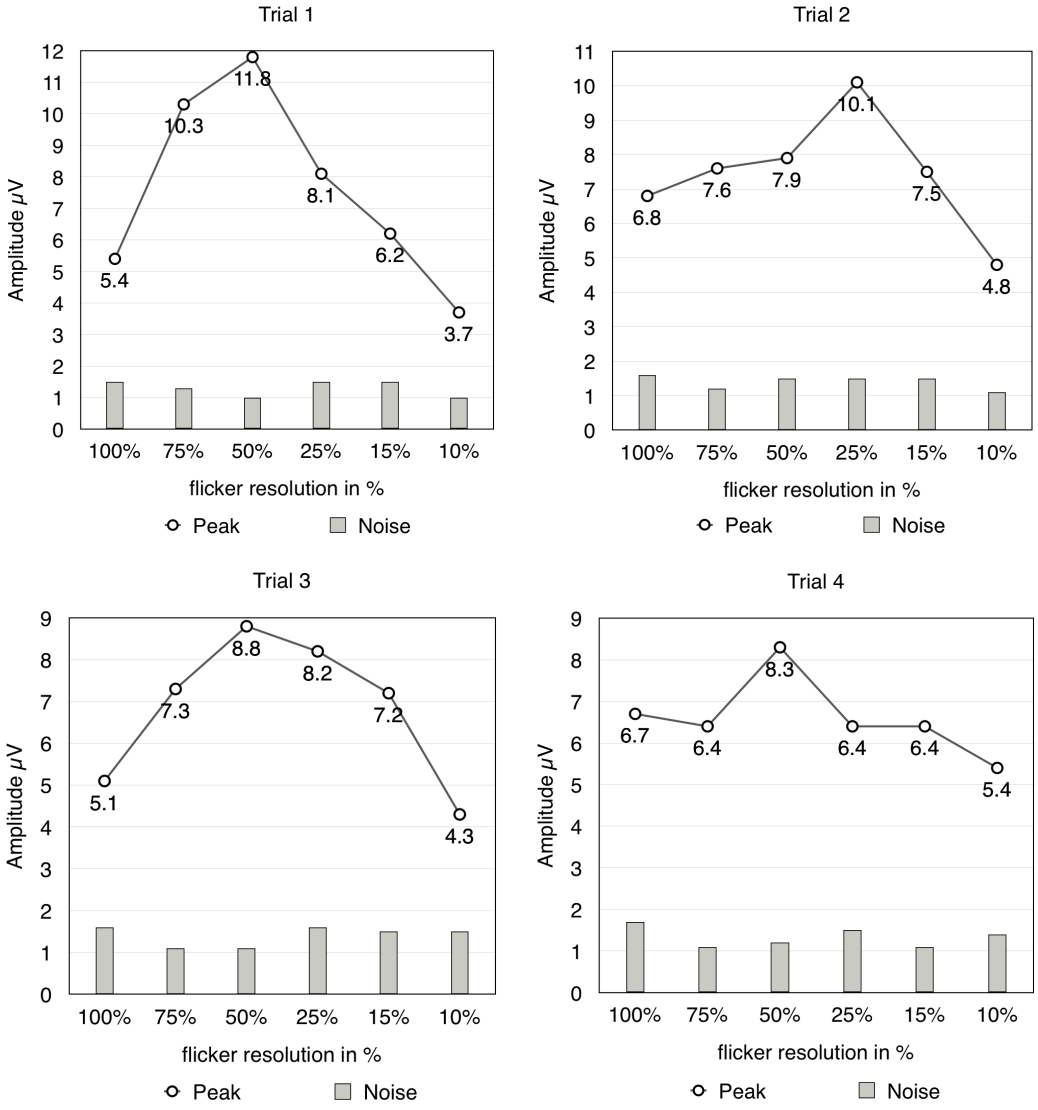

Figure 5-10 RW flickers over white background

Figure 5-10, with less erratic signal levels, exposes very even and balanced overall results producing very dependable brain signal responses. The same phenomenon of improved signals with flickers between 75% and 25% is evident compared to the highest 100% and the lowest 10% resolutions. In the RW experiment, all medium size flickers produced exceptionally high peak levels outperforming all the previous flickers. The highest result at 11.8 μV was registered in Trial 1 for 50% resolution, followed by 10.1 μV achieved in Trial 2 for 25% resolution graphic. The noise level in all trials is very comparable to all the previous results, which suggests that the targeted 10 Hz signal peak increase is possible without increasing the noise level.

Inspecting the individual results, it is quite evident that both BW and RW flickers displayed over the white background have produced stronger peak response compared to the black background. This suggests that brighter backgrounds should work better than darker backgrounds for stimuli presentation using digital screens such as the tested 12.9" tablet.

C. *BW and RW flickers – results comparison*

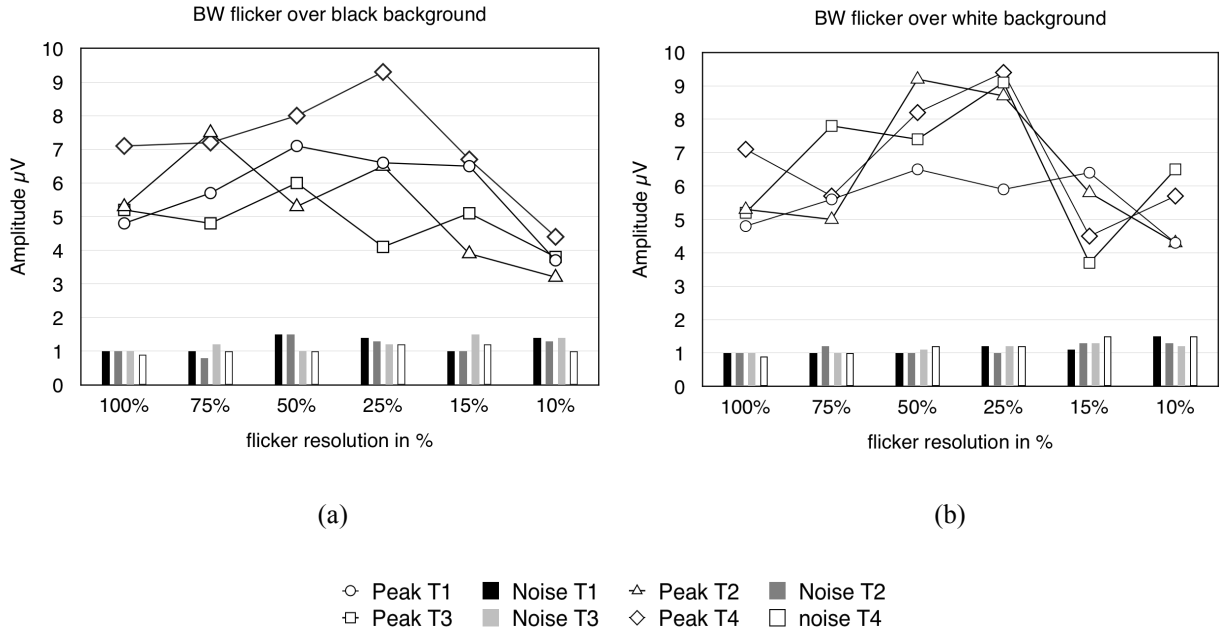

Figure 5-11 BW flickers over black and white background

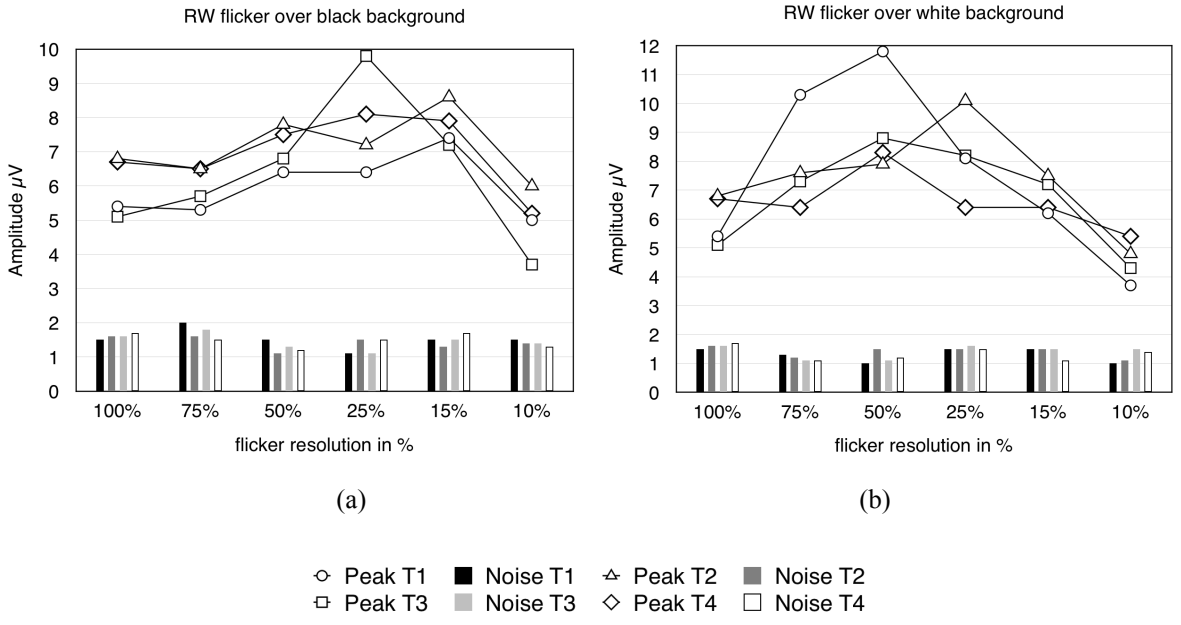

Figure 5-12 RW flickers over black and white background

Figure 5-11 and Figure 5-12 combine results from all 4 trials for all flicker resolutions in order to compare elicited amplitude levels versus registered noise. The overlaid graphs reveal certain tendencies, which otherwise would be difficult to note. For the BW flickers the white background produced significant boost in the peaks amplitudes for resolutions ranging between 50% and 25% with relatively low noise floor. The peak amplitudes for 100% and 75% are in the same range between 5 and 7 for both black and white backgrounds. Flickers with black background exhibit

considerable drop in signal peaks for the 10% variants. Overall, it is safe to state that the white background offers visible improvement in the quality of the elicited EEG signal peaks for BW flickers (Figure 5-11b). As shown in Figure 5-12, the RW flickers in 100% resolution show almost identical response to BW ones. Slight improvement can be seen in the flicker versions with white background starting from 75% resolution with the Trial 1 (T1) recording exceeding the level of 10 μV in amplitude (Figure 5-12b). For black background T3 reached the level of 10 μV for 25% resolution flicker while for white background one trial for each 75% (T1) and 25% (T2) achieved similar scores. RW flickers with black background demonstrate peak improvement for 50%, 25% and 15% resolution. Interestingly both 100% and 10% resolution flickers produced almost identical responses despite such a large difference in resolution. The variants with white background show signal improvement from 75% to 25% resolution. The 15% was still better than 100% full resolution version. Again, a visible drop in peak amplitudes was demonstrated by the smallest 10% resolution graphics. The peak signal strength was better in the medium range of resolutions, which can also be observed in the BW flickers. However, general improvement of the RW flickers over the BW counterparts is undeniable. For RW stimuli, the role of white versus black background seems to be less significant compared to BW graphics, suggesting that the impact of colour saturation is of greater significance.

D. BW and RW flickers – averaged signal peaks comparison

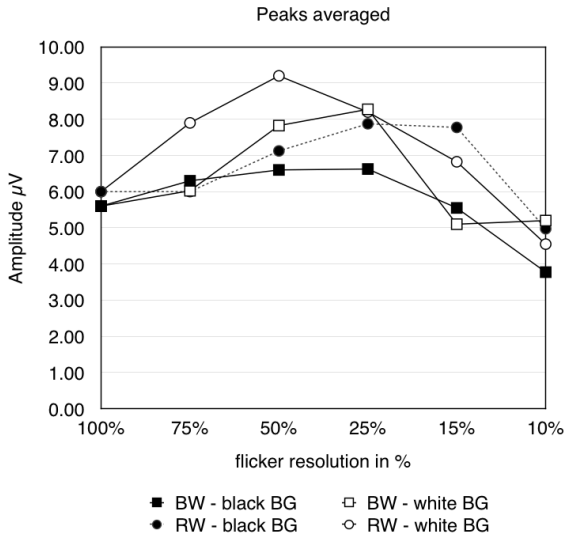

Figure 5-13 Averaged signal peaks for BW and RW flickers with black and white background

Figure 5-13 shows averaged peak values for all four scenarios and from the graph it can be stated that there is a visible tendency of signal peak increase between 75% and 15% for all flickers. The 100% full resolution graphics produced slightly less pronounced peaks while the 10% resolution yielded noticeably the weakest peak response.

The BW flickers with black background (black squares on the graph) show the weakest peak values but still very coherent response curve. The BW flickers with white background show significant peak value increase for 50% and 25% resolution. The RW flickering checkerboards with black background (black dots on the graph) indicate a substantial peak increase for 25% and 15% resolution when compared to BW variants with the same background. This suggests that the saturation of red colour positively impacts the elicited signals. The RW stimuli graphics with white background (white dots on the graph) exhibit the strongest peak values with the most coherent overall performance across all the tested graphic sizes. From this combined positive effect of white background and red colour one could advocate for a theory that indeed certain parameters of the graphics such as colour saturation or brightness of the background can influence brain signals.

(a) (b)

Figure 5-14 Comparison of 100% (a) and 15% (b) checkerboard resolution

The black-white checkerboards of two different resolutions displayed on the 12.9" tablet on the black background.

Also, this plot reconfirms previously expressed findings that the medium sized flickers are most effective. Interestingly, from this graph it is evident that even small size flickers i.e. 15% variant (Figure 5-14b) elicit slightly better brain signals than the 100% size (Figure 5-14a). This implies that using multiple small stimuli graphic elements arranged evenly on the screen should still be effective.

E. BW and RW flickers – averaged signal noise comparison

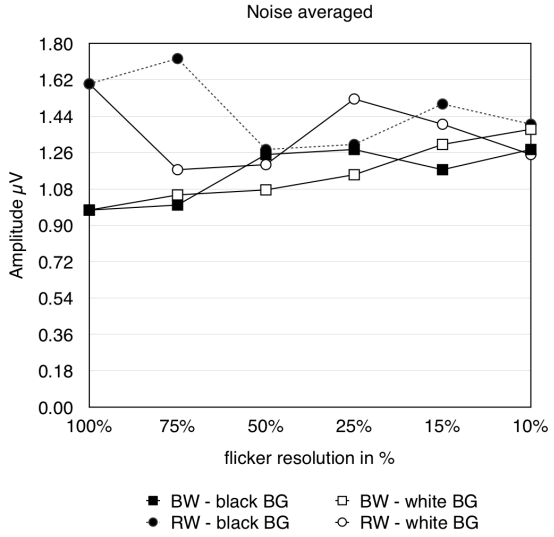

Figure 5-15 Averaged signal noise for BW and RW flickers with black and white background

Figure 5-15 represents averaged noise response for all four recording scenarios. Across all of the flicker types, there is a visible tendency of noise increase from ~1 μV to ~1.5 μV as the stimuli graphic's resolution decreases. However, this increased noise level of approximately 0.5 μV is insignificant when compared to the gain in signal peak values reported earlier in this Section.

5.2.3 Discussion and Conclusions

The purpose of this experiment was to establish whether relative flicker size/resolution has any impact on the quality of the SSVEP signal recordings. This information is crucial when designing stimuli graphics for SSVEP-based BCI systems. The use of multiple flickers for multi-command systems is a necessity, therefore knowing how small the stimuli graphics can be before the signal drops in quality is very important. This experiment initiates a series of tests where colour response in SSVEP will be tested.

- Observation #1

From the results reported in Section 5.2.2 it could be noticed that white (light) background is delivering better results in terms of peak levels compared to black (dark) background for both BW and RW graphics. However, when looking at the level of noise no obvious direct correlation to flicker colour or lightness of background could be observed in either of the scenarios. This suggests that both the red colour of the flickers as well as the lightness of the background have a noticeable impact mainly on the elicited portion of the signals i.e. tested 10 Hz peaks.

- Observation #2

RW stimuli flickers produced better signal peaks compared to BW counterparts. RW graphics with white background demonstrate a significant increase in signal peak for resolution between 75%-25% while with black background similar behavior can be noticed between 50%-15% resolution. Any significance of that should be reconfirmed in further tests with more trials preferably with more subjects. This observation is very important and in accordance with findings reported by Gerloff and Schilling (2012), thus suggesting the significance of colour implementation stimuli based BCI systems.

- Observation #3

Flickers' size and resolution does have an impact on the EEG signal peaks in SSVEP paradigm. With 100% as a starting point and a reference one can notice that with every step of decreasing the flickers' size the elicited signal peaks raised in value. A noticeable decrease of peak level can be observed at 25%, although it still delivered a very good performance in most of the cases, which is comparable to 100% full resolution graphics. Most noticeable decline in peak levels can be distinguished in 10% resolution. A relatively low noise level in all of the observed signals promises a practical usefulness of this variant where extremely small stimuli elements are required in a well-designed BCI system. For all interested in designing multi-command BCI systems these results should offer reassurance that small flicker sizes carefully arranged across the entire stimuli displaying screen will deliver excellent performances. Also knowing that colour red with white outperforms standard black with white combination allows for diversity in designing visually driven BCI systems. Definitely more test trials need to be performed with an extended number of users and the introduction of additional colours and colour combinations.

5.3 Testing Multi-Colour Flickers for Brain Lobe Activations

The purpose of this experiment is to investigate the quality and robustness of the EEG signals elicited by various multi-colour combinations using the SSVEP paradigm and observe any correlation of the elicited peaks with brain lobe activations. The results derived from various multi-colour flickers were compared against the reference black and white monochromatic flicker. The flickers have been designed and rendered as separate video files in Adobe After Effects software. For research consistency, as detailed in Section 1.2, 10 Hz flickers were tested. Three subjects were asked to participate in this experiment using 2 computers and the Emotiv EPOC headset in rotated position. Signal acquisition was performed using Emotiv Xavier Test Bench application. The recorded and saved separate signals were analysed in MATLAB with EEGLAB plugin. All the colour flickers produced very strong and useable SSVEP signals. For more details on the methods used please refer to Section 3.2.

5.3.1 Experiment Setup

Two computers and an Emotiv EPOC wireless EEG headset were used during this experiment. One computer displayed the stimuli graphics while the other PC was capturing all the incoming raw EEG signals. All the graphic elements were designed and rendered in Adobe After Effects and their playback was handled by open source VLC media player. For raw signal acquisition Emotiv Xavier Test Bench application was used. For signal analysis, filtering and results plotting MATLAB and EEGLAB were used. For more details on the software and hardware setup please refer to Section 3.2.

Based on successful preliminary tests with black and white flickers 10 Hz frequency has been chosen for all colour flicker combinations. The Emotiv EPOC headset was rotated to achieve a better response in SSVEP as suggested by Manyakov et al. (2011). This method places more sensors in the occipital lobe of the brain precisely where the visual system's response is located. Both computers were placed on a desk in front of the subjects at approximately equal distance. The stimuli graphics were rendered and played back in 1080 x 1080 pixels resolution using 17" screen MacBook Pro. The PC running acquisition and analysis software used Windows OS. The raw EEG signals were recorded in EDF file format. After importing the captured data into MATLAB using EEGLAB's BIOSIG toolbox the baseline was removed from the signals and they were further filtered using basic FIR filter with boundaries set at 1 Hz and 40 Hz as explained in Section 3.2.2.2. In some of the signals artefacts were visually inspected and manually removed using channel data (scroll) plot function. In EEGLAB, the channel spectra and maps plot was used to examine the existence of desired frequency peaks.

To compare against the most contrasting black and white graphic, a variety of colour combinations were chosen for the test. The following colour combinations were determined for testing: blue-white, blue-magenta, blue-red, green-white, green-blue, green-magenta, magenta-white, red-white, red-green, and red-magenta. These colours represent all the primary colours from the RGB additive colour science. Additionally, magenta as the secondary colour was added to the testing colour pallet. As reviewed earlier in Section 1.8, violet colour successfully elicited useable brain oscillations. The following standard colour coordinates were chosen within the RGB colour space: red (255, 0, 0), blue (0, 0, 255), green (0, 255, 0), magenta (255, 0, 255) and white (255, 255, 255). All the colour patterns are shown in Figure 5-16.

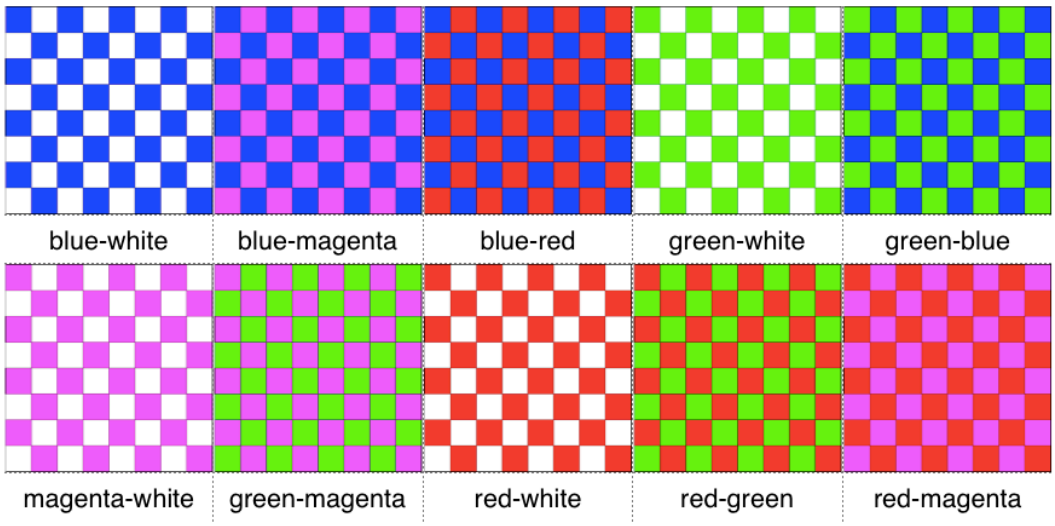

Figure 5-16 Multi-colour flicker graphics tested in the experiment

5.3.2 Test Results

Four test cases were carried out during the experiment. Test cases 1 and 2 (repetition of the same scenario) were performed with subject 1 (wearing glasses) while test case 3 with subject 2 (male) and test case 4 with subject 3 (male). Table 5-4 presents test case 1 results for all colour flickers. Peak values displayed in columns 1 and 2 are based on the channel spectra and maps plots generated by EEGLAB. Their values have been plotted from the Y-axis (Figure 5-17).

Table 5-4 Examples of numeric values derived from plots for Test case 1 – Subject 1

Flicker colours	black-white	blue-white	blue-magenta	blue-red	green-white	green-blue	magenta-white	green-magenta	red-white	red-green	red-magenta
10 Hz peak	18	16	12	13	13	13	14	14	18	14	12
20 Hz peak	10	0	10	0	8	8	0	0	10	0	0

Figure 5-17 shows an example of red-white flicker's response in the raw EEG signal. The brain maps areas pointed by the arrows indicate accumulated brain activity. Plotted, as colour red is the positive polarity while the colour blue indicates negative polarity of the brain's electromagnetic activity. As mentioned before, the headset was rotated ensuring more complete occipital lobe coverage to achieve better results, so the brain maps are also rotated. All the brain activity showed in the frontal lobe in fact took place in the parietal and occipital lobes. In the lower part of the plot there are signal peaks indicating increased amplitude of 10 Hz fundamental frequency and 20 Hz harmonic from which the values were determined (Table 5-4) and plotted.

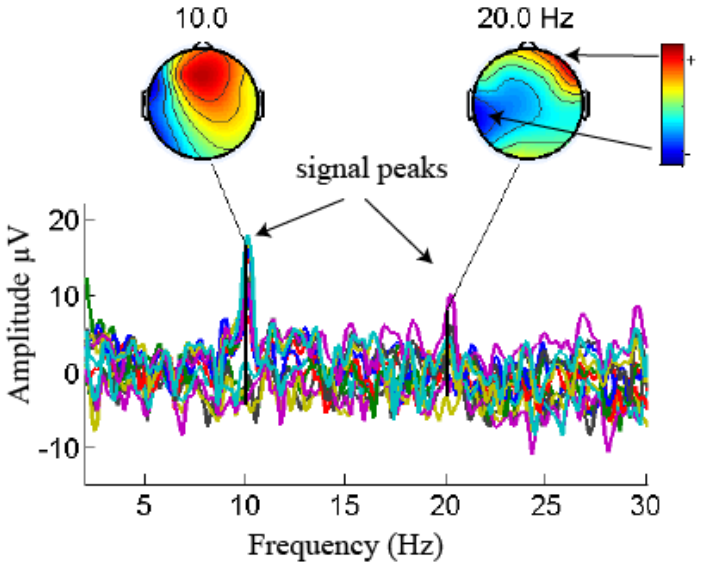

Figure 5-17 Channel spectra and maps with signal peaks and brain activity areas

The arrows in the upper right corner show positive and negative polarities reflecting brain activity.

Additionally, for this experiment, brain lobe activity was estimated using brain map colours generated by the EEGLAB plots. The main motivation was to find out whether any correlation between elicited frequency response and brain area activation could be perceived. Lobe activity values were estimated based on the brain map colours from the same plots. The score of 20 (dark red) was associated with maximum positive activity while the score of -20 (dark blue) indicates a minimum negative activity as shown in Table 5-5. All the in-between values were assigned accordingly.

Table 5-5 Brain maps colour values

Colour range	dark red	light red	orange	yellow	green	cyan	light blue	blue	dark blue
Value assigned to brain activity using brain maps (from -20 to 20)	20	15	10	5	0	-5	-10	-15	-20

Figure 5-18 shows results recorded by subject 1 in test case 1. It presents 10 Hz and 20 Hz peaks for all colour checkerboards tested as well as brain lobe activations. The vertical solid blue bars (a) and (b), indicate peak values elicited by tested colour combinations for the fundamental 10 Hz (a) and harmonic 20 Hz (b). It can be observed that for subject 1, all colour flickers provide a very solid response in the fundamental 10 Hz with black-white, blue-white, and red-white flickers generating the highest brain signal amplitudes with levels between 18 µV and 16 µV. Only 5 out of 11 flickers generated 20 Hz harmonics and their values are between 8 µV and 10 µV. The majority of the flickers generated very clean signals, as shown in Figure 5-18c. The square and round points connected with lines indicate parietal (black squares) and occipital (grey circles) lobe activities for both 10 Hz (Figure 5-18a) and 20 Hz (Figure 5-18b). In this test case an almost exact correlation between 10 Hz peaks occurrence and parietal and occipital lobe positive activations is evident. The 20 Hz harmonics are accompanied by decreased brain activity in the parietal lobe.

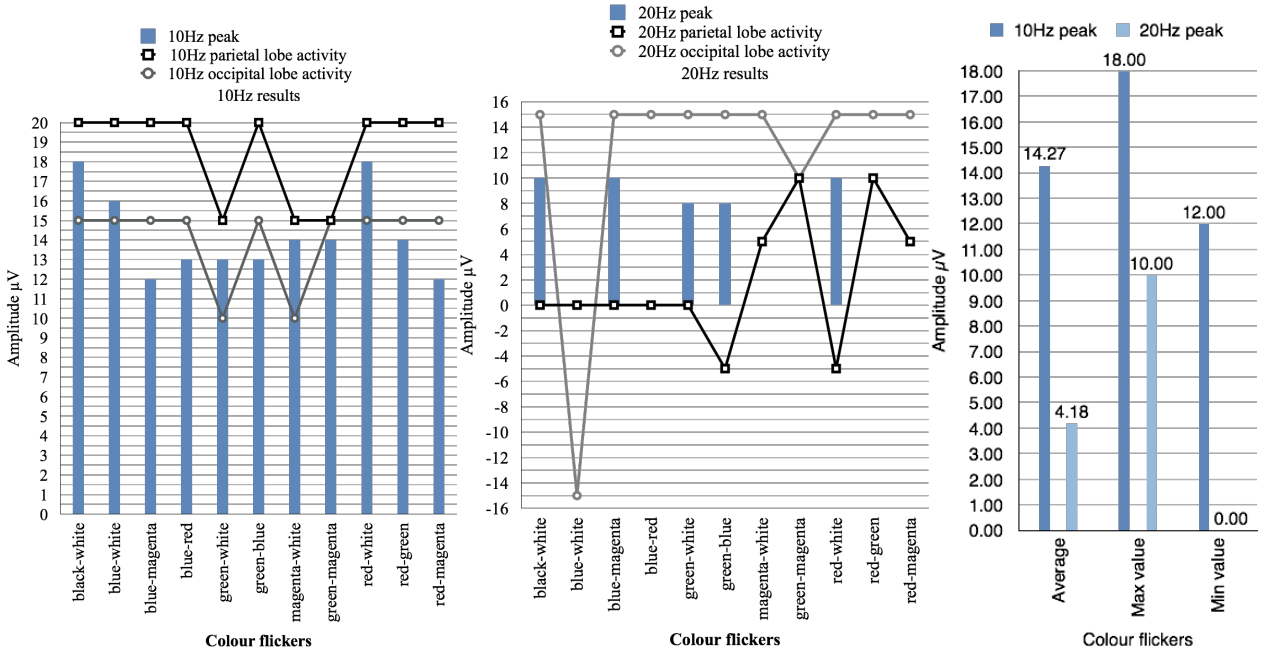

Figure 5-18 Test case 1 – subject 1

Individual flicker results for 10 Hz (a), 20 Hz (b) and statistical data (c). In (a) and (b) blue bars indicate 10 Hz peak response, while black square and circle show parietal and occipital lobe brain activities respectively. On the right, (c) indicates statistical data calculated for the 10 Hz fundamental (dark blue) and 20 Hz harmonic (light blue) showing average, maximum and minimum values.

Figure 5-19 illustrates the best 3 results for 10 Hz peaks accompanied by brain activities maps. It can be noted that 10 Hz brain activity maps look almost identical in all 3 plots. However, there is a noticeable difference in brain activity for 20 Hz harmonics between blue-white (Figure 5-19b) and the 2 other examples shown. Evident is reversed electromagnetic polarity where 20 Hz peak is not formed.

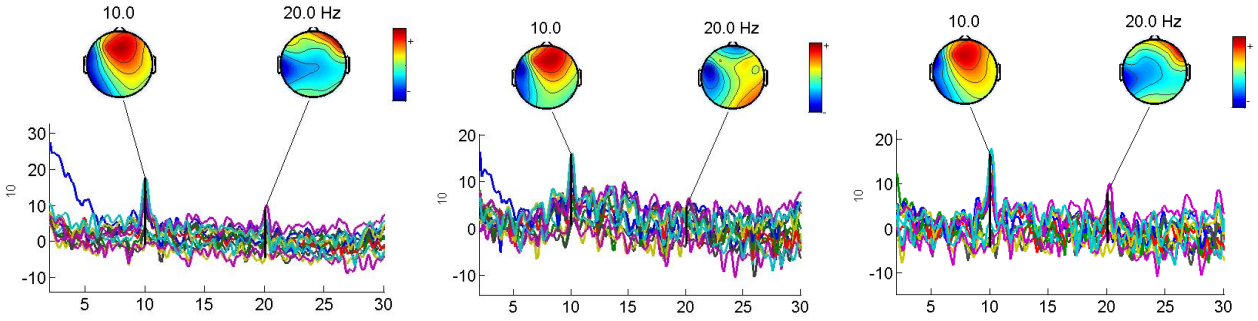

(a) (b) (c)

Figure 5-19 Examples of the highest 10 Hz peaks elicited by subject 1 in test case 1

The following plots represent black-white (a), blue-white, and red-white flicker results. In blue-white (b) one can observe lack of 20 Hz peak accompanied by reversed polarity of the brain activity.

Test case 2 results are shown in Figure 5-20. Since both tests 1 and 2 were carried out with the same subject 1 the results are quite similar. Again, the highest amplitude peaks are registered for black-white at 16 µV, blue-white and red-white both at 17 µV. However, green-blue and green-magenta did not form any 10 Hz peaks at all.

Only 4 out of 11 flickers generated 20 Hz harmonic content in this test case and their amplitude values are lower than the fundamental 10 Hz peaks. In blue-white and red-magenta the harmonics are of considerably lower amplitude when compared to the base 10 Hz. However, in green-blue and red-green the fundamental 10 Hz is rather low and almost comparable to level achieved by 20 Hz harmonics. Interestingly, 20 Hz produced very few peaks even though parietal and occipital lobes show substantial activities in that frequency as it can be observed for black-white, blue-red, magenta-white and green-magenta.

Analysing plots in Figure 5-21 it can be noted that colour flickers (b and c) generate much cleaner signals compared to the black and white reference stimulus (a).

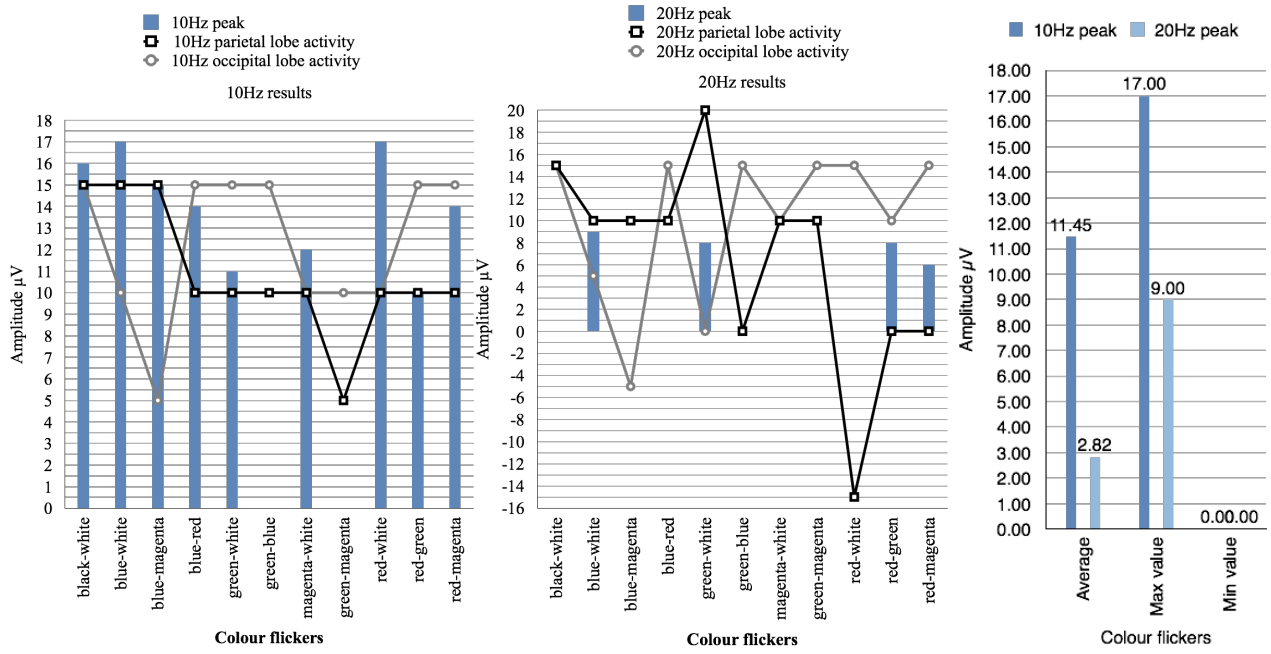

(a) (b) (c)

Figure 5-20 Test case 2 – subject 1 results

Individual flicker results for 10 Hz (a), 20 Hz (b) and statistical data (c). In (a) and (b) blue bars indicate 10 Hz peak response, while black square and circle show parietal and occipital lobe brain activities respectively. On the right, (c) indicates statistical data calculated for the 10 Hz fundamental (dark blue) and 20 Hz harmonic (light blue) showing average, maximum and minimum values.

The brain map plots illustrate quite similar brain lobe activations when compared to test case 1. However, this time the lighter red colour visible in the plots (Figure 5-21) suggest slightly decreased brain activities in the occipital lobe, which could be associated with missing 2 peaks (Figure 5-20a) and lower average peak values (Figure 5-20c) in 10 Hz.

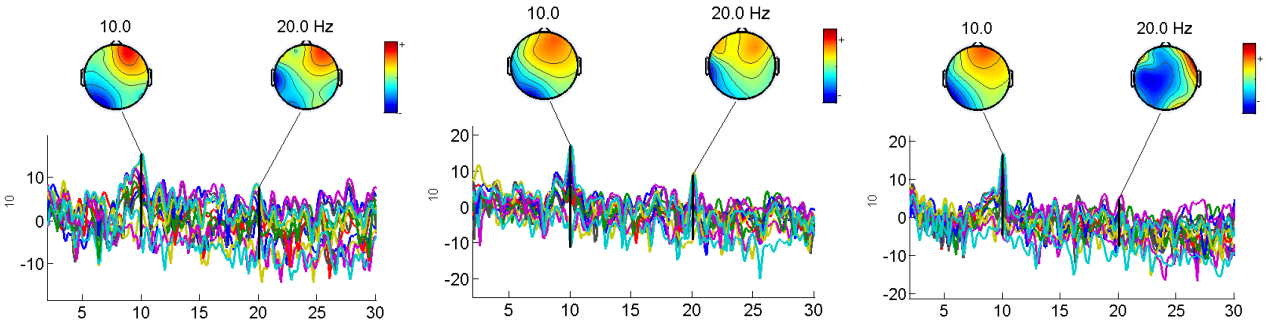

(a) (b) (c)

Figure 5-21 Examples of the highest 10 Hz peaks elicited by subject 1 in test case 2

The following plots represent black-white (a), blue-white, and red-white flicker results. Black-white flicker result (a) is noisier compared to colour counterparts (a and b).

Test case 3 was carried out with subject 2 and the results are shown in Figure 5-22. Except for green-blue, all other colour flickers produced peaks in 10 Hz, although the amplitudes are lower compared to test cases 1 and 2 with subject 1. Only blue-red flicker generated 20 Hz harmonic with amplitude of 8 µV. With the exception of green-magenta and green-blue, parietal and occipital lobe activities match the 10 Hz signal peaks (Figure 5-22a). In 20 Hz harmonic response (Figure 5-22b), as expected, lower activities in both lobes mirror the lack of signal peaks in black-white, blue-white and blue-magenta examples. However, an interesting pattern can be observed in the remaining flickers. Lack of peaks corresponds precisely with considerably decreased parietal lobe activity while at the same time occipital lobe presents contrasting high activity. This could lead to a conclusion that peak occurrence and parietal lobe activity are closely related.

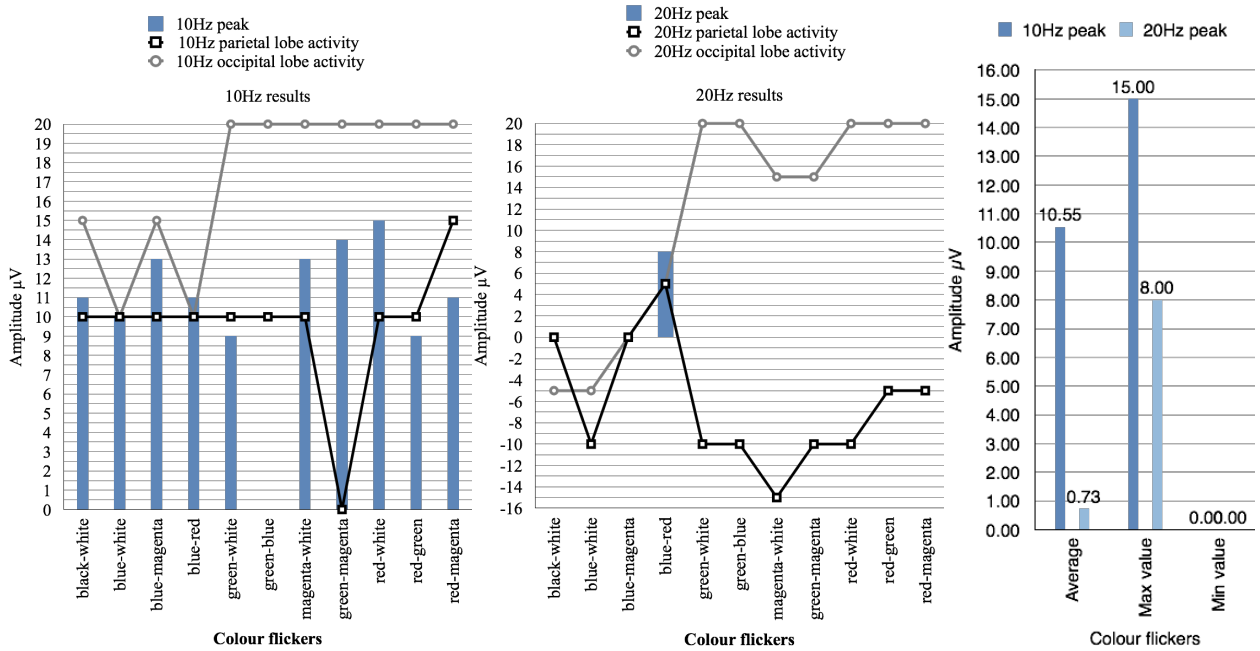

(a) (b) (c)

Figure 5-22 Test case 3 – subject 2 results

Individual flicker results for 10 Hz (a), 20 Hz (b) and statistical data (c). In (a) and (b) blue bars indicate 10 Hz peak response, while black square and circle show parietal and occipital lobe brain activities respectively. On the right, (c) indicates statistical data calculated for the 10 Hz fundamental (dark blue) and 20 Hz harmonic (light blue) showing average, maximum and minimum values.

Figure 5-23 shows plots for 4 best performing stimuli and they are all colour flickers. They all indicate very clean 10 Hz peaks with no 20 Hz harmonic formation, which is desirable for BCI development with minimum signal processing.

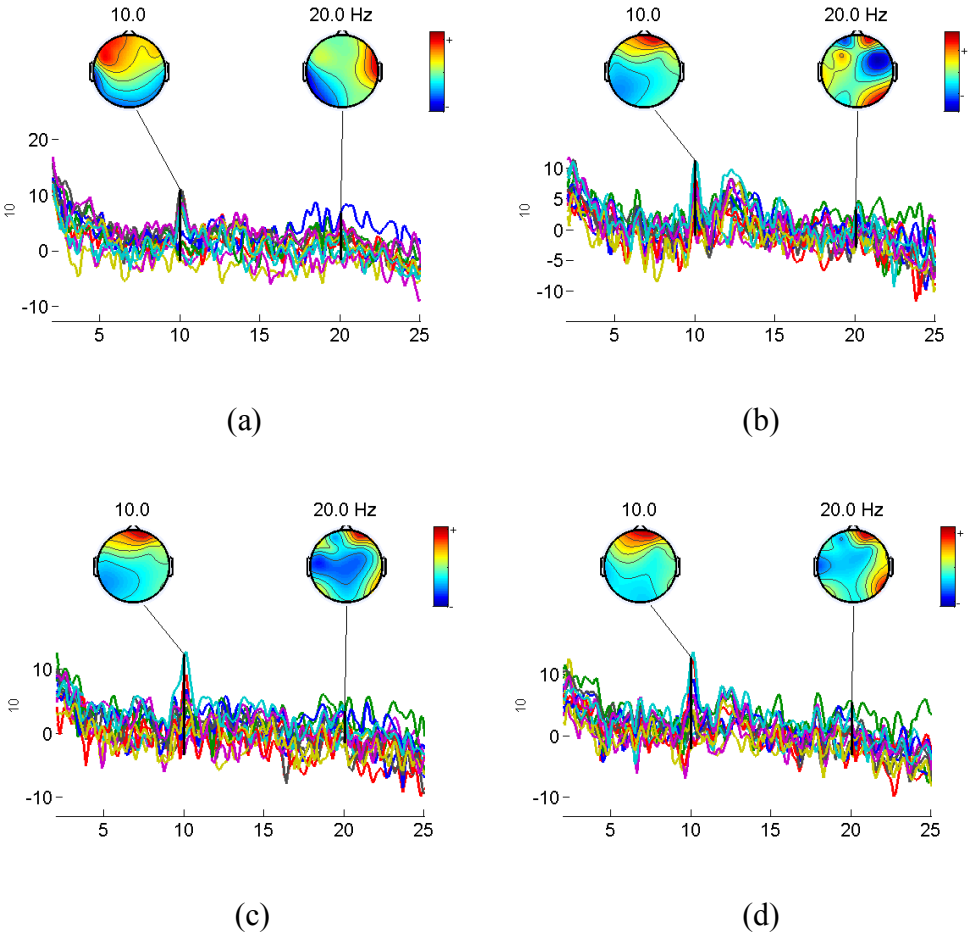

Figure 5-23 Examples of the highest 10 Hz peaks elicited by subject 2 in test case 3

The plots represent blue-magenta (a), magenta-white (b), green-magenta (c), and red-white (d) flicker results.

Test case 4 results with subject 3 participating are shown in Figure 5-24. Two flickers, blue-magenta and magenta-white, did not successfully produce the targeted 10 Hz signal peaks. Six colour flickers, blue-white, red-blue, blue-red, green-blue, green-magenta, red-white and red-magenta produced equally strong signal peaks as the reference black-white, which suggests that subject 3 responded equally to most of the colour flickers regardless of their hue. The correlation between the lack of signal peaks and decreased parietal lobe activity is less pronounced with subject 3 when compared to subject 2 but still present, especially in black-white, blue-magenta, green-white, magenta-white, green-magenta and red-white.

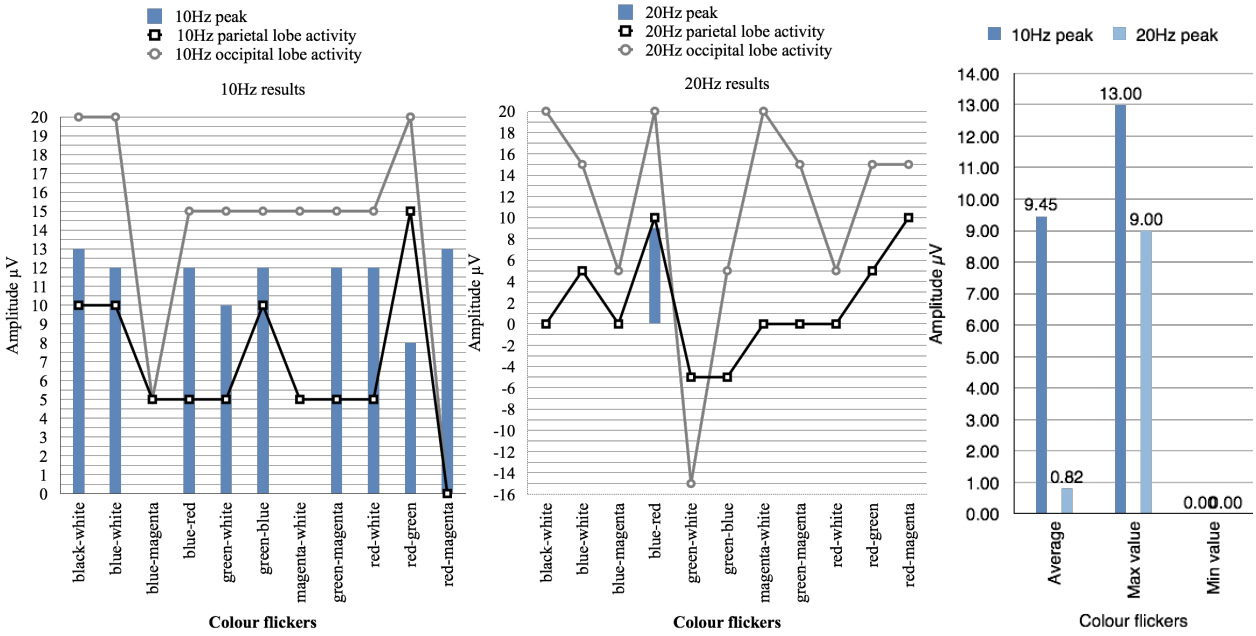

(a) (b) (c)

Figure 5-24 Test case 4 – subject 3 results

Individual flicker results for 10 Hz (a), 20 Hz (b) and statistical data (c). In (a) and (b) blue bars indicate 10 Hz peak response, while black square and circle show parietal and occipital lobe brain activities respectively. On the right, (c) indicates statistical data calculated for the 10 Hz fundamental (dark blue) and 20 Hz harmonic (light blue) showing average, maximum and minimum values.

By observing the plots themselves as shown in Figure 5-25, the signal peaks lack in clarity and are usually accompanied by noisy background in all of the examples. This indicates that although subject 3 produced 10 Hz peaks with most of the tested flickers, the response was not strong enough and the signals were very polluted with high levels of noise.

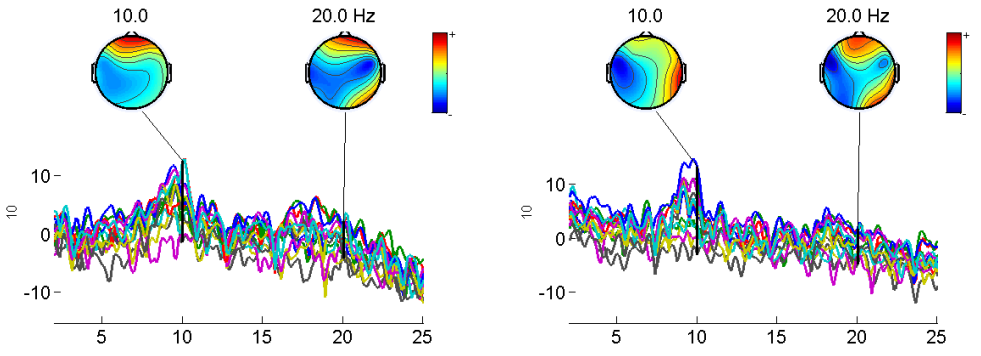

(a) (b)

Figure 5-25 Examples of the highest 10 Hz peaks elicited by subject 3 in test case 4

5.3.3 Discussion and Conclusions

Based on the obtained results it is observed that certain patterns and responses are associated with individual subjects' ability to focus and concentrate during an experiment like this one. It is quite possible that other individual features and probably subjects' mental state at the time of testing were varying. For instance, subject 1 in test cases 1 and 2 produced more consistent and stronger 10 Hz peaks compared to the other 2 subjects, while the same subject 1 produced considerably more 20 Hz harmonic peaks compared to the other 2 subjects. It needs to be reminded that harmonics are to be avoided and treated as artefacts. It is possible that the increased 20 Hz peak harmonic content observed in subject 1 is dependent on the overall strength of the fundamental 10 Hz response. Therefore, it is fair to state that the stronger the main component's response, the higher the chance of eliciting additional harmonics in the brain signals. It is worth mentioning that subject 1 should be considered as a trained subject with considerable amount of time spent on eliciting brain signals through visual stimulation. Thus, as suggested in Section 4 of this thesis, the element of training provides better brain signal response for subject 1 in two test cases.

An interesting respone can be noticed for subject 2. For 20 Hz harmonic signals his patterns show very strong occipital lobe activity despite the lack of peaks and with very minimal parietal lobe activity. The other 2 subjects have not reproduced this behavior. Overall it can be stated that subject 2 exhibited much stronger occipital lobe activity with very minimal parietal lobe activity in both fundamental 10 Hz and 20 Hz harmonic frequencies.

Patterns that are common for most of the subjects can also be observed. One of them is visible correlation between 10 Hz peaks and occipital lobe activity in this frequency. This pattern has been very clearly exhibited by subject 1 in test case 1 where the parietal lobe followed with similar arrangement and by subject 3 in test case 4. Subject 2 in test case 3 also shows traces of this structure. In the 20 Hz harmonic there is also visible correlation between the lack of peaks and minimal activity in the parietal lobe. This can be seen in the results of subjects 2 and 3. Subject 1 repeats this pattern only in test case 1, with less coherence in some of the colour flickers. When analysing 20 Hz responses one can notice another similarity. Both subjects 2 and 3 produced only one peak for the same colour combination of blue-red flicker. It is very promising to see a very structured and solid response of the multi-colour flickers when compared to the black-white reference one. Significantly, the checkerboard flickers with red-white, blue-white, blue-magenta, magenta-white, and green-magenta delivered better results than the traditional black and white reference flicker.

5.4 Testing Multi-Colour Flickers' Performance Against Greyscale Versions

Using iOS global control features available in the utilised 12.9" tablet the author decided to design another test to investigate the role of graphic's colour component on elicited brain signals through visual stimulation. Furthermore, this experiment employs the bespoke MCF application detailed in Section 3.2.3.3. The application can automatically generate multi-colour checkerboard 10 Hz flickers of various preset sizes on white, grey and black backgrounds. This experiment compares signals generated by fully saturated colour flickers against their greyscale versions.

Every colour graphic element is comprised of two main components: luminance and chrominance. Luminance is simply the greyscale representation of graphic elements that are shown by digital displays. In luminance only, the graphics with maximum brightness are shown as white. Their opposite with least amount of brightness are shown as black. Everything in between is shown as different levels of grey. The colour information of the graphics can only be shown when a chrominance element is added to the graphics. In essence the luminance channel is responsible for brightness and the chrominance channel for the colour hue of displayed graphic. In the human eye retina, there are two types of photosensitive cells: rods and cones. Rods respond to different levels of brightness only and are immune to changes in colour. On the other hand, cones are sensitive to colour information. Specifically, there are three types of cones and each type responds to quite narrow spectrum of visible light. One type of the cones is sensitive to light spectrum which can be approximated as red (64% of all cones). Another type (34%) is sensitive to green spectrum of light, while only 2% of the cones respond to blue. For more details on the human retina structure please refer to Section 1.3. It is quite easy to see the relationship between this anatomical structure of the human eye and the RGB additive colour science. In additive colour science, by mixing the primary Red, Green and Blue colours, secondary colours of Cyan (Green+Blue), Yellow (Red+Green) and Magenta (Red+Blue) will be achieved. When all colours are added the white light is produced (Figure 5-26).

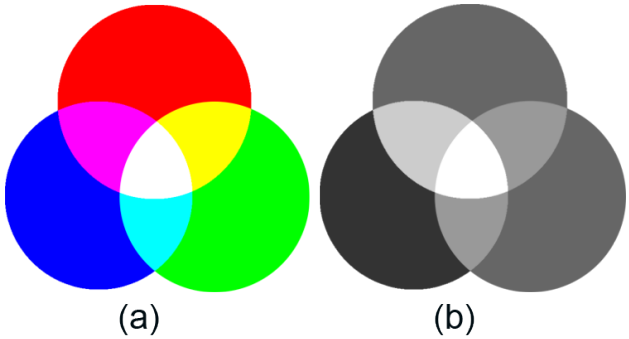

Figure 5-26 RGB colours (a) and their greyscale versions (b)

RGB primary and secondary colour hues shown with chrominance and luminance (a), vs luminance only (b).

The purpose of this Section is to establish whether the chrominance (colour information) of the flickering graphics can have an effect on the elicited brain signals compared to their greyscale (luminance) counterparts. It is worth mentioning that the full colour graphics contain both, chrominance and luminance (Figure 5-26).

5.4.1 Experiment Setup

The hardware and software setup was as follows. Raw EEG brain signals were captured as European Data Format files (EDF) by Emotiv EPOC headset wirelessly communicating with Windows 7 based PC computer running Emotiv Xavier Test Bench software. The signals were analysed in MATLAB using EEGLAB and ERPLAB plugins for basic filtration and plots. For more details on testing method please refer to Section 3.2.

The total of 33 multi-colour combinations were tested with 15 trials per each 2-colour flicker combination. Two testing scenarios were designed. In the first scenario, fully saturated colour flickers were used with graphics containing chrominance and luminance information combined. In the second scenario, greyscale versions of the same flickers were used with graphics containing luminance information only. This resulted in the total number of 990 brain signals recordings captured for this experiment as shown in Figure 5-27.

33 flickers x 15 trials/flicker x 2 scenarios (colour/greyscale) = 990 recordings

Figure 5-27 The total number of tested flickers

Beside the RGB primary and secondary colours, white, black and 50% grey were also used (Figure 5-28). Each trial lasted for approximately 10 seconds. All the signals analysed were taken from the same EEG channel positioned over occipital lobe.

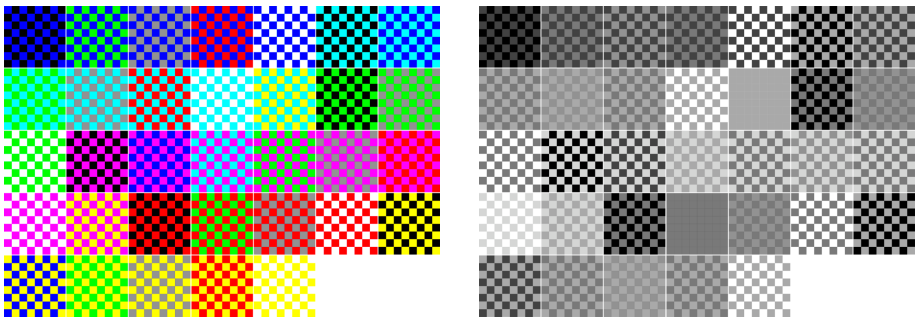

(a) (b)

Figure 5-28 Tested multi-colour checkerboard flickers

The 33 flicker colour versions were presented in two scenarios; the first as full colour checkerboards (a), and the second as their greyscale versions (b).

Since all the tests conducted for this research were carried out using 10 Hz oscillation, to satisfy the results comparability and compatibility requirement, all the 33 flickers were presented as 10 Hz flickers. Subject 1 wearing correcting glasses was exposed to visual stimulation in a normal office environment in daylight. The subject was sitting 50 cm from 12.9" tablet, which was placed inside of a cardboard box with black walls to minimise light reflections and limit influence of ambient light. The tablet screen was set to maximum brightness with colour temperature set to daylight. To realise the greyscale display requirement, the iOS tablet was set to: Settings – General – Accessibility – Display Accommodations – Colour Filter – Greyscale (Figure 5-29).

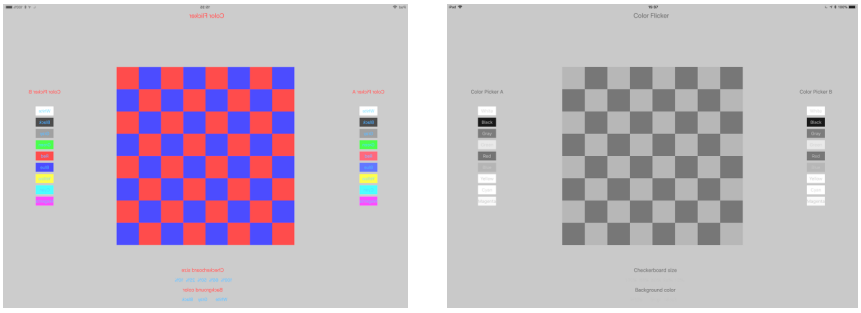

(a) (b)

Figure 5-29 Colour and greyscale tablet screen modes

Tablet screen displaying red-blue graphic set to normal full colour (a) and greyscale mode (b).

Since the brain signal recording session capturing all 33 flickers lasted for several hours, the colour and greyscale versions were captured during two consecutive days. To achieve better coverage of the occipital lobe, which is crucial for accurate SSVEP response, the EPOC headset was rotated as suggested by Manyakov et al. (2011). For more details on the EPOC headset please refer to Section 3.2.1.1.

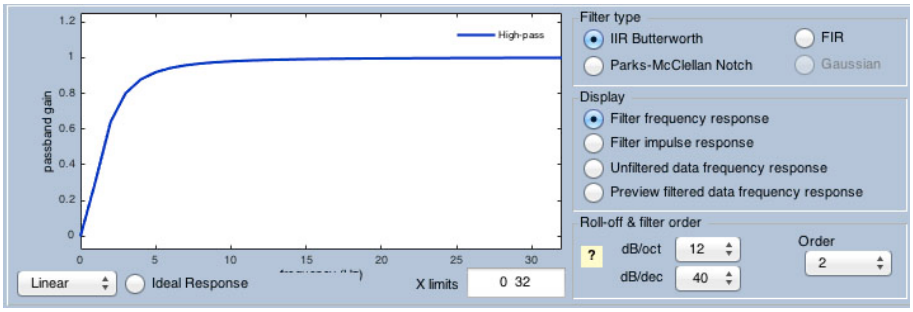

Figure 5-30 Filter settings

Only basic signal processing was applied to captured data including detrending (remove baseline function in EEGLAB) and IIR Butterworth high-pass 2nd order filter with cutoff frequencies set between 1.5 Hz and 2.3 Hz as shown in Figure 5-30 Filter settings, to remove low frequency artefacts.

5.4.2 Test Results

This Section provides tests results. Specifically, 'average' and 'maximum' values are taken into consideration. First, they are presented as bar graph plots derived from statistical data from all 15 trials per each 2-colour flicker combination resulting in 495 trials carried out for each testing scenario, bringing the total number of recorded signals to 990. Next, bar graph plots show values for 6 best performing stimuli with the average calculated from all average values and another average taken from all maximum values to easier identify overall performance difference between both scenarios. Lastly, 10 Hz signal peak amplitude plots for six individual best performing 2-colour patterns are shown. All signal peak values shown in bar graphs are presented in µV.

A. Results for full colour test scenario – luminance + chrominance

This plot summarises maximum and average results registered for full colour flickers consisting of the luminance and chrominance graphic components.

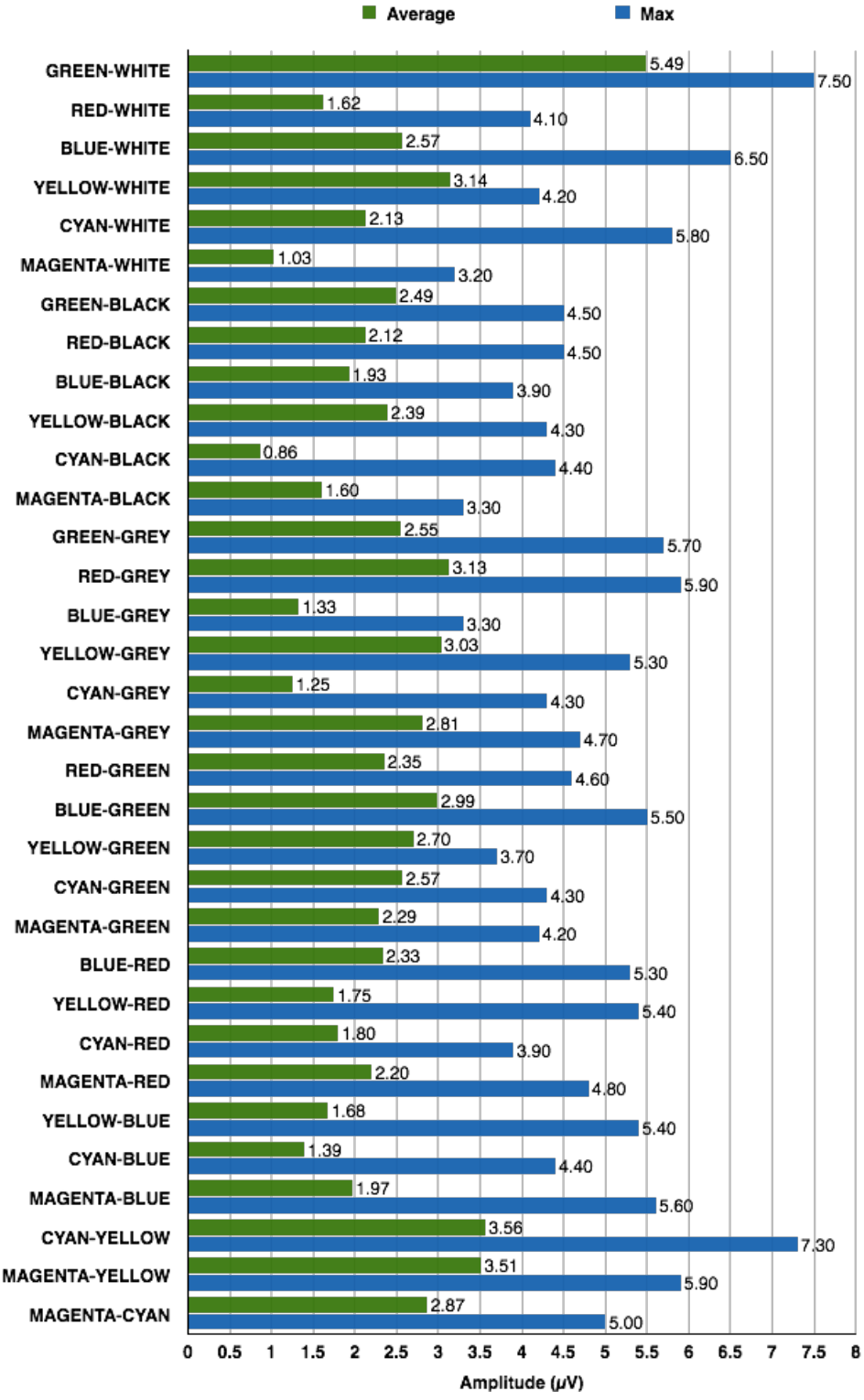

Figure 5-31 Average and maximum values derived from 33 colour flickers

This plot illustrates results for 6 best performing flickers showing their maximum and averaged results. The last, seventh bar, indicates averaged maximum and average results from all flickers tested in this scenario.

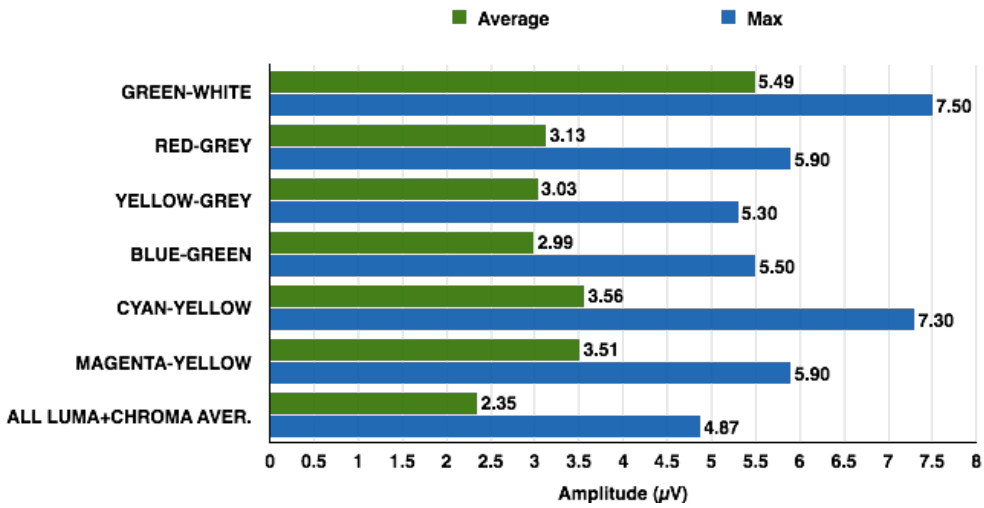

Figure 5-32 Results for 6 best performing colour flickers

The full colour flickers, which elicited the best brain signals, are: green-white, red-grey, yellow-grey, blue-green, cyan-yellow, and magenta-yellow.

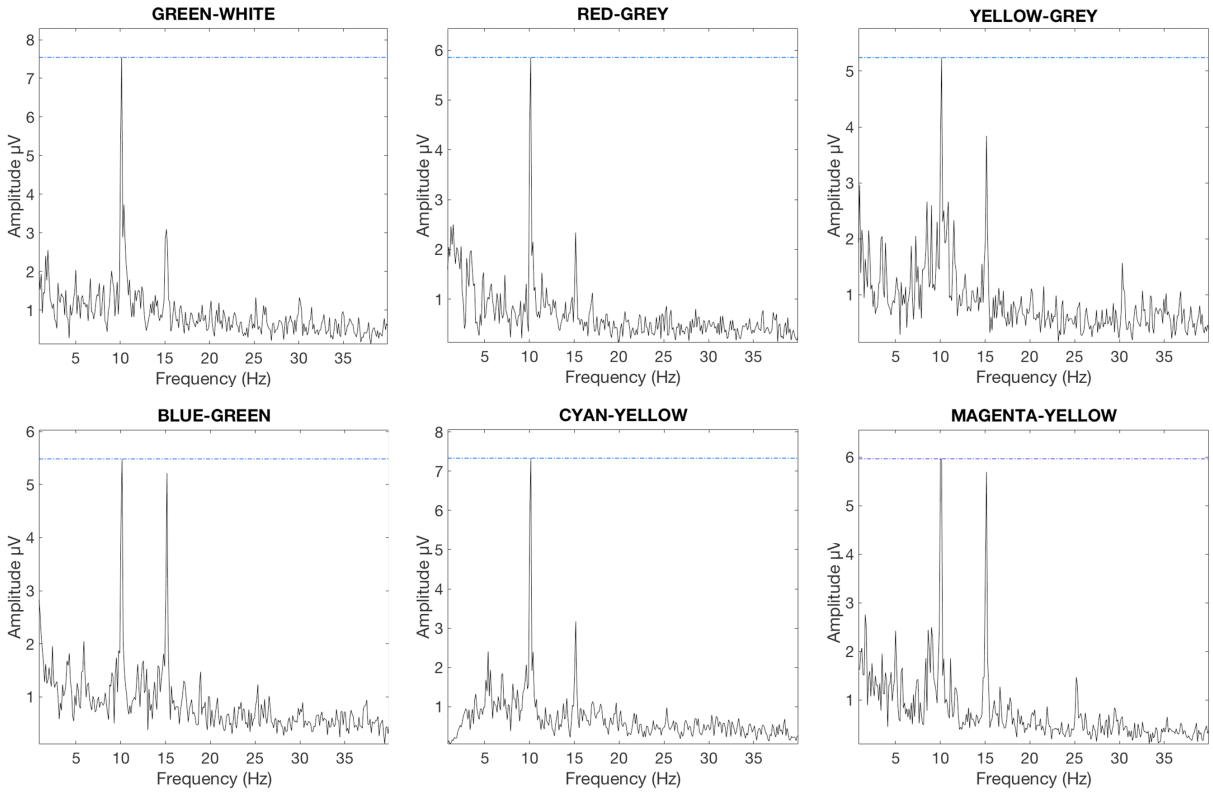

Figure 5-33 Amplitude plots for 10 Hz peaks for 6 best performing full colour patterns

In scenario A (luminance+chrominance) we can observe that the highest 10 Hz peak with maximum (7.50 μV) and average (5.49 μV) values were generated by the green-white flicker (Figure 5-31). Among the 6 best performing stimuli graphics are green-white, red-grey, yellow-grey, blue-green, cyan-yellow and magenta-yellow flickers. The average calculated from all average values is 2.35 μV while the average from all maximum values is 4.87 μV (Figure 5-32). From the individual 10 Hz peak plots shown in Figure 5-33 it can be noted that the green-white, red-grey and cyan-yellow produced the cleanest 10 Hz peaks with very little harmonic content and low noise. The blue-green and magenta-yellow also generated strong 10 Hz fundamental frequency peak but it is accompanied by a very strong 15 Hz inter-harmonic. It is worth mentioning that the 15 Hz inter-harmonic peaks are present in all demonstrated in Figure 5-33 plots.

In scenario B (luminance only) the highest 10 Hz peak with maximum of 5 μV was registered by the red-grey flickering graphic and the highest average value of 2.81 μV was registered by the cyan-yellow flicker (Figure 5-34). The 6 best performing stimuli graphics are red-grey, blue-grey, cyan-green, magenta-red, cyan-yellow and magenta-cyan.

B. Results for greyscale test scenario – luminance only

This plot summarises maximum and average results registered for greyscale flickers consisting of the luminance component only.

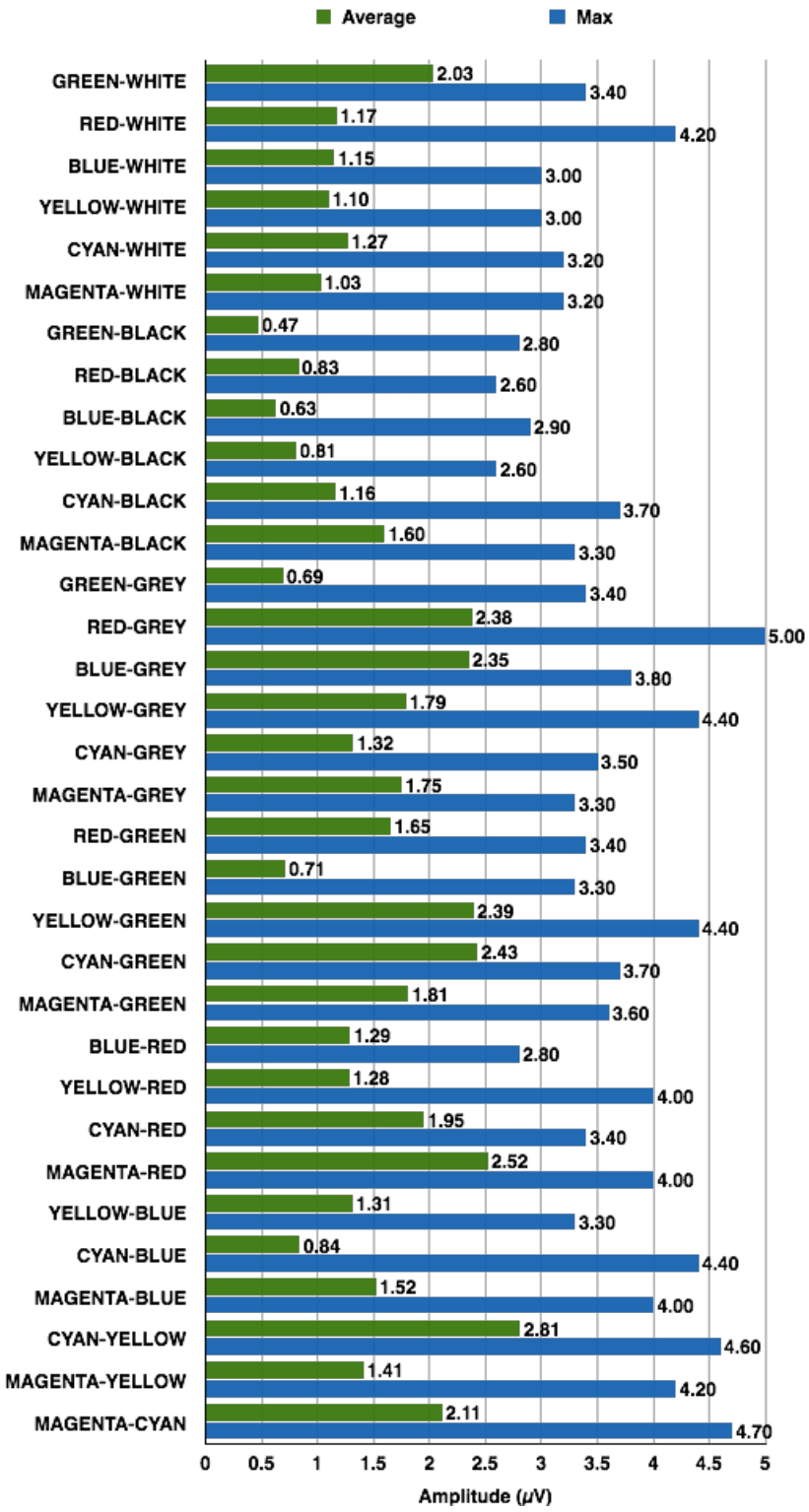

Figure 5-34 Average and maximum values derived from 33 greyscale flickers

This plot shows 6 the best performing flickers with the maximum and average results against averaged maximum and average results from all flickers placed at the bottom of the plot.

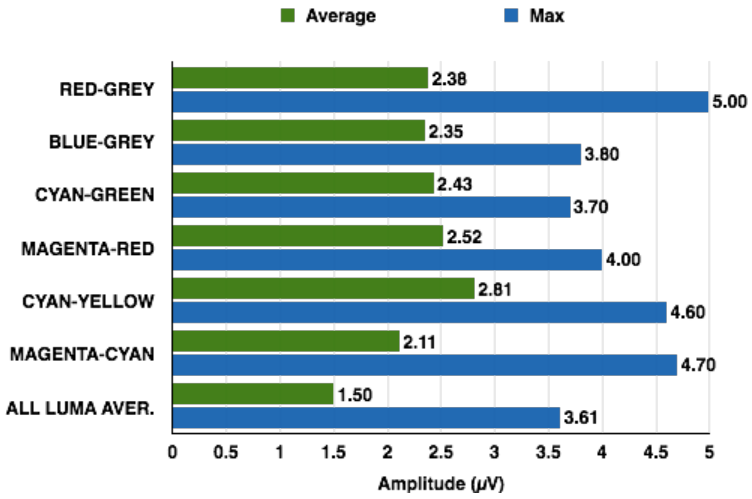

Figure 5-35 Results for 6 best performing greyscale flickers

Average and maximum values for 6 best performing greyscale flickers.

The average calculated from all average values is 1.50 μV while the average from all maximum values is 3.61 μV (Figure 5-35).

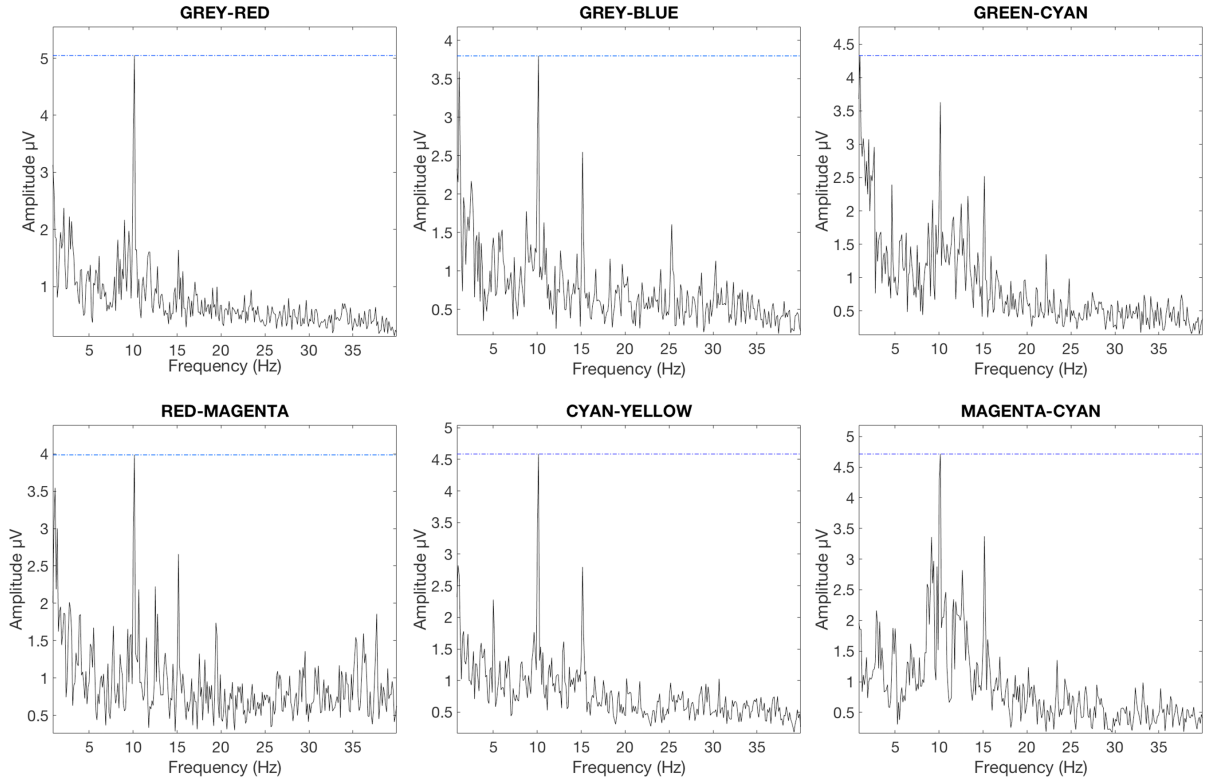

Figure 5-36 Amplitude plots for 10 Hz peaks for 6 best performing greyscale patterns

The best brain signals generated by the greyscale flickers are: grey-red, grey-blue, green-cyan, red-magenta, cyan-yellow, and magenta-cyan.

From the individual 10 Hz peak plots showed in Figure 5-36 one can distinguish that the grey-red not only produced the highest amplitude at 10 Hz but also the cleanest one with no harmonic content and relatively low noise.

The cyan-yellow also generated relatively clean peak at the fundamental 10 Hz with only minor 15 Hz inter-harmonic and low noise. The magenta-cyan produced comparable amplitude at the base 10 Hz but with much more noise and stronger response in 15 Hz. In the remaining grey-blue, green-cyan and red-magenta flickers, although with clearly discernible 10 Hz peaks, very high levels of noise are present in the signals, especially in frequency range below 5 Hz. In the green-cyan the low frequency noise is even higher than the base 10 Hz peak. Beside the grey-red signal, all the remaining best signals demonstrate a 15 Hz harmonic contamination.

5.4.3 Discussion and Conclusions

When recording brain signals in a normal office environment with computer screens, lighting fixtures and people moving around, all being a potential distraction and source of unwanted artefacts, it is to be expected that not all of the recordings will be clean and useable. Therefore, for this particular test 15 trials were recorded for each tested pattern resulting in 495 signal recordings for each scenario A and B. Every trial lasted approximately 10 seconds with 5 seconds breaks between the recordings. Some of the recorded signals did not show any peaks at all, exposing only random noise (Figure 5-37).

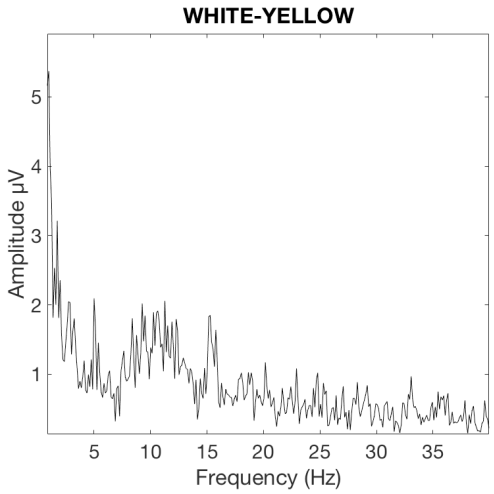

Figure 5-37 lack of peaks in white-yellow flicker

Example of a trial that did not produce any peak in the brain signal.

In certain cases, very low or no base 10 Hz peak was observed with signal carrying only 15 Hz inter-harmonic (Figure 5-38).

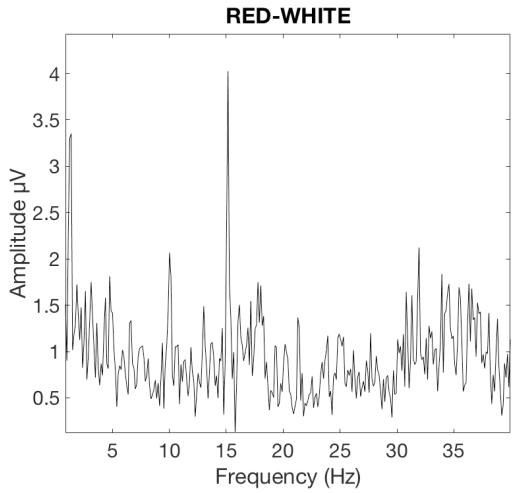

Figure 5-38 Fundamental and harmonic peaks in red-white flicker

Example of a trial with low 10 Hz peak amplitude and strong inter-harmonic response of 15 Hz.

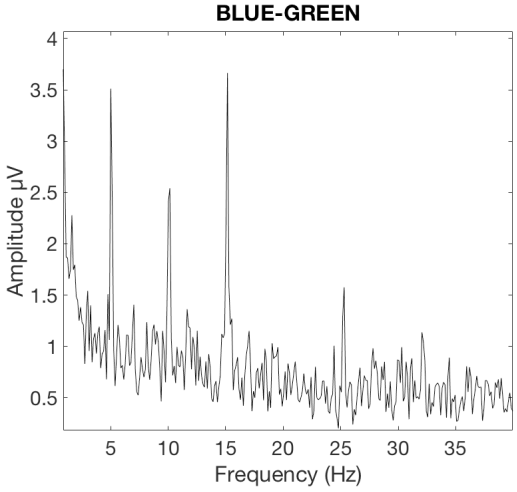

Figure 5-39 Fundamental and harmonic peaks in blue-green flicker

Example of a trial with visible fundamental 10 Hz peak and 5 Hz sub-harmonic and 15 Hz inter-harmonic contamination.

In Figure 5-39 another example of strongly polluted with harmonics signal can be observed. Such poorly recorded signals suggest that due to long recording sessions, subject's brain did not have proper rest between so many trials and the factor of exhaustion and lost concentration influenced some of the resulted signal recordings. However, the main purpose of this work was to establish any correlation between colour saturated flickering graphics as well as their greyscale counterparts and their ability to elicit the tested 10 Hz oscillation. Inspecting the statistical data from the hundreds of trials analysed several observations can be made.

- Observation #1

Poorly recorded signals did occur in both scenarios A and B suggesting that harmonic and noise pollution cannot be linked to either colour or its lack in the flicker, but rather should be associated with short breaks between the trials and very large number of trials captured resulting in excessive tiredness of the subject.

- Observation #2

Majority of harmonic pollution occurred as 5 Hz sub-harmonic and 15 Hz inter-harmonic in relation to the elicited fundamental 10 Hz. No explanation could be found as to why this specific type of harmonic pollution occured in the brain signals elicited through visual stimulation.

- Observation #3

By comparing statistical data between both scenarios, A and B derived from all trials it can be stated that the colour (luminance+chrominance) flickers performed significantly better than their greyscale (luminance) counterparts. Assuming that the values registered by the greyscale flickers are the base of 100%, a 56% increase in the 10 Hz frequency is observed in colour flickers when comparing average values. When averaging only maximum values achieved by each 2-colour flicker a 34% increase can be declared for the benefit of colour flickers.

5.4.4 Summary

These results suggest that indeed the colour (chrominance) information in the graphic flickers influences the strength of elicited brain signals in a positive way. It is still to be understood whether possible simple signal amplification occurs or if much more complicated processes occur in the brain. It is unknown how much of this signal improvement can be attributed to the construction of the eye retina and the fact that it contains separate colour sensitive photocells having direct nerve connection to the brain. More serious questions can be asked. For instance, is the flickering graphic's colour information eliciting the required brain oscillations before the brain is actually analysing the specific colour? How much of this effect, if at all, could be observed with subjects who are colour blind?

Simple comparison of the achieved results between greyscale and colour flickers clearly indicate that even colours such as yellow, cyan or green, which do not produce high contrast ratio with white, can improve the quality of elicited brain signals.

It is suggested then, to use visual stimuli containing colour instead of plain black-white or other greyscale versions for the benefit of elicited signal amplitude strength. Other dependencies such as level of noise and harmonic contamination still need to be examined in future tests.

5.5 Testing Primary and Secondary Colour Flickers with Multiple Subjects

The following experiment constitutes the concluding attempt to establish whether colour information present in flickering graphics impacts the quality of elicited brain signals. In this experiment brain signals are measured using 14 subjects exposed to colour and reference black-white flickers. There are various factors analysed for this experiment. One of them is the element of subject training. Since the author participated in many brain signals recording sessions using visual stimulation, his results are categorised as trained subject's results. All the other participants, who never took part in similar experiments, are treated as untrained subjects. The importance of subject training was already discussed in Section 4. However, the main factor discussed in this experiment relates to a subject's brain response to stimuli flicker employing primary and secondary RGB colours in comparison to traditional black-white counterpart. In essence, this experiment tries to determine the usefulness of colour stimuli application for successful brain signal recording using 1 trained and 13 untrained subjects.

5.5.1 Experiment Setup

The setup in this experiment was identical to conditions detailed in Section 4.2. In this experiment however, the total of 14 subjects were tested. One trained subject, further referred to as subject 1, participated in 3 separate recording sessions, while 13 untrained subjects participated in 1 session each. During the recording session, each subject was exposed to visual stimulation using 6 colour flickers and 1 black-white variant for reference resulting in 7 flickers being recorded. Each flicker was presented individually in 5 trials/repetitions with each trial lasting for 10 seconds. Thus, the total of 16 recording sessions were carried out (3 sessions with the subject 1 and 13 sessions with the remaining subjects). Each participating subject delivered 35 individual brain signal recordings bringing the total number of captured signals to 560 as shown in Figure 5-40. The recording sessions henceforth are referred to as test cases. The selection of these colours has been determined and thoroughly explained in Chapter 1 and detailed in Section 1.6. Figure 5-41 exemplifies the colours used in the experiment.

16 recording sessions x 7 flickers x 5 trials/flicker = 560 recordings

Figure 5-40 The total number of tested flickers in 16 test cases

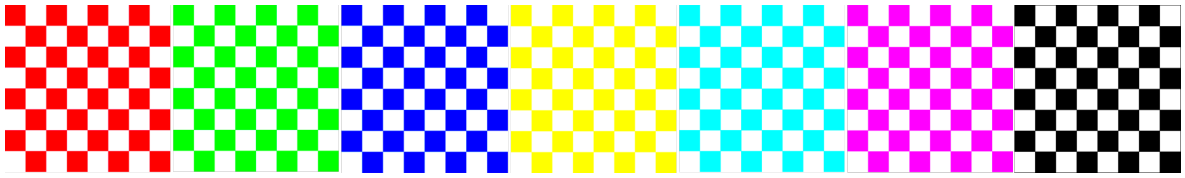

Figure 5-41 Colour flickers used in the experiment

Red-white, green-white, blue-white, yellow-white, cyan-white, magenta-white, and reference black-white.

5.5.2 Test results

Since this is the most comprehensive experiment conducted during this research consisting of 16 test cases resulting in 560 individual brain signal recordings, the results are presented in three stages.

The first stage, stage *A* presents individual subjects' results for each colour tested including the reference black-white flicker. It shows signal peaks generated in each trial presented as bar graph plots reflecting the fundamental 10 Hz peak responses as well as any harmonics present in the signals up to 35 Hz. These plots are very useful in determining the level of signal contamination by harmonics, which are to be avoided.

The second stage, stage *B* presents the results as 7 summary bar graph plots detailing each subject's response to colour flickers and the black-white reference variant. These plots are shown on per single colour basis allowing convenient comparison of all subjects' response to a given colour. The last in this stage plot compares how the different subjects responded to the reference black-white flicker. Maximum and average values are presented.

The third stage, stage *C,* presents bar graph plots summarising 11 successful subjects' results but this time on per subject basis. Again, maximum and average peak results can be observed allowing comparison of individual subject's response to all colours and the reference black-white flickers in one plot. In all plots, the amplitude peak values are expressed in μV. Both summary stages *B* and *C* illustrate only the main 10 Hz component responses without the harmonics, which are extensively discussed in stage *A*.

A. *Individual Subject Results per Colour*

Test case 1 - Subject 1

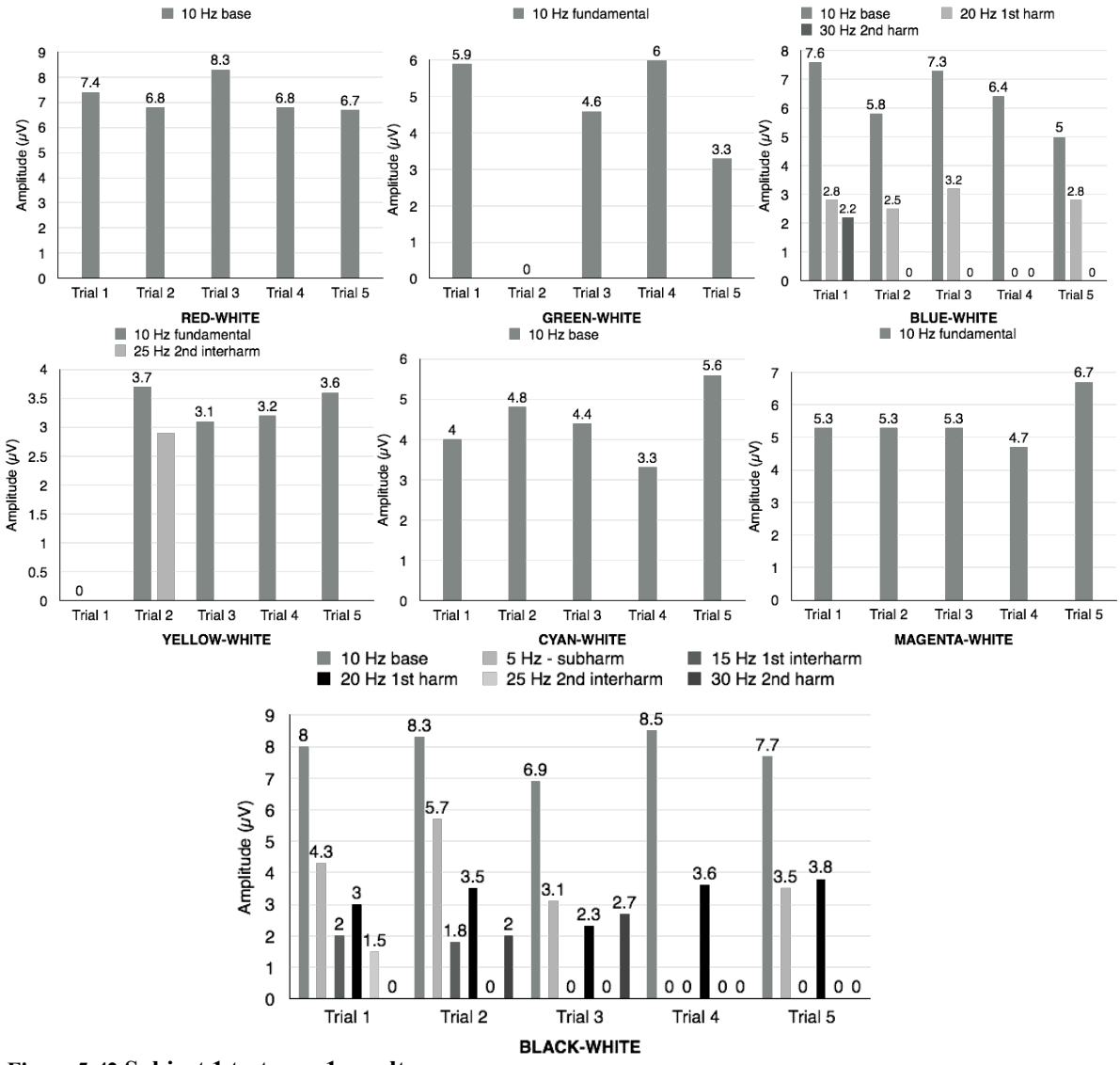

Figure 5-42 Subject 1 test case 1 results

These plots represent the first results achieved by the trained subject 1. The targeted 10 Hz signal peaks are missing only in 2 trials, 1 for green-white and 1 for yellow-white flickers. Overall, the subject presents very good ability to generate stimulated 10 Hz oscillations with all tested colour variants. Red-white, green-white, cyan-white, and magenta-white colour checkerboards generated very clean and free of harmonics 10 Hz peaks in all trials. Blue-white flicker generated 20 Hz harmonics in 4 trials, however with reasonably low amplitudes. The highest 10 Hz peaks can be observed in the black-white reference stimulus with very excessive harmonic content in most of the trials. This level of harmonic contamination would be very difficult to remove. Red-white flicker delivered very consistent, harmonic free and high amplitude 10 Hz peaks.

Test case 2 - Subject 1

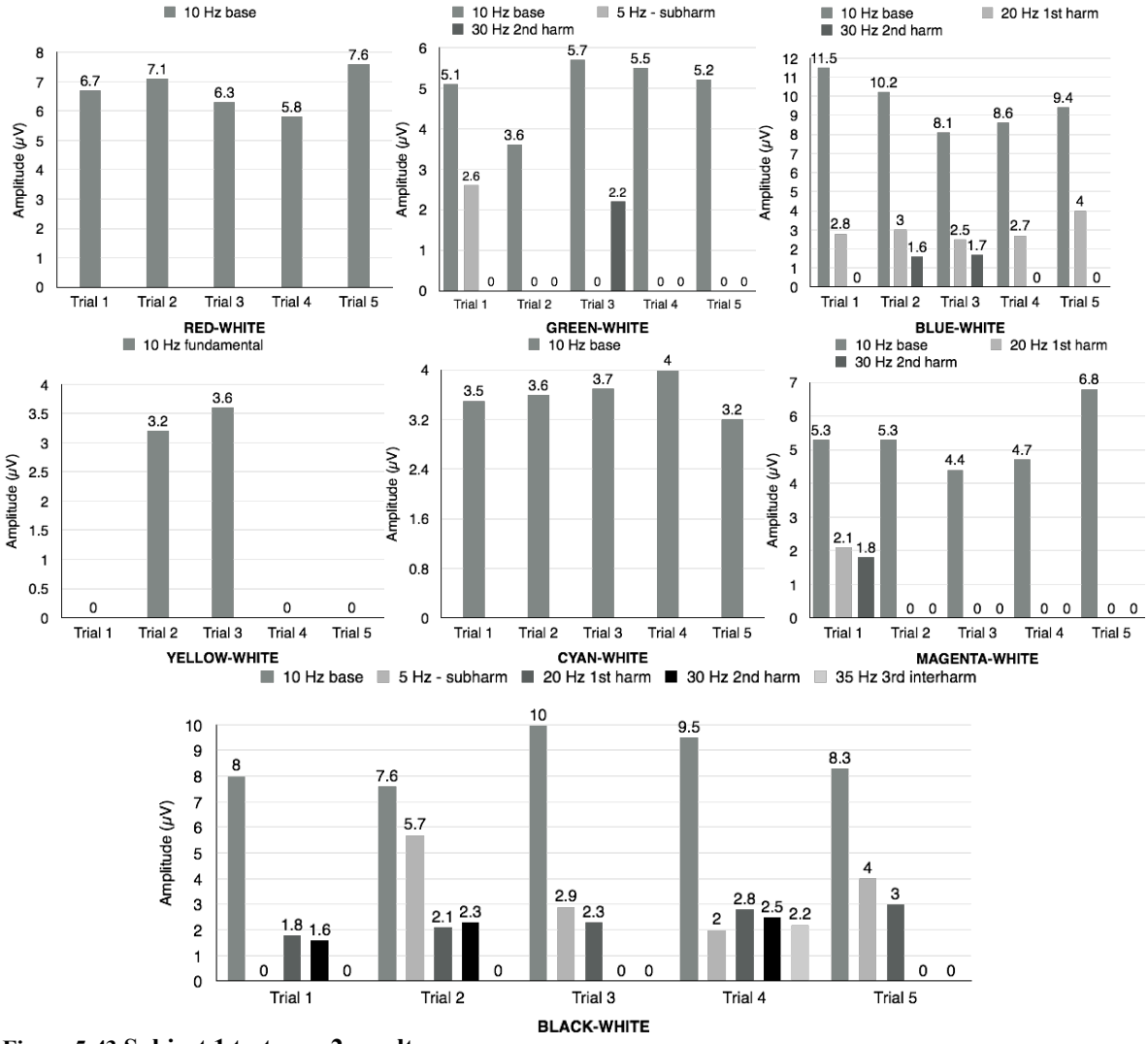

Figure 5-43 Subject 1 test case 2 results

Test case 2 continues to present subject's 1 results. In this test case 3 trials were unsuccessful and all are associated with yellow-white flicker. Similarly, to previous test case, blue-white flicker produced 20 Hz harmonic contaminations with rather low amplitudes, but in this case these are accompanied by very high peak amplitudes for the target 10 Hz. This time only two colours red-white and cyan-white produced harmonic free responses in all trials. The reference black-white flicker generated very high 10 Hz peaks in all trials, but again these are highly contaminated with many harmonic frequencies. The red-white stimulus again produced harmonic free very high 10 Hz peaks.

Test case 3 - Subject 1

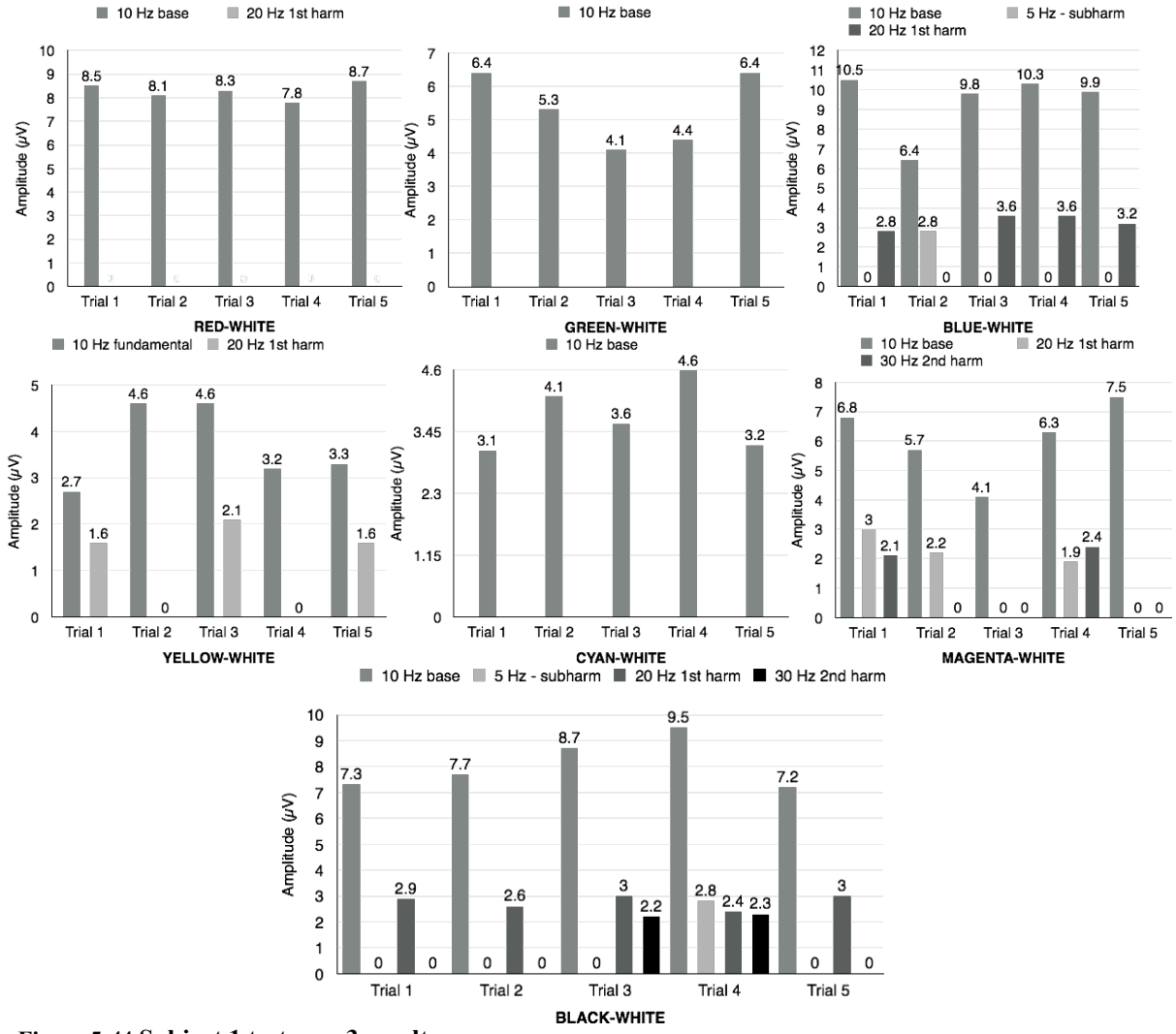

Figure 5-44 Subject 1 test case 3 results

Test case 3 is the last set of results generated by the subject 1 showing all captured trials as successful. Again, similarities between these results and the remaining 2 tests cases can be observed. Blue-white continues to show very high 10 Hz peaks with similar to previous cases 20 Hz contamination. Red-white and cyan-white generated harmonic free responses in all trials, this time also accompanied by green-white variant, which additionally produced high 10 Hz peak levels. The reference black-white checkerboard elicited high 10 Hz peaks with slightly less harmonics compared to the previous 2 test cases. Overall, read-white flicker again deserves to be nominated as the most efficient, harmonic free stimulus for this subject.

Test case 4 - Subject 2

No 10 Hz signal peaks detected.

Test case 5 - Subject 3

No 10 Hz signal peaks detected.

Test case 6 - Subject 4

No 10 Hz signal peaks detected.

Test case 7 - Subject 5

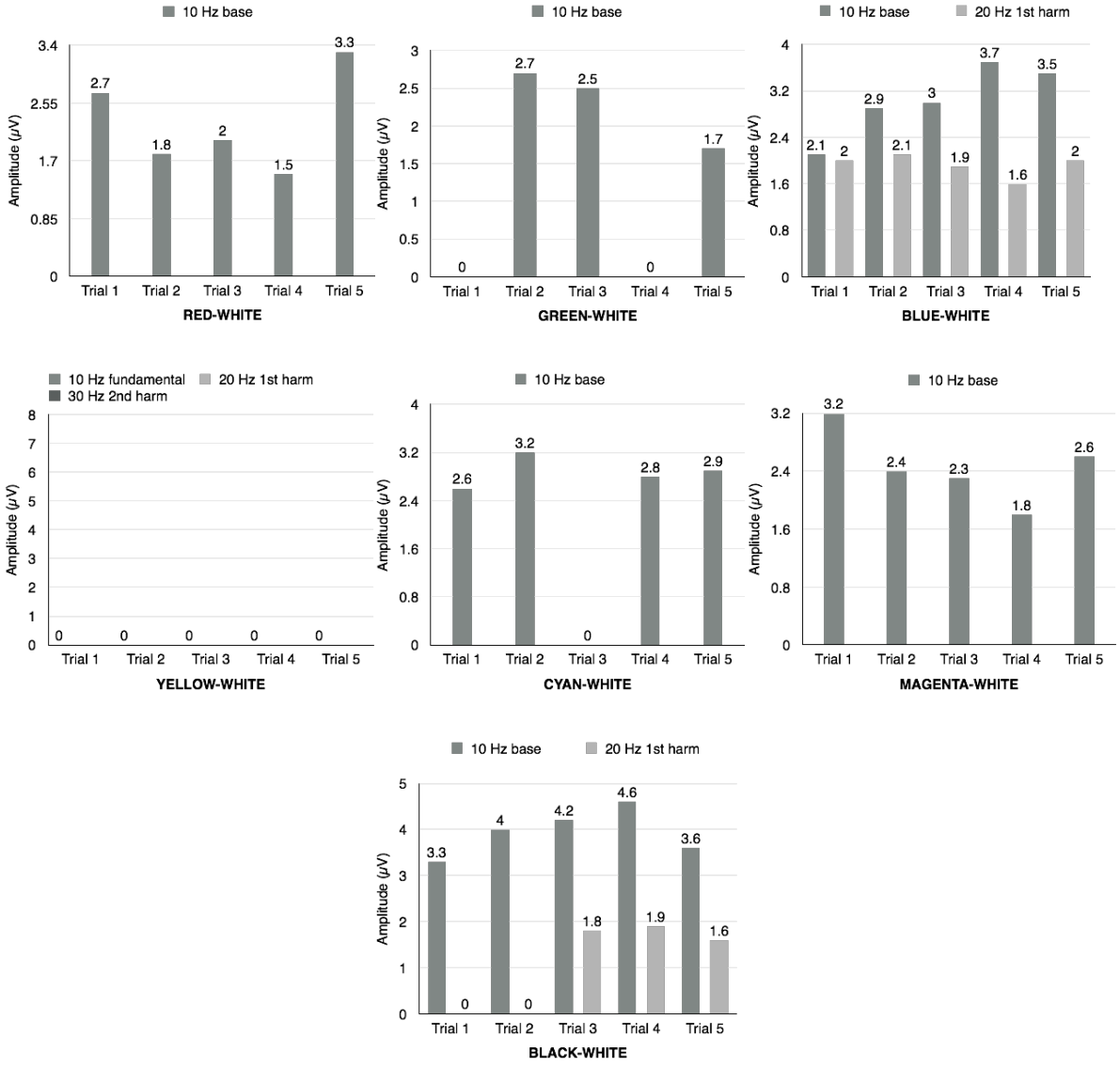

Figure 5-45 Subject 5 test case 7 results

Subject 5 is the first untrained subject who successfully generated 10 Hz peaks. In this test case, the yellow-white variant did not produce any results. There were also 3 unsuccessful trials, 2 for the green-white and 1 for the cyan-white stimuli. Comparably to subject 1, this test case presents blue-

white trials, with all 5 trials corrupted by heavy 20 Hz harmonic responses. Subjects 5 elicited harmonic free all successful trials with red-white and magenta white checkerboards. Very good peaks response is evident in the reference black-white variant. Some level of 20 Hz harmonic contamination is present in 3 trials; however, it is less evident when compared to subject 1. Overall, the levels of elicited 10 Hz peaks are much lower in comparison to subject 1.

Test case 8 - Subject 6

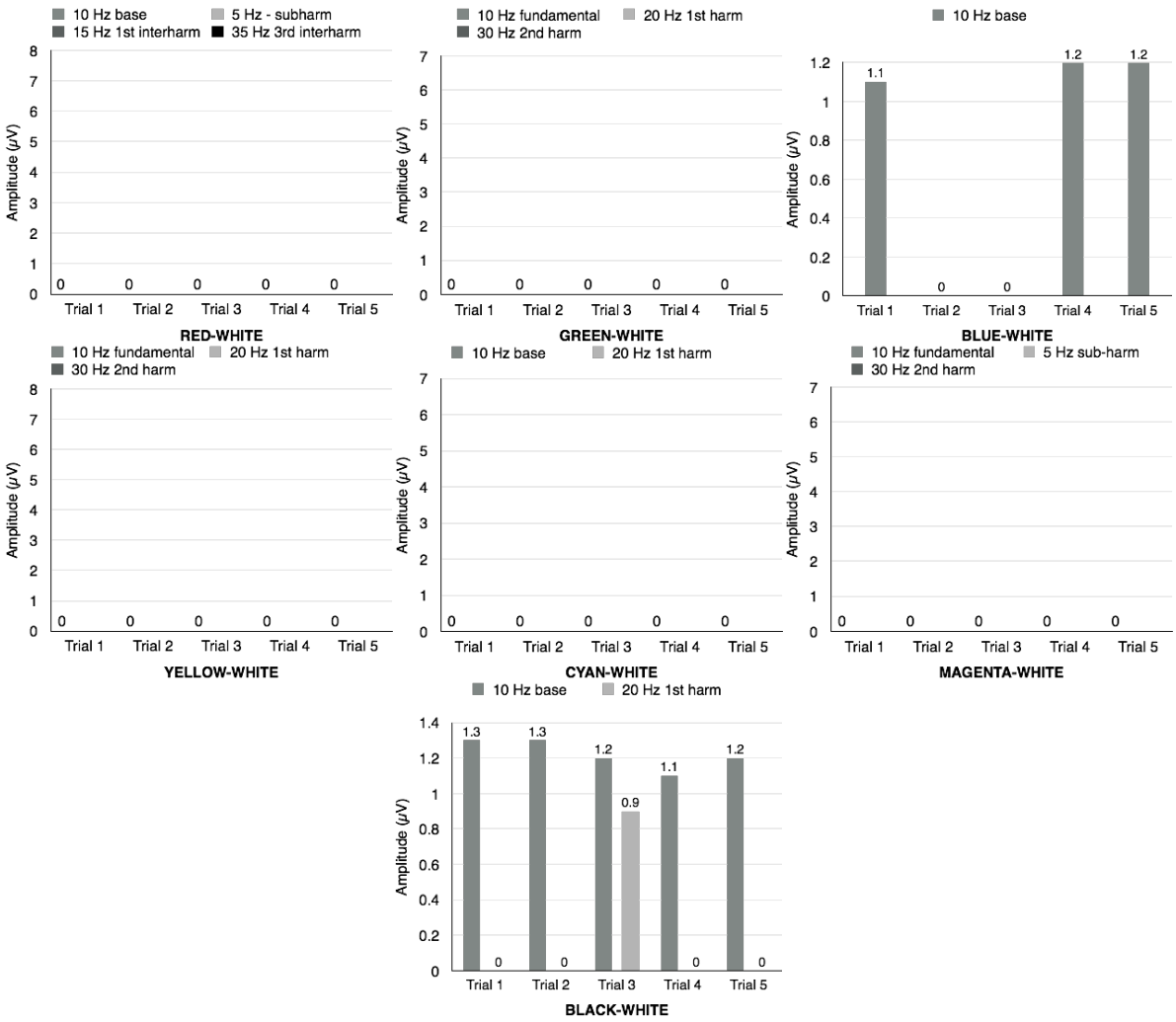

Figure 5-46 Subject 6 test case 8 results

Subject 6 was successful only with 2 flicker colours, blue-white and the reference black-white. The blue-white flicker produced 3 clean 10 Hz peaks and the black-white 4 clean peaks and 1 contaminated with 20 Hz content. However, the overall levels of elicited signals are very low between 1.1 µV and 1.3 µV.

Test case 9 - Subject 7

No 10 Hz signal peaks detected.

Test case 10 - Subject 8

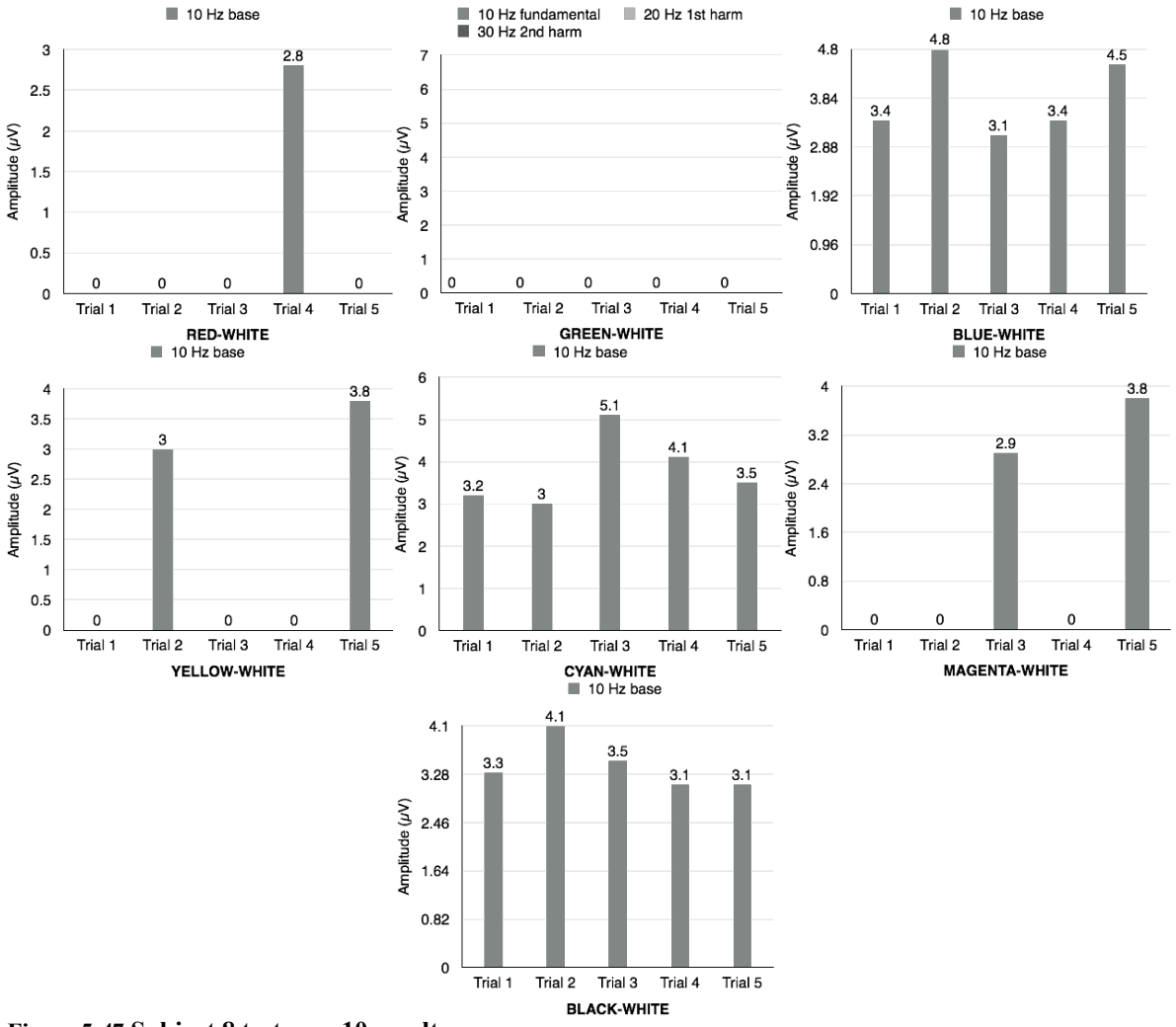

Figure 5-47 Subject 8 test case 10 results

Test case 10 representing subject's 8 results shows very interesting brain response to stimuli presentation. None of the registered trials shows any harmonic content, which is very unusual. Although the green-white flicker did not produce 10 Hz peaks at all, surprisingly, the red-white variant, very successful so far, generated only 1 peak of 10 Hz oscillation. The yellow-white and magenta-white versions produced only 2 successful trials each. The blue-white, cyan-white, and black-white colours all produced very good 10 Hz peak responses. The registered peak amplitudes are lower by approximately 50% in comparison to the trained subject 1.

Test case 11 - Subject 9

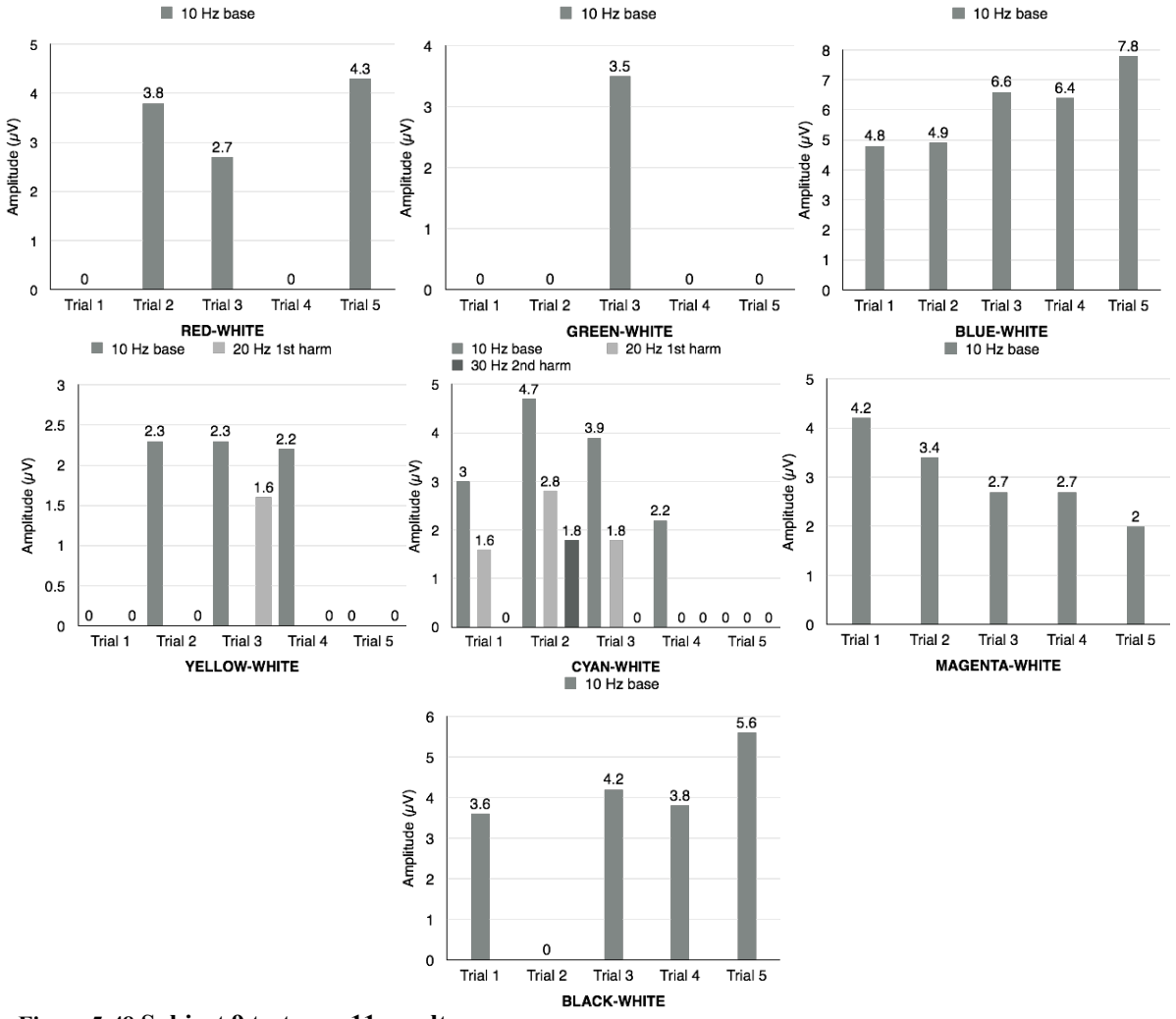

Figure 5-48 Subject 9 test case 11 results

The above results registered for subject 9 show inconsistencies and irregularities, not observed with the previous subjects. In total there are 10 unsuccessful trials in this test case, while other flickers such as blue-white and magenta-white elicited very clean and consistent results. The green-white stimulus produced only 1 successful 10 Hz peak. The usually efficient red-white stimulus generated only 3 positive responses of the brain. Very strong harmonic contamination with this user can be observed only on cyan-white variant, which did not produce any harmonics in any of the previously mentioned test cases. The blue-white checkerboard slightly outperformed the reference black-white version. The generated 10 Hz peaks are again lower in amplitude compared to the trained subject 1.

Test case 12 - Subject 10

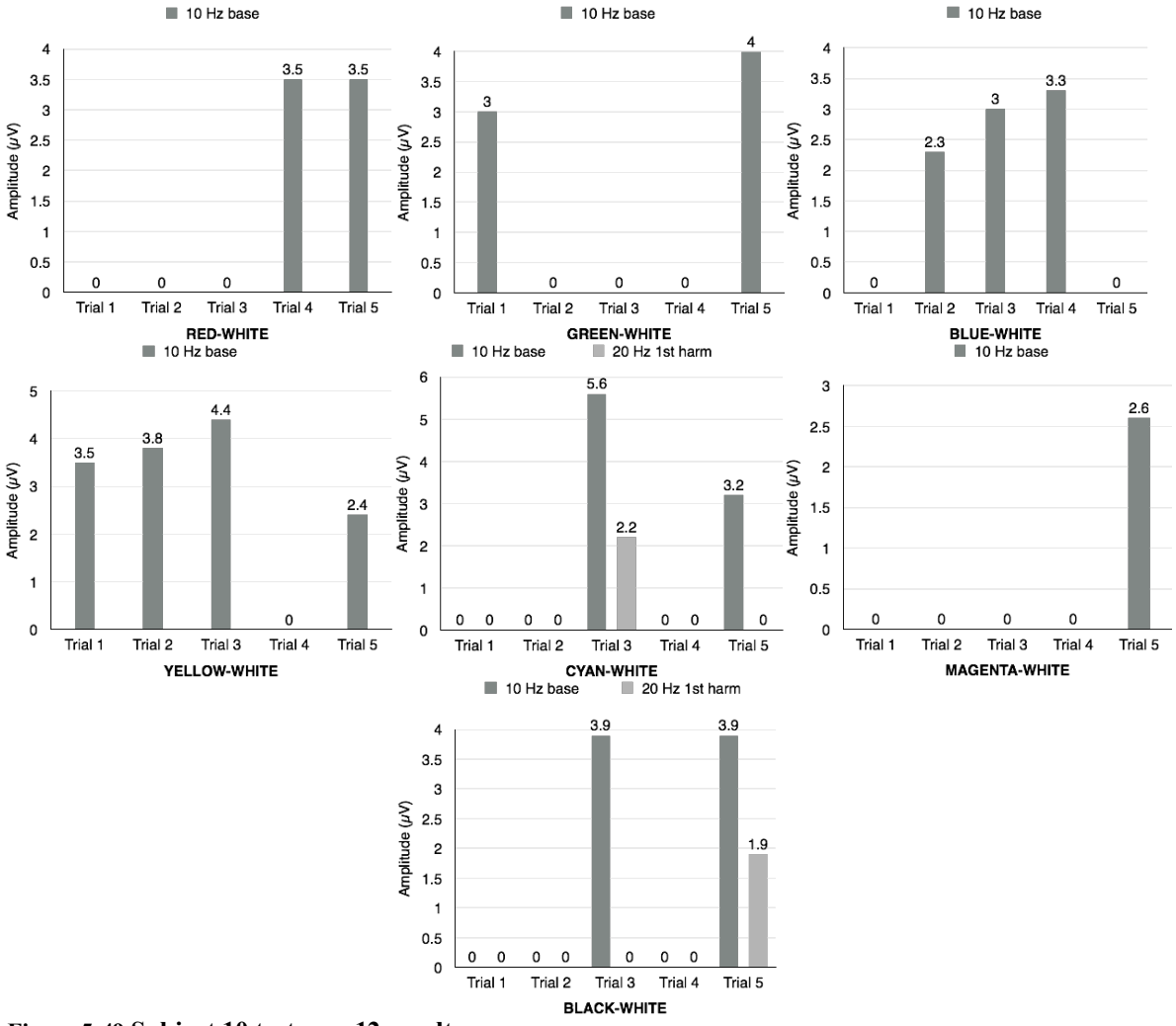

Figure 5-49 Subject 10 test case 12 results

Subject 10 shows very erratic response to presented visual stimuli, which is reflected in the test case 12 results. Every colour flicker produced unsuccessful trials, 19 of them in total. The least successful flicker can be evidenced in the magenta-white plot, with only one 10 Hz peak elicited. The red-white and green-white variants each produced harmonics free 10 Hz peaks. The cyan-white and reference black-white checkerboard also generated 2 successful 10 Hz peaks, however with visible harmonic content. The blue-white flicker elicited 3 peaks, while usually very inefficient yellow-white variant achieved the best results of 4 peaks with this subject.

Test case 13 - Subject 11

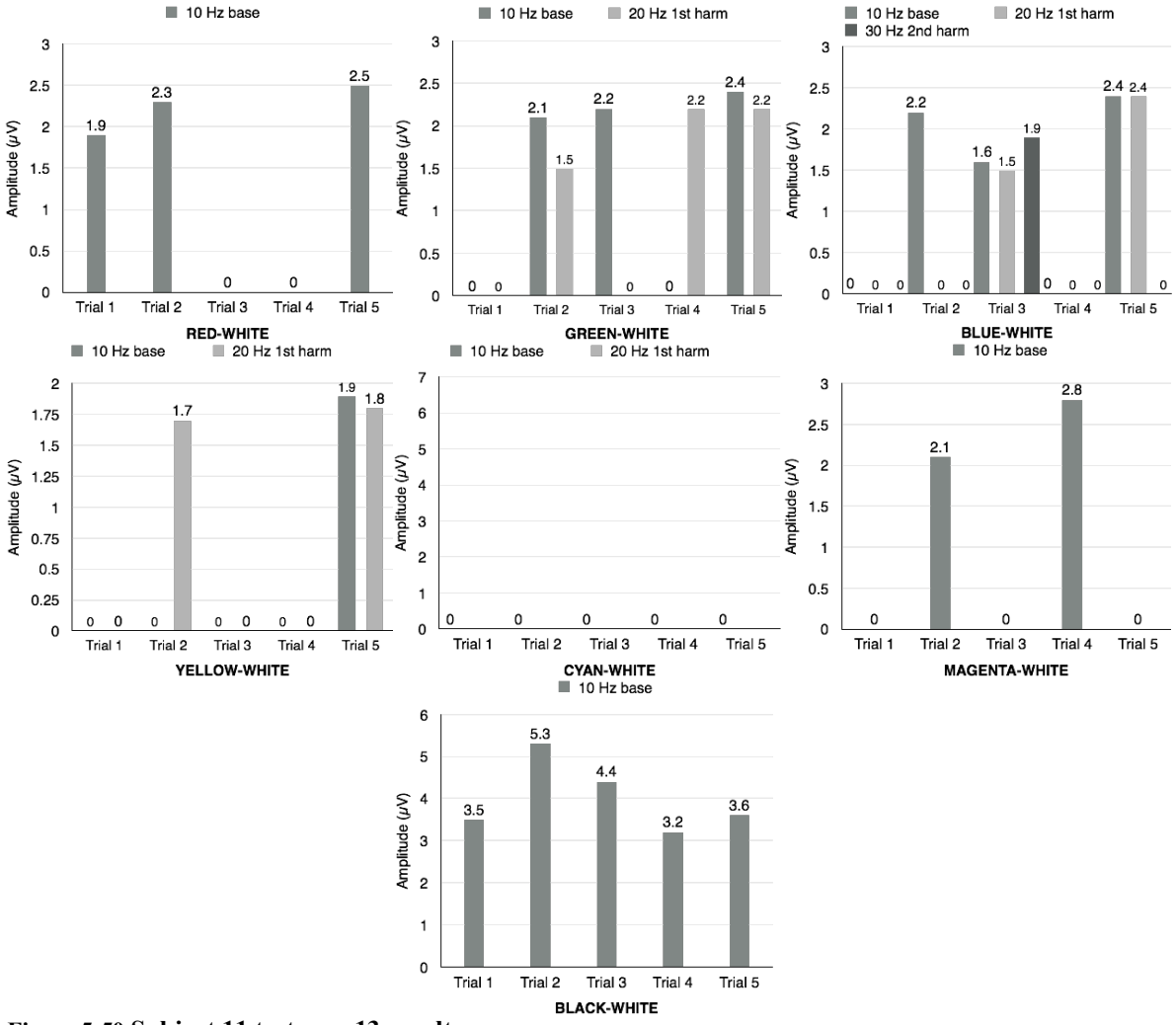

Figure 5-50 Subject 11 test case 13 results

The best harmonics free signal peaks for the subject 11 were produced by the reference black-white stimulus with all 5 successful trials. On the other side of the spectrum is the cyan-white checkerboard with no response in 10 Hz oscillation. The red-white with 3 trials and magenta white with only 2 trials flickers produced clean 10 Hz signal but of very low amplitudes ranging between 1.9 μV and 2.8 μV. The green-white and blue-white variants generated equally weak 10 Hz peaks but with rich harmonic content. The yellow-white shows only 1 peak in 10 Hz but with equally strong 20 Hz harmonic.

Test case 14 - Subject 12

No 10 Hz signal peaks detected.

Test case 15 - Subject 13

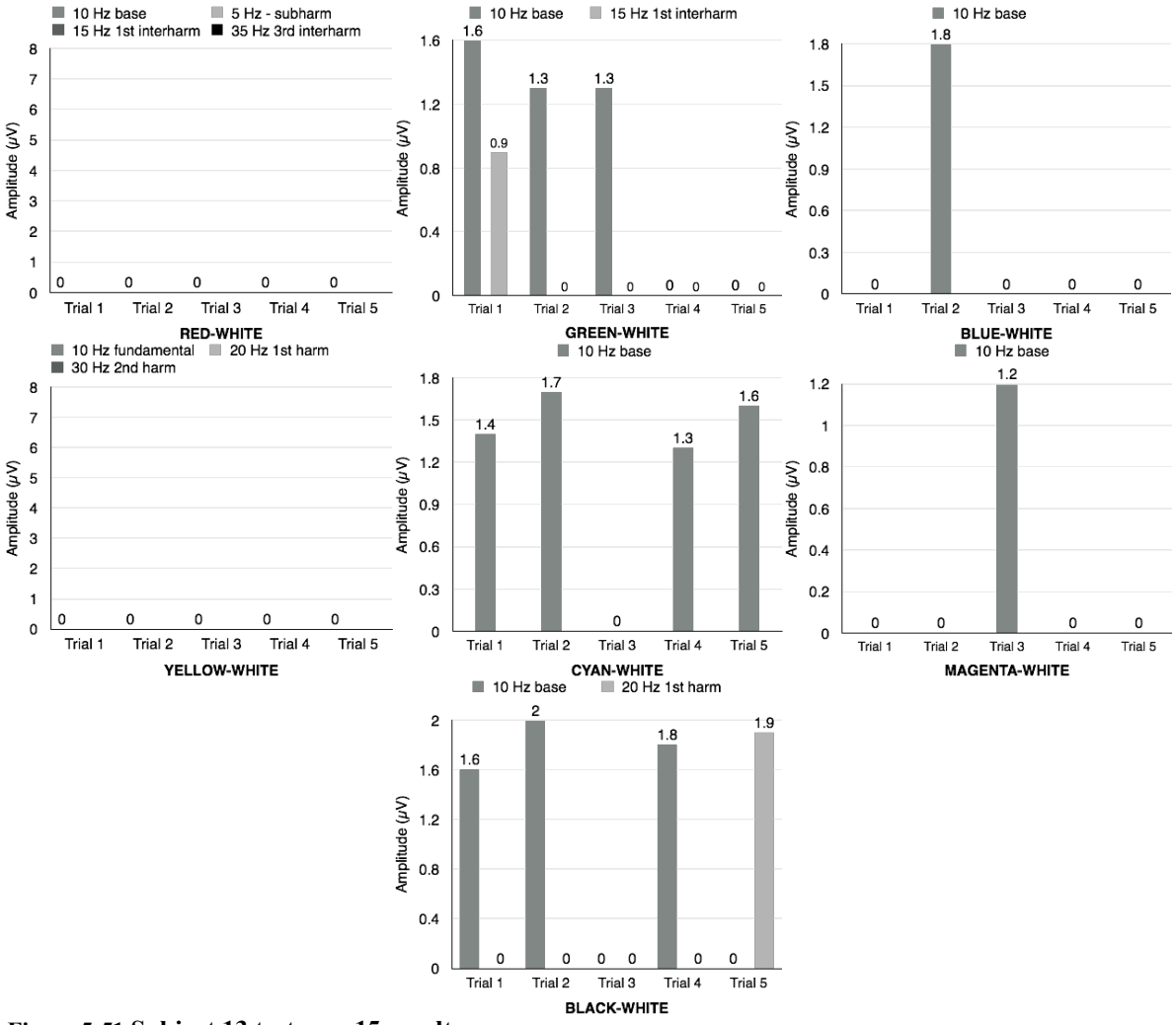

Figure 5-51 Subject 13 test case 15 results

Test case 15 with subject 13 results represents rather poor set of results reflected in the above shown plots. The red-white and yellow-white flickers did not show any 10 Hz results at all, while 2 successful trials can be observed in the blue-white and magenta-white plots. The cyan-white flicker elicited the best signals with plots showing no harmonic contamination. The green-white and black-white counterparts both elicited 3 positive responses in the target 10 Hz with minor harmonic content.

Test case 16 - Subject 14

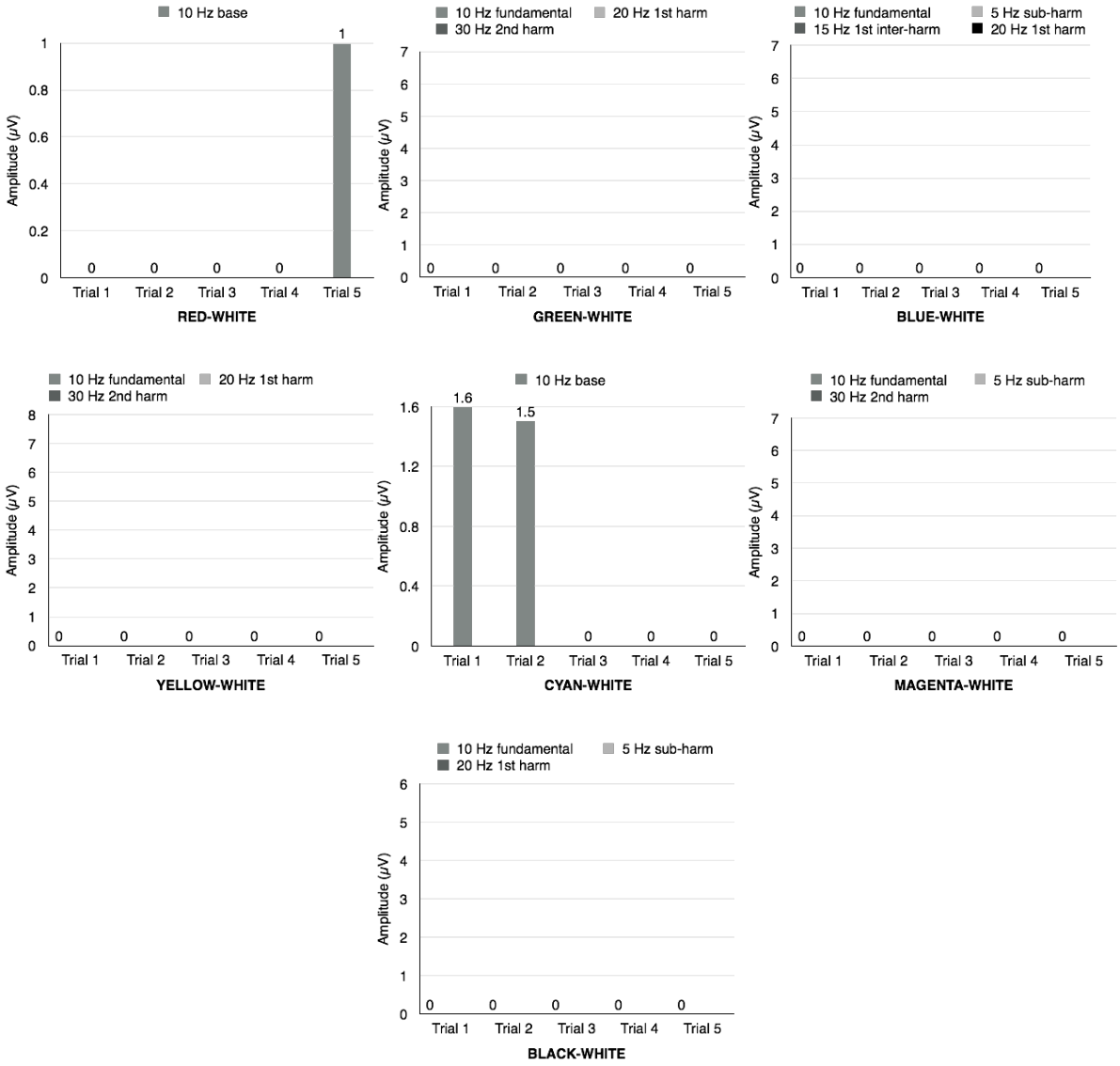

Figure 5-52 Subject 14 test case 16 results

The test case 16 with subject 14 results is another example of very poor brain's response to the visual stimulation. The red-white flicker elicited only 1 target 10 Hz peak with very low amplitude level at just 1 μV. The cyan-white variant generated 2 slightly stronger peaks with values of 1.5 μV and 1.6 μV. All the remaining flickers including the reference black-white variant were unsuccessful.

B. Results Summary – All Subjects per Colour

Colour Red

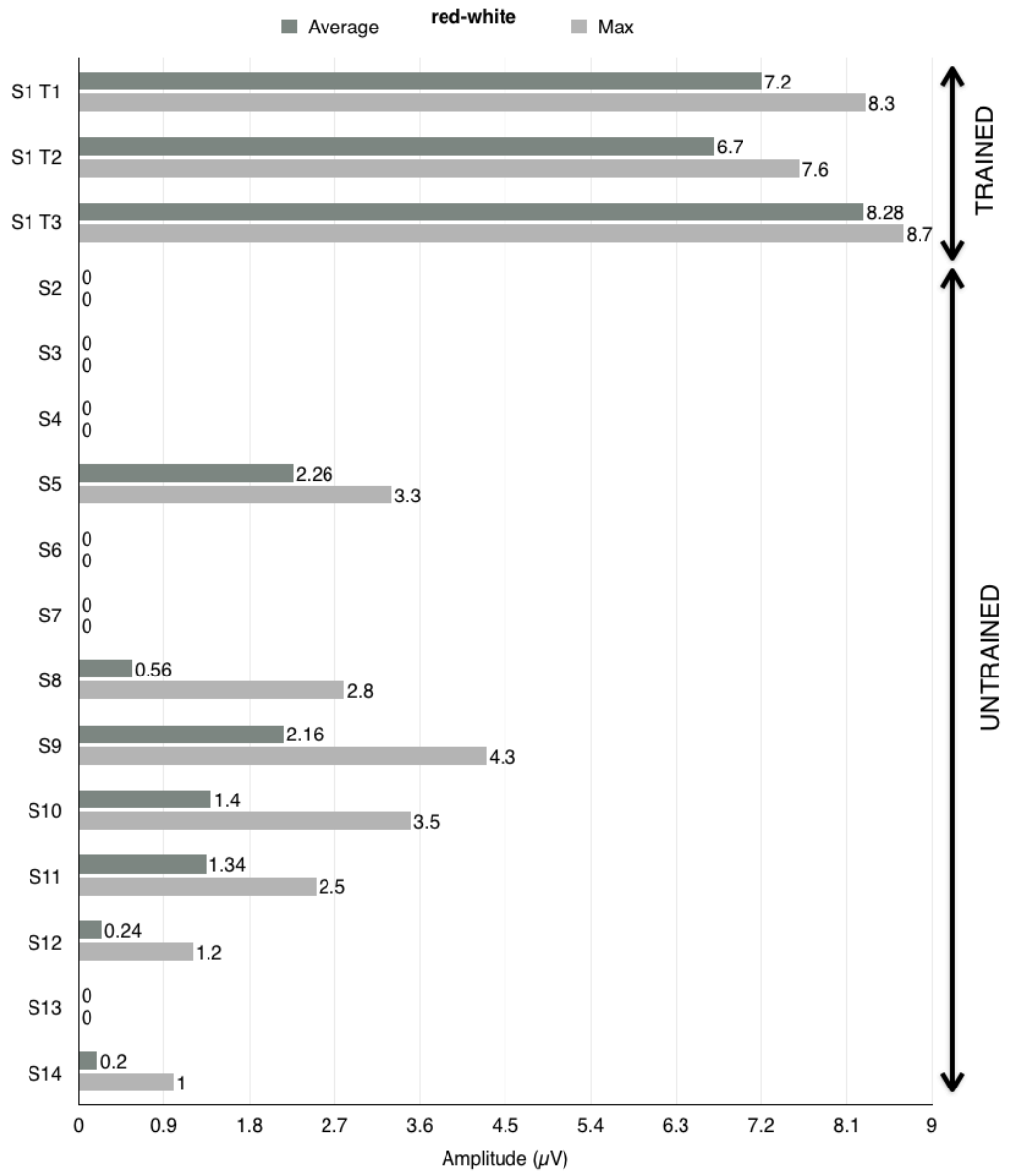

Figure 5-53 Maximum and average results for colour red

This first in a series summary plot using the maximum results (light grey bar) and the statistical average results derived from all 5 trials (dark grey bar) shows how all the participating subjects responded to the red-white checkerboard flicker. Only the main 10 Hz component is detailed in these plots. In the plots the subjects are marked as S1, S2, S3, … and S14. T1, T2, and T3 refer to three tests cases performed by the subject 1. Firstly, a large disproportion in the elicited signal peaks amplitude between the trained subject 1 and all the remaining successful untrained subject can be observed in the plot. Subject 1 manifests very strong and uniform response to the red-white flicker variant across all the 3 test cases. Evident is a very small difference between the maximum and the average results, especially in the test case 3 proving consistent and steady 10 Hz responses to the

red-white checkerboard of the subject. From the untrained subjects, 6 of them did not produce any traces of 10 Hz peaks in their brain signals. Subjects 5 and 9 provided results with the average values exceeding 2 μV, while subjects 10 and 11 generated average signals in the range 1-2 μV. The remaining subjects 8, 12, and 14 generated very low average 10 Hz peaks below 1 μV.

Colour Green

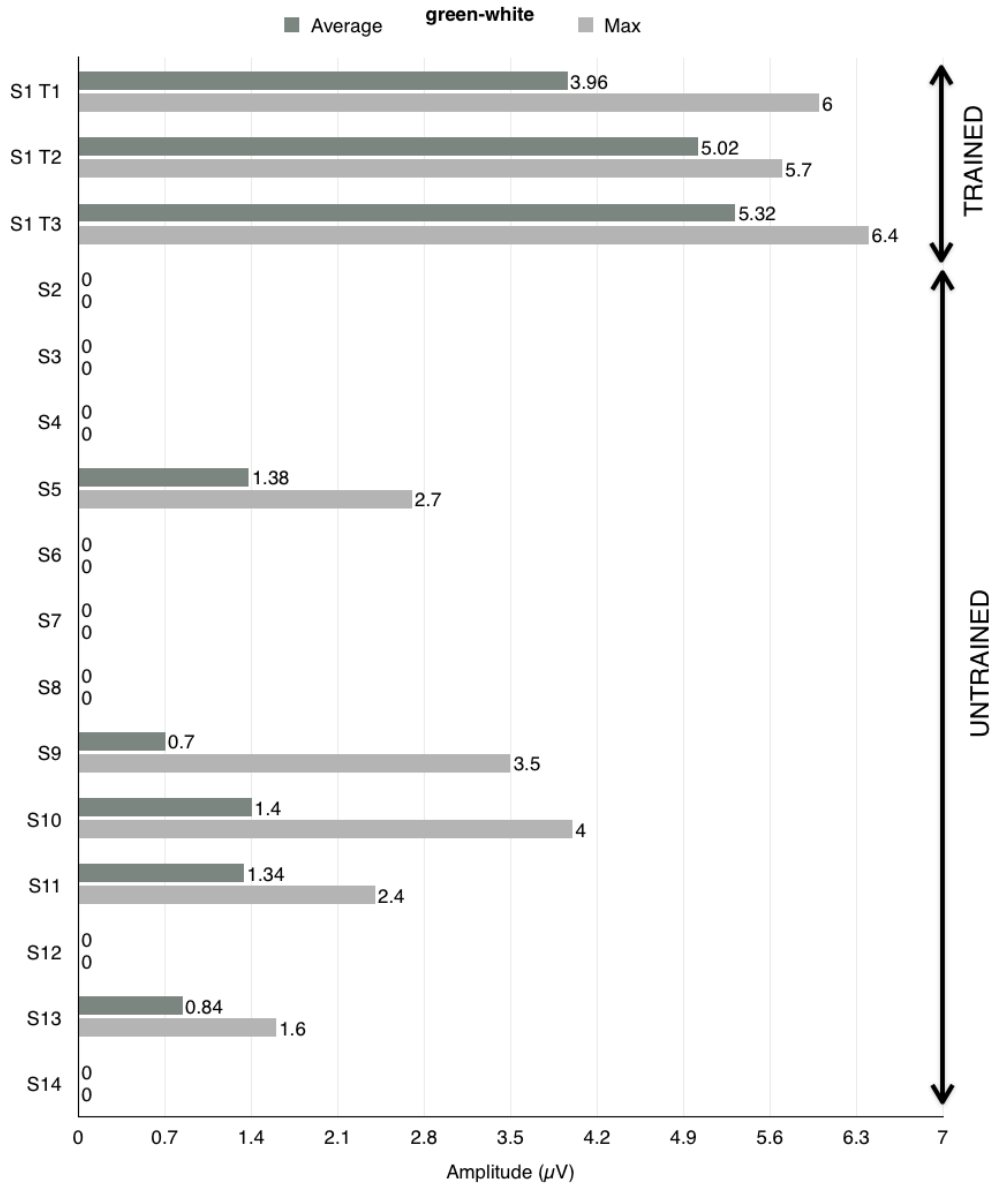

Figure 5-54 Maximum and average results for colour green

Comparably to the red-white colour flicker, the green-white variant exposes a large discrepancy in 10 Hz signal peaks between the trained subject 1 and the untrained subject. Although not as high as the red-white flicker, the green-white variant produced rather steady response in the subject 1 brain, especially evidenced in the test cases 2 and 3. With the colour green-white even more subjects, 8 of them, did not succeed in reproducing the 10 Hz oscillation displayed by the flicker. Subjects such as

9 and 10, present very promising maximum results between 3.5 µV and 4 µV. However, the average results should be more thoroughly analysed as they more accurately represent the subjects' ability to elicit the desired signal peaks. Thus, it must be stated that among these who responded positively to the green-white flicker presentation, i.e. subjects 5, 9, 10, 11, and 13, the registered average levels are very low in the range between 1.4 µV and 0.84 µV.

Colour Blue

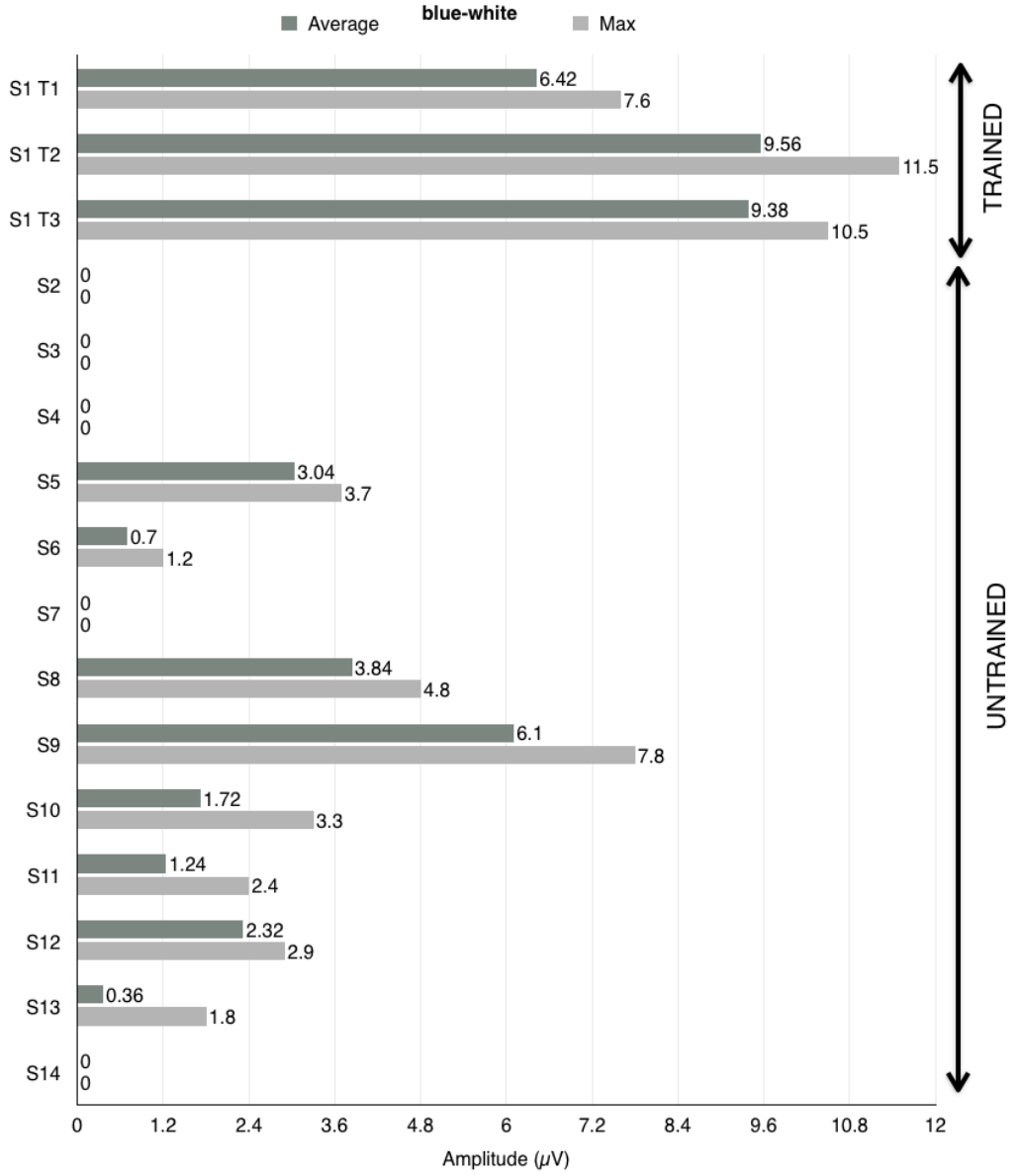

Figure 5-55 Maximum and average results for colour blue

White-blue flicker exhibits similar to the previously submitted results characteristics of clearly visible difference between the subject 1, considered as trained subject, and the remaining untrained subjects. Subject 1 presents very reliable response to the presented blue-white checkerboard stimulus especially affirmed in test cases 2 and 3. Among the untrained subjects, 5 of them did not

reproduce the target 10 Hz frequency in their brain signals. The best average result for the untrained subject can be reported for the subject 9 with value of 6.1 µV. Satisfactory average results in the range between 3.04 µV and 3.84 µV are achieved by subjects 5 and 8. Subject 12 shows rather stable response but with low average value of 2.32 µV. The rest of the subjects, i.e. 6, 10, 11, and 13 represent very low average signal levels between 1.72 µV and 0.36 µV.

Colour Yellow

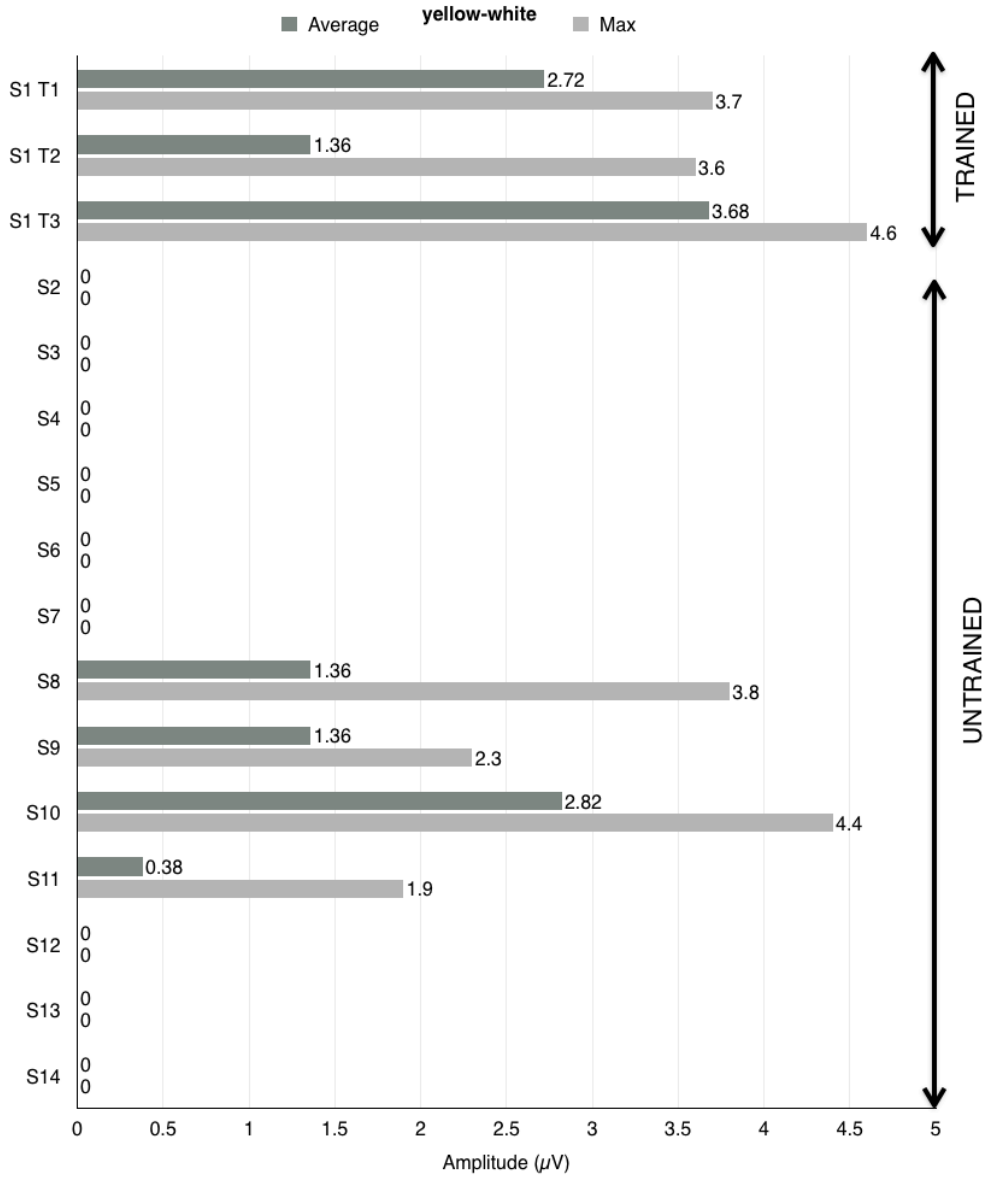

Figure 5-56 Maximum and average results for colour blue

Clearly yellow-white stimulus flicker generates one of the weakest brain responses, which can be affirmed in the above shown results. Subject 1 registered his lowest average results in all 3 test cases with the highest average value of 3.68 µV found in the test case T3. Overall, 10 untrained subject did not produce any brain responses matching the target 10 Hz frequency. It can be observed that subjects 8 and 10 generated rather high maximum values ranging between 3.8 µV and

4.4 µV, however their average scores between 1.36 µV and 2.82 µV confirm that this colour is inefficient. Subject 11 with the weakest result among the successful test cases revels the same tendency of substantial difference between sporadic maximum value and the average counterpart.

Colour Cyan

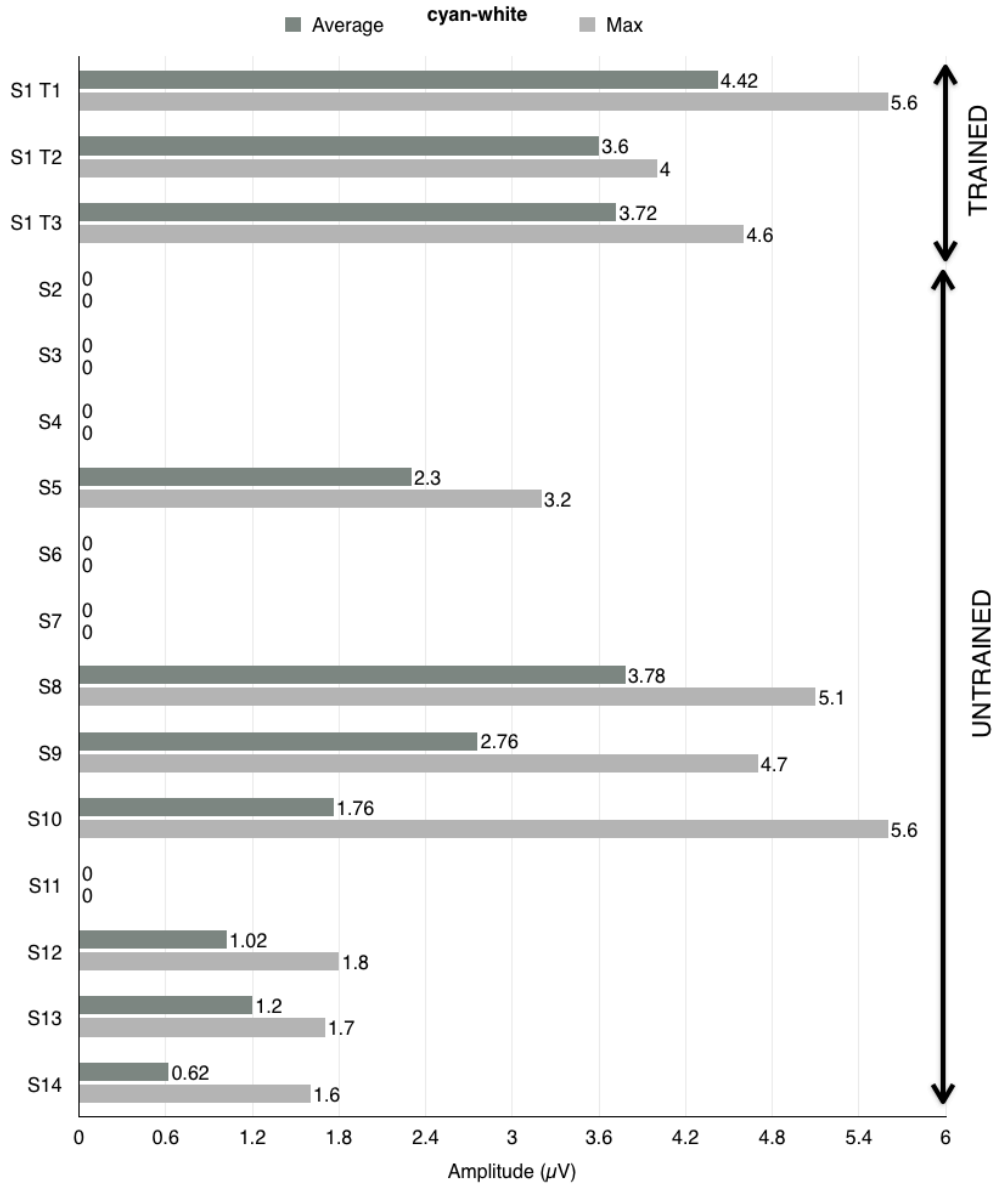

Figure 5-57 Maximum and average results for colour cyan

By analysing the cyan-white colour flicker results one can observe slightly diminished discrepancy between the trained and untrained sections of the plot considering the results of subjects 8, 9, and 10. Although, the trained subject 1 presents more solid and stable response as shown by smaller differences between the maximum and average results for this subject. Among the untrained subjects, 6 of them did not produce any results in stimulated 10 Hz. The untrained subject 8 exposes very comparable maximum and average results when compared to the trained subject 1. Subject 5

shows stable response but with rather low average value of 2.3 μV, while subject 10 generated one of the highest maximum 10 Hz peaks but with even low average result at 1.76 μV. Subjects 12 to 14 although successful, show very weak response to cyan-white flicker with average score between 1.2 μV and 0.62 μV.

Colour Magenta

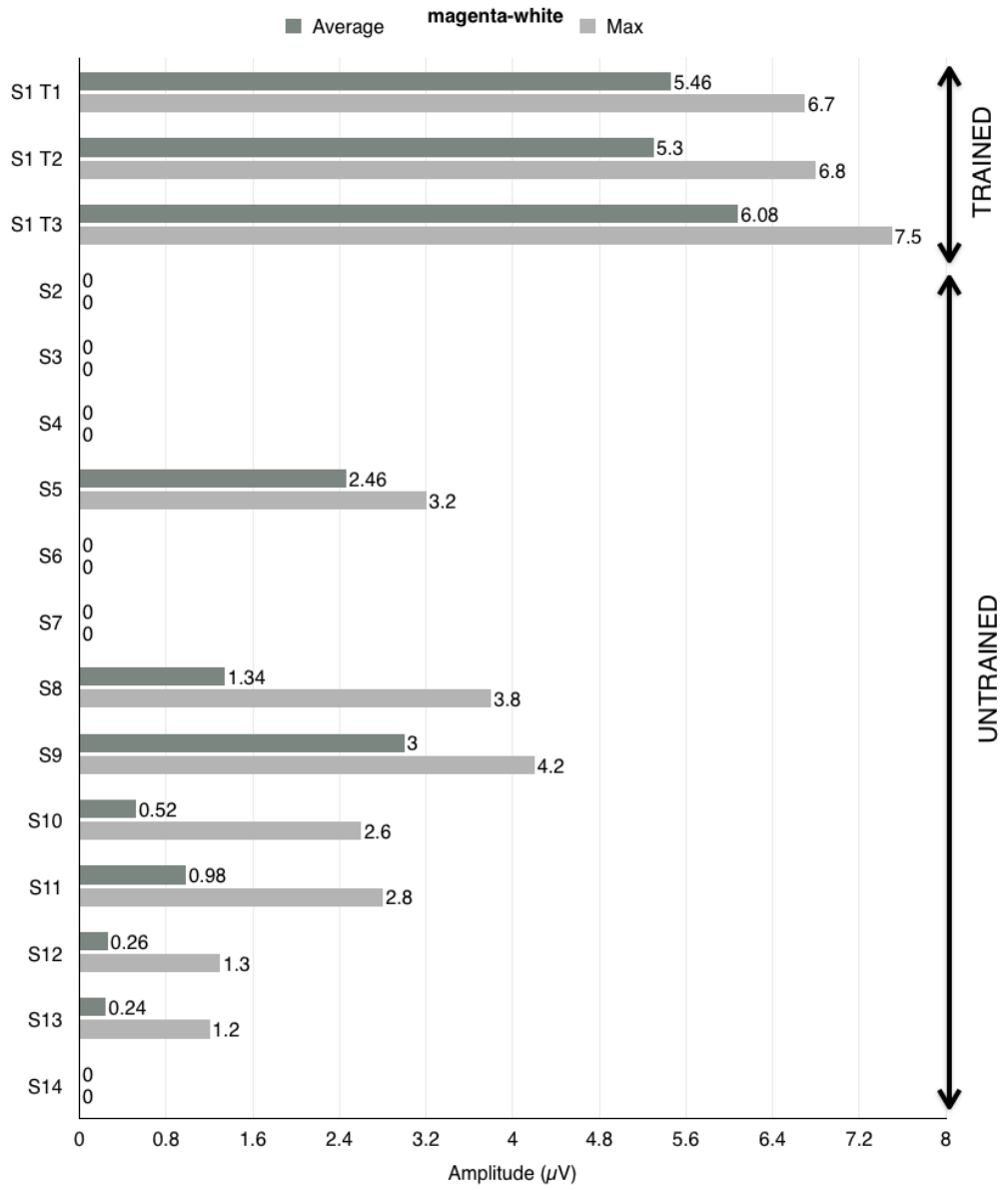

Figure 5-58 Maximum and average results for colour magenta

Magenta-white flicker reveals again a large disproportion in brain response to visual stimulation between the trained subject and the remaining untrained subjects. In all 3 tests cases, the trained subject responded with very solid average signals between 5.3 μV and 6.08 μV. In total, 6 untrained subjects did not produce any 10 Hz peaks in their brain signals. Subjects 5 and 9 responded with stable signals however the levels of the former are not satisfactory with average amplitude at 2.46

µV. Subject 8 represents unstable response with large difference between the maximum of 3.8 µV and the average of only 1.34 µV. Subjects 10 and 11 generated much higher maximum peaks compared to their low average results of 0.52 µV and 0.98 µV respectively. Very similar behaviour can be noticed with subject 12 and 13 signals but with much lower amplitude values.

Black-White

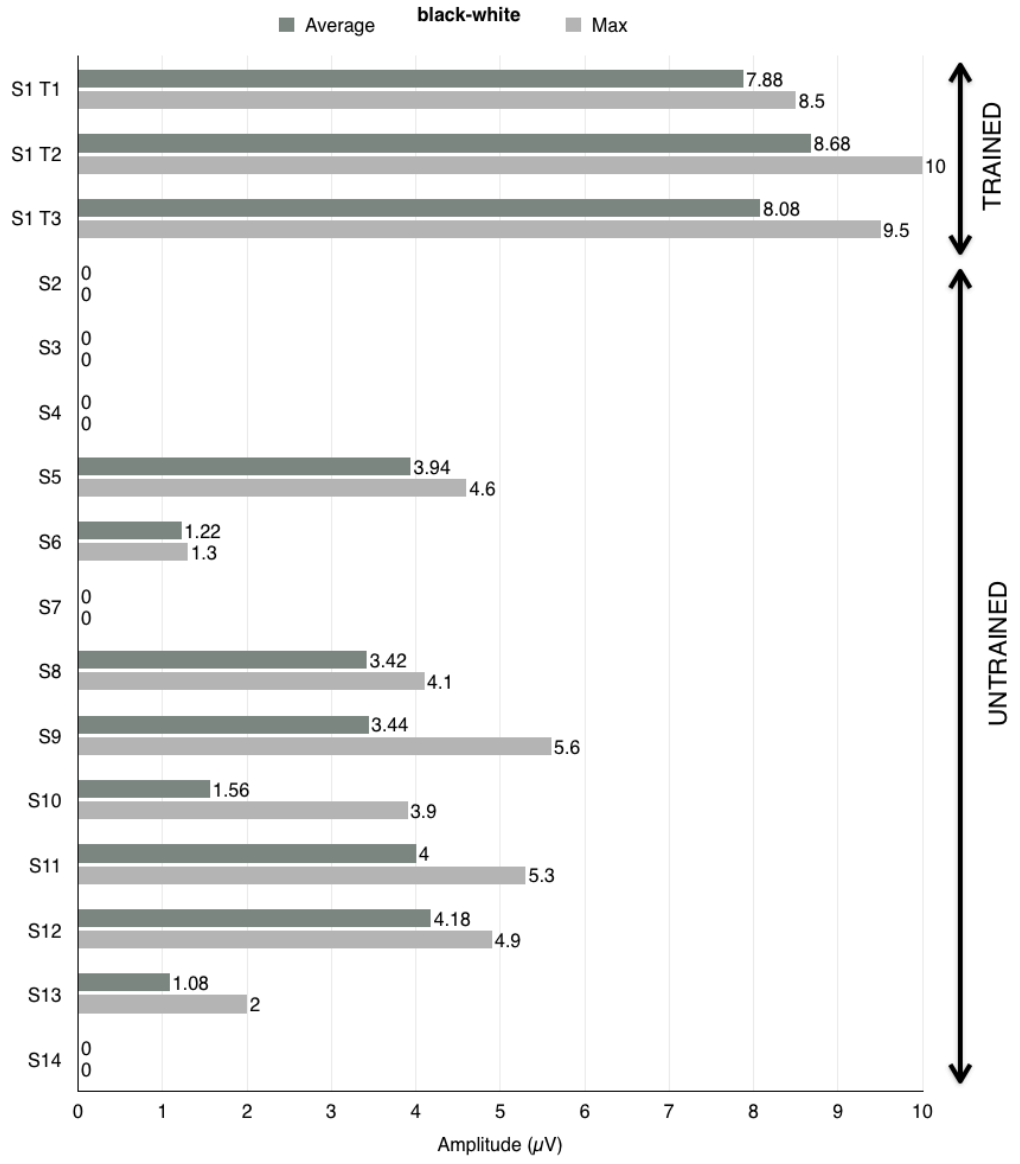

Figure 5-59 Maximum and average results for reference black-white

The black-white reference checkerboard flicker demonstrates very strong and solid response in the trained subject 1 all 3 tests cases. The average amplitude peaks registered for the trials show 7.88 µV, 8.68 µV, and 8.08 µV. In total, 5 subjects did not produce any signals. Subjects 5, 8, 9, 11, and 12 reveal very firm response with average signals between 3.42 µV and 4.18 µV. Subject 10 represents a case where the high maximum of 3.9 µV is accompanied by very weak average level of 1.56 µV. Subjects 6 and 13 represent both weak maximum and average values.

C. Results Summary – All Colours per Subject

Test Case 1 - Subject 1

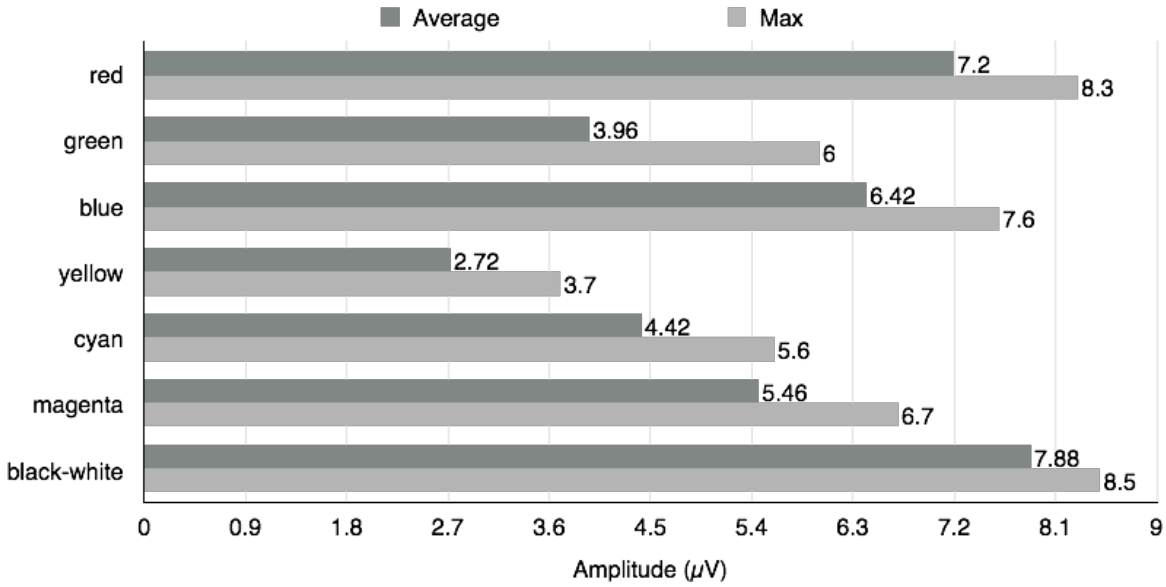

Figure 5-60 Maximum and average results for subject 1 test case 1

The above shown plot represents the first in a series of all colours response results per subject. In test case 1, the subject 1 shows the strongest signals, both maximum and average, generated by the reference black-white stimulus. Only slightly weaker are results produced by the red-white, followed by the blue-white, magenta-white and cyan-white variants. The green-white flicker produced high maximum but the more important average score is weaker. The yellow-white colour produced the weakest signals in the brain.

Test Case 2 - Subject 1

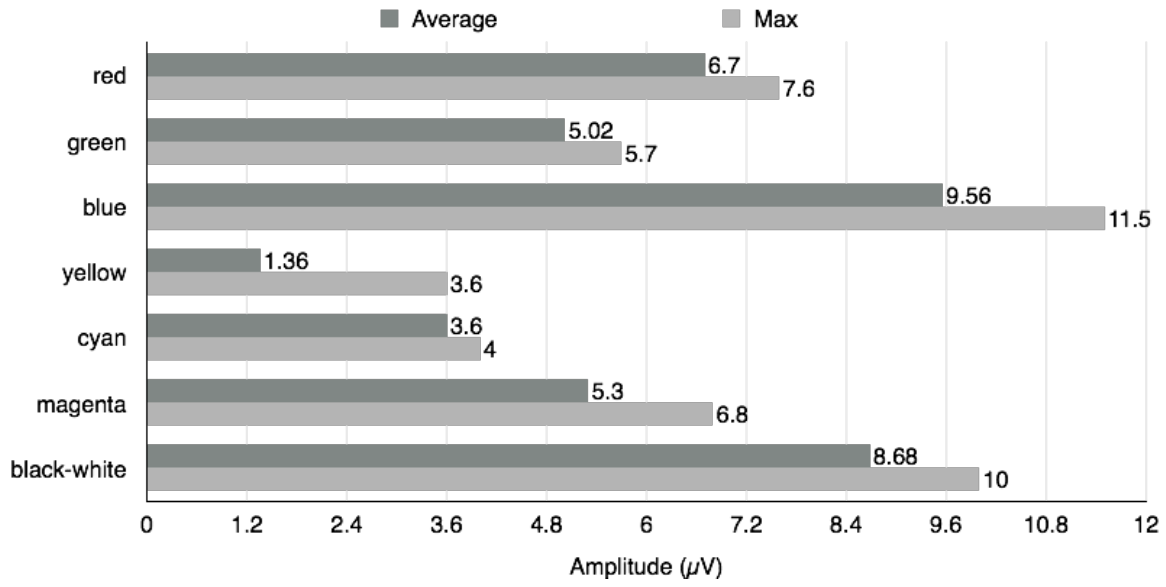

Figure 5-61 Maximum and average results for subject 1 test case 2

In test case 2 of the same subject 1 apparent is the domination of the blue-white flicker, which outperformed the black-white variant. Next is the red-white followed by magenta-white, and green-white. The cyan-white displays solid response but levels are significantly lower than the better performing flicker versions. The yellow-white delivered the poorest brain signals.

Test Case 3 - Subject 1

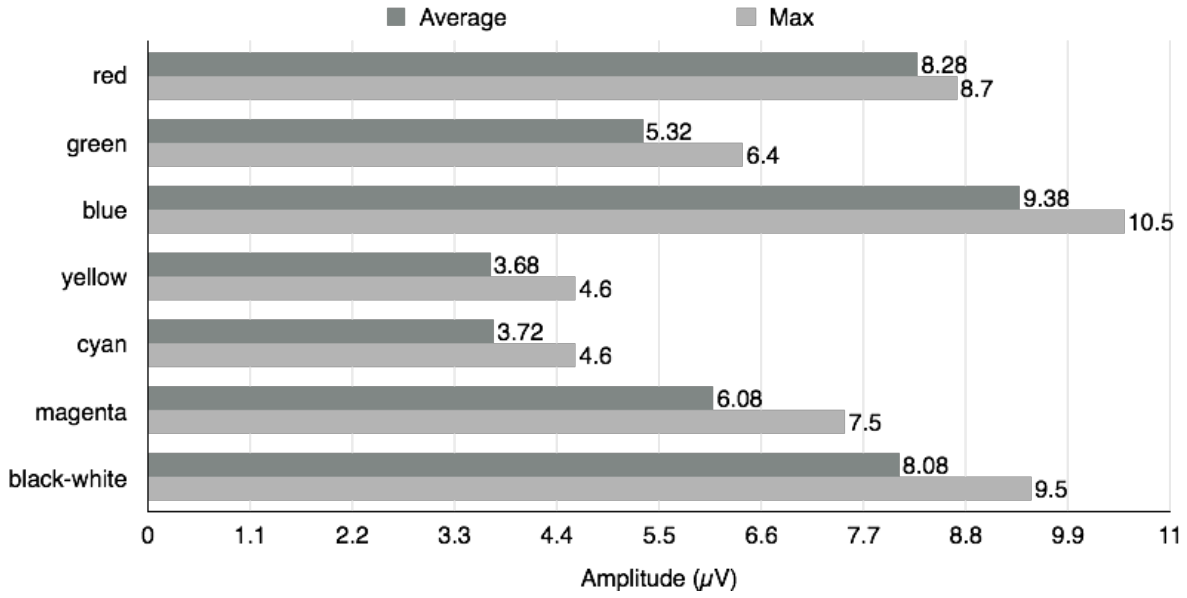

Figure 5-62 Maximum and average results for subject 1 test case 3

In test case 3, the subject 1 exhibits the highest response to the blue-white flicker. The next highest average score belongs to the red-white flicker with very small discrepancy between maximum and average results. The black-white reference produced very high maximum but the average is smaller than the previous 2 flickers discussed. The magenta-white is followed by the green-white version both representing the medium level of response. The lowest 2 scores produced by the yellow-white and cyan-white are very similar in terms of maximum and average levels.

Test Case 4 - Subject 2

No 10 Hz signal peaks detected.

Test Case 5 - Subject 3

No 10 Hz signal peaks detected.

Test Case 6 - Subject 4

No 10 Hz signal peaks detected.

Test Case 7 - Subject 5

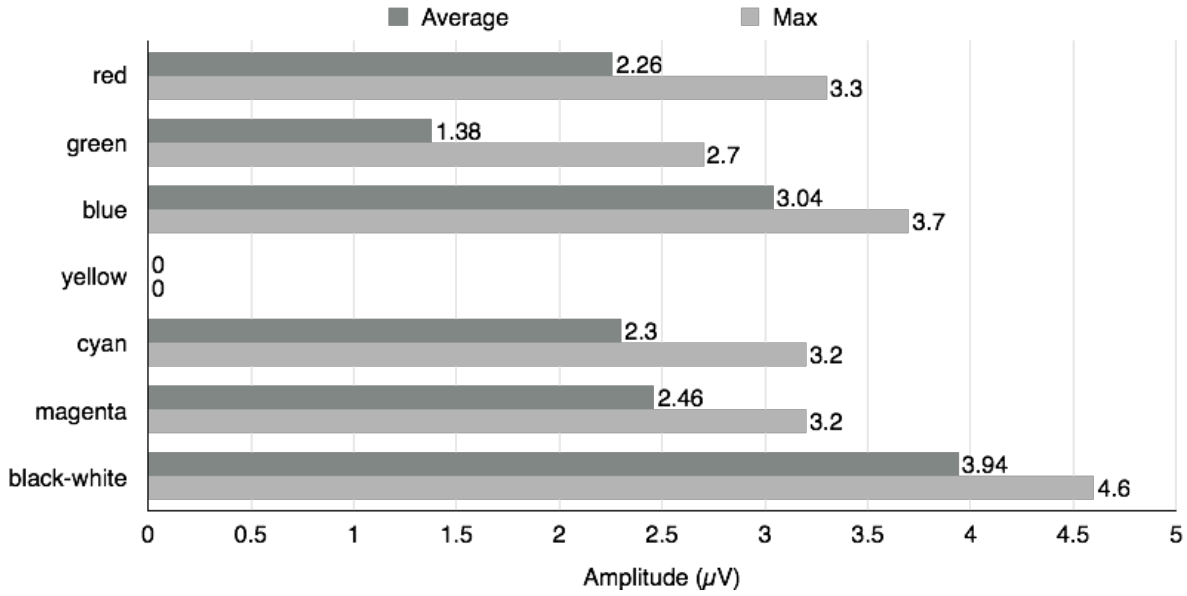

Figure 5-63 Maximum and average results for subject 5

Subject 5 is the first untrained subject who responded positively to visual stimulation. The black-white reference flicker generated the highest levels both maximum and average. The best colour flicker results belong to the blue-white variant, followed by the red-white, magenta-white, and cyan-white stimuli results. The green-white flicker unveils comparable to the rest of the flickers maximum level, but the average response is visibly weaker. The yellow-white did not produce any 10 Hz signals.

Test Case 8 - Subject 6

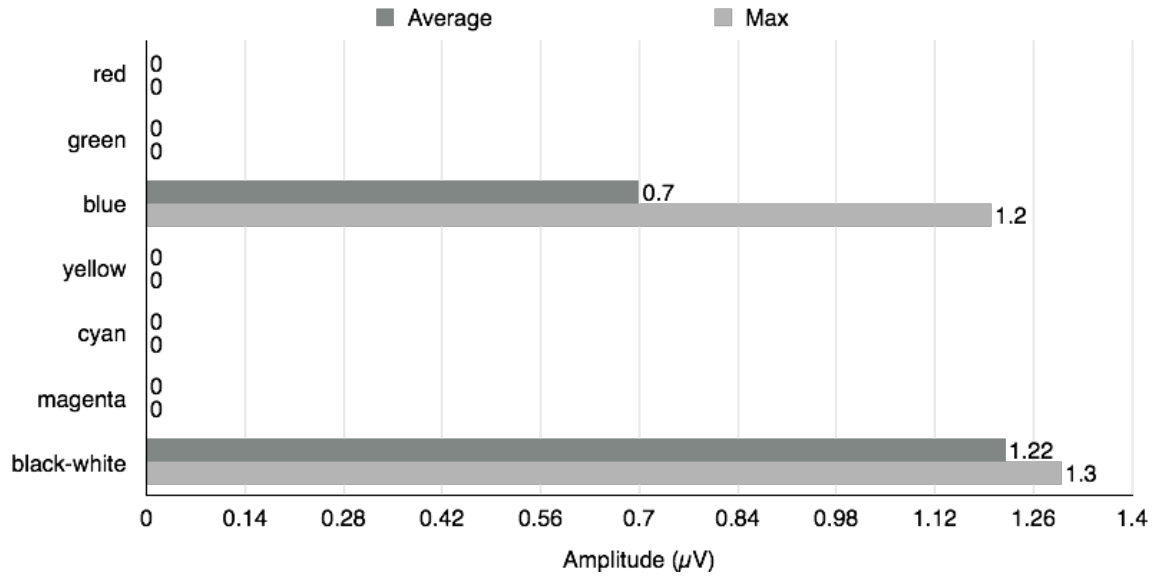

Figure 5-64 Maximum and average results for subject 6

Subject 6 responded only to 2 flickers, the black-white and blue-white, although the signals are very poor.

Test Case 9 - Subject 7

No 10 Hz signal peaks detected.

Test Case 10 - Subject 8

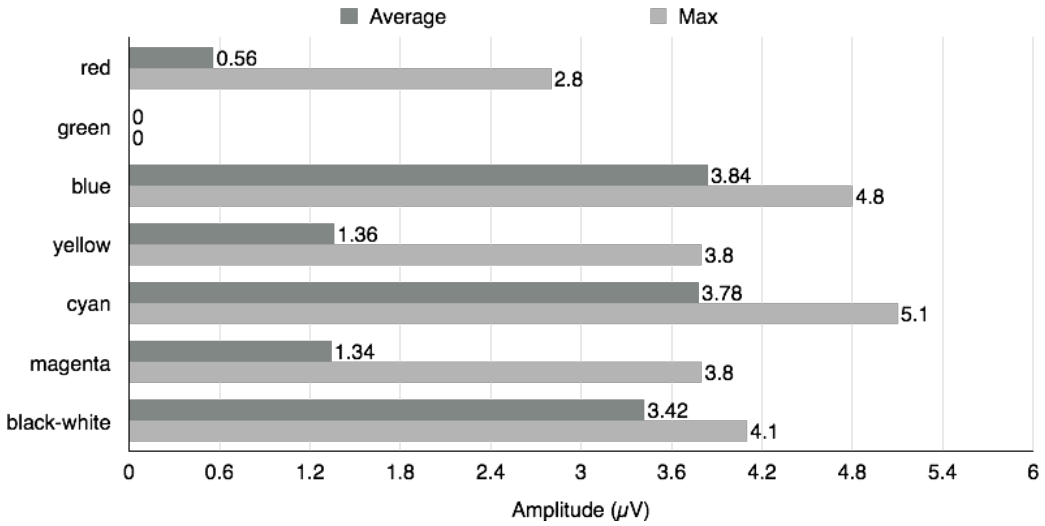

Figure 5-65 Maximum and average results for subject 8

Subject 8 responded equally well to both blue-white and cyan-white flickers. Both colours performed slightly better than the black-white, which represents the third highest average score for this subject. The yellow-white and magenta-white generated almost identical results with large discrepancy between high maximum and low average results. The red-white generated very weak average response, while the green-white did not produce any signals.

Test Case 11 - Subject 9

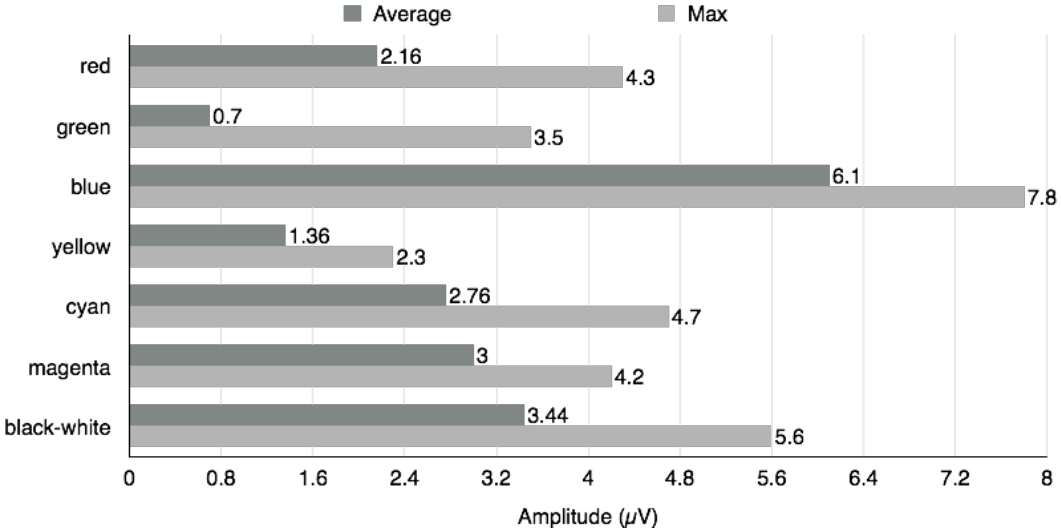

Figure 5-66 Maximum and average results for subject 9

Subject 9 responded with the strongest maximum and average signals to the blue-white colour flicker. The black-white stimulus represents the second highest score for both maximum and average results. These are followed by the magenta-white, cyan-white, red-white, and yellow-white variants with gradually decreasing signals strength. The green-white generated reasonably high maximum signal but with the lowest average result.

Test Case 12 - Subject 10

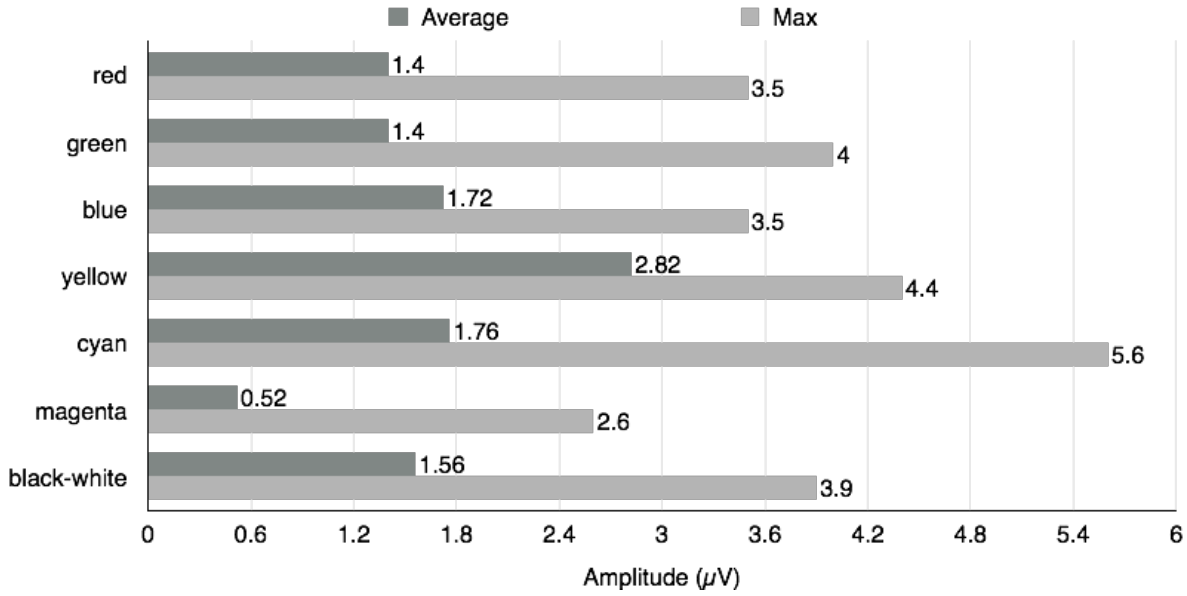

Figure 5-67 Maximum and average results for subject 10

Subject 10 reveals the phenomenon of high maximum peaks with low average results for all the tested colours. As discussed earlier, judging by the average results, the yellow-white flicker variant, which in most tests cases is ranked among the weakest performers, in this test case delivered the highest average result. This is followed by cyan-white and blue-white. The 4th result belongs to the reference black-white checkerboard, which identically to the colour versions shows substantial difference between the maximum and average results. The red-white and green-white stimuli performed almost identically. The lowest average score is registered by the magenta-white flicker revision. Very high maximum results registered by cyan-white, yellow-white, green-white, and red-white flicker revisions show great potential of these colours.

Test Case 13 - Subject 11

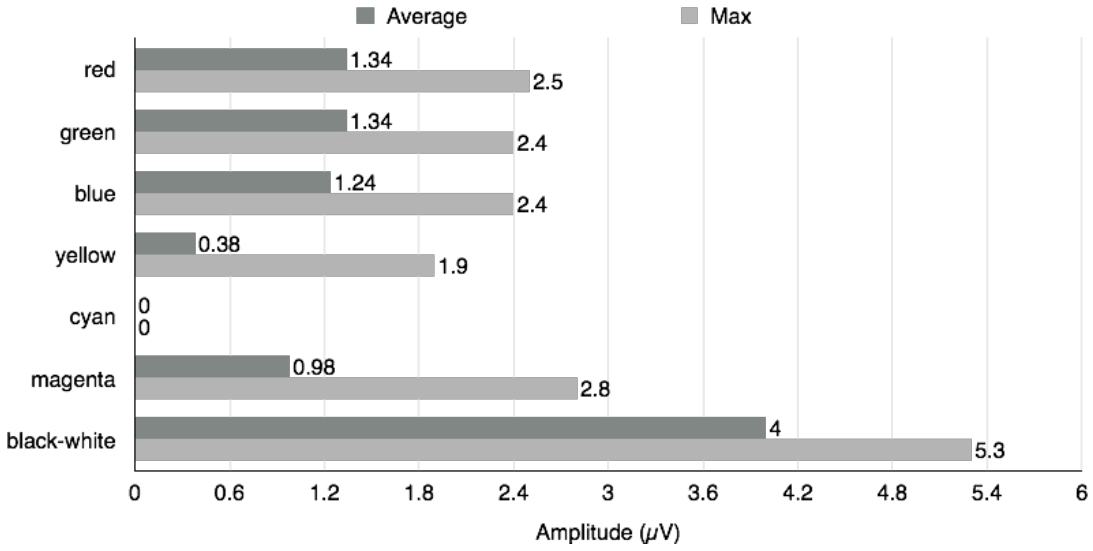

Figure 5-68 Maximum and average results for subject 11

When analysing subject 11 all colours results, one can observe the dominance of the black-white combination with very high maximum results and the highest average result. The next best performing 4 colour flickers, i.e. red-white, green-white, blue-white, and magenta-white delivered very similar results in terms of maximum and average results, with the latter representing approximately half of the maximum peak values. The yellow-white performed the weakest of the successful testcases, while the cyan-white combination did not deliver any results. In general, the average values generated by the colour stimuli are very low compared to the black-white lattice.

Test Case 14 - Subject 12

No 10 Hz signal peaks detected.

Test Case 15 - Subject 13

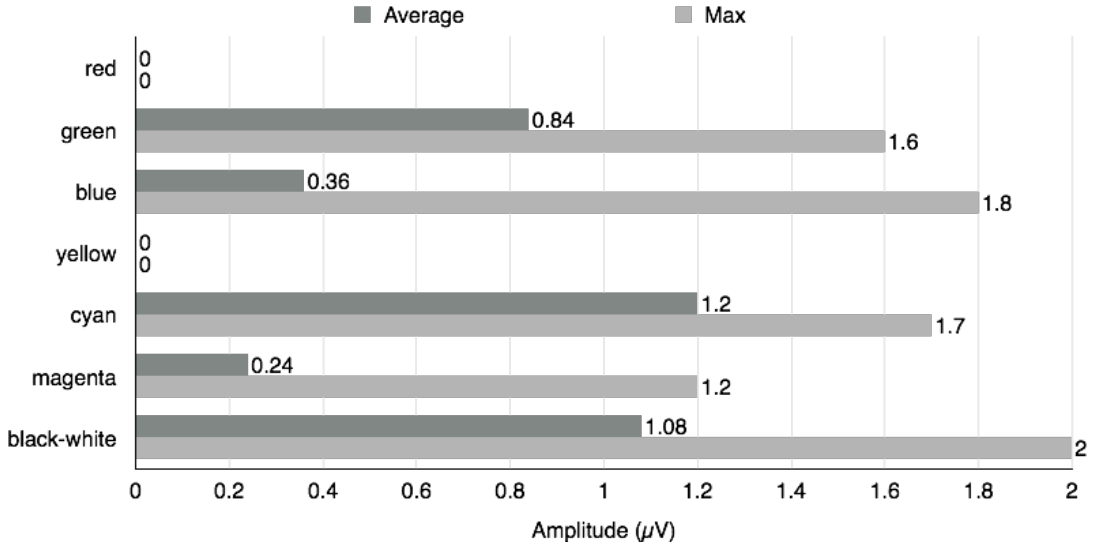

Figure 5-69 Maximum and average results for subject 13

In test case 15, subject 13 shows the highest average result for the cyan-white flicker, closely followed by the black-white, and then green-white versions with all results occupying low range of values. Despite very low peaks values registered by the subject 13, the blue-white delivered one of the highest maximum results together with very low average value. The very same occurrence of high maximum and low average values is evidenced by the magenta-white flicker, which delivered the weakest signal among the successful ones. The red-white and yellow-white were unsuccessful.

Test Case 16 - Subject 14

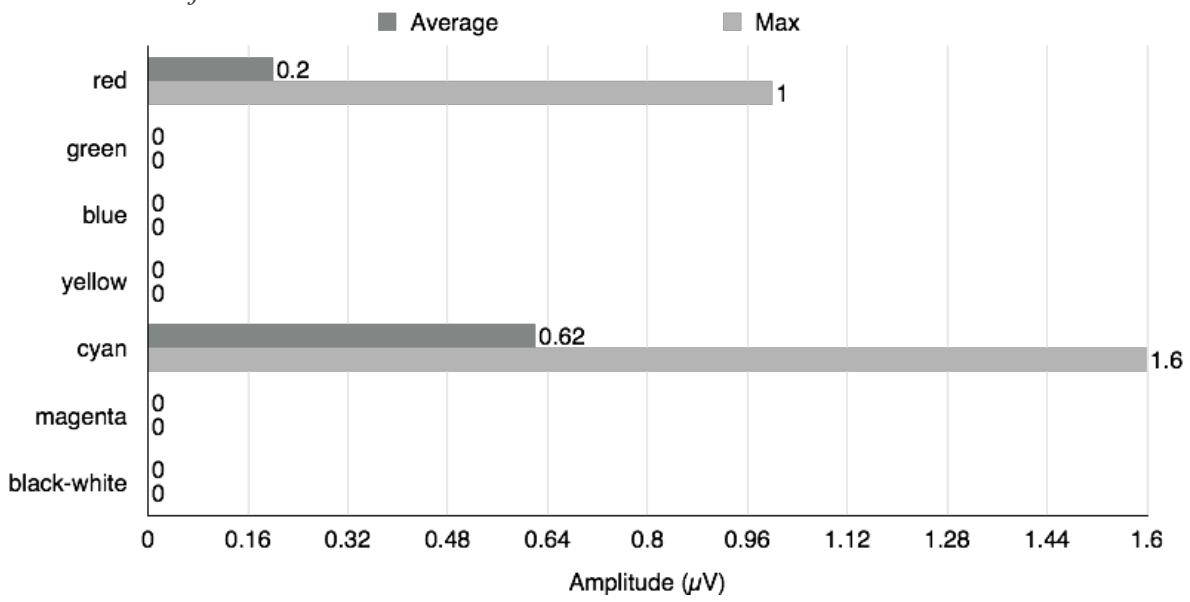

Figure 5-70 Maximum and average results for subject 14

Subject 14 generated the weakest signals in all successful test cases. The large gap between the maximum and average results for the 2 successful flickers is also evident with the subject 14. However, the average levels are extremely low for both cyan-white and red-white stimuli. The remaining flicker variants did not produce any 10 Hz signals.

5.5.3 Experiment Discussion and Observations

This Section provides a thorough discussion of this extensive colour flickers testing experiment involving multiple subject including 1 trained subject and 13 untrained subjects. All the observations have been derived from the above presented graphs and plots.

- Observation #1

The trained subject 1 delivered much higher elicited signal levels in comparison to all untrained subjects for the reference black-white and all colour flickers.

- Observation #2

The consistency of performance can be judged by the discrepancy between the maximum and average results. The larger the discrepancy between the results the lower the performance consistency. The trained subject 1, in all 3 test cases delivered very high level of signal consistency for most of the flickers tested compared to majority of the untrained successful subjects. For the untrained subjects, among the colour combinations tested, the weakest regularity in performance can be observed for the red-white, green-white, and yellow-white flickers. A medium consistency can be attributed to the cyan-white and magenta-white checkerboards, while the best performance consistency is found in blue-white and black-white results. Only subject 5 can be considered as delivering reasonably consistent signals although with significantly lower levels compared to the trained subject 1. Subjects 8 and 9 delivered medium level of quality consistence, while signals produced by subjects 6, 10, 11, 13, and 14 convey very low level of performance consistency.

- Observation #3

From 14 subjects tested, 5 untrained subjects (2, 3, 4, 7, and 12) did not respond to visual stimulation at all. Further 2 untrained subjects (6 and 14) generated weak signals each responding to 2 flickers only. Additionally, further 3 untrained subjects (10, 11, and 13) responded to most of the flicker versions and generated 10 Hz peaks but with low amplitude signals that would require additional signal processing in order to use them in a BCI system. When considering only performance of the untrained subjects, the following observations must be made: 53.8% did not generate useable signals, further 23% generated weak signals with most of the stimuli tested.

- Observation #4

The reference black-white checkerboard is a valid stimulus option and performs exceptionally well for the trained subject 1 generating very strong and stable 10 Hz signal peaks in all 3 test cases. However, only one test case (test case 1) indicates higher 10 Hz signal peaks generated by the

black-white flicker compared to colour versions. Higher 10 Hz peaks generated by the black-white flicker are found in the untrained subjects 5, 6, and 11 in comparison to their colour flicker results. Among the untrained subjects who positively responded to the visual stimulation, 37.5% performed better with the reference black-white graphic. When including the trained subject 1 it is 33.3% of the total positive responses.

- Observation #5

The colour flickers perform better in comparison to the traditional black-white checkerboard. For the trained subject 1, both test cases 2 and 3 indicate higher 10 Hz signal peaks when compared to the reference black-white version. For the untrained subjects, the majority of them i.e. subjects 8, 9, 10, 13 and 14 responded better to colour stimuli. Among the untrained subjects who positively responded to the visual stimulation, 62.5% performed better with the colour graphics. When including the trained subject 1 it is 66.6% of the total positive responses.

- Observation #6

Based on the results collected from all tested 14 subjects, it must be noted that the brain's response to presented flicker versions is very individual. It is very hard to conclude, which particular colour generally delivers the best performance, which could be recommended for all subjects. The following Table 5-6 provides a summary of the results.

Table 5-6 Colour Flickers Performance Results Summary – Multiple Subjects

Subjects	Test case	Best	Worst	Remarks
1	**1**	black-white red-white blue-white	yellow-white green-white cyan-white	black-white rich in harmonics blue-white with 20 Hz harmonic
1	**2**	blue-white black-white red-white	yellow-white cyan-white green-white	black-white rich in harmonics blue-white with 20 Hz harmonic
1	**3**	blue-white red-white black-white	yellow-white cyan-white green-white	black-white rich in harmonics blue-white with 20 Hz harmonic sporadic 20 Hz harmonics in yellow-white and in magenta-white some 20 Hz and 30 Hz
5	**7**	black-white blue-white magenta-white	green-white red-white cyan-white	no signal from yellow-white blue-white with strong 20 Hz harmonics black-white with some 20 Hz harmonics
6	**8**	black-white	blue-white	no signal from red-white, green-white, yellow-white, cyan-white, and magenta-white
8	**10**	blue-white cyan-white black-white	red-white magenta-white yellow-white	subject 8 produced no harmonics in any of the 20 successful trials
9	**11**	blue-white black-white magenta-white	green-white yellow-white red-white	cyan-white with harmonic content
10	**12**	yellow-white cyan-white blue-white	magenta-white red-white green-white	unsuccessful trials in all colours very sporadic 20 Hz response in cyan-white and black-white
11	**13**	black-white red-white green-white	yellow-white magenta-white blue-white	no signals from cyan-white blue-white with 20 Hz and 30 Hz harmonics 20 Hz in green-white and yellow-white
13	**15**	cyan-white black-white	magenta-white blue-white	no signal from red-white and yellow-white
14	**16**	cyan-white	red-white	no signal from green-white, blue-white, yellow-white, magenta-white, and black-white

Based on the Table 5-6 presented above, one can conclude that indeed certain colours perform better than others. Among the best performing checkerboards found in this experiment are: red-white, blue-white, and black-white versions.

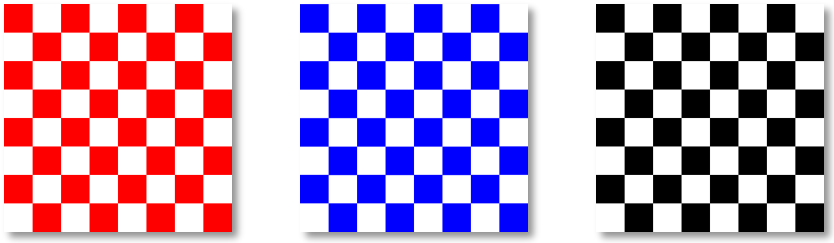

Figure 5-71 The best performing colours in checkerboard flickers

The colours that elicited the best brain signals are red-white, blue-white, and the reference black-white.

The checkerboards, which delivered the worst results, are: yellow-white, green-white, and cyan-white.

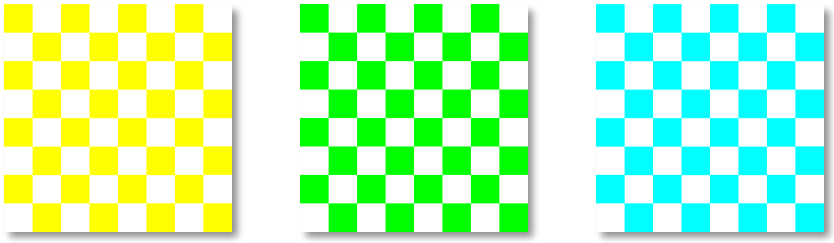

Figure 5-72 The worst performing colours in checkerboard flickers

The colours that elicited the weakest brain signals are yellow-white, green-white, and cyan-white.

Certain minor differences can be observed, especially with the untrained subjects. Most notably however, it is possible to observe certain repeating patterns within each subject's trials. For instance, in subject 1 results the same colours repeat in both best and worst performing categories. Almost identical harmonic response can be identified in all 3 test cases of the subject 1. Very similar harmonics, especially repeating 20 Hz pattern in black-white and blue-white can be found in subject 5 results, and sporadically in subjects 10 and 11 results. While most of the subjects responded better to the primary colours used in red-white and blue-white flickers, others seem to react better to the secondary colours such as cyan or yellow (subjects 10, 13, and 14).

5.6 BCI Application

To validate the author's results, over the last 3 years, several projects have been carried out. These projects were designed for Level 8 undergraduate students. Most projects investigated the ability to increase the robustness of the SSVEP-based BCI systems through improving the quality of elicited brain signals, which was in line with the main scope of this research. Each year, the author had the opportunity to implement his newly designed flickers in BCI systems and test their functionality. The project detailed below has been completed implementing the 4-command BCI system. The scope of the project was to control a miniature smart home with pre-recorded brain signals achieved through visual stimulation. In an off-line BCI system, such as this one, a great attention can be put to recording brain signals of the highest possible quality. Developing this application project was very valuable for this research giving the opportunity of employing all the parameters established in this work. This was the first practical application aimed at confirming the effectiveness of the proposed flicker parameters. In order to comply with the multi-command requirement, RGB LED panels, each controlled by an Arduino board were used. The system was battery powered. After conducting preliminary frequencies tests with the LED boards within the Alpha range, the frequencies of 6 Hz, 7 Hz, 8 Hz, and 9 Hz have been identified as best performing, and thus used in the project. The colours chosen for the stimuli elements were blue, green, red, and magenta as shown in Figure 5-73.

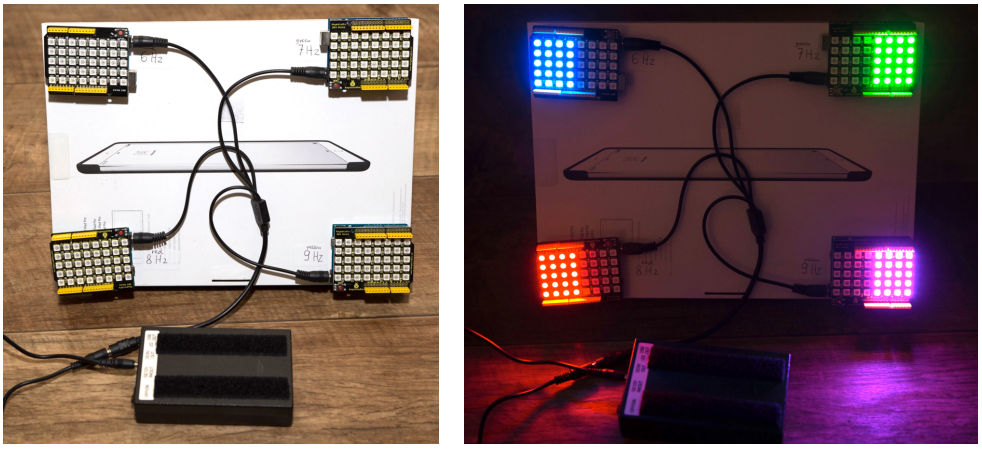

(a) (b)

Figure 5-73 Visual stimulator for the BCI application using RGB 40-LED panels

The stimulator employs four LED panels, each flickering at frequencies of 6 Hz (blue), 7 Hz (green), 8 Hz (red), and 9 Hz (magenta) for a multi-command BCI system controlling miniature smart home: switched off (a) and activated (b).

The most efficient pattern P1 with two flickering rectangles was selected for its abilities to generate clean and strong brain oscillations with minimal artefacts and noise, as detailed in Section 4.3. The resulting elicited brain signals are presented in an FFT plot shown in Figure 5-74, where four distinct signal peaks can be observed.

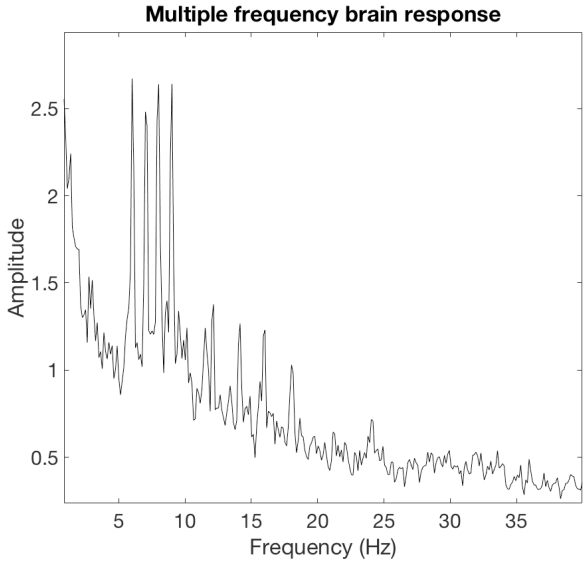

Figure 5-74 Brain signal recording for a four-command BCI system

The captured frequencies can be identified by the visible signal peaks of 6 Hz, 7 Hz, 8 Hz, and 9 Hz.

The off-line recorded signal containing the four frequencies was then used to drive the designed BCI system. The signals were processed in MATLAB using filtering and feature extraction finally to be classified into four separate commands. These commands were used by an Arduino UNO board to control a set of connected devices installed in the miniature smart home as detailed in Figure 5-75. One command was controlling the stepper motor opening the miniature door. Two next two commands were responsible for lighting up LEDs on the first and the second floor of the miniature house. Finally, the last fourth command started the fan on the second floor. A big part of the success in running this BCI can be attributed to the high quality brain signals with minimal noise and artefacts.

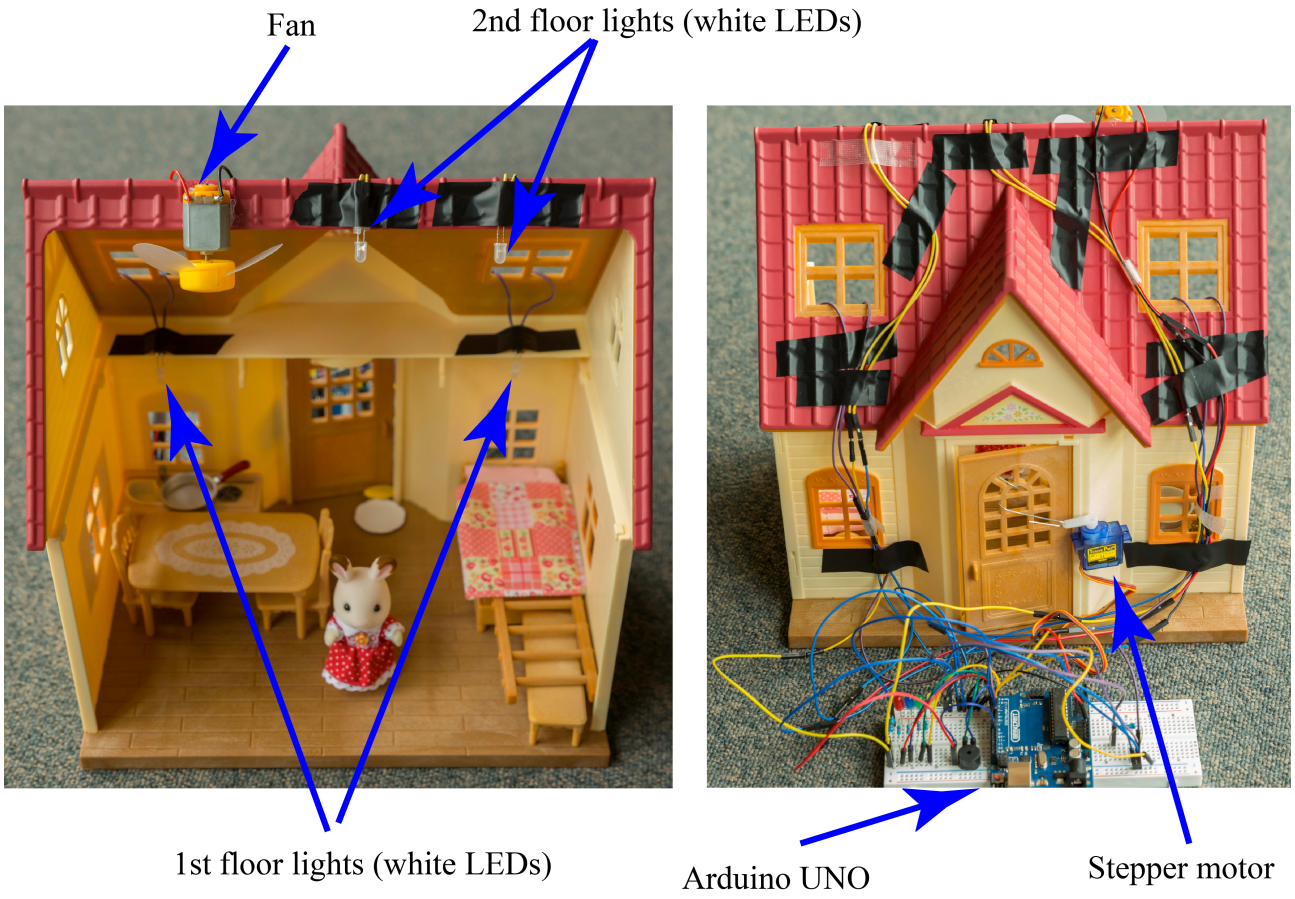

Figure 5-75 Miniature smart home controlled by four-command SSVEP-based offline BCI

Chapter 6 The Element of user Training for SSVEP-based BCI

6.1 Introduction

As already mentioned in Section 3.2.1 a testing scenario engaging multiple subjects was planned and executed. The main purpose of this experiment was to investigate an element of preparatory subject training and how it wll impact the quality of elicited brain signals. The need for this particular experiment became apparent after conducting a number of brain signal recording sessions with subjects without any prior experience in this field. The author, being the first subject undergoing preliminary tests involving brain signals acquisition, using a variety of graphic stimuli elements such as the black and white checkerboard, noticed improvement in the achieved results. This could not have been attributed to the quality of flickers or environmental conditions, which remained constant. A possible explanation suggested that indeed a certain element of subject training could be attributed to the improving results. According to Ballesteros et al. (2018) brain plasticity can be induced by several factors such as physical exercise, cognitive training, video games, and other combined interventions. Brain plasticity is a well-documented phenomenon explaining the brain's ability to adapt to repeated stimulation over prolonged period of time.

In case of the author's elicited brain signals, it has been noticed that the initial tests conducted during early tests did not produce the expected results. The recorded signals when analysed did not demonstrate any visible patterns with peaks matching the flicker's oscillations. An identical pattern was also observed with other undergraduate student subjects supervised by the author during their final year projects development. As will be revealed in this Section, the overall process of generating involuntary brain signals through visual stimulation and possible improvement over time probably depends on the individual abilities and responses of each subject.

For the purpose of this work, the author proposes to define as the "trained" subject/user, a person who has undergone a repeated exposure to the visual stimulation over an extended period of time, preferably over the period of 12 weeks, with at least one 30-minute session per week. A person, who has never experience any visual stimulation through flickers, is considered in this work as an "untrained" subject/user.

6.2 Experiment Setup

For details on the hardware/software used for brain signals recording and testing environment please refer to Chapter 3. For stimuli presentation the iOS 12.9" screen tablet was used as described in Section 3.2.1.3 utilising bespoke MCF application introduced in Section 3.2.3.3 (Szalowski and

Picovici, 2019). As explained in Section 1.2, the 10 Hz frequency has been chosen for all experiments conducted during the research. This frequency is reported to be the most effective in SSVEP stimulation (Regan, 1989). This approach ensures a high degree of results compatibility and comparability. In this experiment, the results of one trained user were compared against results provided by 12 untrained users who had no previous experience with visual stimulation.

The trained user, (subject wearing correcting glasses) was exposed to visual stimulation through the 12.9" tablet placed in a box in a normal office environment in daylight as detailed in Section 3.3.1, Figure 3-55a. In this experiment only black and white checkerboard was used. Three test cases as detailed in Section 6.3, Table 6-1 were carried out. Each test case consisted of 5 trials. Each trial lasted for 10 seconds. Brain signals were recorded and saved as separate EDF files. Short breaks were taken between the trials. All the untrained users followed exactly the same procedure with the exception that only one test case consisting of five trials was carried out per the untrained user (Section 6.3, Table 6-1). The decision for a single test case for the untrained users was made due to the fact that most of the subjects reported tiredness and dizziness after one test case.

As detailed in Section 3.3.2, during the tests conducted, all the subjects were sitting approximately 50 cm from the tablet screen wearing the EEG headset, which streamed digitised signal to the PC computer. The hardware and software was identical to the one detailed in Section 3.2.1.2.

1 flicker x 15 test cases x 5 trials/test case = 75 recordings

Figure 6-1 The total number of recorded signals

For this experiment 15 tests (3 for trained user and 12 for untrained users) resulting in 75 trials altogether were carried out over a period of 8 weeks (please see Figure 6-1 for details). As shown in Section 3.2.1.1, in order to achieve better coverage of the occipital lobe, the EPOC headset was rotated as suggested by Manyakov et al. (2011). Technical details on the headset used, channel selection, and sensor placement can be found in Section 3.2.1.1. All channels were recorded and the signal peaks of interest were found in all 4 channels placed over the occipital lobe. Only channel 1 (AF3) was analysed as explained in Section 5.2.1. The sensor arrangement in the headset is according to the International 10-20 System as detailed in Section 2.5. Only raw, unprocessed brain signals were used in this experiment. From each trial a signal peak plot in the frequency domain was generated. Next, the peak values were entered into spreadsheet software ('Numbers' by Apple) in order to calculate maximum and average values. Finally, based on the achieved statistical data, bar-graph plots were generated for comparison purposes.

6.3 Test Results

This Section presents the test results of the experiments. Individual user's test results are provided, using frequency peak plots that show the highest amplitude achieved from all five trials for each user. Bar graph charts showing achieved amplitude levels for the target 10 Hz peaks in five trials accompany these plots. The choice for the 10 Hz peak analysis is explained in Section 1.2. All the results are arranged on a per user basis starting from the trained user, for the rest of this Section referred to as User 1, followed by all the untrained users, User 2, User 3, User 4, and so forth. Finally, tables with statistics and a bar graph plot present maximum, average, and standard deviation peak levels achieved by all users.

Table 6-1 Test cases conducted in the experiment

Test case	User	Figure
1-3	1	Figure 6-2, Figure 6-3, Figure 6-4
4	2	Figure 6-5
5	3	Figure 6-6
6	4	Figure 6-7
7	5	Figure 6-8
8	6	Figure 6-9
9	7	Figure 6-10
10	8	Figure 6-11
11	9	Figure 6-12
12	10	Figure 6-13
13	11	Figure 6-14
14	12	Figure 6-15
15	13	Figure 6-16

A. Results for trained user – amplitude peaks

Test case 1 – User 1

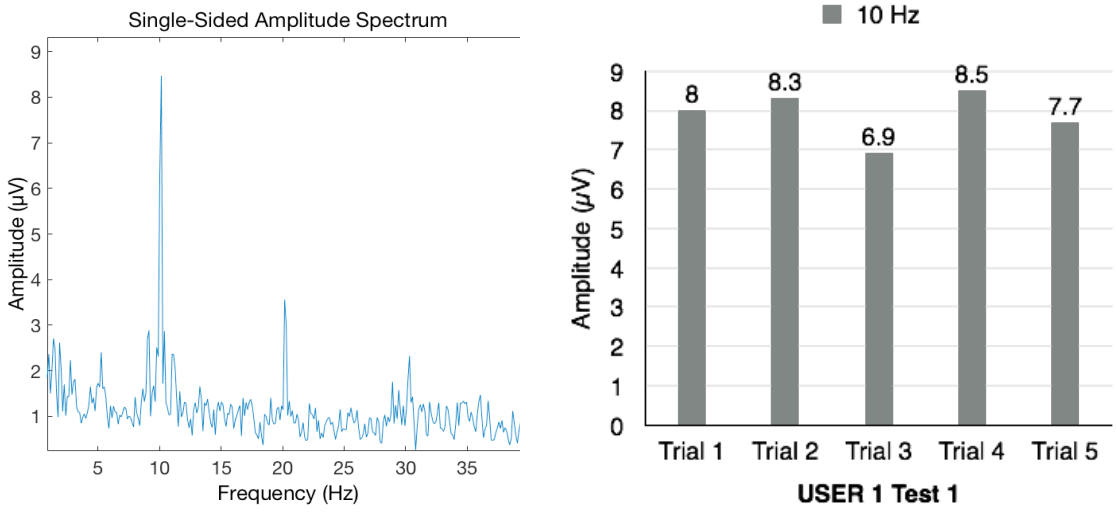

(a) (b)

Figure 6-2 Maximum peak achieved in Test case 1 (a), 10 Hz peaks in all 5 trials (b)

In this test case User 1 generated consistent and good results with minor 20 Hz harmonics. All trials show successful 10 Hz peaks generated in the brain signals.

Test case 2 – User 1

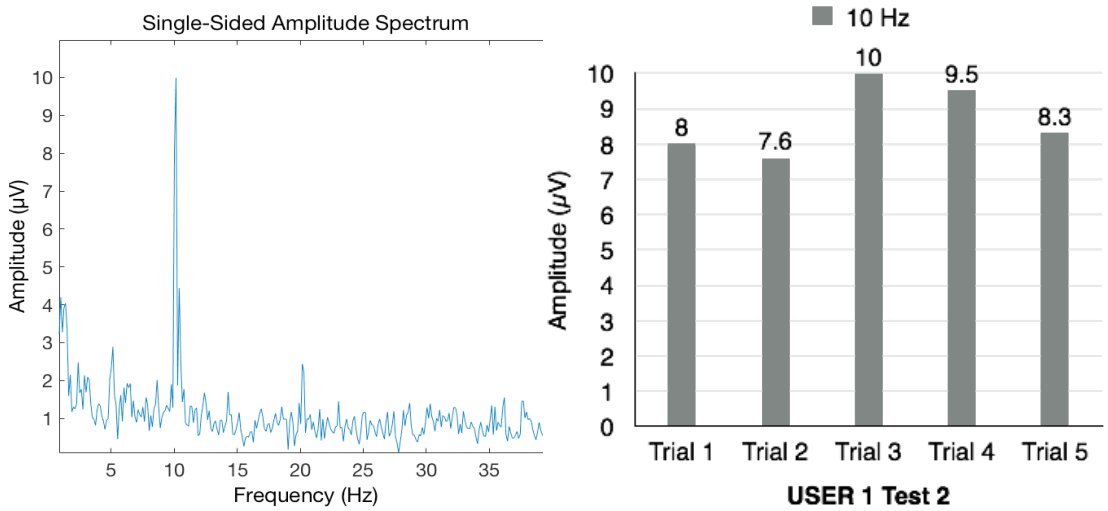

(a) (b)

Figure 6-3 The best maximum 10 Hz peak of User 1 with minimum harmonics (a), 5 successful trials (b)

In this test case User 1 generated the highest amplitude of 10 μV for the target 10 Hz with minimum 20 Hz harmonics. All trials show successful 10 Hz peaks generated in the brain signals.

Test case 3 – User 1

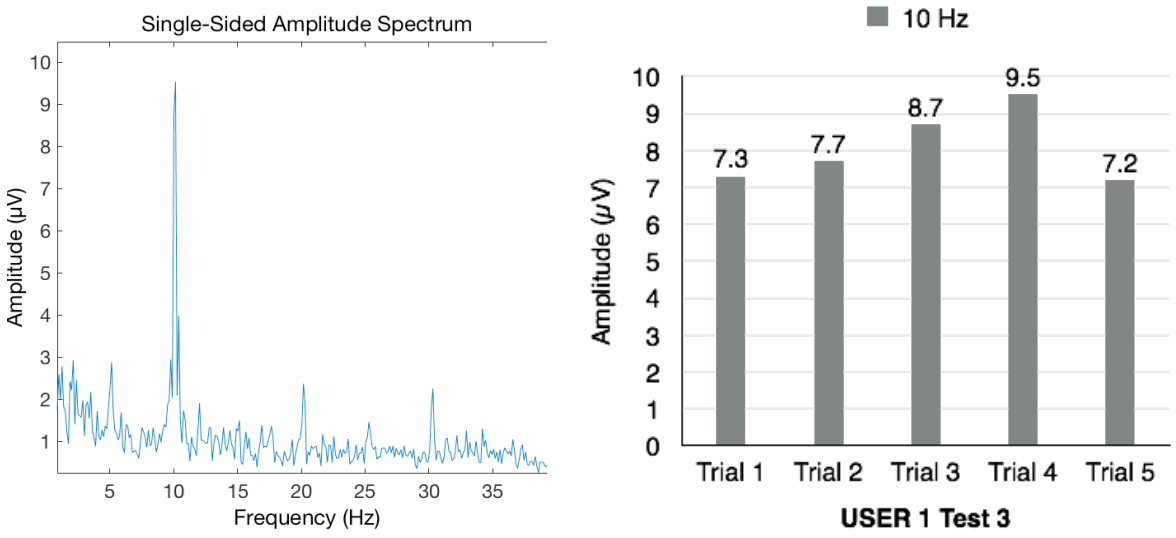

(a) (b)

Figure 6-4 Maximum 10 Hz peak of with harmonics (a), 5 trials with amplitude increasing (b)

Again, very uniform response for the 10 Hz stimulus and successful strong and clean signals in all 5 trials. In test case 3 the second best maximum signals peak of 9.5 μV was generated in trial 4.

B. Results for untrained users – amplitude peaks

Test case 4 – User 2

No 10 Hz peaks found.

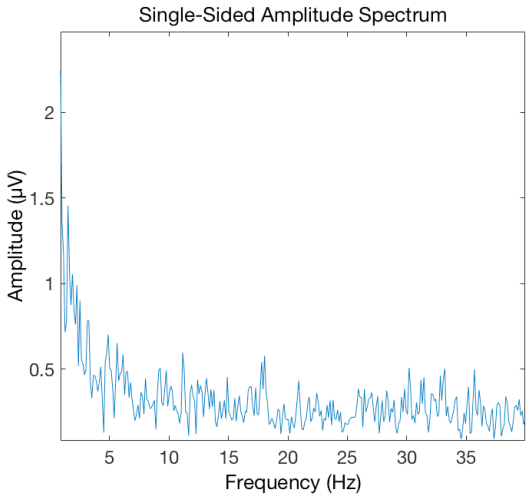

Figure 6-5 No 10 Hz signal peaks were detected in any of the 5 trials recorded from User 2

As shown in Figure 6-5, the User 2 did not produce any 10 Hz peak in elicited brain signals. All results were similar to the sample shown in the figure above with uniform noise across 5 Hz to 40 Hz frequency range without any harmonics present. Below 5 Hz the level of noise is slightly increased.

Test case 5 – User 3

No 10 Hz peaks found.

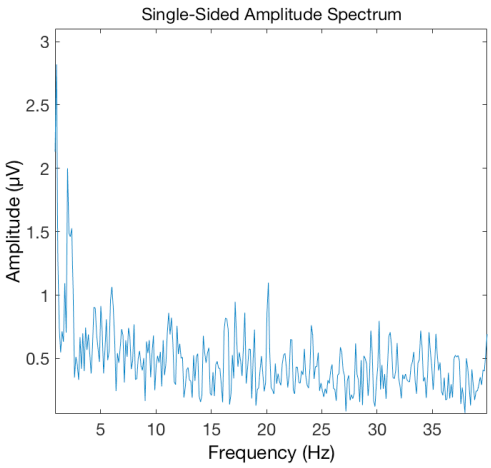

Figure 6-6 No 10 Hz signal peaks were detected in any of the 5 trials recorded from User 3

As shown in Figure 6-6, no 10 Hz peaks were detected in User's 3 test trials. In the example shown, within fairly uniform noise between 5 Hz to 40 Hz, one can observe a slight trace of 20 Hz harmonic and substantial noise level below 5 Hz.

Test case 6 – User 4

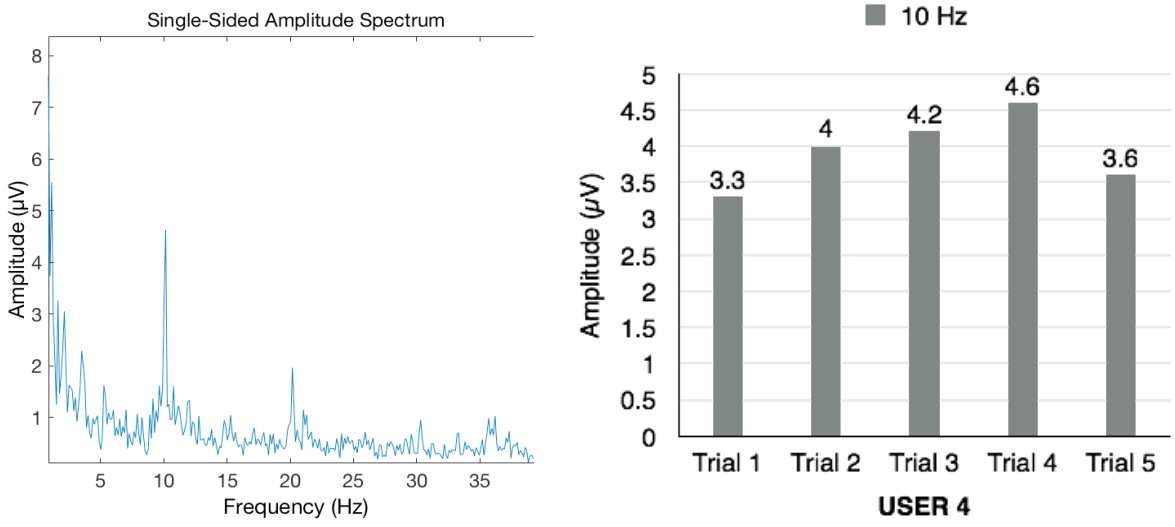

(a) (b)

Figure 6-7 Maximum peak detected in Test case 6 (a), amplitudes of 5 successful 10 Hz peaks (b)

The first successful test case for the User 4 shows a very consistent peak response across all 5 trials with amplitudes gradually increasing with trials (Figure 6-7b). The maximum amplitude level found is 4.6 μV (Figure 6-7a), however this amplitude is noticeably lower when compared to the trained user's results. Also, strong low frequency signal pollution is evident below 5 Hz as well as minor 20 Hz harmonic.

Test case 7 – User 5

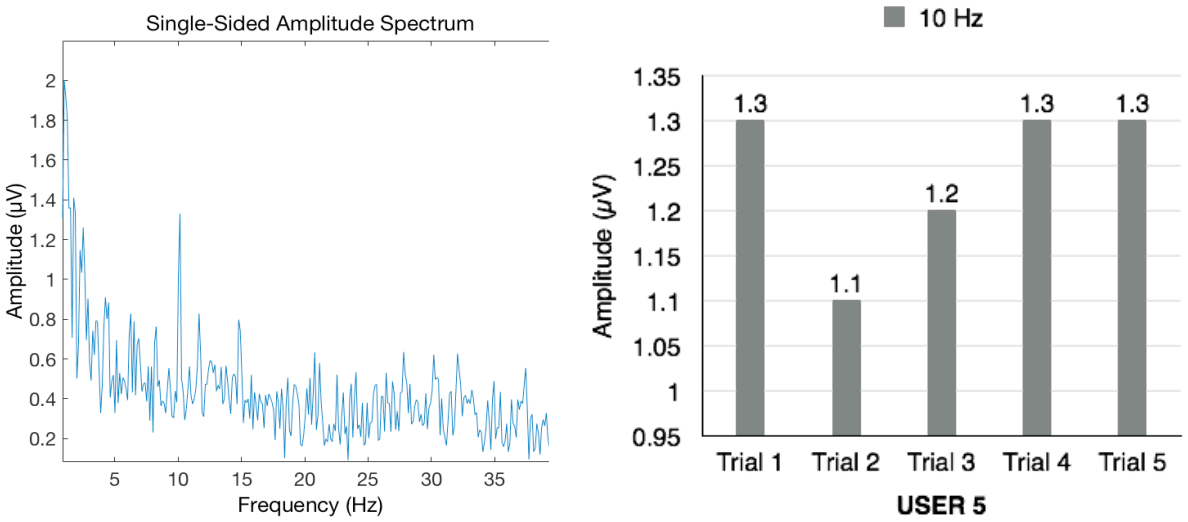

(a) (b)

Figure 6-8 Maximum peak detected in Test case 7 (a), amplitudes of 5 successful 10 Hz peaks (b)

User 5, although having successful 10 Hz peaks in all five trials, exhibits a tendency to generate low frequency noise below 5 Hz that exceeds the amplitude of the targeted 10 Hz peaks (Figure 6-8a). All the peaks are of very low amplitude level between 1.1 μV and 1.3 μV (Figure 6-8b). Figure 6-8a illustrates a representative trial for this user frequency response with the highest 10 Hz peak of 1.3 μV.

Test case 8 – User 6

No 10 Hz peaks found.

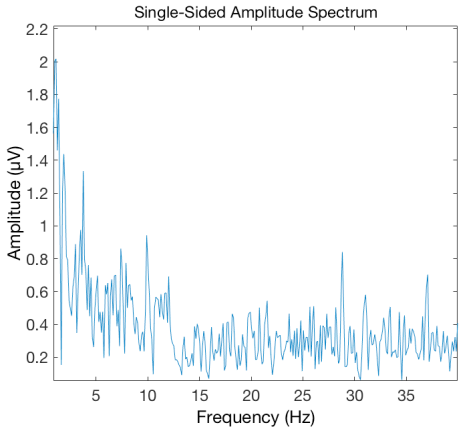

Figure 6-9 No 10 Hz signal peaks were detected in any of the 5 trials recorded from User 6

User 6 did not produce any 10 Hz peaks in elicited brain signals. In the example shown as Figure 6-9 less uniform noise is present across 5 Hz to 40 Hz frequency range with visible spikes, which

cannot be attributed to any of the expected peaks at harmonic frequencies. Below 5 Hz, the level of noise is relatively high compared to the rest of the noise.

Test case 9 – User 7

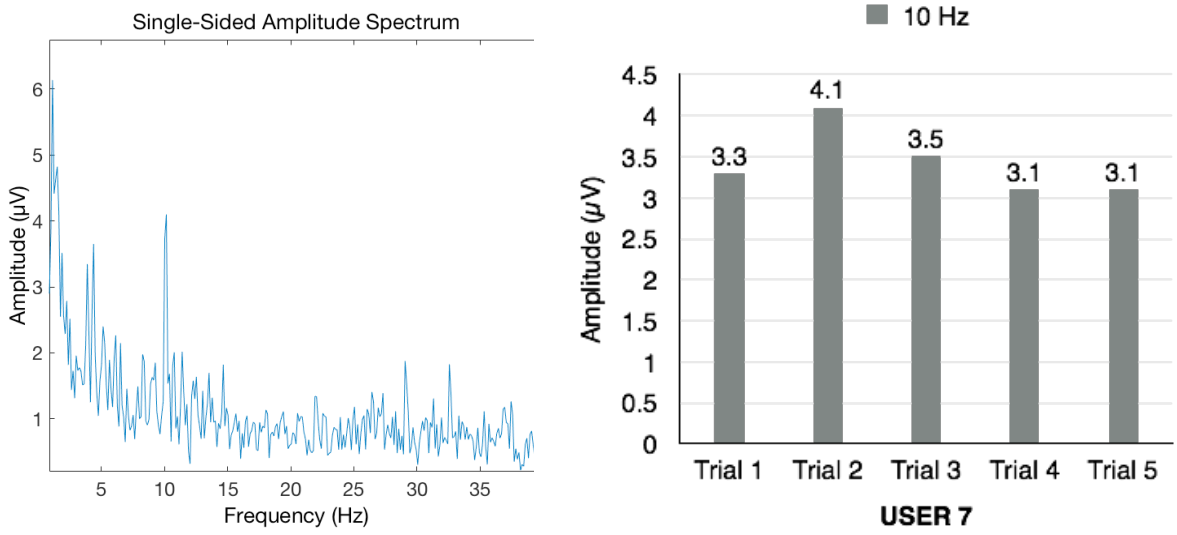

(a) (b)

Figure 6-10 Maximum peak detected in Test case 9 (a), uniform peak response in 5 successful trials (b)

In test case 9 the User 7 generated reasonably useable brain signal peaks at 10 Hz in all 5 successful trials (Figure 6-10b). However, low frequency noise is apparent as seen in previous untrained user tests (Figure 6-10a).

Test case 10 – User 8

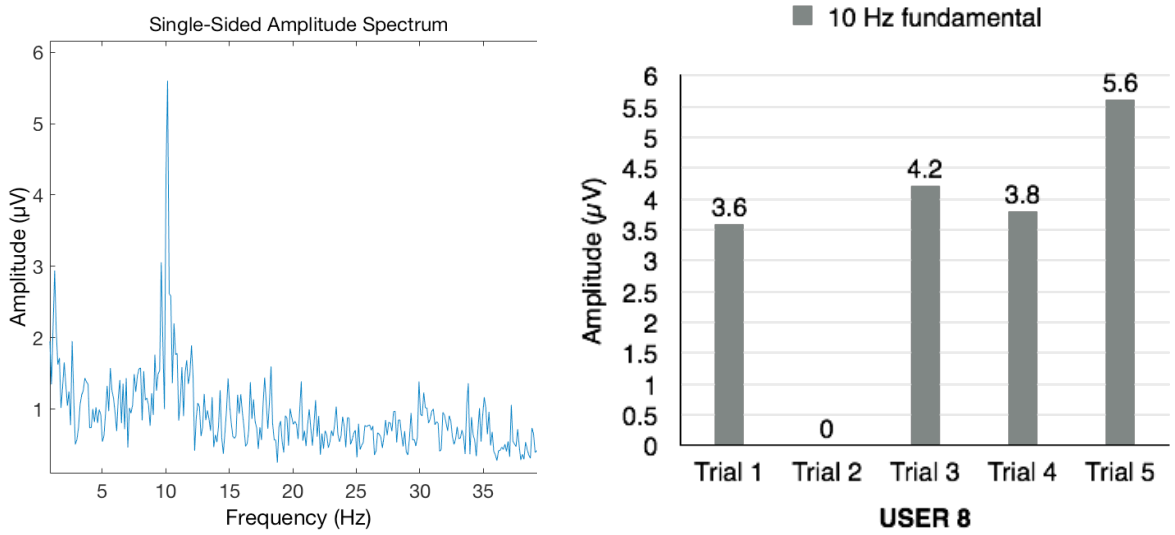

(a) (b)

Figure 6-11 Maximum peak detected in Test case 10 (a), uniform peak response in 5 successful trials (b)

User 8 shows good response with one high amplitude peak registered at 5.6 μV and good average results. Within five trials conducted, one trial was unsuccessful as shown in Figure 6-11b. Figure

6-11a illustrates the best signal response elicited by the user with reasonably low noise and no harmonics. The artefacts usually present below 5 Hz are of reasonably low amplitude.

Test case 11 – User 9

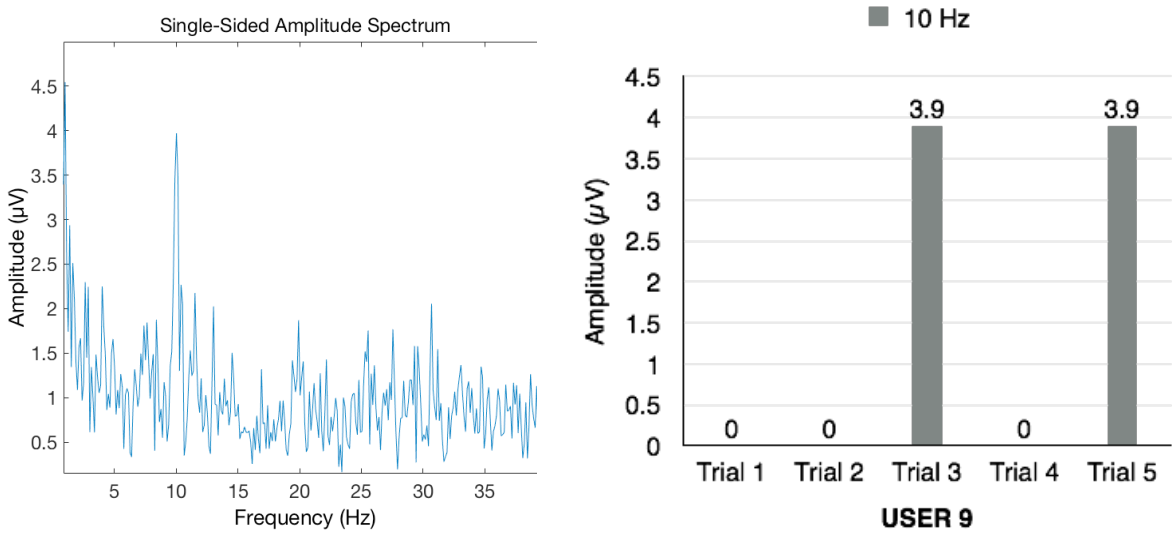

(a) (b)

Figure 6-12 Maximum peak detected in Test case 11 (a), sporadic peak response in 2 trials only (b)

User 9 produced peak levels with amplitude of 3.9 μV in 2 instances, while the remaining 3 trials were unsuccessful (Figure 6-12b). As shown in Figure 6-12a, the level of noise is quite high in comparison to achieved 10 Hz peak.

Test case 12 – User 10

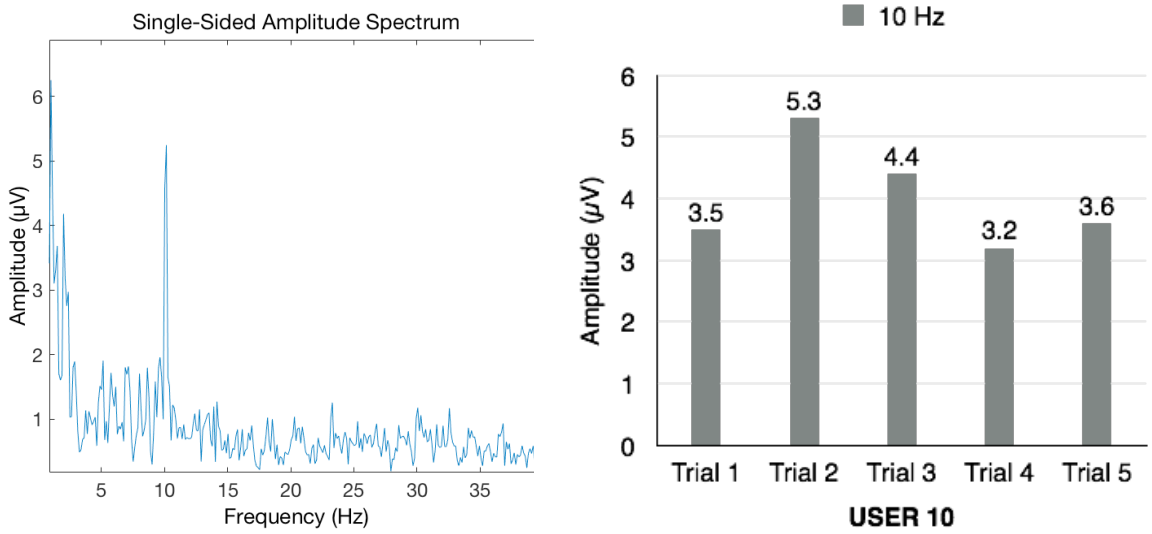

(a) (b)

Figure 6-13 Maximum peak detected in Test case 12 (a), 10 Hz peaks in all 5 trials (b)

As presented in Figure 6-13b, in test case 12, User 10 generated 5 successful 10 Hz peaks with maximum amplitude reaching 5.3 μV. The plot with the highest 10 Hz peak amplitude also reveals

reasonably low broadband noise. However, the low frequency artefacts below 5 Hz are very high (Figure 6-14a).

Test case 13 – User 11

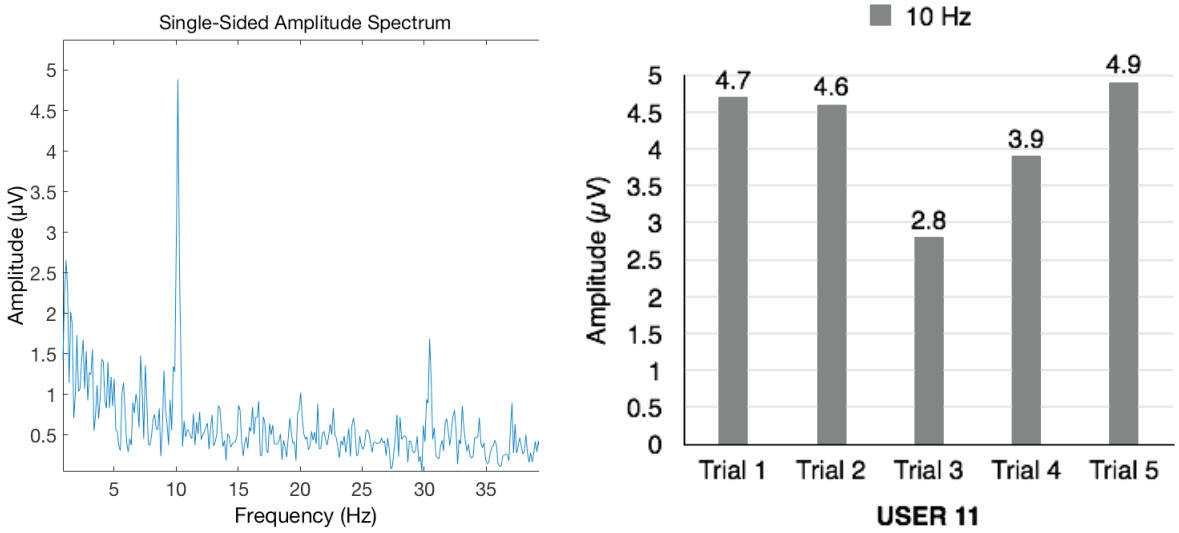

(a) (b)

Figure 6-14 Maximum peak detected in Test case 13 (a), 10 Hz peaks in all 5 trials (b)

User 11 generated very good signal peaks with the highest amplitude of 4.9 μV as shown in frequency domain plot with very little noise and slight traces of 30 Hz harmonics (Figure 6-14a). Three trials display amplitude levels above 4.6 μV, which promises very good statistical average result (Figure 6-14b).

Test case 14 – User 12

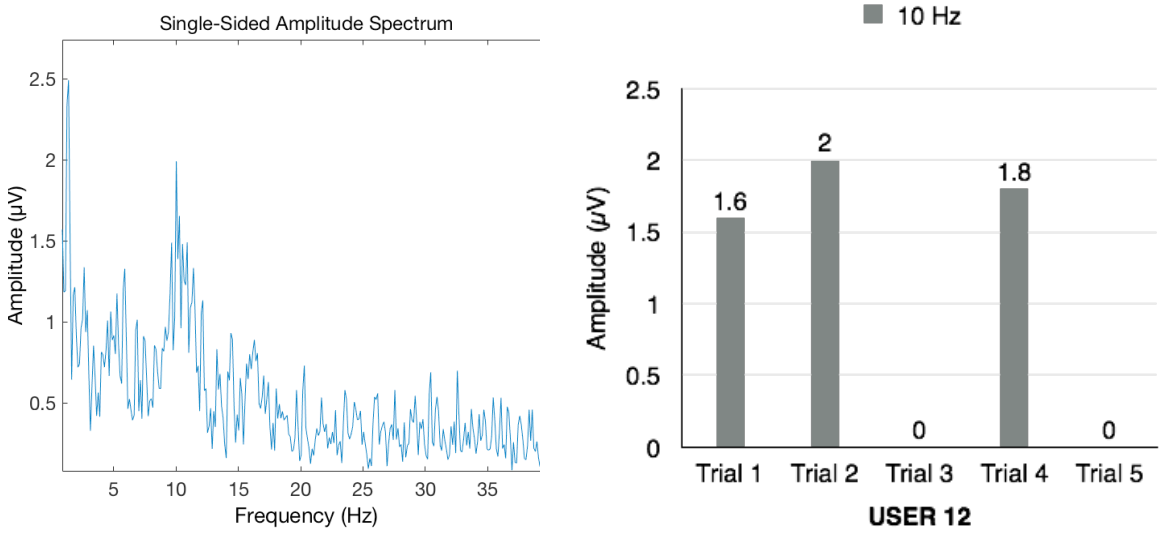

(a) (b)

Figure 6-15 Maximum peak detected in Test case 14 (a), 10 Hz peaks in 5 trials (b)

In test case 14 only 3 trials were successful with the visible 10 Hz peaks exposing very low amplitude levels between 1.6 µV and 2 µV (Figure 6-15b). The highest registered 10 Hz peak shown in Figure 6-15a is very contaminated by noise surrounding the fundamental frequency. This is manifested by a widened signal peak, which characterises poor response in the brain.

Test case 15 – User 13

No 10 Hz peaks found.

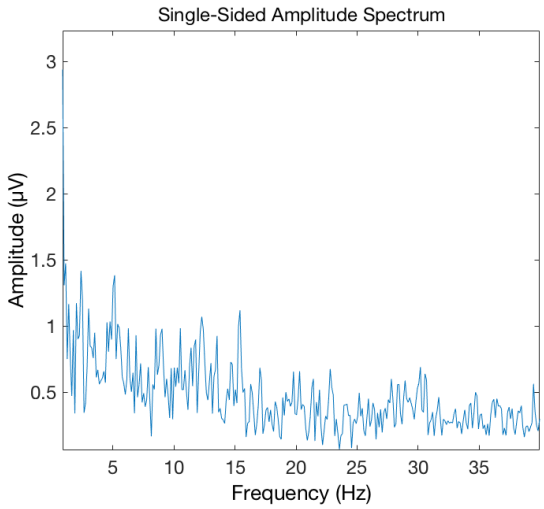

Figure 6-16 No 10 Hz signal peaks were detected in any of the 5 trials recorded from User 13

C. Results comparison for all users

In this plot, the achieved results for all participating users are shown. The bar graph results representing maximum and average results for all successful users are combined for overview and comparison purposes. The two arrows on the right-hand side of the plot indicate the two groups of results; trained and untrained respectively.

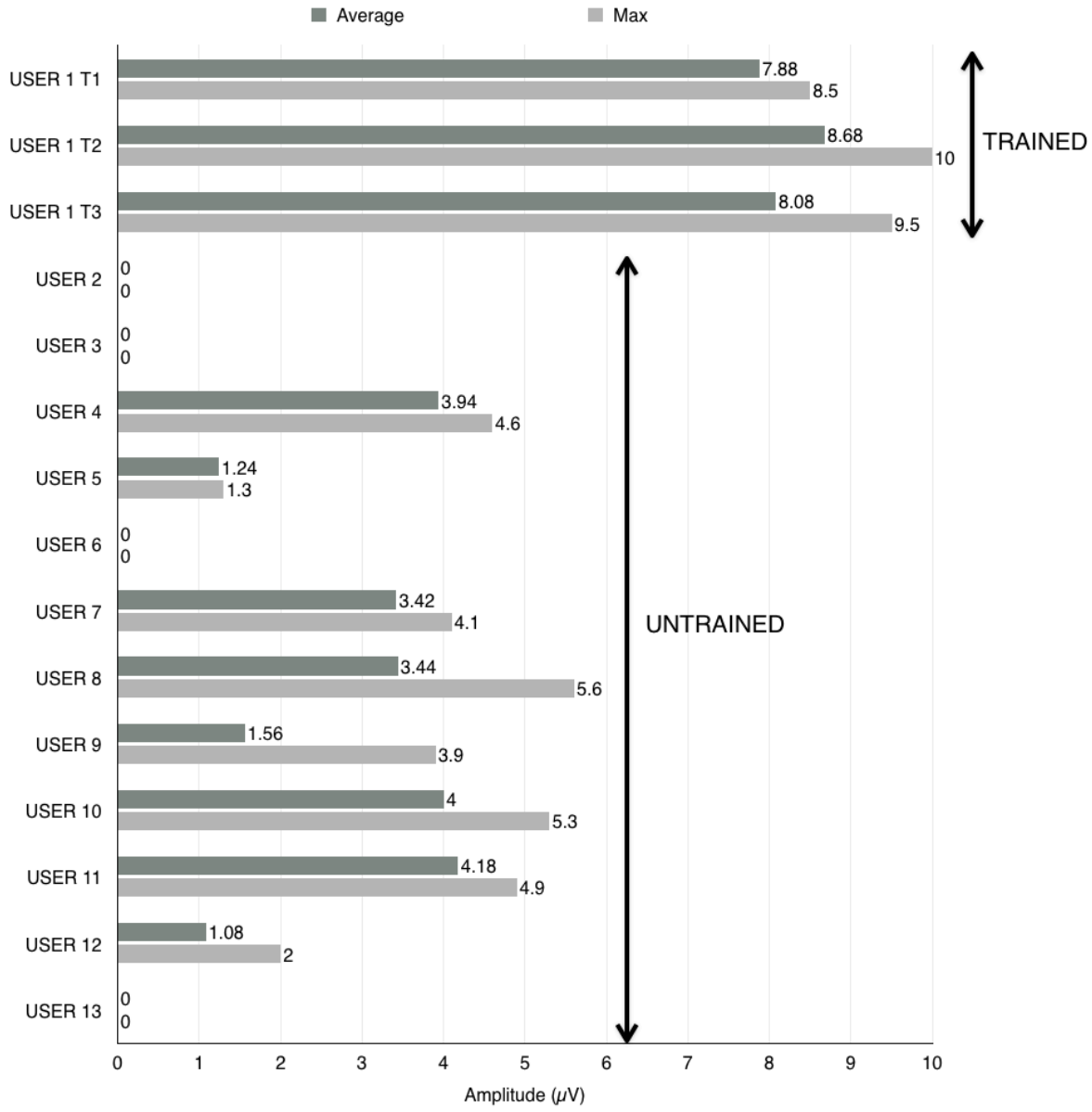

Figure 6-17 Maximum and average values from 5 trials

In this graph, Test case 1, Test case 2, and Test case 3 are marked as T1, T2, and T3 respectively for convenience.

6.4 Experiment Discussion and Observations

The main purpose of this Section is to investigate the importance of user training for SSVEP-based BCI systems. In the majority of literature the SSVEP technique is often described as the one that does not require training and the brain signals it elicits are characterised as involuntary. The majority of the subjects did produce involuntary brain signals of 10 Hz as a result of visual stimulation through black and white checkerboards as expected. However, by viewing the comparison plot (Figure 6-17), there is a discernible difference that can be observed among the achieved results. These differences are detailed in the observations below.

Table 6-2 represents statistics related to all 3 test cases for the trained User 1, while Table 6-3 shows only successful test cases for the untrained users. High standard deviation values in Test cases 10 and 11 are due to unsuccessful trials.

Table 6-2 Trained user statistics

Test case	User number	Max amplitude in μV	Average amplitude in μV	Standard deviation amplitude in μV
1	1	8.5	7.88	0.63
2	1	10	8.68	1.02
3	1	9.5	8.08	0.99
Averaged	→	9.33	8.21	0.88

Table 6-3 Untrained users statistics

Test case	User number	Max amplitude in μV	Average amplitude in μV	Standard deviation amplitude in μV
6	4	4.6	3.94	0.51
7	5	1.3	1.24	0.09
9	7	4.1	3.42	0.41
10	8	5.6	3.44	2.08
11	9	3.9	1.56	2.14
12	10	5.3	4	0.85
13	11	4.9	4.18	0.86
14	12	2	1.08	1
Averaged	→	3.96	2.86	0.99

- Observation #1

User 1, who had previous experience with visual stimulation and for this experiment was considered as a trained user, was able to repeat very similar results in terms of achieved maximum and average 10 Hz peaks in three separately conducted tests, each consisting of five individual trials. The maximum-recorded signal peaks were 8.5 μV, 9.5 μV, and 10 μV, while the average calculated from five trials captured in each test were in the range from 7.88 μV to 8.68 μV as shown in Figure 6-17. Standard deviation was calculated at very low levels; especially in test 1 at 0.63 μV. Test 2 and test 3 show 1.02 μV and 0.99 μV respectively (Table 6). The average value for standard deviation was calculated at 0.88 μV, which suggest very consistent results for this user.

- Observation #2

Four untrained users did not produce any visible 10 Hz signal peaks in any of their trials recorded. These users are User 2, User 3, User 6, and User 13 constituting 33.3% of the untrained participants as detailed in Figure 6-17.

- Observation #3

Among the remaining untrained eight users who successfully produced 10 Hz peaks in their brain signals, User 5 and User 12 achieved the lowest amplitude readings as shown in Figure 6-17. When inspecting their results in detail (Figure 6-8 and Figure 6-15), one will notice that their 10 Hz signal peaks are very low and should be considered as rather unusable for BCI operations due to very low signal-to-noise ratio. Extracting such features would require elaborate and intricate signal processing.

- Observation #4

User 9 produced useable 10 Hz peaks in two trials out of five conducted, as shown in Figure 6-12b. In these successful trials the peaks registered amplitude of 3.9 μV, twice as big as the visible noise. Such signals could be extracted and used in BCI using most of the popular feature extraction algorithms. However, a 40% success rate should not be considered as an optimistic scenario for BCI design.

- Observation #5

Five untrained users (Figure 6-17), constituting a 41.7% success rate, produced satisfactory results with 10 Hz peaks visibly extending above the noise floor, making them useable and relatively easy to extract. User 11 generated very consistent signals with clean 10 Hz peaks (Figure 6-14b), reasonably low standard deviation of 0.86 μV (Table 6-3), and the highest average peak result of

4.18 μV (Figure 6-17), which together with the achieved maximum of 4.9 μV produced a very good result. Even better consistency with standard deviation as low as 0.51 μV was achieved by User 4 (Figure 6-7 and Figure 6-17) with only slightly weaker signal peak readouts of 3.94 μV for average and 4.6 μV for maximum (Figure 6-17 and Table 6-3). Consistent results are also reported for User 7 (Figure 6-17) with very low standard deviation of 0.41 μV (Table 6-3). However, quite strong noise contamination can be observed for this user, especially in the low frequency range below 5 Hz as shown in Figure 6-10. For a successful BCI application, a significant signal filtration set at 5 Hz boundary would have to be applied. For User 10, although slightly less consistent with standard deviation at 0.85 μV, very useable signal peaks can be observed with very high average result of 4 μV and maximum result of 5.3 μV (Figure 6-17), making it the second best maximum result among the untrained users. User 8 generated the highest maximum peak among the untrained users of 5.6 μV and quite high average results of 3.44 μV (Figure 6-17). However, with one unsuccessful trial (Figure 6-11b), this lowered the standard deviation score to 2.08 μV.

- Observation #6

When averaging the maximum and average results achieved by the trained User 1 (Table 6-2) and all the successful untrained eight users (Table 6-3), one can observe that the trained user generated much higher 10 Hz amplitudes. When comparing averaged maximum results, the untrained users generated signals with amplitudes, which are weaker by 57% compared to the trained user. However, when comparing averaged average results, the untrained users generated significantly weaker amplitudes by 65%.

- Observation #7

By comparing the averaged standard deviation statistics between the trained user's three test cases and all the successful untrained users' test cases, certain degree of similarity can be observed. The trained user averaged at 0.88 μV, which is well below the value of 1, while the successful untrained users' averaged result is calculated at 0.99 μV, still fitting the 'less than 1' rule (Table 6-2 and Table 6-3). This suggests that once the user's brain is capable of inducing the stimulated signals, it is rather consistent and stable. The big difference between the trained and untrained user's results lies in the amplitude levels.

6.5 Summary

To summarise the results, it can be stated that a substantial number of the untrained users, i.e. 33.3%, were completely unsuccessful in generating useable brain signals through visual black and white checkerboard stimulation. Two users generated very weak signals, which probably in real live

scenario would not guarantee sufficient results. Additionally, one user generated reasonably good signals in only two trials out of five, which rather eliminates the user as a successful system operator. That means that according to tests conducted for this research, only five, i.e. 41.6% of the untrained users could operate a visually driven BCI without any prior training. The results achieved by the untrained users are rather disappointing and it is hard to predict what the main factor was that limited their ability to generate consistent and repeatable good signals. This phenomenon should be further investigated in order to determine whether poor performance of the untrained users could be attributed to inappropriate mindset, insufficient focus or lack of experience. Based on the presented results the author does not declare holding the undisputed proof that definitely, as a consequence of experimental exposure to visual stimulation, the user's brain undergoes a certain process of training that augments the brain's ability to repeat positive response to such stimulation. It is also unclear, whether such abilities if indeed gained, remain inherited within the trained user's brain. However, based on the presented herewith trained user's results, demonstrating a very high degree of elicited brain signal repeatability and elevated amplitude levels when compared to the untrained users, it can be suggested that user exposure to visual stimulation improves the brain's response, thus positively influencing the overall performance of SSVEP-based BCI systems. In this test variables such as gender or age have not been accounted for. The tests were organised on different days approximately in similar lighting and environmental noise conditions.

Chapter 7 Conclusions

7.1 Introduction

In this thesis a comprehensive assembly of experiments have been carried out in order to determine a set of parameters describing the most effective and practical visual stimuli graphics for the SSVEP-based Brain-Computer Interface system. As it has been thoroughly expressed in Section 1.1, the main motivation and rational of this research was to exhaust as many parameters as possible for the stimuli graphics in order to arrive at settings potentially providing the best response in the brain. After reviewing over three hundred BCI related papers it became apparent that the stimuli graphics, although commonly agreed among the BCI research community as important and sometimes even crucial for a successful BCI operations, lacks in research. The most often used and popular are different revisions of black and white checkerboards as illustrated in Figure 7-1 (Zhu et al., 2010).

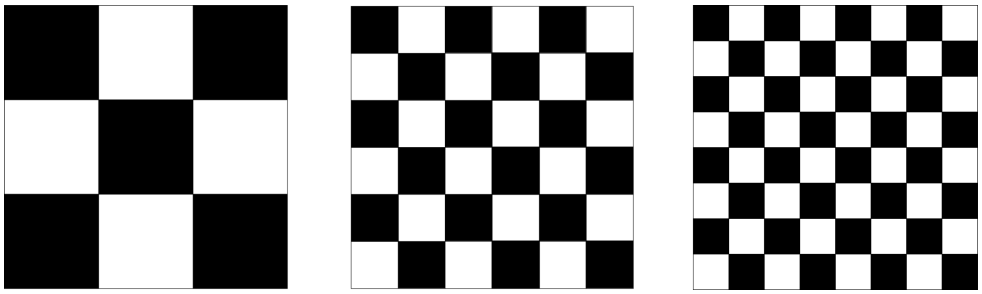

(a) (b) (c)

Figure 7-1 Revisions of black and white checkerboards

Three examples of black and white checkerboard flickers often used in SSVEP related BCI systems. These versions differ in the number and concentration of checkers: (a) 9 checkers, (b) 36 checkers, and (c) 64 checkers.

For the experiments utilising graphic checkerboards, the version with 64 checkers as shown above was used in this research. Based on the correlation recognised by the author, between the human retina and the digital screens, which was thoroughly explained through Sections 1.2 to 1.6, it was decided to implement colours into checkerboard flickers with the expectation to improve the quality of elicited brain signals. The research exploring colour application in BCI and specifically in SSVEP-based systems is minimal. As reviewed in Section 1.8, the existing and exemplified publications are rather isolated and limited in their scope. The main motivation for this research work was to propose a thorough and comprehensive methodology utilising unique and never explored before flicker design approaches using variety of techniques including software and

hardware solutions. In doing so, the proposed methodology was designed such that many parameters were included in the testing scenarios.

In order to provide a unified platform for other researchers potentially interested in continuing similar experiments, the colours, and other desaturated tones such as white, 50% grey, and black used in this thesis are derived from the commonly known RGB additive colour science; namely red, green, blue, as the primary colours; and yellow, cyan, and magenta, as the secondary colours. Additionally, white, 50% grey, and black were included in some of the tests. The choice of colours has been explained in Section 1.6 and exemplified in Figure 7-2.

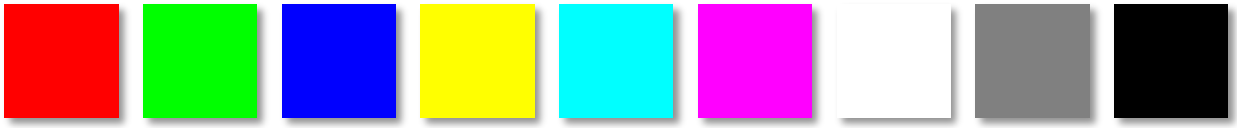

Figure 7-2 The set of RGB primary, secondary colours, and greyscale tones used

The RGB colours and greyscale tones used are: red, green, blue, yellow, cyan, magenta, white, 50% grey, and black.

Through a series of preliminary tests and the achieved early results, other parameters were also considered as potentially influential, and thus included in this research. Among the included additional parameters are flicker size/resolution, various flicker patterns and different types of background for the stimuli presentation.

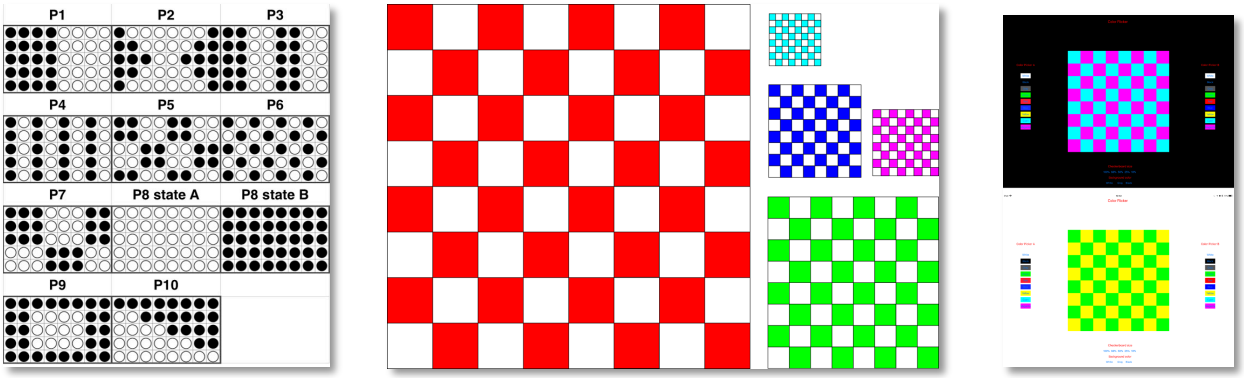

(a) (b) (c)

Figure 7-3 Examples of the parameters investigated during the research

Beside RGB colours as detailed in Figure 7-2, other parameters determining the appearance of stimuli flickers were tested including: patterns (a), size/resolution (b), and backgrounds (c).

Furthermore, as a result of repeated brain signal recording tests performed by the author over an extended period of time, an improvement, mainly visible in targeted 10 Hz peaks, has been perceived in the captured brain signals. This observation paves the path for extensive multi-subject

experiments investigating the difference in the captured brain signals, between trained and untrained subjects.

These final conclusions constitute the author's proposal establishing a set of parameters aiming at generating effective and functional flickering graphics for robust SSVEP-based BCI systems. From the achieved results and detailed in Chapter 4, Chapter 5, and Chapter 6 the following list of conclusions can be assembled.

A. The Element of Training

The element of subject training is important in achieving strong and repetitive brain signal responses elicited through visual stimulation using flickering graphics. Such training should include instructions given to the trainee subject about body and muscle relaxation, taking sufficient breaks between the recording trials, attentive observation of the presentation screen and focusing vision in the centre of the stimulus. The author believes that sufficient exposure of the trainee subject to the flickering graphics over a prolonged period of time, allows the subject to gain experience and adeptness, thus gradually improves the quality of elicited brain signals as it has been evidenced by the results generated by subject 1 through numerous repeated tests (Section 6.4).

B. The Flickering Pattern

The flickering pattern greatly impacts the quality of elicited brain signals, especially in terms of unwanted artefacts such as harmonic content, as evidenced in Sections 4.3, 4.4, and 4.5. The flicker pattern P8 (as detailed in Figure 7-4) with a single flickering element is not recommended. It repeatedly generated the most distorted brain signals with a very high harmonic pollution in multiple frequencies (Figure 7-5).

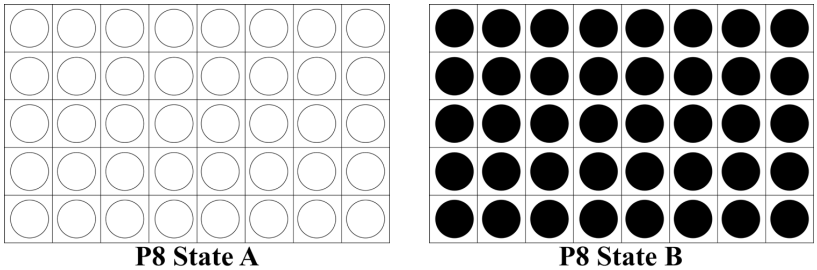

Figure 7-4 Flicker pattern P8 with single flickering element

This pattern is composed of two states alternating, state A and state B, i.e. all LEDs light on and off. Thus, the entire surface of the panel constitutes the flickering element.

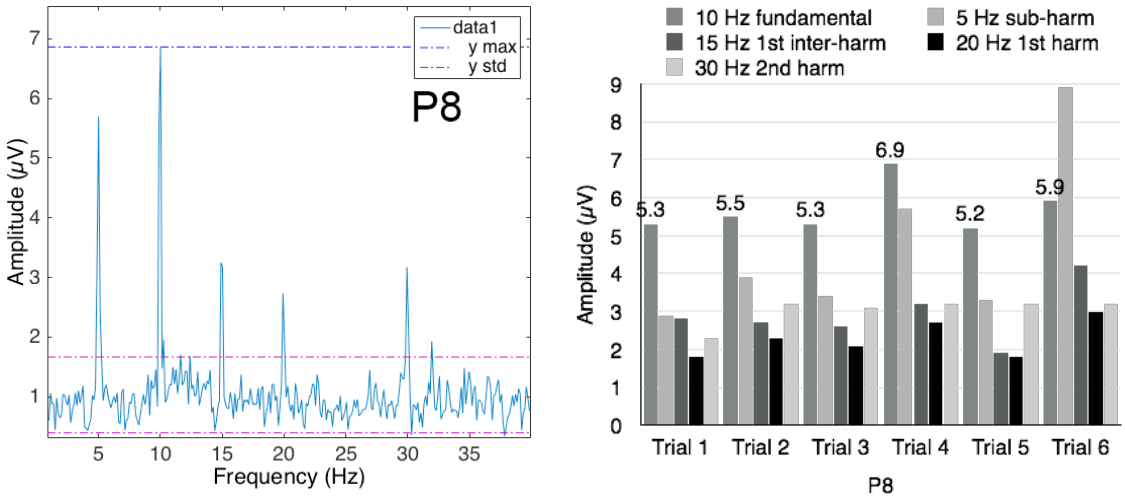

(a) (b)

Figure 7-5 Results for the flicker pattern P8

The amplitude (a) plot reveals multiple harmonics accompanying the elicited 10 Hz fundamental which is further reiterated by (b) showing similar response in all trials.

The patterns, which generated the best results consisted of 2-3 flickering elements as illustrated in Figure 7-6.

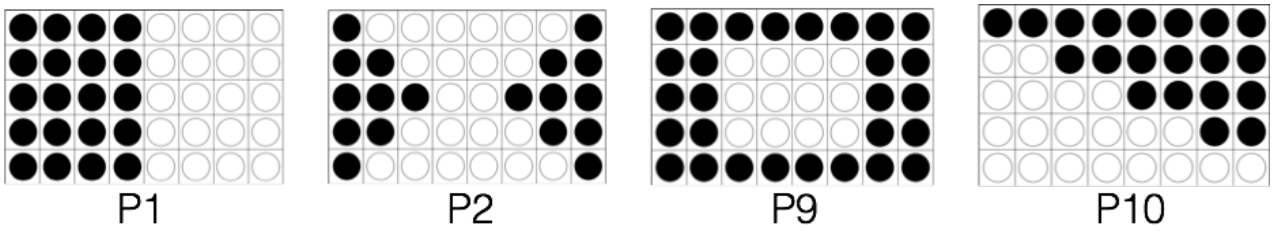

Figure 7-6 The patterns which generated the best brain signals

The flickering patterns P1, P2, P9, and P10 repeatedly generated the strongest and free of harmonics brain signals.

Since the rectangular and triangular shapes produced equally strong results, they are both recommended. Although these patterns were generated using an LED panel, they could be replicated and rendered as computer graphics.

C. The flicker size/resolution

The flicker size/resolution is another parameter influencing the quality of elicited brain signals. From the test results reported in Sections 5.2.2 and 5.2.3, it is evident that the recommended medium sized graphics, in the test referred to as 50%, provided the best results as illustrated in Figure 7-7. For the screen to graphic size ratio please refer to Figure 7-8.

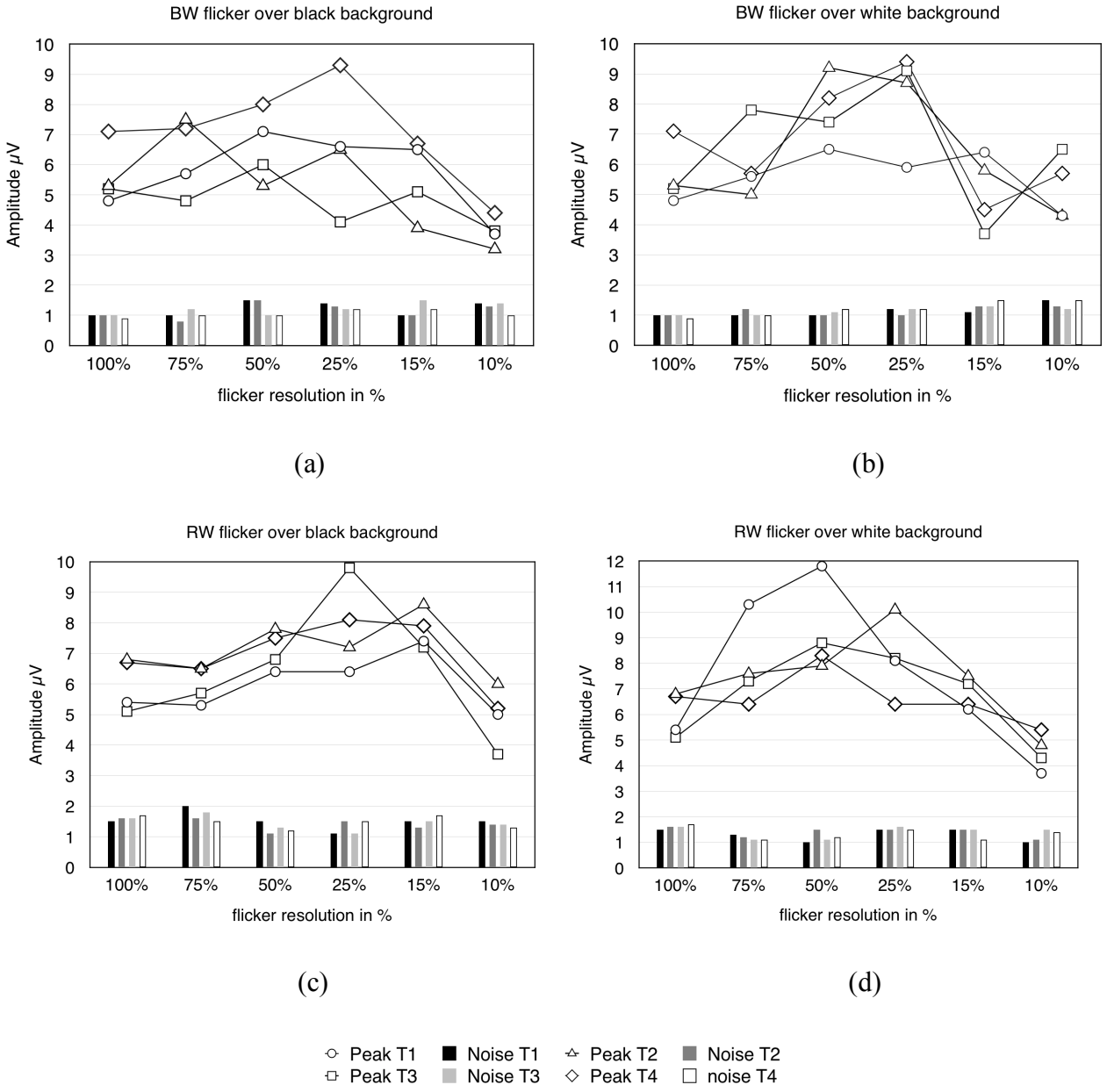

Figure 7-7 Flicker size/resolution results in four trials

The flickers with 50% size exhibit the best performance showing the highest peak values followed by 75% and 25% flickers the plot lines represent peaks and bars represent noise. The plots (a) and (b) are for black-white checkerboard, while (c) and (d) for red-white.

Acceptable results can be observed for the 75% and 25% flicker sizes, which are also recommended. Interestingly, the largest flicker of 100% did not produce the best results and should

be used with caution. The 15% flicker, although very small when presented of the screen, produced surprisingly good results considering the flicker to screen size/resolution ratio.

It should be noted that these types of results must be viewed in relation to the overall flicker presentation screen size in conjunction with the subject's distance from the screen. In this experiment the subject's distance was 50 cm from the 12.9" tablet screen.

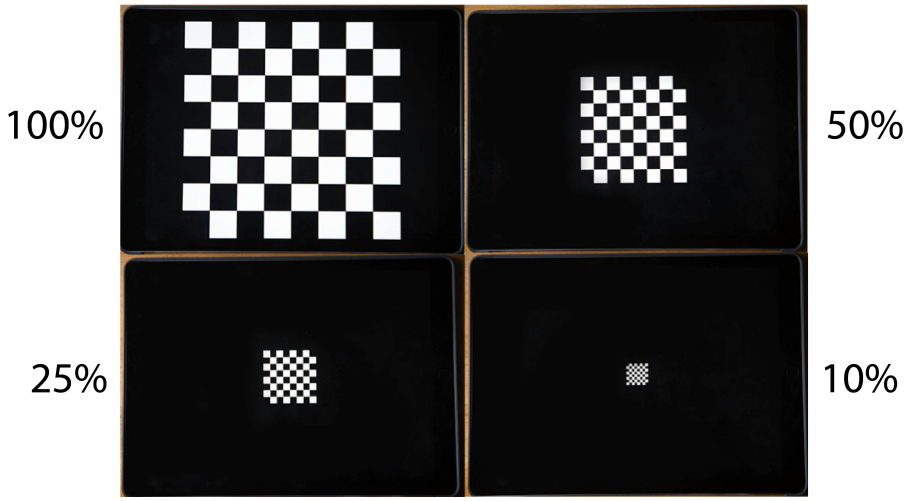

Figure 7-8 The checkerboard patterns in various sizes/resolutions

The 12.9" tablet screen shows 100%, 50%, 25%, and 10% flickers giving an idea about the screen to flicker size ratio.

Although the medium sized graphics worked best, very promising are the results reported for the smallest sizes of 15% and 10%, which generated reasonably useable brain signals.

D. Bright vs Dark Background

It was also decided to experiment with bright (white) and dark (black) backgrounds for stimuli presentation with the intention to discover, whether this variable can alter the brain's response, thus offering any benefits to the elicited brain signals. From the achieved results reported in Sections 5.2.2 and 5.2.3, very slight signal improvement can be observed with the bright (white) background for both the reference black-white flicker and its colour counterpart, the red-white version (Figure 7-9).

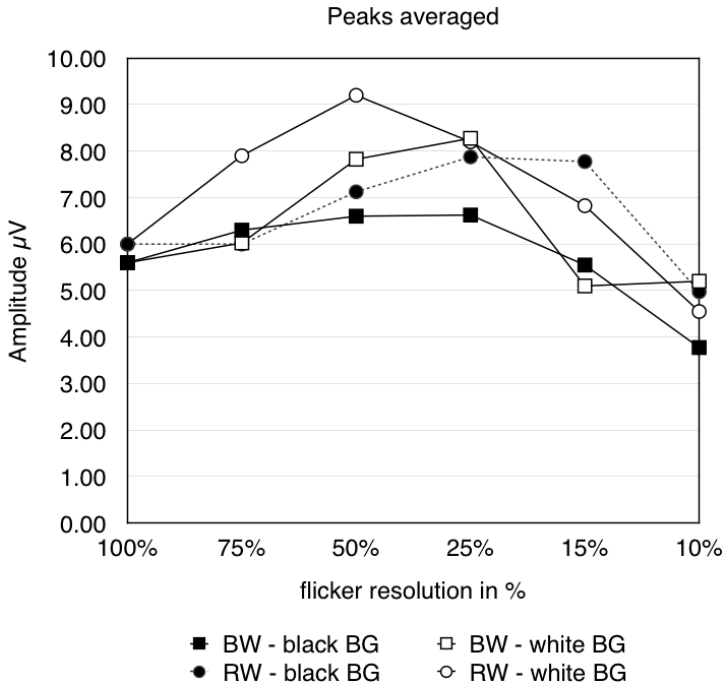

Figure 7-9 The checkerboard patterns in various sizes/resolutions

The results for white background are marked with white circles and squares.

E. Colour vs Black-White for Stimuli Flickers

Throughout this work, various experiment scenarios have been reported aiming at measuring the impact of colour on the brain signals. All the colour and multi-colour flickers were tested against black-white reference stimulus or greyscale counterparts. Depending on testing scenario, one trained subject and multiple untrained subjects were tested.

F. Black-White vs Red-White

The first colour testing experiment scenario used black-white (BW) and red-white (RW) checkerboard flickers as detailed in Section 5.2. From the results a very small amplitude increase could be observed for the RW flicker when compared to the BW reference as illustrated in Figure 7-9. The RW flicker results are shown as the rounded points on the plot, while the BW reference as the square points.

G. Multi-Colour vs Greyscale

From the very extensive multi-colour flicker testing against the greyscale versions the main conclusion suggests that the colour and multi-colour flickers offered significant signal quality improvement demonstrated by the average amplitude increase by 56% (Section 5.4.2). When averaging the maximum results, the quality increase has been calculated at 34% in favour of colour. The comparison of the six best performing flickers for both colour and greyscale are shown in

Figure 7-10. These results give a general suggestion that the use of colour in stimuli flickers is preferable and beneficial for the resulting brain signals.

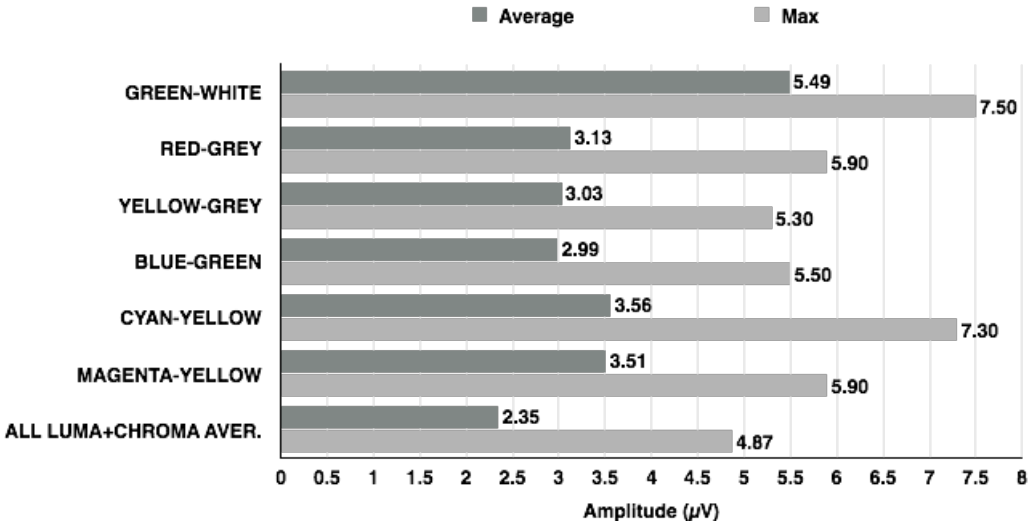

(a)

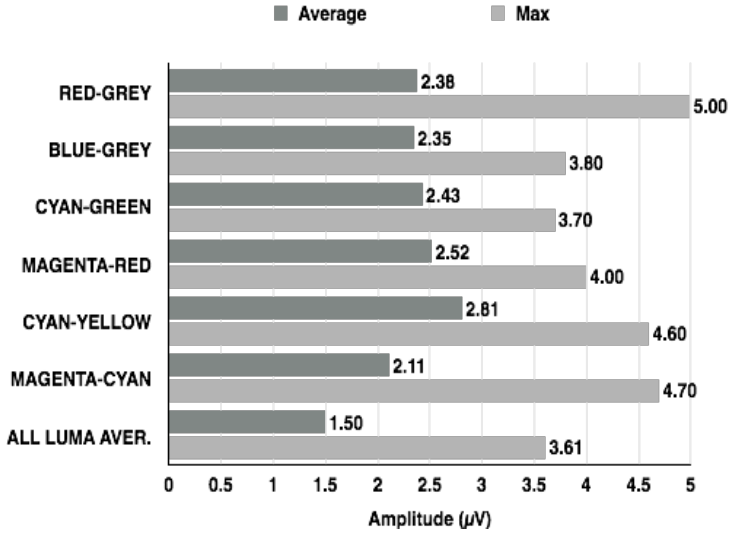

(b)

Figure 7-10 Side-by-side direct comparison of colour (a) vs greyscale (b) results

The comparison reveals only the results for the six best performing flickers in both categories.

H. Primary and Secondary Colours vs Black-White

In a multi-subject experiment, three primary (red, green, and blue) as well as three secondary (yellow, cyan, and magenta) colour flickers were tested against the reference black-white checkerboard (Section 5.5.2). By analysing the 560 brain signals captured from one trained subject and thirteen untrained subjects the general conclusion is that although the black-white graphic

proved to be a valid stimulator, the colours delivered signal quality improvement by 66.6% for the trained subject and by 62.5% for the untrained subjects.

Along the black-white reference flicker, the flickers utilising primary red and blue colours produced the best signals and are to be considered and recommended.

In this experiment, the secondary colours yellow and cyan, and the primary colour green, although occasionally delivered useable results, their overall performance was disappointing and should not be considered and recommended.

I. Conclusions Summary

This conclusions summary, serves the purpose of providing the ultimate suggestion for the most effective flicker configuration.

Firstly, colours should be used as a valid alternative and if needed, an expansion for traditional black-white flickers, which also proved to be a valid option. In most of the cases, the colours are able to deliver equal or higher signal amplitude peaks. The main reason for replacing the black-white flickers with colour versions, especially in multi-flicker arrangements, is to guarantee better recognition of specific flickering graphics by the BCI users. The most recommended colours by the author are red and blue, however it needs to be stated that the choice of colours could be subject dependent. As some of the presented results indicated, other colours such as green or magenta worked better with other subjects. Considering secondary colours such as yellow or cyan, which especially when presented in greyscale mode displayed very low contrast ratio, still were able to produce valid brain signals with some of the subjects. Therefore, more tests are recommended, especially when fine tuning specific colour combinations to specific BCI users.

Secondly, it is recommended to use light (white) background for colour flickers presentation. It provides slight improvement of the elicited brain signals by several microvolts.

Thirdly, some flicker patterns perform better than others and the BCI developers utilising visual stimulation should be aware of this fact. By using flickers with fewer flickering elements (between 2-3) the elicited brain signals will have fewer harmonic, thus making the fundamental frequencies easier to process.

Fourthly, the flicker size/resolution should be carefully chosen in respect to the presentation screen. Graphics, which occupy most of the presentation screen, will not necessarily generate the best signals. Medium sized graphics usually work best. Very small flickering elements will induce brain signals but their amplitude and especially signal to noise ratio will be compromised.

Fifthly, as an aftermath of the conducted series of experiments, it became apparent that certain element of subject/user training occurs. Thus, it is suggested to provide such training to the user/subject using SSVEP-based BCIs. From the achieved results it can be noted that such training could have one of the strongest positive impacts on the quality of elicited brain signals. However, it needs to be stated that a number of untrained users did not respond positively to the visual stimulation. In order to conclusively support the argument of the training importance and observe improvement with the said unsuccessful users, more tests need to be performed as part of the future work.

The author would like to propose the following set of parameters describing the most effective flickers to be implemented in the visually driven BCI system based on the above-analysed research outcomes.

- The following stimuli patterns and sizes are recommended: For he graphic checkerboards presented on a 13" digital display, the square checkerboard consisting of 64 checkers with the side length of 8 cm is recommended. For the 40 LED matrix with the light panel dimension of 3.5 cm x 6.5 cm, the two-field flicker with each field occupying half of the panel is recommended.

- For the stimuli presentation utilising digital screens, the bright (white) background is recommended.

- The colour element present in the visual flickers has been identified as improving the amplitude of the elicited brain signals by over 50%. The following colours are recommended: red, green, blue and magenta. Although it needs to be mentioned that certain user-depended individual response to colours can be observed, and in such cases the resulting brain signals will differ. Therefore, colour selection for the individual user should be tested prior application in the final BCI system.

- Since it has been observed that the user's response to the visual flickers gradually improves over time, possibly due to well documented neural plasticity of the human brain, it is recommended to schedule preliminary user exposure to visual stimulation prior the intended BCI operation.

The author is aware that due to the usage of three different stimuli sources (17 laptop screen, 12.9" tablet and 40 LED matrix) the presented results comparability could be questioned. The author believes that minor discrepancies in colour rendition between these devices did not have an impact

on the achieved results in any significant way. The colour pigmentation present in the retina colour sensitive cells must accept wide spectrum of visible light in order to generate highly complicated colour nuances that humans can perceive. The selected primary and secondary colours tested in this work have been chosen in order to enable other researchers to accurately recreate them using preferred method.

As the final note, the author would like to state that despite paying great attention in designing the experiments to ensure optimal flicker parameters, scenarios variety, and maintaining similar testing conditions, the achieved results should serve as the guideline in designing stimuli graphics for BCIs. Since the element of the individual subject response to stimuli plays an important role, one can expect that certain variance can be observed with their own designs. The need to fine-tune certain parameters to individual users/subject should not be ignored.

7.2 Contribution of the Thesis

The most important research contributions of this work can be summarised as follows:

1) Finding and filling a significant gap in research of flicker design and execution.

Based on the obtained education related to colour science, digital image processing and computer animation, further substantiated by the comprehension of the relationship between the digital screens and the human retina, an extensive set of experiments has been carried out during this research. Understanding this relationship inspired the author to investigate the phenomenon of processing by the brain and the eye, black and white graphics, being the equivalent of white light, versus colour and multi-colour flickers. Basing this research on the fact that white light is comprised of multiple electromagnetic wavelengths (colours) of visible light it has been decided to explore any potential benefit of using colour flickers for SSVEP-based BCI systems.

This new approach to designing and testing the extensive variety of graphic parameters in different scenarios, when presented during national and international conferences, has always been well received and met with great interest among the fellow BCI researchers and in other signal processing related fields.

2) Recognition of the fact that the element of subject/user training for visually driven BCI systems.

This aspect will play an important role in increasing the quality and robustness of the system's operations. In majority of the published work, the SSVEP paradigm is claimed to work with minimal to no training, with this feature being presented as crucial in the systems rapid accessibility. Recognising the effectiveness of the user/subject training supported by the published and presented in this work results should change the perspective for the future SVEP-based BCI developers.

These findings and their potential importance have already been recognised by the fellow researchers, and herewith are cited words of the paper reviewer:

> *"It would be interesting to see if these sorts of improvements can be achieved with a systematic training procedure. It would also be interesting to know if other motivated and practiced subjects (the co-author, say) also exhibit improvements, and if other labs have observed this effect. A practice-time-vs-performance curve would be interesting. Are other groups aware of this? Within the community this would be valuable*

information, so people building BCI systems are aware that use of the system engineers as test subjects can lead to a biased performance estimates."

3) Development of the bespoke Multi Colour Flicker (MCF) Application.

An iOS application automatically generating checkerboard flickers using RGB primary and secondary colours as well as white, 50% grey and black. Additionally, the application offers several useful features such as three types of backgrounds (white, 50% grey, and black) for the stimuli presentation and changeable flickers sizes. The application can work both in vertical and horizontal modes. This is a unique application offering great advantages for colour stimuli testing which did not exist before. Due to programmed automation in flicker presentation the application offers extremely fast workflow saving hundreds of hours otherwise required for manual flicker preparation. Since the application occupies only several hundreds of kilobytes, this workflow preserves gigabytes of storage space which otherwise would be occupied by rendered individual flickering graphics. The MCF is designed to work with Apple iPad tablets which are known for high quality of built-in screens, thus guaranteeing very accurate colour rendition of the generated flickers. The source code has been made available and is attached to this thesis in the digital form in Appendix 2.

4) Brain signals database.

During the years of research several thousands of brain signals obtained through visual stimulation have been recorded which are available as a database for other researchers interested in this type of work. All the recorded files are of European Data File (EDF) format and are tagged according to testing scenario and type of flicker with which they were elicited. The recorded signals have been catalogued and made available in the digital form in Appendix 3.

5) Flickering graphics.

As a consequence of conducted research for designing and developing stimuli graphics, utilising different methods evolving over time as detailed in this thesis, a variety of flickering graphics were generated and rendered. These graphics, in the form of separate digital video files have been made available and are the part of Appendix 4.

6) Use of professional software tools to generate flickers.

Additionally, the project files created using graphics design software (After Effects by Adobe) allowing generating checkerboard flickers of any colour, size, and flickering frequency (by changing relevant parameters) have been made available and included in Appendix 5.

7) Use of Arduino controlled RGB light source to generate flickers.

Beside contemporary and advanced software solution, this research work also utilises hardware, combining commonly known elements such as Arduino UNO microcontroller board with a recently available RGB LED matrix shield in order to assemble a useful and effective brain stimulation device. Using Arduino Integrated Development Environment, almost eight hundred of flicker designs have been programmed during this research, with many of them tried and tested. This hardware and software combination, after selecting required pattern design, allows choosing any desired flickering frequency as well change the LED's brightness. Among the designed flickers are different patterns using traditional white light as well as colour and multi-colour combinations. For the colour flickers, the same primary and secondary RGB colours have been used in order to maintain maximum compatibility with the MCF iOS application mentioned earlier. Almost 800 of preprogrammed sketches including variety of flickering patterns employing primary and secondary colours have been made available and attached to this thesis in Appendix 6.

8) Pioneering BCI projects at IT Carlow.

During the three years of research, the author supervised almost twenty 4-year engineering students working on their final year projects. All the projects were based on BCI systems development utilising the SSVEP technique. Due to this work, the author popularised the idea of BCI development among the IT Carlow students and the lecturing stuff. The students were encouraged to participate in many brain-recording experiments becoming subjects for the majority of the tests reported in this work. The student built BCIs each year gradually developed into more complicated systems. It should be noted that as an outcome of the continued work and showcased projects during these three years, other IT Carlow lecturers expressed their interest and developed BCI systems with their supervised students.

9) MATLAB-based GUI for EDF files.

In order to quickly detect multiple frequencies in the pre-recorded brain signals, a MATLAB model has been designed and developed with a GUI allowing opening recorded EDF files, assigning

channel for analysis, applying filtration by setting filter order and cut-off frequencies, and file segmenting (number of epochs). After signal processing completion, the detected frequencies are listed in the GUI (Figure 7-11) and their plots are displayed for each detected frequency (Figure 7-12). This model constitutes a very convenient method revealing frequencies of interest before the signals are further implemented in the BCI. Full code has been made available and is attached in Appendix 7.

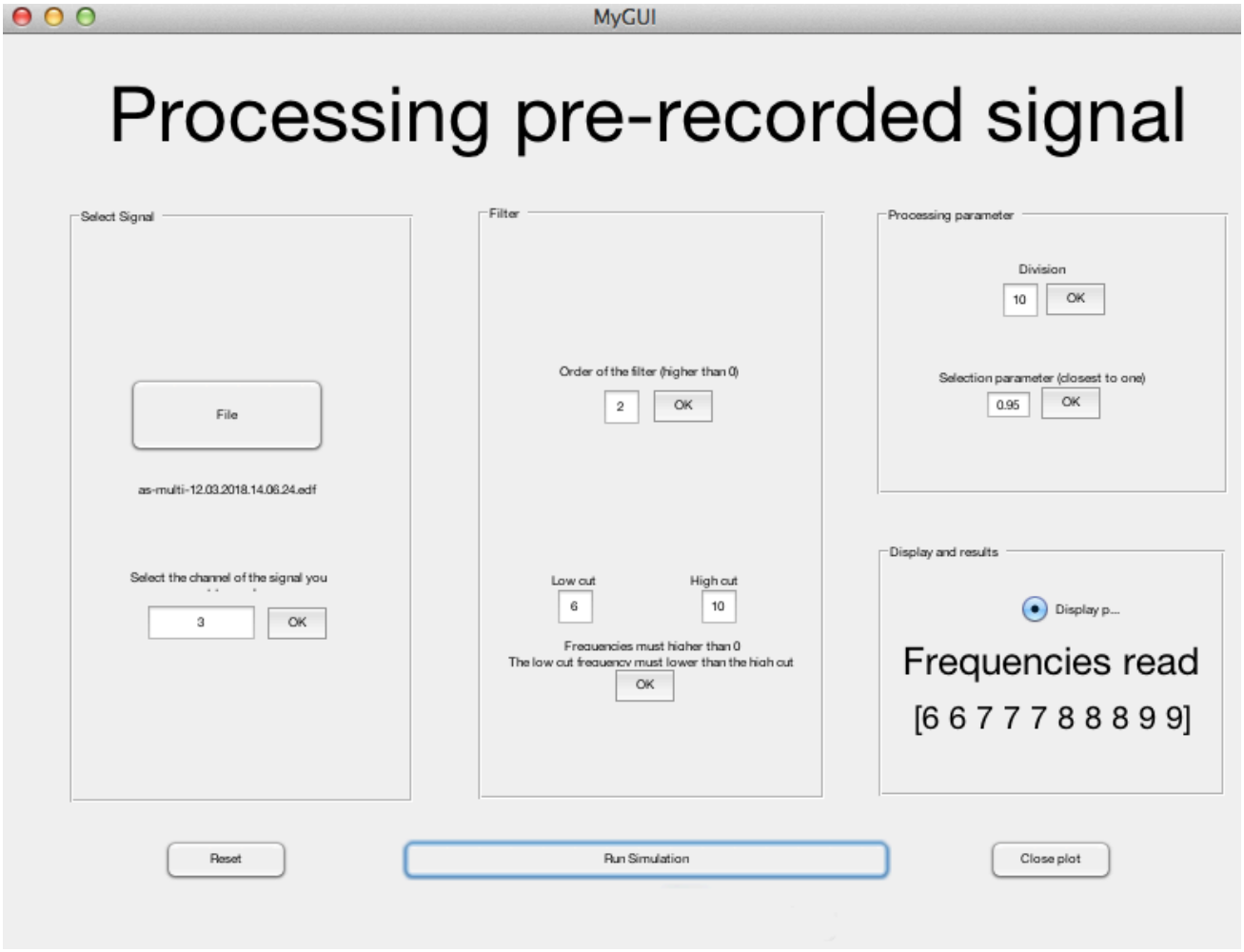

Figure 7-11 MATLAB model detecting frequencies in pre-recorded brain signals

The model's GUI displayed detected sequence of frequencies as they appeared in the captured brain signal recording.

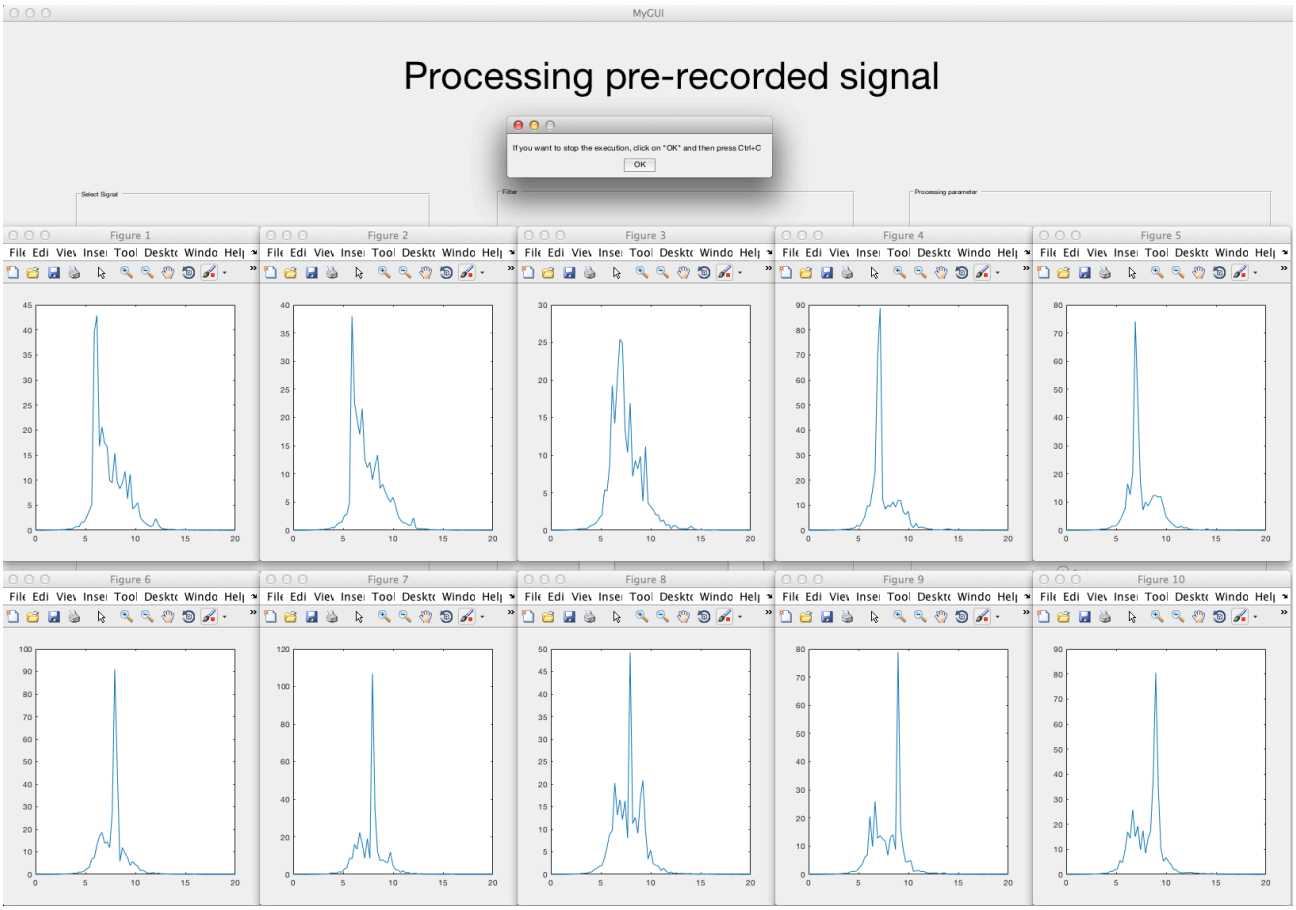

Figure 7-12 GUI with displayed frequency peak plots

The number of plots depends on the signal fragmentation; i.e. number of epochs specified in the GUI.

7.3 Future Research Direction

Although significant amount of effort has been made during this research work to experiment with large variety of testing scenarios there are still possible directions for further improvements and enhancements. In essence there are three areas that could be pursued for further improvements:

1) Widening the base of subjects testing in order to achieve more material for analysis and thus pinpointing even more precisely the relationships between tested parameters and their impact on the elicited brain signals. By doing so, and by concentrating on testing the already determined parameters, new and valuable information could be uncovered and even more precise flicker tuning could be performed for the SSVEP-based BCI systems enhanced effectiveness and improved robustness. Additionally, by continued and repeated testing the same group of subjects, the element of training could be further investigated. This element has been identified as one of the most important to test and reconfirmed by one of the reviewers referring to the author's recent paper publication.

2) Using the most recent technical advancements such as new display devices applying the latest high dynamic range (HDR) technology. Employing such devices in experiments would provide a new type of information not available hitherto. The latest display offerings mounted in tablets and computer monitors implement true 10-bit display technology, which provides more accurate colour rendition, expanded colour spectrum, and most importantly, much higher screen brightness reaching up to 1000 nits. The current traditional screens are 8-bit displays with approximately 400 nits brightness level. It is expected to see a significant shift in achieved results in terms of signal strength as well as artifact and noise content.

3) Extending the scope of interest by combining the utilised visual stimulation with other techniques such as machine learning and neural networks to further improve the operations of SSVEP-based BCIs. A very rapid development and widespread usage of the machine learning technology and neural networks would open new possibilities in visual stimuli applications for the most advanced future BCI systems. It is a common opinion among the BCI researchers and developers that the future of the BCI systems depends on the ability to combine multiple control paradigms into one system. Additionally, it would be very interesting to investigate, whether the application of neural networks in SSVEP-based systems could help in recognising certain colours by the system. The general goal of any BCI system is to enable the maximum number of control commands in combination with maintained robustness which such approach should help achieving.

References

Aftanas, L.I., Golocheikine, S.A. (2001) *Human anterior and frontal midline theta and lower Alpha reflect emotionally positive state and internalized attention: High-resolution EEG investigation of meditation*. Neurosci. Lett, 2001; 310: 57–60.

Ambler, T., Braeutigam, S., Stins, J., Rose, S., Swithenby, S. (2004) *Salience and choice: Neural correlates of shopping decisions.* Psychol. Market 2004, 21, 247–261.

Ambler, T., Ioannides, A., Rose, S. (2000) *Brands on the brain: Neuro-images of advertising.* Bus. Strateg. Rev. 2000, 11, 17–30.

Aminaka, D., Makino, S., Rutkowski, T.M. (2014) *Chromatic SSVEP BCI Paradigm Targeting the Higher Frequency EEG Responses.* In Asia-Pacific Signal and Information Processing Association, 2014 Annual Summit and Conference (APSIPA), Dec 2014, pp.1-7.

Anand, B.K., Chhina, G.S., Singh, B. (1961) *Some aspects of electroencephalographic studies in Yogis.* Electroencephalogr. Clin. Neurophysiol, 1961; 13: 452–456.

Ariely, D., Berns, G.S. (2010) *Neuromarketing: The hope and hype of neuroimaging in business.* Nat. Rev. Neurosci. 2010, 11, 284–292.

Ascher, S. and Pincus, E. (2012) *The filmmaker's handbook. 3rd ed*. New York: Plume.

Association Visual Cortex (no date) *Manumissio Wikispaces.* Available at:http://manumissio.wikispaces.com/Association+Visual+Cortex [Accessed: 17 June 2016].

Astafiev, S.V., Stanley, C.M., Shulman, G.L., Corbetta, M. (2004) *Extrastriate body area in human occipital cortex responds to the performance of motor actions.* Nat Neurosci 7:542-548. 10.1038/un1241.

Aurlien, H., Gjerde, I.O., Aarseth, J.H., Eldøen, G., Karlsen, B., Skeidsvoll, H., Gilhus, N.E. (2004) *EEG background activity described by a large computerized database.* Clinical Neurophysiology, 2004; 115(3): 665–673.

Baillet, S., Mosher, J.C., Leahy, R.M. (2001) *Electromagnetic brain mapping.* IEEE Signal Process. Mag. 2001, 18, 14–30.

Bakardjian, H., Tanaka, T., Cichocki, A. (2010) *Optimisation of SSVEP brain responses with application to eight-command Brain-Computer Interface.* Neuroscience L etters, Vol. 469 Issue 1, pp 34-38.

Ball, T.; Kern, M.; Mutschler, I.; Aertsen, A.; Schulze-Bonhage, A. (2009) *Signal quality of simultaneously recorded invasive and non-invasive EEG*. Neuroimage 2009, 46, 708–716.

Ballesteros, S., Voelcker-Rehage, C. and Bherer, L. (2018) *Cognitive and Brain Plasticity Induced by Physical Exercise, Cognitive Training, Video Games, and Combined Interventions.* Frontiers in Human Neuroscience, [Online]. 12, 169. Available at: https://www.frontiersin.org/articles/10.3389/fnhum.2018.00169/full [Accessed 19 June 2019].

Bensch, M., Karim, A.A., Mellinger, J., Hinterberger, T., Tangermann, M., Bogdan, M., Rosenstiel, W., Birbaumer, N. (2007) *Nessi: An EEG-controlled web browser for severely paralyzed patients.* Comput. Intell. Neurosci. 2007, 2007, 71863.

Birbaumer, N., Elbert, T., Canavan, A.G., Rockstroh, B. (1990) *Slow potentials of the cerebral cortex and behavior.* Physiol. Rev., 1990; 70: 1–41.

Birbaumer, N., Ghanayim, N., Hinterberger, T., Iversen, I., Kotchoubey, B., Kubler, A., Perelmouter, J., Taub, E., Flor, H. (1999) *A spelling device for the paralysed.* Nature 1999, 398, 297–298.

Blabe, C. H., Gilja, V., Chestek, C. A., Shenoy, K. V., Anderson, K. D., and Henderson, J. M. (2015) *Assessment of brain-machine interfaces from the perspective of people with paralysis*. *J. Neural Eng.* 12:043002. doi: 10.1088/1741-2560/12/4/043002.

Black, A.H. (1997) *The Operant Conditioning of Central Nervous System Electrical Activity.* In Psychology of Learning and Motivation, Gordon, H.B., Ed.; Academic Press: New York, NY, USA, 1997; 6: 47–95.

Blankertz, B., Lemm, S., Treder, M., Haufe, S., Müller, K.R. (2011) *Single-trial analysis and classification of ERP components—A tutorial*. Neuroimage 2011, 56, 814–825.

Blankertz, B., Tangermann, M., Vidaurre, C., Fazli, S., Sannelli, C., Haufe, S., Maeder, C., Ramsey, L., Sturm, I., Curio, G., Mueller, K.R. (2010) *The Berlin Brain-Computer Interface: Non-Medical Uses of BCI Technology.* Front. Neurosci. 2010, doi: 10.3389/fnins.2010.00198.

Borisoff, J.F., Mason, S.G., Bashashati, A., Birch, G.E. (2004) *Brain-computer interface design for asynchronous control applications: Improvements to the LF-ASD asynchronous brain switch.* IEEE Trans. Biomed. Eng. 2004, 51, 985–992.

Bostanov, V. (2004) *BCI competition 2003-data sets Ib and IIb: Feature extraction from event-related brain potentials with the continuous wavelet transform and the t-value scalogram.* IEEE Trans. Biomed. Eng. 2004, 51, 1057–1061.

Boye, A.T., Kristiansen, U.Q., Billinger, M., do Nascimento, O.F., Farina, D. (2008) *Identification of movement-related cortical potentials with optimized spatial filtering and principal component analysis*. Biomed. Signal Process. Control 2008, 3, 300–304.

Bramao, I., Faisca, L., Forkstam, C., Reis, A., Petersson, K.M. (2011) *Cortical Brain Regions Associated with Color Processing: An FMRi Study.* Open Neuroimag J 4:164-7310.2174/1874440001004010164.

Brown, P., Salenius, S., Rothwell, J.C., Hari, R. (1998) *Cortical correlate of the piper rhythm in humans.* J. Neurophysiol., 1998; 80: 2911–2917.

Brunner, C., Allison, B.Z., Krusienski, D.J., Kaiser, V., Müller-Putz, G.R., Pfurtscheller, G., Neuper, C. (2010) *Improved signal processing approaches in an offline simulation of a hybrid brain-computer interface.* J. Neurosci. Methods 2010, 188, 165–173.

Cao, T., Wan, F., Mak, P.U., Mak, P.I., Vai, M.I., Hu, Y. (2012) *Flashing Color on the Performance of SSVEP-based Brain-Computer Interfaces.* 34th Annual International Conference of the IEEE EMBS, San Diego, California USA.

Castellanos, N.P., Makarov, V.A. (2006) *Recovering EEG brain signals: Artifact suppression with wavelet enhanced independent component analysis.* J. Neurosci. Methods 2006, 158, 300–312.

Chambayil, B., Singla, R., Jha, R. (2010) *Virtual Keyboard BCI Using Eye Blinks in EEG.* In Proceedings of the 6th IEEE International Conference on Wireless and Mobile Computing, Networking and Communications (WiMob'10), Niagara Falls, ON, Canada, October 2010; pp. 466–470.

Cheng, M., Gao, X., Gao, S., Xu, D. (2001) *Multiple color stimulus induced steady state visual evoked potentials*. Proc. 23rd Annual Conf. IEEE EMBS, Istanbul, 2001, pp. 1012-1014.

Chumerin, N., Manyakov, N.V., Van Vliet, M., Robben, A., Combaz, A., Van Hulle, M.M. (2012) *Processing and Decoding Steady-State Visual Evoked Potentials for Brain-Computer Interfaces*. Laboratorium voor Neuro- en Psychofysiologie, KU Leuven, Belgium, River Publishers, An Edited Volume, 2012; 1-33.

Ciaccio, E., Dunn, S., Akay, M. (1993) *Biosignal pattern recognition and interpretation systems. 2. Methods for feature extraction and selection.* IEEE Eng. Med. Biol. Mag. 1993, 12, 106–113.

CIE (1932) *Commission internationale de l'Eclairage proceedings, 1931.* Cambridge: Cambridge University Press.

Cincotti, F., Mattia, D., Aloise, F., Bufalari, S., Schalk, G., Oriolo, G., Cherubini, A., Marciani, M.G., Babiloni, F. (2008) *Non-invasive brain-computer interface system: Towards its application as assistive technology*. Brain Res. Bull. 2008, 75, 796–803.

Cook, I.A., Warren, C., Pajot, S.K., Schairer, D., Leuchter, A.F. (2011) *Regional Brain activation with advertising images*. J. Neurosci. Psychol. Econ. 2011, 4, 147–160.

Dacey, D.M. (1999) *Primate retina: Cell types, circuits and color opponency.* Progress in Retinal and Eye Research 18: 737–763.

Dal Seno, B., Matteucci, M., Mainardi, L. (2008) *A Genetic Algorithm for Automatic Feature Extraction in P300 Detection*. In Proceedings of the IEEE International Joint Conference on Neural Networks (IJCNN'08), Hong Kong, China, June 2008; pp. 3145–3152.

Daly, J.J., Wolpaw, J.R. (2008) *Brain-computer interfaces in neurological rehabilitation.* Lancet Neurol. 2008, 7, 1032–1043.

Darah Juang, Dr. Dro!: (2017) *Darah Juang, Dr. Dro!: EEG electrode placement for motor imagery, Y01-M01-D10*. [ONLINE] Available at: http://drhdrdro.blogspot.ie/2013/09/eeg-electrode-placement-for-motor.html. [Accessed 01 February 2017].

deCharms, R.C., Christoff, K., Glover, G.H., Pauly, J.M., Whitfield, S., Gabrieli, J.D.E. (2004) *Learned regulation of spatially localized brain activation using real-time fMRI*. Neuroimage 2004, 21, 436–443.

del R Millan, J., Mourino, J., Franze, M., Cincotti, F., Varsta, M., Heikkonen, J., Babiloni, F. (2002) *A local neural classifier for the recognition of EEG patterns associated to mental tasks*. IEEE Trans. Neural Netw. 2002, 13, 678–686.

Demiralp, T., Yordanova, J., Kolev, V., Ademoglu, A., Devrim, M., Samar, V.J. (1999) *Time-frequency analysis of single-sweep event-related potentials by means of fast wavelet transform*. Brain Lang 1999, 66, 129–145.

Dias, N., Kamrunnahar, M., Mendes, P., Schiff, S., Correia, J. (2010) *Feature selection on movement imagery discrimination and attention detection*. Med. Biol. Eng. Comput. 2010, 48, 331–341.

Displaymate.com. (2019). *DisplayMate Monitor Projector and TV Set Up Calibration and Testing*. [online] Available at: http://www.displaymate.com [Accessed 28 Sep. 2019].

Douma, M. curator. (2008) *Color, Art and the Mind. Microconsciousness. What is color?* [ONLINE] Available at: http://www.webexibits.org/causesofcolor/mind.html. [Accessed 31 March 2016].

EEG Headsets | NeuroSky Store (2014) EEG Headsets | NeuroSky Store.

Embrandiri, S. S., Teja, S. S. S., Ramasubba Reddy, M. and Chandrachoodan, N. (2015) *Effect of stimulation shapes on the Steady-State Visual-Evoked response.* 2015 41st Annual Northeast Biomedical Engineering Conference (NEBEC), Troy, NY, 2015, pp. 1-2.doi: 10.1109/NEBEC.2015.7117158.

Emotiv.Store.Compare. (2014) *Compare.* [ONLINE] Available at:http://emotiv.com/ store/compare/. [Accessed 24 October 2014].

EmSense: Quantitative Biosensory Metrics. (no date) Available online: http://www.emsense.com/ (accessed on 9 January 2019).

Epoc. (2015). Epoc. [ONLINE] Available at: https://emotiv.com/epoc.php. [Accessed 20 September 2015].

ERP Info. (2019) *ERPLAB Toolbox — ERP Info*. [online] Available at: https://erpinfo.org/erplab [Accessed 11 May 2019].

Falk, D., Brill, D. and Stork, D. (1986) *Seeing the light.* [Chichester]: Wiley.

Farwell, L.A., Donchin, E. (1988) *Talking off the top of your head: Toward a mental prosthesis utilizing event-related brain potentials*. Electroencephalogr. Clin. Neurophysiol. 1988, 70, 510–523.

Fatourechi, M., Bashashati, A., Ward, R.K., Birch, G.E. (2007) *EMG and EOG artefacts in brain computer interface systems: A survey*. Clin. Neurophysiol. 2007, 118, 480–494.

Fatourechi, M., Birch, G.E., Ward, R.K. (2007) *Application of a hybrid wavelet feature selection method in the design of a self-paced brain interface system.* J. NeuroEng. Rehabil. 2007, 4, 1–13.

Fazel-Rezai, R., Abhari, K. (2009) *A region-based P300 speller for brain-computer interface.* Can. J. Elect. Comput. E. 2009, 34, 81–85.

Felzer, T., Freisieben, B. (2003) *Analyzing EEG signals using the probability estimating guarded neural classifier*. IEEE Trans. Neural Syst. Rehabil. Eng. 2003, 11, 361–371.

Fernández, T., Harmony, T., Rodríguez, M., Bernal, J., Silva, J., Reyes, A., Marosi, E. (1995) *EEG activation patterns during the performance of tasks involving different components of mental calculation*. Electroencephalogr. Clin. Neurophysiol, 1995; 94, 175–182.

Ferrez, P.W., del R. Millan, J. (2008) *Error-related EEG potentials generated during simulated brain-computer interaction*. IEEE Trans. Biomed. Eng. 2008, 55, 923–929.

Fisch, B.J. (2002) *Fisch and Spehlmann's EEG Primer: Basic Principles of Digital and Analog EEG.* 3e. 3 Edition. Elsevier, 2002.

Fisher, C.E., Chin, L., Klitzman, R. (2010) *Defining neuromarketing: Practices and professional challenges*. Harv. Rev. Psychiatry 2010, 18, 230–237.

Fisher, R.S., Harding, G., Erba, G., Barkley, G.L., Wilkins, A. (2005) *Photic- and pattern-induced seizures: a review for the epilepsy foundation of america working group*. Epilepsia, 2005; 46(9): 1426-1441.

Fitzgibbon, S.P., Lewis, T.W., Powers, D.M.W., Whitham, E.M., Willoughby, J.O., Pope, K.J. (2013) *Surface Laplacian of Central Scalp Electrical Signals is Insensitive to Muscle Contamination*. IEEE Transactions on Biomedical Engineering, 2013; 60(1): 4–9.

Florian, G., Pfurtscheller, G. (1995) *Dynamic spectral analysis of event-related EEG data.* Electroencephalogr. Clin. Neurophysiol. 1995, 95, 393–396.

Fonseca, C., Cunha, J.P.S., Martins, R.E., Ferreira, V.M., de Sa, J.P.M., Barbosa, M.A., da Silva, A.M. (2007) *A Novel Dry Active Electrode for EEG Recording.* IEEE Trans. Biomed. Eng. 2007, 54, 162–165.

Fun of gaming: Measuring the human experience of media enjoyment. (no date) Available online: http://fuga.aalto.fi/ (accessed on 7 January 2019).

Furdea, A., Halder, S., Krusienski, D.J., Bross, D., Nijboer, F., Birbaumer, N., Kübler, A. (2009) *An auditory oddball (P300) spelling system for brain-computer interfaces*. Psychophysiology 2009, 46, 617–625.

Galán, F., Nuttin, M., Lew, E., Ferrez, P.W., Vanacker, G., Philips, J., Millán, J.D.R. (2008) *A brain-actuated wheelchair: Asynchronous and non-invasive brain-computer interfaces for continuous control of robots*. Clin. Neurophysiol. 2008, 119, 2159–2169.

Galloway, N. (1990) *Human brain electrophysiology: Evoked potentials and evoked magnetic fields in science and medicine*. Br. J. Ophthalmol. 1990, 74, 255.

Gao, J., Yang, Y., Lin, P., Wang, P., Zheng, C. (2010) *Automatic removal of eye-movement and blink artefacts from EEG signals*. Brain Topogr. 2010, 23, 105–114.

Gargiulo, G., Calvo, R.A., Bifulco, P., Cesarelli, M., Jin, C., Mohamed, A., van Schaik, A. (2010) *A new EEG recording system for passive dry electrodes.* Clin. Neurophysiol. 2010, 121, 686–693.

Garrett, D., Peterson, D.A., Anderson, C.W., Thaut, M.H. (2003) *Comparison of linear, nonlinear, and feature selection methods for EEG signal classification*. IEEE Trans. Neural Syst. Rehabil. Eng. 2003, 11, 141–144.

Gerloff, M., Schilling, M. (2012) *Subject response variability in terms of colour and frequency of capacitive SSVEP measurements.* Biomedical Engineering / Biomedizinische Technik. Vol. 57, Issue SI-1 Track-F, Pages 95-98. ISSN (Online) 1862-287X.

Ghafar, R., Hussain, A., Samad, S.A., Tahir, N.M. (2008) *Comparison of FFT and AR Techniques for Scalp EEG Analysis*. In Proceedings of the 4th Kuala Lumpur International Conference on Biomedical Engineering 2008, Kuala Lumpur, Malaysia, June 2008; Abu Osman, N.A., Ibrahim, F., Wan Abas, W.A.B., Abdul Rahman, H.S., Ting, H.-N., Magjarevic, R., Eds.; Springer Berlin Heidelberg: Berlin, Germany, 2008; Volume 21, pp. 158–161.

Ghanbari, A.A., Kousarrizi, M.R.N., Teshnehlab, M., Aliyari, M. (2009) *Wavelet and Hilbert transform-based Brain Computer Interface*. In Proceedings of the International Conference on Advances in Computational Tools for Engineering Applications (ACTEA'09), Beirut, Lebanon, July 2009; pp. 438–442.

Grosse-Wentrup, M., Buss, M. (2008) *Multiclass common spatial patterns and information theoretic feature extraction*. IEEE Trans. Biomed. Eng. 2008, 55, 1991–2000.

Henze, D. A., Borhegyi, Z., Csicsvari, J., Mamiya, A., Harris, K. D., and Buzsaki, G. (2000) *Intracellular features predicted by extracellular recordings in the hippocampus in vivo. J. Neurophysiol.* 84, 390–400.

Hering, E. (1878) *Zur Lehre von Lichtsinne.* Wien, Gerolds Sohn.

Hering, E. (1964) *Outlines of a Theory of the Light Sense.* Cambridge, MA, Harvard University Press.

Hinterberger, T., Schmidt, S., Neumann, N., Mellinger, J., Blankertz, B., Curio, G., Birbaumer, N. *(2004) Brain-computer communication and slow cortical potentials*. IEEE Trans. Biomed. Eng., 2004; 51: 1011–1018.

Hinterberger, T., Schmidt, S., Neumann, N., Mellinger, J., Blankertz, B., Curio, G., Birbaumer, N. (2004) *Brain-computer communication and slow cortical potentials*. IEEE Trans. Biomed. Eng. 2004, 51, 1011–1018.

Hochberg, L.R., Serruya, M.D., Friehs, G.M., Mukand, J.A., Saleh, M., Caplan, A.H., Branner, A., Chen, D., Penn, R.D., Donoghue, J.P. (2006) *Neuronal ensemble control of prosthetic devices by a human with tetraplegia.* Nature 2006, 442, 164–171.

Hoffmann, U., Vesin, J.M., Ebrahimi, T., Diserens, K. (2008) *An efficient P300-based brain-computer interface for disabled subjects*. J. Neurosci. Methods 2008, 167, 115–125.

Hubbard, B.B. (1998) *The World According to Wavelets: The Story of a Mathematical Technique in the Making.* A.K. Peters: Natick, MA, USA, 1998.

Huster, R.J., Mokom, Z.N., Enriquez-Geppert, S., Hermann, C. (2014) *Brain-computer interfaces for EEG neurofeedback: Peculiarities and solutions*. International Journal of Psychology, 2014; 91(1): 36-45.

Hwang, H., Kwon, K., Im, C. (2009) *Neurofeedback-based motor imagery training for brain-computer interface (BCI)*. J. Neurosci. Methods, 2009; 179: 150–156.

Isa, I.S., Hussain, Z., Sulaiman S.N. and Hamzah, N.H. (2012) *Study on EEG Steady State Alpha Brain Wave Signals Based on Visual Stimulation for FES.* Computers, Automatic Control, Signal Processing and Systems Science.

Jacobs, G.H. (2014) *The Discovery of Spectral Opponency in Visual Systems and its Impact on Understanding the Neurobiology of Color Vision.* Journal of the history of the neuroscience. 2014;23(3):287-314.

Jain, A.K., Duin, R.P.W., Jianchang, M. (2000) *Statistical pattern recognition: A review.* IEEE Trans. Pattern Anal. 2000, 22, 4–37.

Jasper, H.H. (1958) *The ten-twenty electrode system of the International Federation.* Electroencephalogr. Clin. Neurophysiol. 1958, 10, 371–375.

Jinghai, Y., Derong, J., Jianfeng, H. (2009) *Design and Application of Brain-Computer Interface Web Browser Based on VEP*. In Proceedings of the International Conference on Future BioMedical Information Engineering (FBIE'09), Sanya, China, 13–14 December 2009; pp. 77–80.

Jung, T.P., Makeig, S., Humphries, C., Lee, T.W., McKeown, M.J., Iragui, V., Sejnowski, T.J. (2000) *Removing electroencephalographic artefacts by blind source separation*. Psychophysiology,2000; 37(2): 163–178.

Kaiser, J. (2001) *Self-initiation of EEG-based communication in paralyzed patients*. Clin. Neurophysiol, 2001; 112: 551–554.

Kanayama, N., Sato, A., Ohira, H. (2007) *Crossmodal effect with rubber hand illusion and gamma-band activity.* Psychophysiology, 2007: 44(3): 392–402.

Karim, A.A., Hinterberger, T., Richter, J., Mellinger, J., Neumann, N., Flor, H., Kübler, A., Birbaumer, N. (2006) *Neural internet: Web surfing with brain potentials for the completely paralyzed.* Neurorehabil. Neural Repair 2006, 20, 508–515.

Kayikcioglu, T., Aydemir, O. (2010) *A polynomial fitting and k-NN based approach for improving classification of motor imagery BCI data*. Pattern Recogn. Lett. 2010, 31, 1207–1215.

Keren, A.S., Yuval-Greenberg, S., Deouell, L.Y. (2010) *Saccadic spike potentials in gamma-band EEG: Characterization, detection and suppression.* NeuroImage, 2010; 49(3): 2248–2263.

Khalid, M.B., Rao, N.I., Rizwan-i-Haque, I., Munir, S., Tahir, F. (2009) *Towards a Brain Computer Interface Using Wavelet Transform with Averaged and Time Segmented Adapted Wavelets*. In Proceedings of the 2nd International Conference on Computer, Control and Communication (IC4'09) Karachi, Sindh, Pakistan, February 2009; pp. 1–4.

Kirmizi-Alsan, E., Bayraktaroglu, Z., Gurvit, H., Keskin, Y.H., Emre, M., Demiralp, T. (2006) *Comparative analysis of event-related potentials during Go/NoGo and CPT: Decomposition of electrophysiological markers of response inhibition and sustained attention*. Brain Research, 2006; 1104(1): 114–128.

Kisley, M.A., Cornwell, Z.M. (2006) *Gamma and Beta neural activity evoked during a sensory gating paradigm: Effects of auditory, somatosensory and cross-modal stimulation*. Clinical Neurophysiology, 2006; 117(11): 2549–2563.

Kleber, B., Birbaumer, N. (2005) *Direct brain communication: neuroelectric and metabolic approaches at Tübingen*. Cogn. Process, 2005; 6: 65–74.

Klimesch, W. (1997) *EEG-Alpha rhythms and memory processes*. Int. J. Psychophysiol, 1997; 26: 319– 340.

Konrad, P., Shanks, T. (2010) *Implantable brain computer interface: Challenges to neurotechnology translation.* Neurobiol. Dis. 2010, 38, 369–375.

Krusienski, D.J., McFarland, D.J., Wolpaw, J.R. (2006) *An Evaluation of Autoregressive Spectral Estimation Model Order for Brain-Computer Interface Applications*. In Proceedings of the 28th Annual International Conference of the IEEE Engineering in Medicine and Biology Society (EMBS'06), New York, NY, USA, September 2006; pp. 1323–1326.

Krusienski, D.J., Schalk, G., McFarland, D.J., Wolpaw, J.R. (2007) *A mu-rhythm matched filter for continuous control of a brain-computer interface.* IEEE Trans. Biomed. Eng. 2007, 54, 273–280.

Kübler, A., Birbaumer, N. (2008) *Brain-computer interfaces and communication in paralysis: Extinction of goal directed thinking in completely paralysed patients?* Clin. Neurophysiol. 2008, 119, 2658–2666.

Kübler, A., Kotchoubey, B., Kaiser, J., Wolpaw, J.R,. Birbaumer, N. (2001) *Brain-Computer Communication: Unlocking the Locked in.* American Psychological Association: Washington, 2001.

Kun, L., Sankar, R., Arbel, Y., Donchin, E. (2009) *Single trial independent component analysis for P300 BCI system.* In Proceedings of the 31th Annual International Conference of the IEEE Engineering in Medicine and Biology Society (EMBCS'09), Minneapolis, MN, USA, September 2009; pp. 4035–4038.

Lakany, H., Conway, B.A. (2007) *Understanding intention of movement from electroencephalograms.* Expert. Syst. 2007, 24, 295–304.

Laureys, S., Boly, M., Tononi, G. (2009) *Functional Neuroimaging. In The Neurology of Consciousness.* Steven, L., Giulio, T., Eds.; Academic Press: New York, NY, USA, 2009; pp. 31–42.

Lebedev, M.A., Nicolelis, M.A.L. (2006) *Brain-machine interfaces: Past, present and future.* Trends Neurosci. 2006, 29, 536–546.

Lee, K.H., Williams, L.M., Breakspear, M., Gordon, E. (2003) *Synchronous Gamma activity: A review and contribution to an integrative neuroscience model of schizophrenia.* Brain Res. Rev, 2003; 41: 57–78.

Lee, P., Hsieh, J., Wu, C., Shyu, K., Wu, Y. (2008) *Brain computer interface using flash onset and offset visual evoked potentials*. Clin. Neurophysiol. 2008, 119, 605–616.

Lemm, S., Blankertz, B., Dickhaus, T., Müller, K.-R. (2011) *Introduction to machine learning for brain imaging*. NeuroImage 2011, 56, 387–399.

Li, Y., Guan, C., Li, H., Chin, Z. (2008) *A self-training semi-supervised SVM algorithm and its application in an EEG-based brain computer interface speller system.* Pattern Recogn. Lett. 2008, 29, 1285–1294.

Lin, C.J., Hsieh, M.H. (2009) *Classification of mental task from EEG data using neural networks based on particle swarm optimization*. Neurocomputing 2009, 72, 1121–1130.

Lins, O.G., Picton, T.W., Berg, P., Scherg, M. (1993) *Ocular artefacts in recording EEGs and event-related potentials II: Source dipoles and source components.* Brain Topogr. 1993, 6, 65–78.

Liu, Y., Zhou, Z., Hu, D. (2011) *Gaze independent brain-computer speller with covert visual search tasks*. Clin. Neurophysiol. 2011, 122, 1127–1136.

Manyakov, V.N., Chumerin, N., Combaz, A., Robben, A., Van Vliet, M., De Maziere, P. A. (2011) *Brain-Computer Interface Research at Katholieke Universiteit Leuven*, Proc. of the 4th Int. Symp. on Appl. Sci. in Biomedical and Commun. Technologies, ACM.

Martinez, P., Bakardjian, H., Cichocki, A. (2007) *Fully online multicommand brain-computer interface with visual neurofeedback using SSVEP paradigm.* Computational Intelligence and Neuroscience, 2007; 2007: 9.

Marz, M. (2018) *Understanding Power System Interharmonics*. [online] Transmission & Distribution World. Available at: https://www.tdworld.com/smart-grid/understanding-power-system-interharmonics [Accessed 19 Sep. 2018].

Mason, S.G., Birch, G.E. (2000) *A brain-controlled switch for asynchronous control applications.* IEEE Trans. Biomed. Eng. 2000, 47, 1297–1307.

McFarland, D.J., Anderson, C.W., Muller, K.R., Schlogl, A., Krusienski, D.J. (2006) *BCI meeting 2005-workshop on BCI signal processing: Feature extraction and translation.* IEEE Trans. Neural Syst. Rehabil. Eng. 2006, 14, 135–138.

McFarland, D.J., Krusienski, D.J., Wolpaw, J.R. (2006) *Brain-Computer Interface Signal Processing at the Wadsworth Center: mu and Sensorimotor Beta Rhythms.* In Progress in Brain Research; Christa, N., Wolfgang, K., Eds.; Elsevier: New York, NY, USA, 2006; Volume 159, pp. 411–419.

McFarland, D.J., Wolpaw, J.R. (2005) *Sensorimotor rhythm-based brain-computer interface (BCI): Feature selection by regression improves performance.* IEEE Trans. Neural Syst. Rehabil. Eng. 2005, 13, 372–379.

Microsoft Research—Computational (no date) User Experiences: Brain-Computer Interfaces. Available online:http://research.microsoft.com/en-us/um/redmond/groups/cue/bci/ (accessed on 12 July 2011).

Middendorf, M., McMillan, G., Calhoun, G., Jones, K.S. (2000) *Brain-computer interfaces based on the steady-state visual-evoked response.* IEEE Trans. Rehabil. Eng. 2000, 8, 211–214.

Millan, J.R. (2004) *On the Need for On-Line Learning in Brain-Computer Interfaces.* In Proceedings of the IEEE International Joint Conference on Neural Networks, (IJCNN'04), Budapest, Hungary, July 2004; pp. 2877-2882.

Millan, J.R., Mourino, J. (2003) *Asynchronous BCI and local neural classifiers: an overview of the adaptive brain interface project*. IEEE Trans. Neural Syst. Rehabil. Eng. 2003, 11, 159–161.

Mima, T., Simpkins, N., Oluwatimilehin, T., Hallett, M. (1999) *Force level modulates human cortical oscillatory activities*. Neurosci. Lett., 1999; 275: 77–80.

Mohri, M., Rostamizadeh, A., Talwalkar, A. (2012) *Foundations of Machine Learning.* The MIT Press, ISBN 9780262018258, 2012.

Moore, M.M. (2003) *Real-world applications for brain-computer interface technology.* IEEE Trans. Neural Syst. Rehabil. Eng. 2003, 11, 162–165.

Mouli, S., Palaniappan, R., Sillitoe, I.P., Gan, J.Q. (2013) *Performance Analysis of Multi-frequency SSVEP-BCI Using Clear and Frosted Colour LED Stimuli.* Proceedings of IEEE 13th International Conference on Bioinformatics Bioengineering (BIBE), pp 1-4.

Mousavi, E.A., Maller, J.J., Fitzgerald, P.B., Lithgow, B.J. *(2011) Wavelet common spatial pattern in asynchronous offline brain computer interfaces*. Biomed. Signal Process. Control 2011, 6, 121–128.

Muller-Putz, G.R., Pfurtscheller, G. (2008) *Control of an Electrical Prosthesis With an SSVEP-Based BCI.* IEEE Trans. Biomed. Eng. 2008, 55, 361–364.

Müller-Putz, G.R., Scherer, R., Pfurtscheller, G., Rupp, R. (2005) *EEG-based neuroprosthesis control: A step towards clinical practice*. Neurosci. Lett. 2005, 382, 169–174.

Muller, M.M., Andersen, S., Trujillo, N.J., Valdes-Sosa, P., Malinowski, P., Hillyard, S.A. (2006) *Feature-selective attention enhances color signals in early visual areas of the human brain.* Proc Natl Acad Sci USA. 2006; 103(38):14250-14254.

Nakamishi, M., Wang, Y., Wang, Y. T., Mitsukura, Y., Jung, T.P (2014) *Generating Visual Flickers for Eliciting Robust SteadyState Visual Evoked Potentials at Flexible Frequencies Using Monitor Refresh Rate.* Plos ONE, 9, 6, pp. 112, Academic Search Complete, EBSCOhost, [Accessed 24 February 2015].

Nakamishi, M., Wang, Y., Wang, Y. T., Mitsukura, Y., Jung, T.P., (2013) *An Approximation Approach for Rendering Visual Flickers in SSVEP-Based BCI Using Monitor Refresh Rate*. 35th Annual International Conference of the IEEE EMBS, Osaka, Japan.

Neuro Insight. (no date) Available online: http://www.neuro-insight.com/ (accessed on 9 January 2019).

Neuroconsult. (no date) Available online: http://www.neuroconsult.at/ (accessed on 8 January 2019).

Neurodevice.pl. (2019) *g.Nautilus – wireless EEG system with active electrodes Neuro Device.* [online] Available at: http://www.neurodevice.pl/en/produkt/g-nautilus-wireless-eeg-system-with-active-electrodes/ [Accessed 8 May 2019].

Neuromarketing, Neuroscientific Consumer Testing. NeuroFocus. (no date) Available online: http://www.neurofocus.com/ (accessed on 8 January 2019).

Nicolas-Alonso, L.F, Gomez-Gil, J. (2012) *Brain Computer Interfaces, a Review.* Sensors, 2012; 12(2): 1211-1279.

Niedermeyer, E., Lopes da Silva, F.H. (1993) *Electroencephalography: Basic principles, clinical applications and related fields, 3rd edition.* Lippincott, Williams & Wilkins, Philadelphia, 1993.

Nolan, H., Whelan, R., Reilly, R.B. (2010) *FASTER: Fully Automated Statistical Thresholding for EEG artifact Rejection*. Journal of Neuroscience Methods, 2010; 192(1): 152–162.

Odom, J.V., Bach, M., Barber, C., Brigell, M., Marmor, M.F., Tormene, A.P., Holder, G.E. (2004) *Visual evoked potentials standard (2004).* Doc. Ophthalmol. 2004, 108, 115–123.

Orban, G.A. (2008) *Higher Order Visual Processing in Macaque Extrastriate Cortex.* Physiol Rev January 1, 2008; 88:(1) 59-89.

Palaniappan, R. (2005) *Brain Computer Interface Design Using Band Powers Extracted During Mental Tasks*. In Proceedings of the 2nd International IEEE EMBS Conference on Neural Engineering (NER'05), Arlington, VA, USA, March 2005; pp. 321–324.

Perlstein, W.M., Cole, M.A., Larson, M., Kelly, K., Seignourel, P., Keil, A. (2003) *Steady-state visual evoked potentials reveal frontally-mediated working memory activity in humans*. Neurosci. Lett. 2003, 342, 191–195.

Peterson, N.N., Schroeder, C.E., Arezzo, J.C. (1995) *Neural generators of early cortical somatosensory evoked potentials in the awake monkey*. Electroencephalography and Clinical Neurophysiology, 1995; 96: 248-260.

Pfurtscheller, G., Allison, B.Z., Bauernfeind, G.n., Brunner, C., Solis Escalante, T., Scherer, R., Zander, T.O., Mueller-Putz, G., Neuper, C., Birbaumer, N. (2010) *The hybrid BCI.* Front. Neurosci. 2010, doi: 10.1186/1744-9081-6-28.

Pfurtscheller, G., Brunner, C., Schlögl, A., Lopes da Silva, F.H. (2006) *Mu rhythm (de)synchronization and EEG single-trial classification of different motor imagery tasks*. Neuroimage, 2006; 31: 153–159.

Pfurtscheller, G., Guger, C., Müller, G., Krausz, G., Neuper, C. (2000) *Brain oscillations control hand orthosis in a tetraplegic*. Neurosci. Lett. 2000, 292, 211–214.

Pfurtscheller, G., Lopes da Silva, F.H. (1999) *Event-related EEG/MEG synchronization and desynchronization: Basic principles*. Clin. Neurophysiol., 1999; 110: 1842–1857.

Pfurtscheller, G., Neuper, C. (2001) *Motor imagery and direct brain-computer communication.* Proc. IEEE, 2001; 89: 1123–1134.

Pfurtscheller, G., Neuper, C., Flotzinger, D., Pregenzer, M. (1997) *EEG-based discrimination between imagination of right and left hand movement*. Electroencephalogr. Clin. Neurophysiol., 1997; 103: 642–651.

Pineda, J. A. (2005) *The functional significance of mu rhythms: Translating 'seeing' and 'hearing' into 'doing'.* Brain Research Reviews, 2005; 50(1): 57-68.

Pires, G., Castelo-Branco, M., Nunes, U. (2008) *Visual P300-Based BCI to Steer a Wheelchair: A Bayesian Approach.* In Proceedings of the 30th Annual International Conference of the IEEE Engineering in Medicine and Biology Society (EMBS'08), Vancouver, Canada, August 2008; pp. 658–661.

Polich, J. (2007) *Updating P300: An Integrative theory of P3a and P3b*. Clinical Neurophysiology, 2007; 118(10): 2128-2148.

Processing Images. (2017) *Processing Images*. [ONLINE] Available at:https://developer.apple.com/library/content/documentation/GraphicsImaging/Conceptual/CoreImaging/ci_tasks/ci_tasks.html. [Accessed 15 October 2017].

Rakotomamonjy, A., Guigue, V. (2008) *BCI Competition III: Dataset II-Ensemble of SVMs for BCI P300 Speller.* IEEE Trans. Biomed. Eng. 2008, 55, 1147–1154.

Ramoser, H., Muller-Gerking, J., Pfurtscheller, G. (2000) *Optimal spatial filtering of single trial EEG during imagined hand movement*. IEEE Trans. Rehabil. Eng. 2000, 8, 441–446.

Rebsamen, B., Burdet, E., Cuntai, G., Chee Leong, T., Qiang, Z., Ang, M., Laugier, C. (2007) *Controlling a Wheelchair Using a BCI with Low Information Transfer Rate.* In Proceedings of the IEEE 10th International Conference on Rehabilitation Robotics (ICORR'07), Noordwijk, The Netherlands, June 2007; pp. 1003–1008.

Regan, D. (1989) *Human Brain Electrophysiology: Evoked Potentials and Evoked Magnetic Fields in Science and Medicine.* Elsevier: New York, NY, USA, 1989.

Research Use of Emotiv EPOC. (2015) *Research Use of Emotiv EPOC.* [ONLINE] Available at: http://neurofeedback.visaduma.info/ emotivresearch_o.htm. [Accessed 12 March 2015].

Rinck, P. (2016) *Magnetic Resonance in Medicine.* The Basic Textbook of the European Magnetic Resonance Forum. 9th edition; 2016. Electronic version 9, published 1 March 2016.

Rohani, D.A., Henning, W.S., Thomsen, C.E., Kjaer, T.W., Puthusserypad, S., Sorensen, H.B.D. (2013) *BCI using imaginary movements: The simulator.* Computer Methods and Programs in Biomedicine , 2013; 111(2): 300 – 307.

Ruiting, Y., Gray, D.A., Ng, B.W., Mingyi, H. (2009) *Comparative Analysis of Signal Processing in Brain Computer Interface*. In Proceedings of the 4th IEEE Conference on Industrial Electronics and Applications (ICIEA'09), Xi'an, China, May 2009; pp. 580-585.

Russell, S.J., Norvig, P. (2010) *Artificial Intelligence: A Modern Approach.* Third Edition, Prentice Hall, ISBN 9780136042594, 2010.

Samar, V.J., Bopardikar, A., Rao, R., Swartz, K. (1999) *Wavelet analysis of neuroelectric waveforms: A conceptual tutorial*. Brain Lang 1999, 66, 7–60.

Sccn.ucsd.edu. (2019). *Chapter 09: Decomposing Data Using ICA - SCCN*. [online] Available at: https://sccn.ucsd.edu/wiki/Chapter_09:_Decomposing_Data_Using_ICA [Accessed 28 Sep. 2019].

Sccn.ucsd.edu. (2019) *EEGLAB Plugins - SCCN*. [online] Available at: https://sccn.ucsd.edu/wiki/EEGLAB_Plugins [Accessed 11 May 2019].

Scherer, R., Muller, G.R., Neuper, C., Graimann, B., Pfurtscheller, G. (2004) *An asynchronously controlled EEG-based virtual keyboard: Improvement of the spelling rate*. IEEE Trans. Biomed. Eng. 2004, 51, 979–984.

Schlögl, A., Lee, F., Bischof, H., Pfurtscheller, G. (2005) *Characterization of four-class motor imagery EEG data for the BCI-competition. 2005*. J. Neural Eng. 2005, 2, L14.

Schmidt, R.F., Thews, G. (1983) *Human Physiology (second completely revised edition)*. Berlin, Heidelberg, New York: Springer-Verlag. p. 725. ISBN 0-387-11669-9.

Sellers, E.W., Vaughan, T.M., Wolpaw, J.R. (2010) *A brain-computer interface for long-term independent home use*. Amyotroph. Lateral Scler. 2010, 11, 449–455.

Senkowski, D., Herrmann, C.S. (2002) *Effects of task difficulty on evoked gamma activity and ERPs in a visual discrimination task*. Clin. Neurophysiol. 2002, 113, 1742–1753.

Serruya, M.D., Hatsopoulos, N.G., Paninski, L., Fellows, M.R., Donoghue, J.P. (2002) *Brain-machine interface: Instant neural control of a movement signal*. Nature 2002, 416, 141–142.

Shenoy, P., Krauledat, M., Blankertz, B., Rao, R.P.N., Müller, K.-R. (2006) *Towards adaptive classification for BCI*. J. Neural Eng. 2006, 3, R13.

Silvoni, S., Volpato, C., Cavinato, M., Marchetti, M., Priftis, K., Merico, A., Tonin, P., Koutsikos, K., Beverina, F., Piccione, F. (2009) *P300-based brain-computer interface communication: evaluation and follow-up in amyotrophic lateral sclerosis*. Front. Neurosci. 2009, 3, 60.

Sinclair, C.M., Gasper, M.C., Blum, A.S. (2007) *Basic Electronics in Clinical Neurophysiology*. In The Clinical Neurophysiology Primer; Blum, A.S., Rutkove, S.B., Eds.; Humana Press Inc.: Totowa, NJ, USA, 2007; pp. 3–18.

Singla, R., Khosla, A., Jha, R. (2014) *Influence of stimuli colour in SSVEP-based BCI wheelchair control using support vector machines*. Journal of Medical Engineering & Technology. 2014;38(3):125-134.

Soneira, R.M. (2015) *iPad 2015 Display Technology Shoot-Out*. Available at: http://www.displaymate.com/ iPad_2015_SchootOut_1.htm [Accessed: 27 March 2016].

Squires, N.K., Squires, K.C., Hillyard, S.A. (1975) *Two varieties of long-latency positive waves evoked by unpredictable auditory stimuli in man*. Electroencephalogr Clin Neurophysiol., 1975; 38(4): 387-401.

Store.arduino.cc. (2019) *Arduino Uno Rev3*. [online] Available at: https://store.arduino.cc/arduino-uno-rev3 [Accessed 26 Jan. 2019].

Sur, S., Sinha, V.K. (2009) *Event-related potential: anoverview*. Ind. Psychiatry J, 2009; 18(1): 70-73.

Szalowski, A, and Picovici, D. (2015) *Investigating the robustness of constant and variable period graphics in eliciting steady state visual evoked potential signals using Emotiv EPOC, MATLAB, and Adobe after effects*. 2015 26th Irish Signals and Systems Conference (ISSC), Carlow, 2015, pp. 1-8.
doi: 10.1109/ISSC.2015.7163777.

Szalowski, A. and Picovici, D. (2019) *The element of user training for SSVEP-based BCI*. Irish Signals and Systems Conference 2019, Maynooth University Maynooth, 17-18 June 2019

Taheri, B.A., Knight, R.T., Smith, R.L. (1994) *A dry electrode for EEG recording*. Electroencephalogr. Clin. Neurophysiol. 1994, 90, 376–383.

Tan, L., (2007) *Digital Signal Processing: Fundamentals And Applications*. Academic Press.

Tanaka, K., Matsunaga, K., Wang, H.O. (2005) *Electroencephalogram-based control of an electric wheelchair*. IEEE Trans. Robot. 2005, 21, 762–766.

Te-Won, L., Lewicki, M.S., Girolami, M., Sejnowski, T.J. (1999) *Blind source separation of more sources than mixtures using overcomplete representations*. IEEE Signal Process. Lett. 1999, 6, 87–90.

Tello, R.M., Müller, S.M., Bastos, T.F., Ferreira, A. (2014) *Evaluation of different stimuli color for an SSVEP-based BCI*. XXIV Congresso Brasileiro de Engenharia Biomedica - CBEB 2014.

Teplan, M. (2002) *Fundamentals of EEG measurement*. Meas. Sci. Rev. 2002, 2, 1–11.

The Harvard University Gazette. (1998) *Brain's Color Processor is Located* [ONLINE] Available at: http://news.harvard.edu/gazette/1998/08.06/BrainsColorProc.html. [Accessed 1 March 2016].

Townsend, G., LaPallo, B.K., Boulay, C.B., Krusienski, D.J., Frye, G.E., Hauser, C.K., Schwartz, N.E., Vaughan, T.M., Wolpaw, J.R., Sellers, E.W. (2010) *A novel P300-based brain-computer interface stimulus presentation paradigm: Moving beyond rows and columns*. Clin. Neurophysiol. 2010, 121, 1109–1120.

Treder, M.S., Blankertz, B. (2010) *(C) overt attention and visual speller design in an ERP-based brain-computer interface*. Behav. Brain Funct. 2010, 6, 28.

Treder, M.S., Schmidt, N.M., Blankertz, B. (2011) *Gaze-independent brain-computer interfaces based on covert attention and feature attention*. J. Neural Eng. 2011, 8, 066003.

Tsui, C., Gan, J. (2007) *Asynchronous BCI Control of a Robot Simulator with Supervised Online Training*. In Intelligent Data Engineering and Automated Learning—IDEAL 2007; Yin, H., Tino, P., Corchado, E., Byrne, W., Yao, X., Eds.; Springer: Berlin, Germany, 2007; 4881: 125–134.

Unimed-electrodes.co.uk. (2019) *Unimed | MULTI-Cap 'Cup' - For Use With Standard EEG Disc Electrodes.* [online] Available at: http://www.unimed-electrodes.co.uk/MULTICap-Cup--For-Use-With-Standard-EEG-Disc-Electrodes/299 [Accessed 8 May 2019].

Usakli, A.B. (2010) *Improvement of EEG signal acquisition: An electrical aspect for state of the art of front end*. Comput. Intell. Neurosci. 2010, 2010, 630649.

Vasquez, P.M., Bakardjian, H., Vallverdu, M., Cichocki, A. (2008) *Fast multi-command SSVEP brain machine interface without training.* In Proceedings of the 18th International Conference on Artificial Neural Networks, 2008; 300–307.

Vecchiato, G., De Vico Fallani, F., Astolfi, L., Toppi, J., Cincotti, F., Mattia, D., Salinari, S., Babiloni, F. (2010) *The issue of multiple univariate comparisons in the context of neuroelectric brain mapping: An application in a neuromarketing experiment.* J. Neurosci. Methods 2010, 191, 283–289.

Vidaurre, C., Krämer, N., Blankertz, B., Schlögl, A. (2009) *Time domain parameters as a feature for EEG-based brain-computer interfaces*. Neural Netw. 2009, 22, 1313–1319.

Vigário, R.N. (1997) *Extraction of ocular artefacts from EEG using independent component analysis*. Electroencephalogr. Clin. Neurophysiol. 1997, 103, 395–404.

Waldert, S. (2016). *Invasive vs. Non-Invasive Neuronal Signals for Brain-Machine Interfaces: Will One Prevail?. Frontiers in Neuroscience*, 10.

Wallstrom, G.L., Kass, R.E., Miller, A., Cohn, J.F., Fox, N.A. (2004) *Automatic correction of ocular artefacts in the EEG: a comparison of regression-based and component-based methods*. Int. J. Psychophysiol. 2004, 53, 105–119.

Wang, Y., Gao, X., Hong, B., Jia, C., Gao, S. (2008) *Brain- Computer Interfaces Based on Visual Evoked Potentials*. Feasibility of Practical System Designs. IEEE Engineering In Medicine And Biology Magazine, 2008.

Wang, Y., Wang, Y. T., Jung, T. P., (2010) *Visual stimulus design for high-rate SSVEP.* Electronic Letters, 46: 1057-1058.

Webvision.med.utah.edu. (2019) *Simple Anatomy of the Retina by Helga Kolb – Webvision.* [online] Available at:https://webvision.med.utah.edu/book/part-i-foundations/simple-anatomy-of-the-retina/ [Accessed 30 May 2019].

Wolpaw, J.R. (2007) *Brain–computer interfaces as new brain output pathways*. J. Physiol. 2007, 579, 613–619.

Wolpaw, J.R., Birbaumer, N., Heetderks, W.J., McFarland, D.J., Peckham, P.H., Schalk, G., Donchin, E., Quatrano, L.A., Robinson, C.J., Vaughan, T.M. (2000) *Brain-computer interface technology: A review of the first international meeting*. IEEE Trans. Rehabil. Eng. 2000, 8, 164–173.

Xiang, L., Dezhong, Y., Wu, D., Chaoyi, L. (2007) *Combining spatial filters for the classification of single-trial EEG in a finger movement task*. IEEE Trans. Biomed. Eng. 2007, 54, 821–831.

Xiaorong, G., Dingfeng, X., Ming, C., Shangkai, G. (2003) *A BCI-based environmental controller for the motion-disabled.* IEEE Trans. Neural Syst. Rehabil. Eng. 2003, 11, 137–140.

Yijun, W., Ruiping, W., Xiaorong, G., Bo, H., Shangkai, G. (2006) *A practical VEP-based brain-computer interface.* IEEE Trans. Neural Syst. Rehabil. Eng. 2006, 14, 234–240.

Yijun, W., Xiaorong, G., Bo, H., Chuan, J., Shangkai, G. (2008) *Brain-computer interfaces based on visual evoked potentials.* IEEE Eng. Med. Biol. Mag. 27, pp 64–71.

Yijun, W., Xiaorong, G., Bo, H., Chuan, J., Shangkai, G. (2008) *Brain-computer interfaces based on visual evoked potentials.* IEEE Eng. Med. Biol. Mag. 2008, 27, 64–71.

Zeki, S., Marini, L. (1998) *Three cortical stages of colour processing in the human brain.* Brain 121 (Pt 9):1669-85.10.1093/brain/121.9.1669.

Zhang, L., He, W., He, C., Wang, P. (2010) *Improving Mental task classification by adding high frequency band information*. J. Med. Syst., 2010; 34: 51–60.

Zhu, D., Bieger, J., Garcia Molina, G., Aarts, R.M. (2010) *A survey of stimulation methods used in SSVEP-Based BCIs*. Comput. Intell. Neurosci. 2010, doi: 10.1155/2010/702357.

List of Publications:

Conference published papers:

- Szalowski, A. and Picovici, D. (2019) "*The element of user training for SSVEP-based BCI"*, 2019 30th Irish Signals and Systems Conference (ISSC2019), Conference paper, Publisher: IEEE, ISBN: 978-1-7281-2800-9/19/.

- Szalowski, A and Picovici, D. (2019) *"Testing performance of multicolour checkerboard flickers against their greyscale versions for SSVEP-based BCI," 2019 7th International Winter Conference on Brain-Computer Interface (BCI)*, Gangwon, Korea (South), 2019, pp. 1-6. doi: 10.1109/IWW-BCI.2019.8737261.

- Szalowski, A and Picovici, D. (2018) *"The influence of flickering patterns on the quality of brain signals for Brain-Computer Interface," 2018 29th Irish Signals and Systems Conference (ISSC)*, Belfast, 2018, pp. 1-6. doi: 10.1109/ISSC.2018.8585359.

- Szalowski, A. and Picovici, D. (2017) "Investigating stimuli graphics' size and resolution performance in Steady State Visual Evoked Potential," 2017 28th Irish Signals and Systems Conference (ISSC), Killarney, 2017, pp. 1-6. doi: 10.1109/ISSC.2017.7983618.

- Szalowski, A and Picovici, D. (2016) *"Investigating brain signal peaks vs electroencephalograph electrode placement using multicolour 10 Hz flickering graphics stimulation for Brain-computer Interface development," 2016 27th Irish Signals and Systems Conference (ISSC)*, Londonderry, 2016, pp. 1-5.
  doi: 10.1109/ISSC.2016.7528453.

- Szalowski, A. and Picovici, D. (2016) "Investigating colour's effect in stimulating brain oscillations for BCI systems," *2016 4th International Winter Conference on Brain-Computer Interface (BCI)*, Yongpyong, 2016, pp. 1-4.
  doi: 10.1109/IWW-BCI.2016.7457449.

- Szalowski, A and Picovici, D. (2015) "Investigating the robustness of constant and variable period graphics in eliciting steady state visual evoked potential signals using Emotiv EPOC, MATLAB, and Adobe after effects," *2015 26th Irish Signals and Systems Conference (ISSC)*, Carlow, 2015, pp. 1-8. doi: 10.1109/ISSC.2015.7163777.

Book chapters:

- Szalowski, A., Pege, T., and Picovici, D. (2018) "*MCF – Multi Colour Flicker iOS Application for Brain-Computer Interface research",* Part of book: "Advances in Intelligent Systems and Computing - Intelligent Computing – Proceedings of the 2018 Computing Conference, Volume 1", Publisher: Springer, November 30th 2018, ISSN 2194-5357, ISSN 2194-5365 (electronic), ISBN 978-3-030-01173-4, ISBN 978-3-030-01174-1 (eBook).

- Szalowski, A. and Picovici, D. (2019) "*Investigating colour response in SSVEP paradigm for BCI development",* Part of book: "Theoretical Investigations and Applied Studies in Engineering", Publisher: EKIN Publishing House, March 15th, (ISBN: 978-605-327-856-6).

Journals:

- Szalowski, A. and Picovici, D. (2015) "*Low-cost Brain-Computer Interfaces",* Publisher: by Scholars Journal of Engineering and Technology, September 2015, (www.saspublisher.com), online (ISSN 2321-435X) printed (ISSN 2347-9523).

Magazine:

- Szalowski, A. (2017) *"Colour in the brain"*, Part of Radius-Research, Development & Innovation magazine, Publisher: Institute of Technology Carlow, Winter 2017, Issue 6, ISSN: 2009-9339

Appendices:

Appendix 1: The digital version of the thesis

Appendix 2: The source code of MCF application for iOS devices

Appendix 3: Brain signals recorded during the research (EDF format)

Appendix 4: Multi-colour checkerboard flickers (video files)

Appendix 5: After Effects project file allowing to render individual flickers

Appendix 6: Arduino sketches for RGB 40 LED shield

Appendix 7: MATLAB-based GUI for detecting frequency peaks in brain signals (for EDF files)

Appendices available on attached DVD disc.